ISBN: 978-82-575-1747-2
ISSN: 1894-6402

Norwegian University
of Life Sciences

Postboks 5003
NO-1432 Ås, Norway
+47 67 23 00 00
www.nmbu.no

Philosophiae Doctor (PhD), Thesis 2017:81

Øyvind Salvesen

96307 / ANDVORDGRAFISK.NO

Norwegian University of Life Sciences
Faculty of Veterinary Medicine
Department of Production Animal Clinical Sciences

Philosophiae Doctor (PhD)
Thesis 2017:81

The cellular prion protein and the inflammatory response

Øyvind Salvesen

The cellular prion protein and the inflammatory response

Øyvind Salvesen

Thesis for the degree of *Philosophiae Doctor* (PhD)

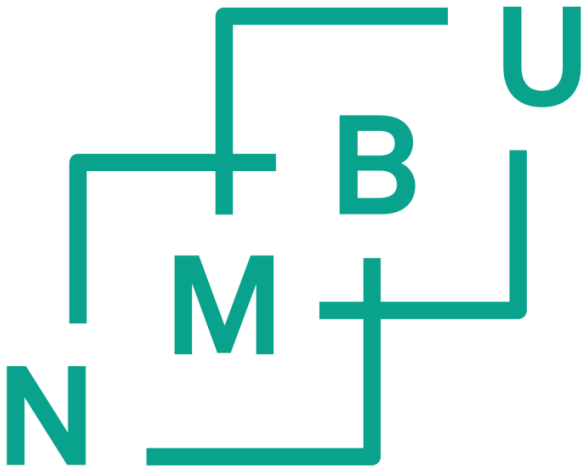

Norwegian University of Life Sciences

Faculty of Veterinary Medicine

Department of Production Animal Clinical Sciences

Section of Small Ruminant Research

Sandnes 2017

Thesis number: 2017:81

ISSN: 1894-6402

ISBN: 978-82-575-1747-2

Contents

Acknowledgements

The present work was conducted at the Section of Small Ruminant Research (Sandnes) in collaboration with the Department of Basic Sciences and Aquatic Medicine (Oslo), at the Norwegian University of Life Sciences (NMBU), between 2014 and 2017. It was part of the project "*Norwegian dairy goats naturally devoid of the prion protein – a break-through in the battle against prions?"* financed by the Research Council of Norway. I highly appreciate the opportunity I have been given by NMBU.

First, I would like to express my sincere gratitude to my main supervisor Cecilie Ersdal. Thank you for always being optimistic, and for great support and valuable feedback. I would also like to acknowledge my co-supervisors, Michael A. Tranulis and Arild Espenes, for constructive criticism, good discussions, and backing of my PhD.

Thanks to Malin for all the help during the experiments and for shared coffee-times, and to Maren, Susan, and Trond for helping me to develop laboratory skills. Thanks to Giulia, Jorke, and Liv Heidi for support and discussions, and Agnes for help with breeding of goats.

A special acknowledgement to the great staff in Sandnes: Suzan, Wenche, Siri, Silje, Solfrid, Eli, Tom, Anita, Unni, Liv, Helge, Jon Ludvig, Garmann, Asbjørn, Eimo, Ane, Michaela, Anne Mette, Marianne, Clare, and Snorre. I have enjoyed working with you all and could not have completed the PhD without you.

Thanks to Kerstin Skovgaard, Peter Heegaard, and Karin Tarp for great support during my research exchange at the Technical University of Copenhagen.

I highly appreciate all the constructive feedback from Lucy Robertson who proofread my manuscripts.

Thanks to my wonderful family and friends and to Nina for great patience and love.

Finally, I would like to acknowledge my PhD committee for evaluating this thesis.

Abbreviations

AD	Alzheimer's disease
ADAM	A disintegrin and metalloproteinase
AMPA	α-amino-3-hydroxy-5-methyl-4-isoxazolepropionic acid
AP	Activator protein
APP	Acute phase protein
BLAST	Basic local alignment search tool
cAMP	Cyclic adenosine monophosphate
CD14	Cluster of differentiation 14
CNS	Central nervous system
COX2	Cyclooxygenase 2
DEGs	Differentially expressed genes
DIC	Disseminated intravascular coagulation
DNA	Deoxyribonucleic acid
EAE	Experimental autoimmune encephalomyelitis
ECM	Extracellular matrix
Edbg	Edinburg *Prnp* knockout mice
EDTA	Ethylenediaminetetraacetic acid
ELISA	Enzyme-linked immunosorbent assay
ER	Endoplasmic reticulum
FOXO3	Forkhead box O3
FPKM	Fragments per kilobase of transcript per million fragments mapped
GFAP	Glial fibrillary acidic protein
GPI	Glycosylphosphatidylinositol
HES-1	Hairy and enhancer of split 1
HP	Haptoglobin
Iba1	Ionized calcium binding adaptor molecule 1
IFN	Interferon (type I)
IFNAR	Interferon-α/β receptor
IHC	Immunohistochemistry
IL	Interleukin
iNOS	Inducible nitric oxide synthase
IPA	Ingenuity pathway analysis
ISGs	Interferon stimulated genes
KO	Knockout
LPS	Lipopolysaccharide
LPB	LPS binding protein
LR	Laminin receptor
MAPK	Mitogen-activated protein kinase
MD2	Myeloid differentiation factor 2
MDD	Major depression disorder
mGluRs	Metabotropic glutamate receptors
MHC	Major histocompatibility complex
MMP	Matrix metalloproteinase
mRNA	Messenger ribonucleic acid

MSA	Multiple sequence alignment
MSB	Martius-Scarlet-Blue
MTF-1	Metal regulatory transcription factor 1
Ngsk	Nagasaki *Prnp* knockout mice
NMDA	N-methyl-D-aspartate
PBMC	Peripheral blood mononuclear cells
PKA	Pro-survival protein kinase A
PNS	Peripheral nervous system
PRND	Doppel protein gene
PRNP	Prion protein gene
Prnp	Murine prion protein gene
$PRNP^{+/+}$	Normal goats (wild type)
$PRNP^{Ter/Ter}$	PrP^{C}-deficient goats (mutant)
PrP^{C}	Cellular prion protein
PrP^{Sc}	Pathological form of the prion protein
qPCR	Quantitative polymerase chain reaction (real-time)
RNA	Ribonucleic acid
RNA-seq	RNA sequencing
ROS	Reactive oxygen species
SAA	Serum amyloid A
SH-SY5Y	Human neuroblastoma cell line
SNP	Single nucleotide polymorphisms
SOD	Superoxide dismutase
SP-1	Specificity protein 1
SPRN	Shadoo protein gene
STI1	Stress-induced phosphoprotein 1
TACE	Tumor necrosis factor-α converting enzyme
TFNAR	Tumor necrosis factor-α receptor
TGF	Transforming growth factor
TLR4	Toll-like receptor 4
TNF	Tumor necrosis factor
YY-1	Yin-Yang 1
ZrchI	Zürich I *Prnp* knockout mice
ZrchIII	Zürich III *Prnp* knockout mice

Abbreviations of proteins involved in the TLR4-pathway are given in Figure 5.

Additional gene abbreviations can be found in the papers and their supplementary files.

Summary

The cellular prion protein (PrP^C) is known for its pivotal role in the development of prion diseases, such as Creutzfeldt-Jakob disease in humans and scrapie in small ruminants. In these diseases, PrP^C is converted into a pathological form, PrP^{Sc}. The accumulation of this misfolded isoform in the brain results in fatal neurodegeneration. Several decades of research have revealed clues to the normal biological function of PrP^C, yet still without a definite conclusion. Unravelling normal PrP^C biology is important not only to understand the pathogenesis of prion disorders, but also to identify potential side effects of future treatments involving blocking of PrP^C or removal of the PrP^C-encoding gene (*PRNP*).

We utilized a unique line of Norwegian dairy goats that carry a stop mutation early in the *PRNP* to study PrP^C physiology. These goats are the only known mammals that are naturally devoid of PrP^C ($PRNP^{Ter/Ter}$). By using next generation RNA sequencing, we identified a primed state of interferon-stimulated genes in circulating blood cells and tissues of $PRNP^{Ter/Ter}$ goats (Papers II, III, and IV). When exposed to systemic lipopolysaccharide (LPS), PrP^C-deficient goats suffered a prolonged sickness behavior and displayed an expression profile skewed towards a type I interferon signaling response in the brain (Paper III). In the lungs, a tissue with a more severe response to LPS, loss of PrP^C resulted in increased activation of pro-inflammatory pathways and remodeling of the extracellular matrix (Paper IV), which indicates augmented damage to the lung parenchyma. Taken together, we propose that PrP^C is a modulator of inflammatory pathways, particularly downstream of type I interferons, and protects vulnerable tissues against inflammatory stress. Being located at the cell surface, our findings corroborate the theory of PrP^C as a scaffolding protein, which can interact with various forms of multiprotein complexes and regulate downstream signaling.

In addition to exploring the function of PrP^C, the current thesis extends the existing knowledge of the inflammatory response in small ruminants. Systemic administration of LPS mimics the initial events of sepsis and is a well-established method of studying the innate immune system. We provide evidence that both leukocytes and tissues increase transcription of acute-phase protein genes at the beginning of an inflammation, and we identify *SAA3* as a particularly useful biomarker (Papers I, III, and IV). In the choroid plexus,

a profound activation of the transcriptome and increased number of Iba1-positive cells were observed. Being located at the blood-brain interface, we confirm that this tissue plays a crucial role in the interaction between systemic circulation and the brain. Alterations in the hippocampus transcriptome were mild, which suggests that this brain region is relatively protected from circulating endotoxins. Yet, the clinical response and activation of astrocytes confirms that inflammation was present (Paper III). As described in paper IV, the lungs were the most affected organ, characterized by substantial activation of the transcriptome and morphological changes compatible with acute lung injury. The high pulmonary sensitivity of goats towards systemic endotoxins implies that limiting pulmonary inflammation is of special importance for treating septic patients. In light of the increasing problem of antimicrobial resistance against antibiotics, understanding the molecular mechanisms of inflammation is a prerequisite for designing new therapeutic strategies.

Sammendrag (summary in Norwegian)

Det normale prionproteinet (PrP^{C}) finnes hos alle pattedyr og er kjent for sin rolle i utviklingen av prionsykdommer. Disse inkluderer blant annet Creutzfeldt-Jakobs sykdom hos mennesker, skrantesjuke (CWD) hos hjortedyr, og skrapesjuke (scrapie) hos småfe. Sykdommene skyldes at en unormal, feilfoldet variant av prionproteinet (PrP^{Sc}) akkumulerer i sentralnervesystemet og fører til degenerasjon av nerveceller. Prionsykdommer kan ikke behandles og er alltid dødelige. Flere tiår med forskning har indikert at PrP^{C} er involvert i en rekke normale biologiske funksjoner, men noen endelig konklusjon har uteblitt. Kartlegging av PrP^{C} sin fysiologiske funksjon er viktig for å forstå utviklingen av prionsykdommer, samt å identifisere potensielle bivirkninger av framtidige behandlingsformer som kan involvere blokkering av PrP^{C} eller fjerning av genet som koder for prionproteinet (*PRNP*).

I denne doktorgraden har vi studert en unik genetisk linje av norske melkegeiter som har en stopmutasjon tidlig i *PRNP*. Disse geitene er de eneste naturlig forekommende pattedyrene som er uten PrP^{C} ($PRNP^{Ter/Ter}$). I tillegg til at de mest sannsynlig ikke kan utvikle scrapie, utgjør disse dyrene en unik mulighet til å studere den normale funksjonen til PrP^{C}. Vi brukte RNA-sekvensering for å lete etter gener som er forskjellig uttrykt i geiter med og uten PrP^{C}. Denne metoden avdekker alle de uttrykte genene i et vev på et gitt tidspunkt (transkriptom). Tap av PrP^{C} førte til økt utrykk av interferon-stimulerte gener i perifere mononukleære blodceller og enkelte vev (Artikkel II, III og IV). Geiter uten PrP^{C} viste også en forlenget sykdomsatferd etter lipopolysakkarid (LPS)-stimulering av det medfødte immunforsvaret (Artikkel III). Samtidig påviste vi en økt aktivering av betennelsesfremmende gener i lungene, sammen med gener involvert i remodelering av ekstracellulærmatriks. Dette indikerer at tap av PrP^{C} fører til en ubalansert betennelsesprosess og gir økt skade av lungevevet (Artikkel IV). Vi foreslår derfor at PrP^{C} regulerer viktige signalveier for immunresponsen, særlig nedstrøms for type I interferoner, og beskytter sårbare vev ved betennelsestilstander. PrP^{C} er et overflateprotein og kan sannsynligvis påvirke flere typer proteiner på celleoverflaten og dermed modulere signalisering inn i cellen.

I tillegg til å studere PrP^C sin normalfunksjon, utvider denne doktorgraden dagens kunnskap om betennelsesprosessen hos småfe. Systemisk administrering av LPS stimulerer en sepsis-lignende tilstand (blodforgiftning), og er en veletablert metode for å studere det medfødte immunforsvaret. I artikkel I beskriver vi at genuttrykket av akuttfaseproteiner øker dramatisk i hvite blodceller etter LPS-stimulering. Selv om leveren er det viktigste organet i akuttfaseresponsen betyr trolig dette at hvite blodceller bidrar til syntese av akuttfaseproteiner både i blod og betent vev som de infiltrerer. Akuttfaseproteinet SAA3 ser ut til å være en spesielt sensitiv biomarkør for betennelse i hvite blodceller og vev hos geiter. Immunhistokjemisk undersøkelse av plexus choroideus (kapillærnett i hjernens hulrom) avdekket aktivering av Iba1-positive celler, og i tillegg sannsynlig rekruttering av monocytter fra blod. Sammen med en tydelig akuttfaserespons på gennivå bekrefter dette at plexus choroideus spiller en viktig rolle i kommunikasjonen mellom den systemiske sirkulasjonen og hjernen. Forholdsvis få gener var aktivert i hippocampus etter LPS, noe som indikerer at denne delen av hjernen er relativt beskyttet mot systemisk betennelse. Aktivering av GFAP-positive astrocytter og den kliniske responsen peker likevel mot at en viss grad av betennelse var tilstede.

I artikkel IV beskriver vi at lungene var det mest berørte organet etter LPS-administrering. Det var en uttalt aktivering av transkriptomet, særlig gener involvert i presentasjon av antigener, nedbrytning av proteiner og syntese av kollagen. Histologisk observerte vi karakteristiske multifokale forandringer med akutt lungeskade som inkluderte infiltrasjon av nøytrofile betennelsesceller, økt mengde alveolemakrofager, ødem og hyaline lungesepta. Dette tyder på at småfelunger er spesielt følsomme for sirkulerende endotoksiner, og at det derfor er essensielt å begrense lungeskade hos pasienter med sepsis. Kartlegging av molekylære mekanismer involvert i forsvaret mot bakterier er vesentlig for å utvikle nye behandlingsstrategier i forbindelse med økende grad av antibiotikaresistente bakterier.

List of papers

Paper I:

Øyvind Salvesen, Malin R. Reiten, Peter M. H. Heegaard, Michael A. Tranulis, Arild Espenes, Kerstin Skovgaard and Cecilie Ersdal (2016)**.** Activation of innate immune genes in caprine blood leukocytes after systemic endotoxin challenge. *BMC Veterinary Research* 12(1):241.

Paper II:

Giulia Malachin, Malin R. Reiten, **Øyvind Salvesen**, Håvard Aanes, Jorke H. Kamstra, Kerstin Skovgaard, Peter M. H. Heegaard, Cecilie Ersdal, Arild Espenes, Michael A. Tranulis and Maren K. Bakkebø MK (2017). Loss of prion protein induces a primed state of type I interferon-responsive genes. *PLoS One* 12(6):e0179881.

Paper III:

Øyvind Salvesen, Malin R. Reiten, Arild Espenes, Maren K. Bakkebø, Michael A. Tranulis and Cecilie Ersdal (2017)**.** LPS-induced systemic inflammation reveals an immunomodulatory role for the prion protein at the blood-brain interface. *Journal of Neuroinflammation* 14(1):106.

Paper IV:

Øyvind Salvesen, Malin R. Reiten, Jorke H. Kamstra, Maren K. Bakkebø, Arild Espenes, Michael A. Tranulis and Cecilie Ersdal (2017)**.** PrP^{C} modulates pathways of inflammation during LPS-induced acute lung injury. *Submitted to Frontiers in Immunology.*

Introduction

The cellular prion protein

The cellular prion protein (PrP^C) is an evolutionarily conserved protein that is expressed in most tissues and has been extensively studied for several decades. A large body of knowledge supports that the pathological isoform (PrP^{Sc}), and thus also PrP^C, is necessary for the development of human and animal prion disorders (Aguzzi 2006; Prusiner 1982). Still, the normal functions of PrP^C are not fully understood. Because PrP^C levels decrease during the progression of prion disorders (Mays et al. 2014) and a loss of PrP^C signaling or gain of PrP^C-mediated toxic signaling may be involved in neuronal cell death (Winklhofer et al. 2008), identifying the normal functions of PrP^C could contribute to a better understanding of the pathogenesis of prion disorders. This literature review presents some of the major proposed functions of PrP^C, a short summary of prion diseases, a description of the lipopolysaccharide model, and an explanation of the unique line of Norwegian dairy goats that laid the foundation for this doctoral work.

The prion protein gene

The cellular PrP is encoded by the prion protein gene (*PRNP*), which is located on chromosome 13 in goats, chromosome 2 in mice, and chromosome 20 in humans. The *PRNP* gene is remarkably conserved among mammals (Puckett et al. 1991; Choi et al. 2006; Harrison et al. 2010; Lee et al. 1998). Together with the two paralogs, *PRND* and *SPRN*, encoding Doppel and Shadoo, *PRNP* constitute the core members of the mammalian prion gene family. Similar to *PRNP*, *SPRN* is highly expressed in neurons of the central nervous system (CNS), and it is thought to have neuroprotective roles (Watts et al. 2007). Conversely, the Doppel protein is most abundant in the male reproductive system (Tranulis et al. 2001) and is involved in the maturation and fertility of spermatocytes (Espenes et al. 2006).

The regulation of *PRNP* expression is complex, and there are numerous binding sites for transcription factors upstream of the transcription start site. For example, SP-1, MTF-1, AP-1, AP-2 and FOXO3 all activate *PRNP* expression, whereas YY-1 and HES-1 are considered to be repressors (Burgess et al. 2009; Bellingham et al. 2009; Wright et al.

2009; Mahal et al. 2001; Kim et al. 2008). Interestingly, a variety of physiological conditions may modulate the expression of the *PRNP* gene, particularly different forms of stress. For instance, Shyu and colleagues reported upregulation of *PRNP* in response to heat shock, hyperbaric oxygen, and hypoglycemia in neuroblastoma cells (Shyu et al. 2000; Shyu et al. 2004; Shyu et al. 2005a).

PrP^C biosynthesis and intracellular trafficking

The human PrP^C is synthesized as a precursor protein of 253 amino acids with a 22 amino acid N-terminal signal peptide. After translocation into the endoplasmic reticulum (ER), the protein is glycosylated, disulfide bonds are formed, and the C-terminal signal sequence is replaced by a glycosylphosphatidylinositol (GPI) anchor (Stahl et al. 1987). Asparagine-linked glycosylation is possible at two sites, both of which are variably occupied resulting in di-, mono- and un-glycosylated molecules (Ermonval et al. 2003; Zahn et al. 2000). Reportedly, the GPI anchor of PrP^C likely associates with lipid rafts already as an immature precursor in the ER (Sarnataro et al. 2004). Both the glycans and the GPI anchor are further modified after transportation to the Golgi apparatus. Interestingly, two transmembrane topologies, ^{Ctm}PrP and ^{Ntm}PrP, have been described for PrP^C, which correspond to COOH- and NH2-terminal transmembrane segments (Hegde et al. 1998; Kim et al. 2002). These do not follow the secretory route and are probably retained within the ER and Golgi apparatus (Stewart et al. 2005).

The mature PrP^C is transported to the cell surface and incorporated into lipid-rafts and invaginated raft structures called caveolae (Sarnataro et al. 2004). An emerging consensus supports that PrP^C continuously cycles between the plasma membrane and endocytic compartments via complex cellular events (Shyng et al. 1993; Magalhães et al. 2002). Investigations performed by electron microscopy have suggested that clathrin-coated pits are the main pathway for endocytic uptake of PrP^C (Shyng et al. 1994). The constant cycling affects the availability of PrP^C at the cell surface and thus likely influences physiological activity (Negro et al. 2001).

Prion protein structure

In humans and small ruminants, PrP^C consists of an approximately 100 amino acid NH2 terminal flexible tail, a globular domain of about another 100 amino acids, and a short COOH-terminal tail (Zahn et al. 2000; Lysek et al. 2005). A hydrophobic section spans the transition between the N- and C-terminal domains, and this section may be involved in the dimerization of PrP^C (Béland et al. 2013). Among the most conserved segments of mammalian PrP^C is the copper-binding octapeptide region that, for most species, contains four or five repetitions of the sequence PHGGGWGQ (Wopfner et al. 1999; Kim et al. 2008). The globular domain comprises three α-helixes that correspond to residues 144-154, 173-194, and 200-228 and two short anti-parallel β-sheets that correspond to residues 128-131 and 161-164 (Zahn et al. 2000). A single disulfide bond links two cysteines at position 179 of the second helix and 214 of the third helix. This bond plays a role in the folding and stability of PrP^C, and it likely affects the pathological conversion of PrP^C and the stabilization of PrP^{Sc} aggregates (Herrmann et al. 1998; Maiti et al. 2001; Welker et al. 2001). The primary structure of PrP^C is highly preserved in mammals, visualized by the multiple sequence alignment below (Figure 1). In non-mammalian species, such as chickens, turtles, and frogs, PrP^C only share approximately 30 % of residues with mammalian PrP^C. Nevertheless, the three-dimensional (tertiary) architecture is strikingly similar in all vertebrates, an observation that supports the theory of an evolutionarily conserved biological role of PrP^C (Calzolai et al. 2005).

```
Mouse  --MANLGYWLLALFVTMWTDVGLCKKRPKP-GGWNTGGSRYPGQGSPGGNRYPPQ-GGTWGQPHGGGWGQPHGGSWGQPHGGSWGQ
Goat   MVKSHIGSWILVLFVAMWSDVGLCKKRPKPGGGWNTGGSRYPGQGSPGGNRYPPQGGGGWGQPHGGGWGQPHGGGWGQPHGGGWGQ
Human  --MANLGCWMLVLFVATWSDLGLCKKRPKP-GGWNTGGSRYPGQGSPGGNRYPPQGGGGWGQPHGGGWGQPHGGGWGQPHGGGWGQ
          :::* *:*.***: *:*:********* ********************** ** **************.*******.***

Mouse  PH-GGGWGQGGGTHNQWNKPSKPKTNLKHVAGAAAAGAVVGGLGGYMLGSAMSRPMIHFGNDWEDRYYRENMYRYPNQVYYRPVDQ
Goat   PHGGGGWGQ-GGSHSQWNKPSKPKTNMKHVAGAAAAGAVVGSLGGYMLGSAMSRPLIHFGNDYEDRYYRENMYRYPNQVYYRPVDQ
Human  PH-GGGWGQGGGTHSQWNKPSKPKTNMKHMAGAAAAGAVVGGLGGYMLGSAMSRPIIHFGSDYEDRYYRENMHRYPNQVYYRPMDE
       ** ****** **:*.**********:**:**********.*************:****.*:*********:**********:*:

Mouse  YSNQNNFVHDCVNITIKQHTVTTTTKGENFTETDVKMMERVVEQMCVTQYQKESQAYYDGRRSSSTVLFSSPPVILLISFLIFLIVG
Goat   YSNQNNFVHDCVNITVKQHTVTTTTKGENFTETDIKIMERVVEQMCITQYQRESQAYY--QRGASVILFSPPPVILLISFLIFLIVG
Human  YSNQNNFVHDCVNITIKQHTVTTTTKGENFTETDVKMMERVVEQMCITQYERESQAYY--QRGSSMVLFSSPPVILLISFLIFLIVG
       ***************:*****************:*:*********:***:.******  .*.:* :***.***************
```

Figure 1. Multiple sequence alignment of the prion protein amino acid sequence generated with Clustal W (1.83) software. Sequences from mouse (*Mus musculus*), goat (*Capra hircus*), and human (*Homo sapiens*) are shown. The highly conserved amino acid sequence across species is visualized by * in the figure. Colors indicate physiochemical properties: Small hydrophobic, acidic, basic, hydroxyl + sulfhydryl + amine.

Proteolytic processing of PrP^C

Figure 2 displays how PrP^C can be proteolytically processed in several ways. Alpha-cleavage may occur just outside of the hydrophobic domain of the prion protein and is presumably mediated by a disintegrin and metalloproteinase (ADAM) proteases (McDonald et al. 2014; Walmsley et al. 2009). Alpha-cleavage is thought to take place in the late Golgi apparatus or endosomal compartment (Walmsley et al. 2009), but it may also be generated at the cell membrane (McDonald et al. 2014). Consequently, the N1 fragment is secreted, whereas the C1 fragment is attached to the cell membrane. Interestingly, as much as 50 % of mature PrP^C were found to be in C1 form in the cerebral cortex of sheep (Campbell et al. 2013). Importantly, some of the most significant proposed biological functions of PrP^C, such as myelin homeostasis and neuroprotection, involve α-cleavage (Guillot-Sestier et al. 2009; Küffer et al. 2016). Beta-cleavage occurs within the octapeptide region and generates fragments N2 and C2 (McMahon et al. 2001). It is primarily observed under pathological conditions, and it seems to be stimulated by oxidative stress and in the presence of reactive oxygen species (ROS) and Cu^{2+} (McMahon et al. 2001). However, enzymatic processing by ADAM8 is also possible (McDonald et al. 2014). More recently, γ-cleavage was identified in un-glycosylated PrP^C (Lewis et al. 2016). It possibly occurs around residues 170-200, thus creating C3-fragments. The relevance of this previously overlooked processing step is not known, but increased levels of C3 in human prion disease may suggest a pathological role of γ-cleavage (Lewis et al. 2016). Finally, full-length PrP^C may be shed in a soluble form mediated by ADAM10 (Altmeppen et al. 2011) or in association with exosomes (Fevrier et al. 2004).

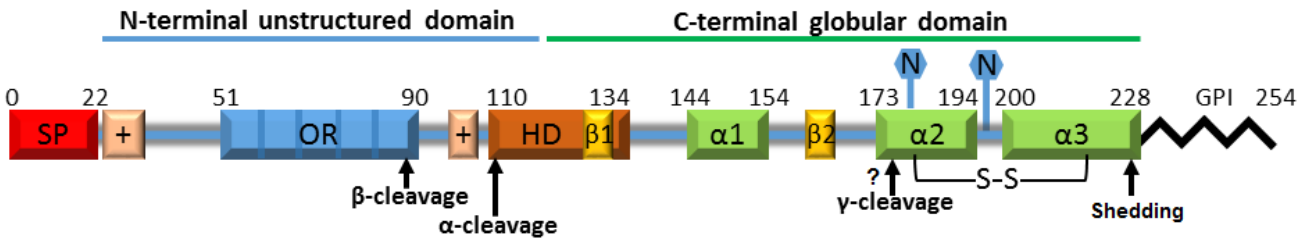

Figure 2. Schematic overview of the mammalian prion protein structure and sites of processing. The signal peptide (SP) is removed in the endoplasmic reticulum. The unstructured N-terminal domain contains two positively charged motifs and the octapeptide repeat region (OR). A hydrophobic domain (HD) spans across the transition of the N- and C-terminal domains. The globular domain contains three α-helixes and two short β-strands. Processing sites are indicated by arrows. Modified from (Bakkebø et al. 2015; Creative Commons License).

Proposed functions of PrP^C

PrP^C knockout models

Soon after it was discovered that PrP^{Sc} is the causative agent of prion diseases, *Prnp* knockout (KO) mice were generated to aid in the search for loss-of-function phenotypes. Surprisingly, the first two *Prnp* KO strains, Zürich I (ZrchI) and Edinburgh (Edbg), presented no developmental alterations or major phenotypical disturbances (Manson et al. 1994; Büeler et al. 1992). Later investigations have shown that PrP^C is dynamically expressed during the developmental stages of nervous tissue and peripheral organs including the heart, liver, lungs, and intestines, which suggests a potential role of PrP^C in embryogenesis (Peralta et al. 2012; Tremblay et al. 2007). Still, experimental ablation of *PRNP* in cattle (Richt et al. 2007) and goats (Yu et al. 2006) produced no pathological phenotypes similar to the initial findings in mice. Conversely, *Prnp* deletion resulted in severe ataxia and Purkinje cell degeneration in a mouse strain known as Nagasaki (Ngsk) (Sakaguchi et al. 1996). Initially, this observation was falsely attributed to the loss of PrP^C, but later investigations demonstrated that overexpression of the gene encoding Doppel caused this phenotype (Moore et al. 1999). Altogether, the initial findings from *Prnp* KO mice seemed to rule out a major physiological role of PrP^C. It was therefore hypothesized that the absence of PrP^C may be compensated for by unknown mechanisms, so a post-natal KO was generated to study the brain upon acute loss of PrP^C in adult mice. Although a subtle electrophysiological alteration was observed in the hippocampus, no evidence of neurodegeneration or histopathological changes was noted (Mallucci et al. 2002).

Nevertheless, later investigations of *Prnp*-ablated mice have revealed a variety of subtle phenotypes and proposed functions of PrP^C. Some of these findings were contradictory, which may have been due to the genetic backgrounds of the mouse models used (Wulf et al. 2017). Of particular importance is the flanking gene problem described in KO strains with a mixed genetic background (Nuvolone et al. 2016). Except from the recently generated Zürich III (ZrchIII) strain (Nuvolone et al. 2016) and the initial Edbg strain (Manson et al. 1994), all *Prnp* KO models have been generated with mixed genetic backgrounds. For this reason, some of the following proposed functions of PrP^C should be considered with caution.

Proposed functions in the central nervous system

Research has shown that PrP^C is expressed most abundantly in the brain, particularly in neurons and to a lesser extent in the supporting cells: astrocytes, microglia, and oligodendroglia (Bertuchi et al. 2012; Moser et al. 1995; Adle-Biassette et al. 2006). Its high expression in neuronal cells, compared to other cell types and tissues, suggests that PrP^C plays a special role in the CNS. Furthermore, the main site of PrP^{Sc} aggregation and pathology is within the CNS, which has led to the brain being the primary focus in prion research.

Neuroprotection

A common model for studying the neuroprotective roles of PrP^C is to induce acute cerebral infarction by occlusion of the middle cerebral artery (Longa et al. 1989). Several studies have reported that *Prnp* KO mice show larger infarction volumes compared with wild type controls or animals that overexpress PrP^C (Steele et al. 2009; Shyu et al. 2005b; Weise et al. 2004; Mitteregger et al. 2007). Notably, PrP^C was upregulated in peri-infarcted regions of wild type mice and rats, and the extent of the upregulation was dependent on the severity of the infarction (Weise et al. 2004; Mitteregger et al. 2007; Mitsios et al. 2007). Likewise, increased PrP^C expression was detected in surviving peri-infarcted neurons of humans 2-34 days after a brain stroke (Mitsios et al. 2007). Taken together, these findings suggest that PrP^C regulates ischemia-induced neuronal cell death *in vivo* (Weise et al. 2004). Under ischemic conditions, PrP^C seems to be proteolytically processed by α-cleavage, which results in the release of N1 fragments with neuroprotective properties (Mitteregger et al. 2007; Guillot-Sestier et al. 2009). Spudich and colleagues proposed that enlarged cerebral infarct sizes in *Prnp* KO animals were linked to increased signaling and activation of ERK1/2, STAT1, caspase-3, and their involvement in apoptosis and neuronal death (Spudich et al. 2005).

Another approach to study neuroprotective roles of PrP^C involves the induction of apoptosis by staurosporine and anisomycin. In primary hippocampal neurons, PrP^C interacts with stress-induced phosphoprotein 1 (STI1), which leads to activation of the pro-survival protein kinase A (PKA) and mitogen-activated protein kinase (MAPK) pathways. This, in turn, protects neurons from apoptosis and promotes neuritogenesis of hippocampal neurons (Zanata et al. 2002; Lopes et al. 2005; Chiarini et al. 2002).

Furthermore, STI1 was upregulated in cerebral infarcted regions of humans and rodents, and the STI1-PrP^C-interaction seemed to recruit bone marrow-derived cells into ischemic brain regions (Beraldo et al. 2013), thus triggering a self-protective mechanism to facilitate recovery after brain infarction (Lee et al. 2013). Finally, it has been suggested that the role of PrP^C in attenuating N-methyl-D-aspartate (NMDA) signaling may participate in the protection against ischemia (Black et al. 2014).

Protection against oxidative stress

Oxidative stress is the result of an imbalance between the production of ROS and the effectiveness of the biological system's antioxidant defense. Disturbances in this equilibrium may result in peroxides or free radicals damaging different cell components including DNA, lipids, and proteins (Burton et al. 2011). Early studies showed that brain samples from *Prnp* KO mice displayed higher levels of oxidative stress markers compared to wild type mice (Wong et al. 2001b). Furthermore, an astrocyte cell line derived from *Prnp* KO mice was more susceptible to treatment with oxidative stress agents, such as hydrogen peroxide and metal ions, compared with controls (Bertuchi et al. 2012). It can thus be presumed that PrP^C participates in the protection of neurons, glial cells, and perhaps other cell types against oxidative stress. As an attempt to deduce the mechanisms involved, Brown and colleagues measured the Cu/Zn superoxide dismutase (SOD) activity, an important antioxidative enzyme. They found decreased SOD activity in *Prnp* KO mice (Brown et al. 1997b) and conversely increased SOD activity in mice overexpressing PrP^C (Brown et al. 1998), which implies that PrP^C regulates the SOD activity or has SOD-like properties. Although the SOD-like activity of PrP^C has been widely described (Brown et al. 1999b; Treiber et al. 2007; Brown et al. 1997b; Brown et al. 1998), several studies have challenged these findings (Hutter et al. 2003; Sakudo et al. 2003; Zocche Soprana et al. 2011), and the topic remains controversial.

PrP^C and behavior

Despite the initial observations that *Prnp* KO mice did not reveal notable behavioral disturbances (Büeler et al. 1992; Manson et al. 1994), a variety of experiments have been performed in an effort to deduce any behavioral phenotype. An early study on ZrchI mice demonstrated a slight increase in locomotor activity during exploration of an unfamiliar environment (Roesler et al. 1999), but contradictory results have also been reported

(Coitinho et al. 2003; Rial et al. 2009). In addition, several studies described reduced anxiety in *Prnp* KO mice (Lobão-Soares et al. 2007; Rial et al. 2009; Schmitz et al. 2014), particularly after acute stress such as foot shock or forced swimming (Nico et al. 2005). Moreover, a depressive-like behavior was described during forced swimming and tail suspension tests in animals that lack PrP^C (Gadotti et al. 2012). These findings propose that PrP^C may participate in the adaptation to stress, which could explain the increased aggressive actions in animals devoid of PrP^C (Büdefeld et al. 2014). More recently, deficits in nesting, basal anxiety, memory, and learning were observed in an age-dependent manner of *Prnp* KO mice (Schmitz et al. 2014). The authors of this study linked these findings to reduced neurofilament-phosphorylation in KO mice that resulted in impaired organization of the cytoskeleton of hippocampal neurons.

Circadian rhythm

One of the first phenotypes described in *Prnp* KO mice (ZrchI and Edbg) indicated that PrP^C regulated the circadian rhythm and sleep patterns (Tobler et al. 1996). In PrP^C-deficient mice, there was an increase in slow wave activity following sleep deprivation (Huber et al. 1999), which possibly reflects that PrP^C has a role in neurotransmission (Huber et al. 2002). Another explanation could be that PrP^C is involved in the homeostasis of hormones; indeed, dysregulated serum levels of melatonin were reported in ZrchI and Edbg mice (Brown et al. 2002). Melatonin is a key regulator of the circadian rhythm and sleep cycle, and lower melatonin levels during the dark phase could explain sleep disruption in *Prnp* KO mice. Later, a PrP^C-dependent regulation of hormones produced by the hypothalamic-pituitary-adrenal axis was linked to alterations in the circadian rhythm (Sánchez-Alavez et al. 2007). Strikingly, sleep deficits are a major clinical phenotype in the human prion disorders fatal familial insomnia (Medori et al. 1992) and Creuzfeldt-Jakob disease (Landolt et al. 2006). Regardless of these observations, there is still no consensus as to how PrP^C regulates sleep at the molecular level. Further studies, including research on goats devoid of PrP^C, are ongoing (M. A. Tranulis, personal communication).

Memory and cognition

Studies have shown that PrP^C is highly expressed in the hippocampus, a brain region that is important for learning, spatial navigation, and the consolidation of short-term memory to long-term memory. Several studies reported impaired memory and cognitive deficits in *Prnp* KO mice (Manson et al. 1995; Coitinho et al. 2003) and that the phenotypes could be rescued by reintroducing PrP^C (Whittington et al. 1995; Criado et al. 2005). Conflicting results, however, have been found (Lledo et al. 1996; Büeler et al. 1992; Lipp et al. 1998), and a definitive role of PrP^C in memory remains to be resolved. In humans, a single polymorphism (Val129) in the *PRNP* gene has been associated with early cognitive decline (Croes et al. 2003) and reduced cognitive performance in elderly patients (Berr et al. 1998). Conversely, humans carrying Met129 displayed better long-term memory than those with Val129 (Papassotiropoulos et al. 2005), which could mean that polymorphisms at codon 129 are related to cognitive performance.

A role for PrP^C in the peripheral nervous system

More recently, a widespread late adult-onset demyelination of the peripheral nervous system (PNS) was discovered in animals without PrP^C. The phenotype has been reported in both ZrchI and Edbg mice (Bremer et al. 2010) in addition to the newly generated ZrchIII line (Nuvolone et al. 2016). The demyelination is morphologically characterized by reduced axonal density with infiltration of macrophages and functionally by deficits in afferent and efferent signal transduction. A series of experiments showed that normal cleavage of neuronal PrP^C was important in myelin maintenance, and an interaction with Schwann cell receptors was indicated (Bremer et al. 2010). Later, Küffer and colleagues demonstrated that PrP^C probably promotes myelin maintenance by activating the G-coupled receptor 126 (GPR126) on the surface of Schwann cells. Residues 23-33 of the N-terminal domain reportedly bind GPR126 and induce signaling through the cyclic adenosine monophosphate (cAMP)-dependent PKA-pathway (Küffer et al. 2016). The authors also suggested that GPR126-dependent myelin maintenance in young *Prnp* KO mice was compensated for by type IV collagen or laminin (Paavola et al. 2014; Petersen et al. 2015). This observation may explain why the phenotype is only manifested in adults.

PrP^C, the immune system and inflammation

Most immunological research on PrP^C has been focused on pathogenic or therapeutic features, and studies on *Prnp*-ablated mice have not identified a definite role of PrP^C in the immune system. Early studies displayed no gross defects in the number or maturation of the different compartments of the immune system (Reviewed in Isaacs et al. 2006). Later, fine-tuned regulations were identified in *Prnp* KO mice, which suggest that functions of PrP^C in the immune system are subtle or may only be critical under certain circumstances. Recent work has proposed a role for PrP^C in immunological quiescence and encouraged further inflammatory studies in PrP^C-deficient animals (Bakkebø et al. 2015).

Expression of PrP^C on immune cells

The cellular PrP is expressed by hematopoietic stem cells in the bone marrow and is important for their self-renewal under stressful conditions (Zhang et al. 2006). Levels of PrP^C are dynamically altered during hematopoietic differentiation (Dodelet et al. 1998), which implies a possible role of PrP^C in the development of these cells. In human immune cells, PrP^C is expressed on monocytes, lymphocytes, neutrophils, platelets, and red blood cells, albeit at varying levels (Dürig et al. 2000; Holada et al. 2000; Haddon et al. 2009; Barclay et al. 2002). Importantly, there are species differences of PrP^C expression on blood cell types (Barclay et al. 2002; Holada et al. 2000). In sheep and goats, several studies demonstrate a lack of cell surface PrP^C in granulocytes, whereas most PrP^C is limited to peripheral blood mononuclear cells (PBMCs) (Halliday et al. 2005; Reiten et al. 2015; Dassanayake et al. 2012). Early work proposed that PrP^C participates in the differentiation and activation of T-cells (Mabbott et al. 1997; Bainbridge et al. 2005) and knockdown of PrP^C resulted in T-cells developing a more pro-inflammatory phenotype (Hu et al. 2010). On the other hand, no abnormalities in T-cell proliferation rates were observed in goats without PrP^C (Reiten et al. 2015), and a definite role for PrP^C in activating T-cells remains elusive. In murine neutrophils, upregulation of PrP^C depended on the serum levels of TGF-β and glucocorticoids, which again are reliant on the activation of the hypothalamic-pituitary-adrenal axis (Mariante et al. 2012). These data indicate a novel interplay between PrP^C in neutrophils and the regulation of the neuro-immuno-endocrine system, which exemplifies the intricate role of PrP^C in physiological responses.

PrP^C and inflammation

Inflammation is a complex biological response of body tissues to invading pathogens or harmful stimuli, such as injury or irritants. Hallmarks of acute inflammation include pain, swelling, heat, redness, and loss of function. Key events in this process at the cellular level are infiltration of leukocytes, phagocytosis of microbes or debris, and synthesis of inflammatory mediators that facilitate the immune response. A balanced inflammatory response should eliminate the initial cause of cell injury, remove necrotic cells, and initiate tissue repair (Ashley et al. 2012). A commonly used model for acute inflammation is zymozan-induced acute inflammatory peritonitis. After such challenge, fewer neutrophils and an increased number of monocytes were recruited to the peritoneum of *Prnp* KO mice (de Almeida et al. 2005). Similarly, *Prnp* KO mice demonstrated reduced leukocyte infiltration in the bronchoalveolar fluid after intratracheal instillation of silica (Linden et al. 2008). When exposed to systemic lipopolysaccharide (LPS), peripheral leukocyte counts were higher in *Prnp* KO mice than in wild types. This finding indicates that fewer peripheral blood leukocytes were recruited in *Prnp* KO mice (Liu et al. 2014). In the same study, the regulation of pro- and anti-inflammatory cytokines in the brain and spleen differed between the groups, and a dramatically increased mortality rate was observed in *Prnp* KO mice, which proposes that PrP^C had a protective role after bacterial LPS challenge (Liu et al. 2014). An altered cytokine profile between groups including mice overexpressing PrP^C, KO mice, and wild type mice was also observed in experimentally induced colitis, which demonstrates a cytoprotective function of PrP^C (Martin et al. 2011). In several neuroinflammatory conditions, loss of PrP^C exacerbates the disease progression (Tsutsui et al. 2008; Gourdain et al. 2012; Nasu-Nishimura et al. 2008). Mice that overexpress PrP^C displayed an additional reduced inflammation, which suggests that PrP^C protects against experimental autoimmune encephalomyelitis (Gourdain et al. 2012).

Taken together, PrP^C may play important roles in the development and maintenance of the immune system. While PrP^C appears to be upregulated upon neutrophil and T-cell activation, expression is not a criterion for T-cell proliferation. Several studies indicate that PrP^C is involved in the recruitment of leukocytes to sites of inflammation and participates in the complex regulation of pro- and anti-inflammatory mediators.

PrP^C and metal homeostasis

The ability of the octapeptide domain of PrP^C to bind divalent metal ions, and importantly copper, has been recognized for decades (Hornshaw et al. 1995; Brown et al. 1997a). Early work by Pauly and colleagues described copper-stimulated endocytosis of PrP^C from the plasma membrane in neuroblastoma cells (Pauly et al. 1998). Later, the PrP^C-Cu^{2+}-interaction was linked to protection against oxidative stress (Watt et al. 2007; Rachidi et al. 2003), uptake of glutamate in astrocytes (Brown et al. 1999a), and regulation of the NMDA receptor (Gasperini et al. 2015), among others. In addition, copper binds the non-octapeptide region of PrP^C and possibly regulates conversion into the pathological form PrP^{Sc} (Giachin et al. 2015). Zinc may also bind the octapeptide region, albeit at a lower affinity than copper, and mediate endocytosis of PrP^C (Perera et al. 2001; Walter et al. 2007; Jackson et al. 2001). In neuronal cells, PrP^C facilitated zinc uptake through interaction with the glutamate receptor AMPA, a process dependent on zinc directly binding PrP^C (Watt et al. 2012). The interactions between PrP^C and both Cu^{2+} and Zn^{2+} have been linked to α-cleavage (McDonald et al. 2014) and β-cleavage (Watt et al. 2005) of the protein, which indicate a physiological relevance of these interactions.

As first identified in neuroblastoma cells, PrP^C appears to facilitate iron transport and uptake into cells (Singh et al. 2009c) by acting as a ferrireductase (Singh et al. 2013; Haldar et al. 2015). Consequently, *Prnp* KO mice displayed a phenotype of iron deficiency in the brain, spleen, and liver, which was reflected in altered hematological parameters and reduced serum iron (Singh et al. 2009b). The latter, however, could not be reproduced in goats without PrP^C (Reiten et al. 2015), and the significance of this interaction remains unclear.

To date, the *in vivo* physiological role of PrP^C in the homeostasis of copper and zinc is not entirely understood, but the high conservation of the metal-binding octapeptide region across mammalian and avian species suggests that it might be important. Notably, levels of copper, zinc, and iron may be altered during prion disease (Wong et al. 2001a; Singh et al. 2009a), which could potentially reflect a loss-of PrP^C function.

Selected PrP^C ligands and interacting partners

One approach to understand the function of PrP^C is to identify molecules that either bind or interact with the protein. As it is located at the plasma membrane, it has been proposed that PrP^C is involved in transmembrane signaling by binding to ligands and that the protein serves as a platform for different signaling molecules (Reviewed in Linden 2017).

The laminin receptor (LR) was originally identified as a binding protein for laminin, which is an extracellular glycoprotein that provides cellular adhesion to the basement membrane. Research has revealed that the LR acts as a receptor for PrP^C on the plasma membrane of mammalian cells, thus facilitating internalization of PrP^C through clathrin-coated pits (Rieger et al. 1997; Gauczynski et al. 2001). Moreover, PrP^C may act as a high-affinity receptor for laminin. The binding of laminin to PrP^C was found to induce neurogenesis in hippocampal neurons (Graner et al. 2000) and modulate memory consolidation in the rat brain (Coitinho et al. 2006), which suggests that PrP^C plays a role in neuronal plasticity. Because PrP^C lacks an intracellular domain, a co-receptor is likely necessary to mediate signal transduction. Several proteins that interact with PrP^C have been identified, such as neural cell adhesion molecule 1 and metabotropic glutamate receptors, which mediate neurite outgrowth (Santuccione et al. 2005; Beraldo et al. 2011). Additionally, PrP^C interacts with several extracellular matrix proteins (Hajj et al. 2007), cell junction proteins (Besnier et al. 2015), and cytoskeletal proteins (Zafar et al. 2011). Other putative binding partners, such as GPR126, STI1, metal ions, and the AMPA receptor, have been mentioned in previous sections. Although a variety of interacting partners have been identified, functional studies should be performed to consider their biological relevance (Wulf et al. 2017).

In the pathogenesis of Alzheimer's disease (AD), β-secretase 1 cleaves the amyloid precursor protein resulting in a fragment called sAPPβ, which is further processed into amyloid beta peptides (Aβ). The cortical plaques of AD brains largely consist of Aβ. It has been suggested that PrP^C can interact with β-secretase 1 and inhibit the production of Aβ, thereby protecting against AD (Parkin et al. 2007). Conflicting results have been reported, and overexpression of PrP^C increased amyloid precursor protein cleavage (McHugh et al. 2012). Moreover, genetic removal of PrP^C in a mouse model expressing human amyloid precursor protein did not affect the processing or levels of Aβ (Whitehouse et al. 2016).

Prion diseases

Prion diseases are a family of invariably fatal neurodegenerative disorders that occur in humans and a range of animals (Table 1). The disorders may be inherited, spontaneous (possibly somatic *PRNP* mutations), or infectious. According to the "protein-only" hypothesis, the host-encoded PrP^{C} is converted into a pathological form (PrP^{Sc}) (Prusiner 1982). Prions act as templates generating aggregates of misfolded PrP^{Sc}. The diseases are characterized by neurodegenerative changes, primarily vacuolization and gliosis, and accumulation of PrP^{Sc} in the CNS and to a lesser extent in peripheral tissues (Collinge 2016). A protein as a transmissible agent stands in contrast to all other known infectious agents including bacteria, viruses, parasites, and fungi, all of which contain nucleic acids. Although PrP^{Sc} constitutes the infectious component of the disease, prion diseases are entirely dependent on endogenous PrP^{C} expression. This criterion has been repeatedly confirmed by PrP^{Sc} inoculation of *Prnp* KO animals, which are unable to replicate prions and are resistant to prion diseases (Büeler et al. 1993; Prusiner et al. 1993).

Table 1. Prion diseases and etiology

Host	Disease	Etiology
Human	Creutzfeldt-Jakob disease	Spontaneous
	Variant Creutzfeldt-Jakob disease	Infectious, BSE-contaminated food
	Iatrogenic Creutzfeldt-Jakob disease	Surgical and medical treatments
	Kuru	Infectious, cannibalism (eradicated)
	Familial Creutzfeldt-Jakob disease	Germline *PRNP* mutation
	Fatal familial insomnia	Germline *PRNP* mutation
	Gerstmann-Sträussler-Schenker Syndrome	Germline *PRNP* mutation
Sheep and goat	Classical scrapie	Infectious
	Atypical scrapie (Nor98)	Spontaneous
Cattle	Classical bovine spongiform encephalopathy	Infectious
	Atypical bovine spongiform encephalopathy (H-type and L-type)	Spontaneous
Cervids	Chronic wasting disease	Infectious
Cat	Feline spongiform encephalopathy	Infectious, BSE-contaminated food
Mink	Transmissible mink encephalopathy	Infectious, unknown source

The primary route of infection is uptake of prions via the alimentary tract. However, transmission via gums, skin, and conjunctiva or iatrogenic via blood transfusion, intramuscular injections, and surgical procedures are also possible (Houston et al. 2000; Hunter et al. 2002; Buchanan et al. 1991; Thomzig et al. 2007). Secretion of PrP^{Sc} into the environment occurs primarily via feces and body fluids, such as amniotic fluid, milk, saliva, and urine (Lacroux et al. 2007; Lacroux et al. 2008; Gough et al. 2010). Prions bind strongly to soil and can probably persist in the environment for years (Brown et al. 1991) or even longer indoors (Georgsson et al. 2006). As shown in Figure 3, low levels of PrP^{Sc} can be absorbed from the soil and transported to plant leaves, yet the infectivity of this route needs further clarification (Pritzkow et al. 2015).

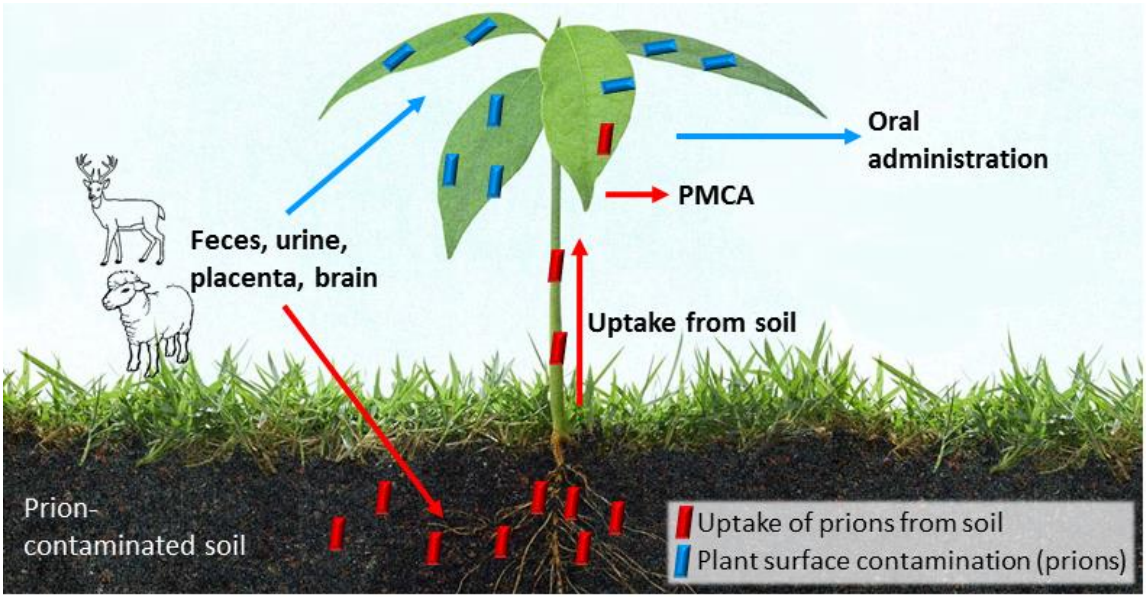

Figure 3. Transmission of prions via soil and plants. Prions can be detected by protein misfolding cyclic amplification (PMCA) in plants grown in prion-contaminated soil. Oral administration of plants with prion surface contamination caused prion disease in hamsters. Modified from (Pritzkow et al. 2015; Creative Commons License).

The exact mechanism by which PrP^{Sc} induces neurodegeneration is currently not known. Initially, the co-occurrence of PrP^{Sc} accumulation and spongiform changes in the brain led scientists to believe that PrP^{Sc} might have toxic effects itself (Forloni et al. 1993). Several studies have proposed that low molecular weight PrP^{Sc} oligomers possess neurotoxic functions (Masel et al. 2005; Kazlauskaite et al. 2005). Another theory suggests that a neurotoxic signal is triggered through PrP^{C} (Brandner et al. 1996). Depletion of neuronal PrP^{C} late in the preclinical phase (Cre-Lox recombination) reversed spongiform changes

and avoided clinical disease, despite continuous accumulation of PrP^{Sc} from non-neuronal cells (Mallucci et al. 2003). Conversely, in a different mouse-model with only PrP^{C} expression of astrocytes, neurodegeneration was evident at the ultrastructural level, and the mice developed clinical disease (Jeffrey et al. 2004). The authors postulated that neurotoxicity could be mediated by the prions or other factors released from astrocytes. Because levels of PrP^{C} decrease when it is misfolded into PrP^{Sc}, it has also been hypothesized that loss of the normal function of PrP^{C} is a participating factor in the early disease development (Hetz et al. 2003). As previously described, a range of neuroprotective functions have been attributed PrP^{C}, such as protection against oxidative stress and regulation of apoptosis (Steele et al. 2009). A similar hypothesis proposes that PrP^{Sc} modifies (or subverts) the normal cytoprotective function of PrP^{C}, thus triggering neurotoxic signaling (Harris et al. 2006). In conclusion, the diversity of prion disorders in regard to histopathology and phenotype suggests that the neurodegenerative changes are potentially triggered by a combination of mechanisms. The toxic effects are perhaps not only related to PrP^{C} and the pathological isoform, but also to imbalances in physiological homeostasis. In the case of prolonged stress, as seen in prion disorders, activated immune cells and repair mechanisms might gradually be overwhelmed, which can escalate into pro-inflammatory and toxic signaling (Jalland 2017).

The occurrence of scrapie in small ruminants, variant Creutzfeldt-Jakob disease in humans, and to some extent chronic wasting disease in deer, is strongly influenced by polymorphisms in the *PRNP* gene. Some polymorphisms can increase the risk of developing diseases, while others may prolong the incubation period or even confer resistance. In goats, a variety of mutations have been described including silent mutations, a three-octapeptide-repeat variant, and the nonsense mutation described in this thesis (Goldmann et al. 1998; Fragkiadaki et al. 2011; Benestad et al. 2012). In natural outbreaks of caprine classical scrapie, the H/R_{143}, R/H_{154}, and R/Q_{211} polymorphisms have been associated with a decrease in disease susceptibility (Bouzalas et al. 2010; Billinis et al. 2002; Barillet et al. 2009). Similarly, the Q/K_{222} polymorphism is associated with a marked resistance towards scrapie (Aguilar-Calvo et al. 2014; Acutis et al. 2012). In sheep, particularly polymorphisms in codon 136, 154 and 171 are important for the susceptibility to classical scrapie (Tranulis 2002).

Lipopolysaccharide in experimental models

Bacterial LPS, or endotoxins, are part of the outer cell membrane complex of most Gram-negative bacteria, and they are potent stimulators of the innate immune response. In contrast to exotoxins secreted by bacteria into the surroundings, endotoxins are only released after destruction of the bacterial cell wall. Traditionally, purified LPS has been used to study the inflammatory response by mimicking sepsis, along with *in vitro* studies of LPS-stimulated cells (Alexander et al. 2001). A variety of other applications exist, including studies of major depression disorder (MDD). Since the behavioral response to LPS has striking similarities with depressive behavior, it has been proposed that cytokines released in response to LPS participate in the development of MDD in humans (Schiepers et al. 2005; Hickie et al. 1995). Indeed, MDD patients had higher levels of antibodies against the LPS of enterobacteria than normal volunteers. This observation could be caused by intestinal mucosal dysfunction resulting in increased translocation of Gram-negative bacteria into the blood stream, followed by subsequent release of low levels of LPS (Maes et al. 2008).

LPS structure

Bacterial LPS consists of a highly conserved lipid component (Lipid A), which exerts the endotoxic activity. Lipid A is linked by a core oligosaccharide to a polysaccharide chain, known as the O-antigen (Figure 4). The O-antigen, which projects from the cell surface, differs between species and is responsible for the serological specificity of bacteria.

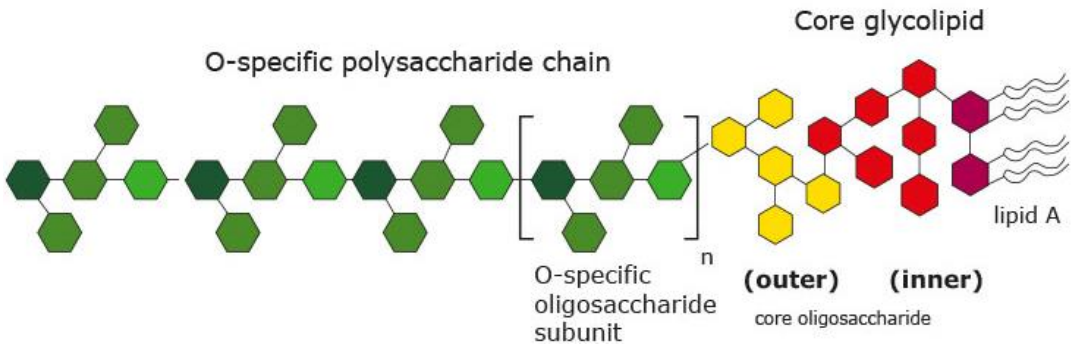

Figure 4. Schematic presentation of the lipopolysaccharide structure. Reproduced with permission from Biomin®.

LPS receptor complex and signaling pathways

Endotoxins elicit a broad spectrum of biological effects that are key events in the defense against Gram-negative bacteria. In mammals, professional phagocytes are the primary target cells involved in protection against LPS. However, a range of other cell types express the toll-like receptor 4 (TLR4) complex that is essential for the defense against endotoxins (Vaure et al. 2014).

The first protein involved in the recognition of LPS is the LPS binding protein (LBP). This protein is a soluble acute phase protein (APP) produced mainly by hepatocytes, and LBP circulates at low levels in the blood stream (Schumann et al. 1990). After endotoxin challenge, LPB is rapidly upregulated and acts as a shuttle protein that opsonizes LPS and catalyzes the delivery to the co-receptor CD14 (Hailman et al. 1994). Moreover, CD14 facilitates the transfer of LPS to the heterodimer that consists of myeloid differentiation factor 2 (MD2) and TLR4. Upon stimulation, the LBP-CD14-MD2-TLR4 complex undergoes dimerization, and induction of the signaling machinery is initiated (Park et al. 2009).

As seen in Figure 5, TLR4 signaling can be divided into the early phase MyD88-dependent pathway and the late phase TRIF-dependent pathway. In the MyD88-dependent pathway, TIRAP facilitates the association between MyD88 and the cytoplasmic domain of TLR4 to initiate downstream signaling (Kagan et al. 2006). Upon stimulation, IRAK 1/4 is recruited, which leads to activation of TRAF6 and TAK1 (Lye et al. 2008; Kim et al. 2007). Furthermore, TAK1 activates the IKK complex and MAPK, which are responsible for phosphorylation of various transcription factors (NFκB, AP-1). Activated transcription factors are translocated to the nucleus where they induce transcription of pro-inflammatory cytokines (e.g., TNF-α, IL-1β, IL-6) and enzymes (e.g., iNOS and COX2) (Sato et al. 2005; Chang et al. 2001). In the TRIF-dependent pathway, TRIF associates with the adaptor molecule TRAM, thus resulting in the activation of IRF3 and transcription of type I interferons (Yamamoto et al. 2003). Notably, macrophages from mice that are deficient in both MyD88 and TRIF showed a complete loss of NFκB activation after LPS challenge, which demonstrates the essential role of both of these pathways in the endotoxin defense (Yamamoto et al. 2003).

The secreted type I interferons, primarily INF-β, may act on nearby cells or by autocrine signaling on the same cell. Type I interferons bind to a common receptor (IFNAR) and activate JAK1 and TYK2, which phosphorylate latent cytoplasmic transcription factors STAT1 and STAT2. Finally, STAT1/2 assembles with IRF9 to form the ISGF3 complex, which translocates to the nucleus and activates transcription of interferon-stimulated genes (ISGs) (Ivashkiv et al. 2014).

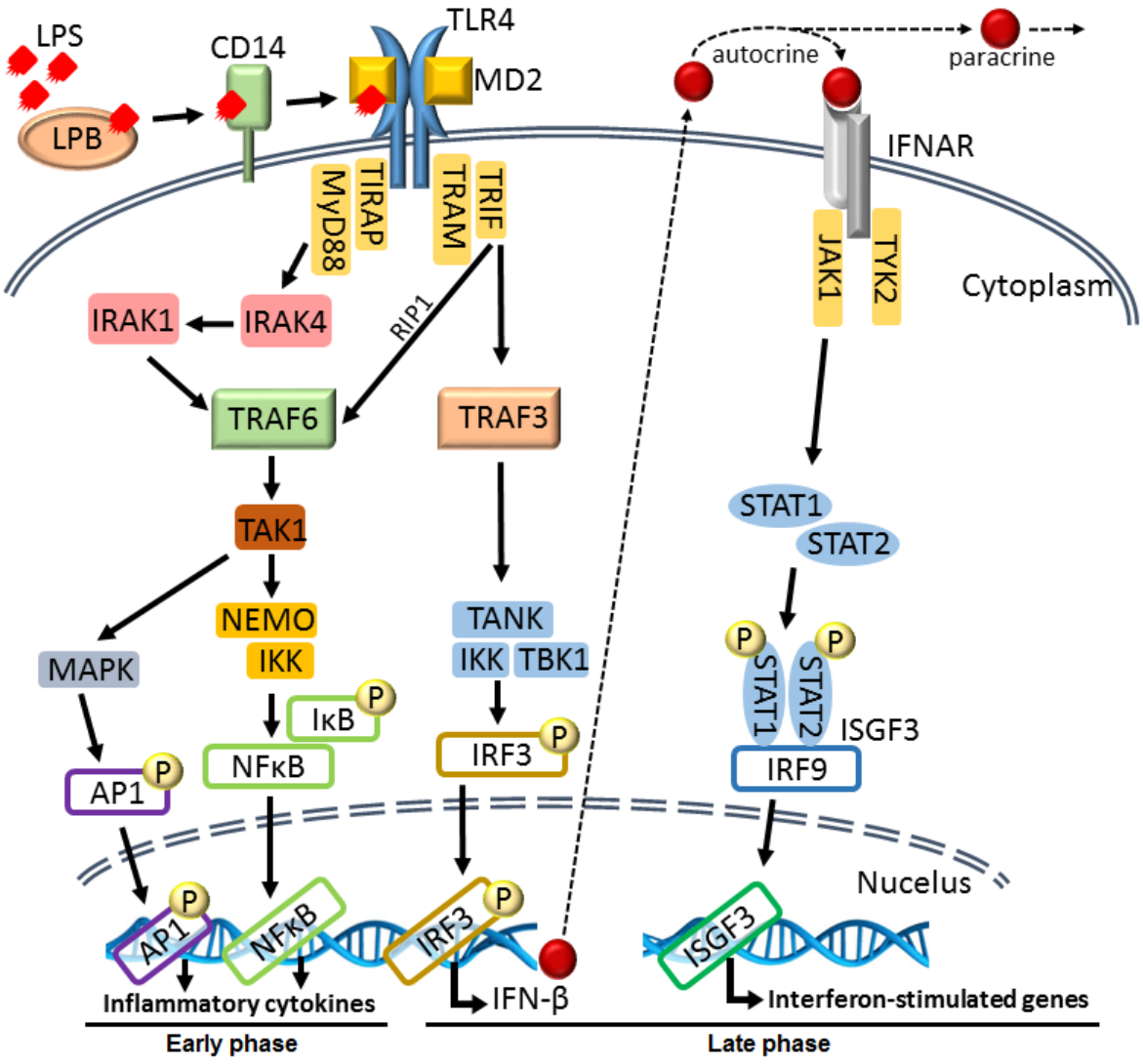

Figure 5. Simplified presentation of the LPS-TLR4 signaling pathway and interactions with interferon signaling. Abbreviations: CD14, cluster of differentiation 14; MyD88, myeloid differentiation marker 88; TIRAP, TIR domain-containing adaptor protein; TRIF, TIR-containing adapter molecule; TRAM, TRIF-related adapter molecule; IRAK, interleukin-1 receptor-associated kinase; TRAF, tumor necrosis factor receptor-associated factor; TAK, transforming growth factor-β-activated kinase; MAPK, mitogen-activated protein kinase; NEMO, NFκB essential modulator; IKK, IκB kinase; AP1, activator protein 1, NFκB, nuclear factor-κB; IRF, interferon response factor; RIP, receptor interacting protein; JAK1, janus kinase 1; TYK2, tyrosine kinase 2; STAT, signal transducer and activator of transcription; ISGF3, interferon stimulated gene factor-3; IFN, interferon.

Physiological and pathological effects of LPS

As described above, the TLR4-signaling cascade culminates in the release of pro-inflammatory cytokines, chemokines, and enzymes. The ensuing physiological response comprises the interaction between the immune, neuroendocrine, and autonomic nervous system. Endotoxins mimic the consequences of sepsis, including fever caused by elevation of the thermoregulatory set point, leukopenia due to diapedesis, glucocorticoid release in response to activation of the hypothalamic-pituitary-adrenal axis, and modulation of CNS centers that control behavioral parameters associated with locomotor activity, thirst, appetite and social interaction. This behavioral state is referred to as sickness behavior and typically develops during the course of an infection (Dantzer 2009).

In normal immunoreactions, low and balanced levels of the inflammatory mediators lead to activation of antimicrobial, antiviral, and antitumoral defense mechanisms (Figure 6). However, under dysregulated and unbalanced levels, higher levels of these mediators, particularly TNF-α, IL-1 and IL-6, may evoke more dramatic or even life-threatening effects, as observed in septic shock (Annane et al. 2005). Such effects can involve vasodilatation, diminished myocardial contractility, and widespread endothelial injury that activates the coagulation system and causes disseminated intravascular coagulation (DIC). Unless treated, the combination of DIC, heart failure, and widespread vasodilation culminates in hypoperfusion of vital organs and multiorgan system failure, which usually is fatal (Thiemermann et al. 1995).

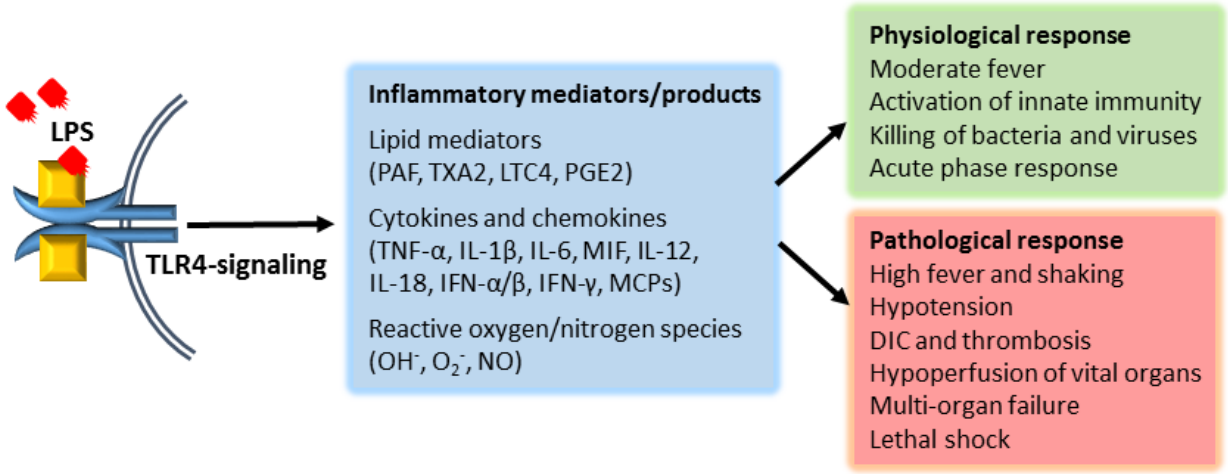

Figure 6. Overview of physiological and pathological effects of LPS. Abbreviations: PAF, platelet-activating factor; TXA2, thromboxane A2; LTC4, leukotriene C4; PGE2, prostaglandin E2; MIF, macrophage migration inhibitory factor; MCP, membrane cofactor protein.

Norwegian dairy goats devoid of prion protein

In 2012, Norwegian researchers discovered a nonsense mutation early in the *PRNP* gene of Norwegian dairy goats (Benestad et al. 2012). The mutation in codon 32 creates a stop signal, thus terminating the translation of PrP^C and leaving only seven amino acids of the mature protein (Figure 7). Homozygous goats that carry the mutation on both chromosomes ($PRNP^{Ter/Ter}$) are devoid of PrP^C and supposedly resistant to scrapie. An inoculation study of Norwegian dairy goats with different *PRNP* genotypes is ongoing (C. Ersdal; personal communication). Goats that are heterozygous for the mutation ($PRNP^{+/Ter}$) display half the amount of PrP^C on the cell surface of peripheral blood mononuclear cells (PBMCs) (Reiten et al. 2015), which suggests that no compensatory expression from the normal allele is present. An initial genetic survey revealed an allele frequency of about 11 % and comprised samples (*n* = 192) from several unrelated flocks (Benestad et al. 2012). A later investigation of Norwegian goat bucks (*n* = 1984) detected an allele frequency of 5.8 %, with 10.9 % of the goats being carriers of the Ter-mutation (M. A. Tranulis; personal communication).

To the best of our knowledge, this is the first report of naturally-occurring PrP^C-deficient animals. The use of a non-transgenic, small ruminant model provides new opportunities for the study of PrP^C physiology. Goats have a longer life expectancy than laboratory rodents and serve as a natural host for prion diseases. They are housed under natural environmental conditions, which contribute to normal development of the immune system. The latter strengthens their suitability as a model to study PrP^C and prion diseases, but also adds complexities, which complicates the analysis of subtle phenotypes.

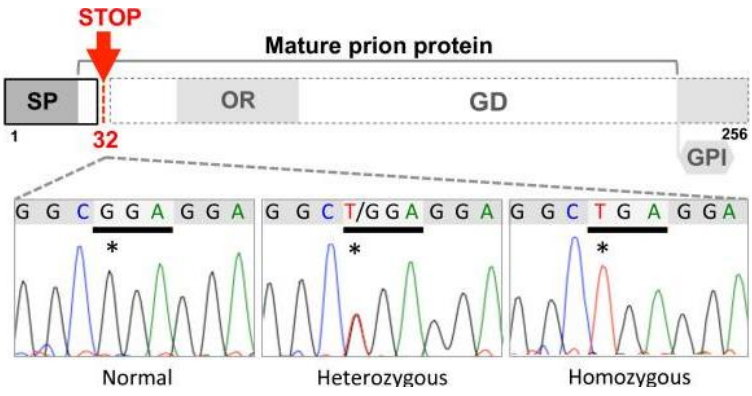

Figure 7. Graphical overview of the prion protein structure and stop mutation in Norwegian dairy goats. Reproduced from (Benestad et al. 2012; Creative Commons License).

Aims of the thesis

The main aim of this doctoral work was to search for loss-of-function phenotypes in goats naturally devoid of PrP^C during acute inflammatory stress. We performed a systemic LPS challenge and asked whether PrP^C influences:

- Clinical and behavioral responses
- Hematological and biochemical parameters
- Expression of leukocyte innate immune genes
- Transcriptome responses in the brain and peripheral tissues
- Morphological alterations in the brain and peripheral tissues

In addition, we aimed to increase the current knowledge of the innate immune response in goats. To obtain this, we characterized the transcriptome and histopathological response to endotoxins in normal goats (*PRNP*$^{+/+}$).

A parallel study was designed to investigate whether loss of PrP^C affects the transcriptome of peripheral blood mononuclear cells.

Summary of papers

Paper I

Activation of innate immune genes in caprine blood leukocytes after systemic endotoxin challenge

Background: Sepsis is a serious health problem associated with a range of infectious diseases in animals and humans. Early events of this syndrome can be mimicked by experimental administration of lipopolysaccharides (LPS). Compared with mice, small ruminants and humans are highly sensitive to LPS, making goats valuable in inflammatory models. We performed a longitudinal study in eight Norwegian dairy goats that received LPS (0.1 µg/kg, *Escherichia coli* O26:B6) intravenously. A control group of five goats received corresponding volumes of sterile saline. Clinical examinations were performed continuously, and blood samples were collected throughout the trial.

Results: Characteristic signs of acute sepsis, such as sickness behavior, fever, and leukopenia appeared within 1 hour of LPS administration. A high-throughput longitudinal gene expression analysis of circulating leukocytes was performed, and genes associated with the acute phase response, type I interferon signaling, LPS cascade, and apoptosis, in addition to cytokines and chemokines were targeted. Pro-inflammatory genes, such as IL1B, CCL3, and IL8, were significantly upregulated. Interestingly, increased mRNA levels of seven interferon stimulated genes (ISGs) were observed peaking at 2 hours, corroborating the increasing evidence that ISGs respond immediately to bacterial endotoxins. A slower response was manifested by four extrahepatic acute phase proteins (APP) (*SAA3*, *HP*, *LF,* and *LCN2*) reaching maximum levels at 5 hours.

Conclusions: We report an immediate induction of ISGs in leukocytes in response to LPS supporting a link between the interferon system and defense against bacterial infections. The extrahepatic expression of APPs suggests that leukocytes contribute to synthesis of these proteins at the beginning of a systemic inflammation. Taken together, these findings provide insights into the dynamic regulation of innate immune genes, as well as raising new questions regarding the importance of ISGs and extrahepatic APPs in leukocytes after systemic endotoxin challenge.

Paper II

Loss of prion protein induces a primed state of type I interferon-responsive genes

The cellular prion protein (PrP^C) has been extensively studied because of its pivotal role in prion diseases; however, its functions remain incompletely understood. A unique line of goats has been identified that carries a nonsense mutation that abolishes synthesis of PrP^C. In these animals, the PrP^C-encoding mRNA is rapidly degraded. Goats without PrP^C are valuable in re-addressing loss-of-function phenotypes observed in *Prnp* knockout mice. As PrP^C has been ascribed various roles in immune cells, we analyzed transcriptomic responses to loss of PrP^C in peripheral blood mononuclear cells (PBMCs) from normal goat kids (n = 8, $PRNP^{+/+}$) and goat kids without PrP^C (n = 8, $PRNP^{Ter/Ter}$) by mRNA sequencing. PBMCs normally express moderate levels of PrP^C.

The vast majority of genes were similarly expressed in the two groups. However, a curated list of 86 differentially expressed genes delineated the two genotypes. About 70 % of these were classified as interferon-responsive genes. In goats without PrP^C, the majority of type I interferon-responsive genes were in a primed, modestly upregulated state, with fold changes ranging from 1.4 to 3.7. Among these were *ISG15*, *DDX58* (RIG-1), *MX1*, *MX2*, *OAS1*, *OAS2,* and *DRAM1*, all of which have important roles in pathogen defense, cell proliferation, apoptosis, immunomodulation, and DNA damage response.

Our data suggest that PrP^C contributes to the fine-tuning of resting state PBMCs expression level of type I interferon-responsive genes. The molecular mechanism by which this is achieved will be an important topic for further research into PrP^C physiology.

Paper III

LPS-induced systemic inflammation reveals an immunomodulatory role for the prion protein at the blood-brain interface

Background: The cellular prion protein (PrP^C) is an evolutionary conserved protein abundantly expressed in the central nervous system, but also peripherally including the immune system. A line of Norwegian dairy goats naturally devoid of PrP^C (*PRNP*$^{Ter/Ter}$) provides a novel model for studying PrP^C physiology.

Methods: In order to explore putative roles for PrP^C in acute inflammatory responses, we performed a lipopolysaccharide (LPS, *Escherichia coli* O26:B6) challenge of 16 goats (8 *PRNP*$^{+/+}$ and 8 *PRNP*$^{Ter/Ter}$) and included 10 saline-treated controls (5 of each *PRNP* genotype). Clinical examinations were performed continuously, and blood samples were collected throughout the trial. Genome-wide transcription profiles of the choroid plexus, which is at the blood-brain interface, and the hippocampus were analyzed by RNA sequencing, and the same tissues were histologically evaluated.

Results: All LPS-treated goats displayed clinical signs of sickness behavior, which were of significantly ($p < 0.01$) longer duration in animals without PrP^C. In the choroid plexus, a substantial alteration of the transcriptome and activation of Iba1-positive cells were observed. This response included genotype dependent differential expression of several genes associated with the immune response, such as *ISG15*, *CXCL12*, *CXCL14,* and acute phase proteins, among others. Activation of cytokine-responsive genes was skewed towards a more profound type I interferon response, and a less obvious type II response, in PrP^C-deficient goats. The magnitude of gene expression in response to LPS was smaller in the hippocampus than in the choroid plexus. Resting state expression profiles revealed a few differences between the *PRNP* genotypes.

Conclusion: Our data suggest that PrP^C act as a modulator of innate immunity signaling, particularly downstream of interferons, and probably contributes to protection of vulnerable tissues against inflammatory damage.

Paper IV

PrP^C modulates pathways of inflammation during LPS-induced acute lung injury

Background: A naturally occurring mutation in the *PRNP* gene of Norwegian dairy goats terminates synthesis of the cellular prion protein (PrP^C), rendering homozygous goats ($PRNP^{Ter/Ter}$) devoid of the protein. Although extensively studied, the function of PrP^C during acute pulmonary inflammation has not been investigated earlier. We examined transcriptional and morphological alternations in the lungs after lipopolysaccharide (LPS) challenge of goats with and without PrP^C.

Methods: Acute pulmonary inflammation was induced by intravenous injection of LPS (*Escherichia coli* O26:B6) in 16 goats (8 $PRNP^{Ter/Ter}$ and 8 $PRNP^{+/+}$). A control group of 10 goats (5 $PRNP^{Ter/Ter}$ and 5 $PRNP^{+/+}$) received sterile saline. Clinical examinations included recordings of respiratory rate and signs of respiratory distress. A full necropsy was performed, and lung tissue was collected for RNA-seq and histopathological analysis.

Results: Systemic LPS challenge induced sepsis-like clinical signs including tachypnea and respiratory distress. A total of 432 ($PRNP^{+/+}$) and 596 ($PRNP^{Ter/Ter}$) genes were differentially expressed compared with the saline control of the matching genotype. When assigned to gene ontology categories, biological processes involved in remodeling of the extracellular matrix (ECM), were exclusively enriched in PrP^C-deficient goats. These genes included a range of collagen-encoding genes and proteases such as metalloproteinases (*MMP1*, *MMP2*, *MMP14, ADAM15*) and cathepsins. Several pro-inflammatory upstream regulators (TNF-α, IL1-β, IFN-γ, TGF-β) showed increased activation scores in goats devoid of PrP^C. Histological examination of lungs revealed multifocal areas with alveolar bleedings, edema, neutrophil infiltration, and higher numbers of alveolar macrophages, with no significant differences between *PRNP* genotypes.

Conclusion: LPS challenge induced marked alterations in the lung tissue transcriptome that corresponded with histopathological and clinical findings in both genotypes. In goats devoid of PrP^C, increased activation of upstream inflammatory regulators was present, and enrichment of ECM components indicated an augmented damage to the lung parenchyma. This suggests that PrP^C has a protective role during acute pulmonary inflammation, possibly by modulating inflammatory pathways.

Methodological considerations

In the present work, clinical and a variety of laboratory-based methods were used. The materials and methods are primarily described in papers I-IV, but some additional considerations are discussed in the following sections.

Animals

The Norwegian dairy goats included in this doctoral work were recruited from the research heard at the Norwegian University of Life Sciences at Ås. The entire research heard of about 100 winter-fed goats was previously *PRNP* genotyped, and goats that were homozygous for the stop-mutation ($PRNP^{Ter/Ter}$) or with a normal PrP^{C} gene ($PRNP^{+/+}$) were selected for the studies. Based on health surveillance through membership in the goat health monitoring service and the Norwegian Association of Sheep and Goat Farmers (Nagel-Alne et al. 2014), the general health status of the herd is considered very good. Housing conditions are representative of a Norwegian dairy goat farm. This factor is of relevance when studying the immune system, but it may also add complexity, especially compared to inbred mice that are housed in a pathogen-depleted environment. Four $PRNP^{+/+}$ goats were recruited from a local farmer. Goats included in the LPS study were transported to Sandnes and acclimatized for at least three weeks before the experiment.

At the research facilities, animals of both genotypes were housed together, fed the same feed, and handled by the same persons to avoid confounding environmental factors. Goats were age-matched within the experiments, and the sexes were equally distributed in the PBMC study (Paper II). One buck was excluded when analyzing transcriptomes in the LPS study, leaving only female goats (Papers III and IV). All included animals had no history of disease, and they were considered healthy based on clinical examinations and hematological and biochemical analysis during the acclimatization period. Gross pathology and histology did not reveal any signs of diseases, but half of the goats had minor areas of lungworm changes in the lungs. Lung tissues used in paper IV were collected away from these areas.

Genetic pitfalls – the flanking gene problem

A flanking gene problem means that nearby genes that flank the targeted locus might be responsible for phenotypic effects ascribed the null mutation (Crusio 2004). This linked region gradually decreases as crossing over occurs during homologous recombination. A few phenotypes first attributed to *Prnp* were later linked to flanking genes, such as the signal-regulatory protein-α gene (*Sirpa*, phagocytic ability) (Nuvolone et al. 2013). To date, the exact distribution of polymorphisms in genes linked to the mutation in Norwegian dairy goats remains to be determined. Preliminary analysis of single nucleotide polymorphisms (SNPs), however, indicates that homozygosity in both directions is relatively short (personal communication, Dag Inge Våge). In this line of goats, transcription of *SIRPA* was similar in the two genotypes of all analyzed tissues and increased synchronically upon LPS challenge. More than 15 SNPs were identified by RNA sequencing (RNA-seq) in the *SIRPA* gene. These appeared randomly distributed, which suggests that sufficient crossover occurred. Consequently, these findings indicate that polymorphisms in the *SIRPA* gene do not confound the phenotypes described in this thesis. In line with these results, both genotypes performed similarly in a phagocytosis assay (Reiten et al. 2015). Nevertheless, a full sequencing of the *PRNP* flanking region should be performed to identify potentially linked genes. Additional cross-validation of our results in cell-culture systems or *Prnp* KO mice would be of great interest in the future.

Ethical considerations

The animal experiments were performed in compliance with ethical guidelines and approved by the Norwegian Animal Research Authority with regard to the Norwegian regulation on animal experimentation (FOR-2015-06-18-761). The LPS study was classified as a procedure of moderate severity that causes short-term moderate pain, suffering, or distress. The three Rs (replace, reduce, refine) are guiding principles for ethical use of animals in research (Russell et al. 1959) and were implemented as follow. A replacement for the live animals was not possible since we aimed to study the *in vivo* role of PrP^C during acute inflammation. To reduce the number of animals and maximize the output information, we collected an extensive amount of material from the included animals. Such material involved clinical recordings and blood sampling (EDTA, whole blood, PAXgene RNA tubes) throughout the experimental period and a range of different tissues

for RNA analyses, histology, immunohistochemistry, and western blotting. In addition, we used powerful tools, such as RNA-seq, to obtain widespread data, and cell cultures replaced live animals in some follow-up studies. Finally, the experiment was refined by performing a pilot titration study to determine a proper dose-response relationship. Based on this, both the first and second dosages of LPS were reduced to avoid unnecessary distress and sensitization. Goats were also housed in social groups and given environmental enrichments during the experiment. Euthanasia was performed by an overdose of pentobarbital that was given rapidly intravenously, which leads to immediate loss of consciousness.

Methods

Table 2. Summary of methods used in this thesis

Method	Paper I	Paper II	Paper III	Paper IV
Clinical recordings	X		X	X
Hematology, flow cytometry	X		X	
Biochemistry	X		X	
Enzyme-linked immunosorbent assay (ELISA)	X			
RNA isolation	X	X	X	X
cDNA synthesis	X	X	X	X
Fluidigm Biomark HD	X	X		
LightCycler 480 qPCR	X	X	X	X
Illumina HiSeq 2000 transcriptome analysis		X	X	X
IFN-α stimulation of SH-SY5Y cells		X		
Western blotting		X		
Gross pathology				X
Histopathology			X	X
Immunohistochemistry			X	X
MSB staining				X

Experimental protocol - LPS challenge

We used purified LPS to stimulate the innate immune system and study PrP^C during acute systemic inflammation. One concern when comparing results derived from LPS studies is the highly variable sensitivity to LPS across different species. Compared with mice, goats and humans are remarkably sensitive to the effects of LPS. The dose of LPS (2-4 ng/kg) that induces clinical symptoms in humans (Talwar et al. 2006; Smith et al. 1994) is about 1 million times lower than the LD_{50} dose that is typically used in mice (1-25 mg/kg) (Reynolds et al. 2002). Therefore, the validity of extrapolating rodent inflammatory responses to human medicine has been debated (Seok et al. 2013). In goats, even a dose of 2 ng/kg induced mild fever and tachycardia in our pilot titration study (unpublished), which indicates a high sensitivity to LPS. Nevertheless, discrepancies between human and ruminant immunology also apply. Small ruminants are probably particularly sensitive to LPS due to the constitutive presence of pulmonary intravascular macrophages (Sone et al. 1999). In humans, these cells may only be induced under certain conditions (Dehring et al. 1989), and a direct extrapolation of pulmonary inflammation in small ruminants to human medicine should be performed with caution.

The physiological response to LPS also depends upon the bacterium and serotype from which it is derived. For instance, LPS from bacteria that have the O-chain with repeating disaccharides are less pyrogenic than LPS produced by colonies that lack the O-chain (Komuro et al. 1989). Similarly, LPS purified from three different types of *Escherichia coli* induced serotype-specific changes on body temperature in rats (Dogan et al. 2000). We selected the *E. coli* O26:B6 serotype because it elicits a reproducible pathophysiological response in goats (Takeuchi et al. 1997). Another technical issue is the potential of contamination from other bacterial products during the purification process (Tapping et al. 2000). Nevertheless, LPS is simple to administer, and the response is reproducible within experiments, as we also observed. Systemic administration of LPS is therefore considered a useful model to study early events of sepsis.

Gene expression studies

The study of gene expression represents a major contribution to the results obtained in the present thesis. Relative gene expression was examined by real-time qPCR (Papers I-IV) including the high throughput Fluidigm Biomark HD platform (Papers I and II). We also analyzed the full transcriptome of PBMCs and several tissues by RNA-seq (Papers II, III, and IV). Generally, changes in mRNA expression are considered reliable indicators of changes in protein levels, and thus they provide valuable information on biological systems (Koussounadis et al. 2015).

Extraction of RNA from leukocytes and tissues

In contrast to DNA, RNA is relatively unstable and rapidly degraded if not handled correctly. We used commercially available PAXgene Blood RNA tubes and RNAlater to stabilize and protect the integrity of RNA in blood leukocytes and tissue samples, respectively. To avoid degradation, tissue samples were collected within 15 minutes after euthanasia. Isolation of RNA was performed using PAXgene Blood RNA kits and RNeasy Lipid Tissue Mini kits from Qiagen. The integrity of extracted RNA was measured by the Bioanalyzer system in all individual samples to ensure high quality RNA for downstream analyses.

Upon LPS challenge, blood leukocytes migrated into tissues, which led to a dynamic change in the circulating leukocyte population throughout the experiment. Because the total population of blood leukocytes was considered to be one compartment, changes in cell population probably contribute to the regulation of some of the genes in paper I. Fortunately, the leukocyte cell composition was similar between *PRNP* genotypes, meaning that the comparison between genotypes was not biased (Paper II).

A challenge when extracting RNA from tissues is that the cellular composition and distribution may vary across samples, especially in heterogeneous tissues. Tissue samples from the hippocampus, choroid plexus, and lung were taken at standardized areas to include similar cell types. For example, the dorsal area of the caudal lung lobe has a relative uniform composition without larger bronchi. The choroid plexus is a very homogenous tissue, and both the choroid plexus and the hippocampus are easily identified areas. In addition, morphological evaluations were always performed from corresponding

areas to assess potential differences in a cell population, such as infiltration of inflammatory cells. In this thesis, transcriptional responses in tissues as a whole are described, and thus phenotypes related to loss of PrP^C in a single cell type might be masked.

Quantitative real-time polymerase chain reaction (qPCR)

Real-time qPCR is a refinement of the original PCR and makes it possible to determine the quantity of a specific RNA (cDNA) or DNA sequence in a sample (Kubista et al. 2006; Higuchi et al. 1993). Target DNA is amplified by the binding of specific primers and a DNA polymerase, and quantification is achieved by using a fluorescent reporter that incorporates double-stranded amplicons (non-specific detection). A computer software analyzes fluorescent signals in real-time, and the threshold value (C_p) is determined when the detection signal rises appreciably above the background level (Pfaffl 2001). The relative expression of the target gene can be calculated by using one or several stably expressed genes as reference.

In this thesis, gene expression studies were performed by LightCycler 480 qPCR (Papers I-IV) and high-throughput qPCR on the Fludigm Biomark HD platform (Papers I and II). In both cases, non-specific probes such as SYBRGreen and EvaGreen were used as fluorophores. The Fluidigm Biomark can combine 96 samples with 96 primer assays in 9216 simultaneous reactions, and is therefore far more efficient and cost reducing than conventional qPCR. Since a large number of genes and samples were analyzed at the same time, inter-run differences and pipetting errors were reduced. Moreover, two primer assays were designed for each target gene, and the correlation of these was calculated to validate that the correct gene was being amplified. The specificity of the primers was also verified *in silico* by BLAST search against the *Capra hircus* genome. When possible, primers were designed to span exon-exon junctions to avoid the risk of false positives from amplifying any contaminating genomic DNA. A disadvantage with chip-based qPCR is that the annealing temperature cannot be optimized for each primer set. Therefore, only primer assays with a PCR efficacy near 100 % and a correlation coefficient above 0.95 were included. Both the RNA extraction and cDNA synthesis protocol included a DNase step to remove genomic DNA, and potential contamination was assessed by including a non-reverse transcriptase in the cDNA synthesis. Melting curves and a no-template control

were evaluated in each reaction to monitor unspecific amplifications or primer dimers. To account for instability in PCR amplifications or pipetting errors (LightCycler 480), samples were run in duplicate or triplicate reactions. The expression levels were normalized against several reference genes (*HPRT1*, *HMBS*, *ACTB,* and *HSP90AA1*) that served as internal controls (Papers I and II). These genes were validated by the geNorm and Normfinder software to be stably expressed and unaffected by treatment or genotype. When validating RNA-seq data, a single stably expressed reference gene (*ACTB*) was used as internal control (Papers III and IV).

RNA sequencing

Next-generation technology is used in RNA-seq to reveal the cellular transcriptome at a given moment in time. Compared with microarrays, RNA-seq quantifies more RNA species, covers a wider dynamic range of gene expression, and has a higher efficacy in identifying truly differentially expressed genes (DEGs) (Marioni et al. 2008). Conversely, RNA-seq is still relatively expensive, and downstream analyses of large data sets require a range of different software as well as bioinformatic skills. We isolated RNA from PBMCs and several tissues, which were shipped on dry ice to the Beijing Genomics Institute (Paper II) and Novogene (Papers III and IV). All included samples were quality checked after transportation and assigned the highest quality level (level A). This step is important because degraded RNA might bias the estimation of gene expression and DEGs (Gallego Romero et al. 2014). Novogene performed downstream processing of RNA-seq data, and details are not discussed in the current section. An excellent overview of the different steps in RNA-seq, as well as challenges and advantages, have previously been reviewed by Wang and colleagues (Wang et al. 2009).

In the LPS study, we extracted RNA from 125 samples (5 tissues, 25 animals) that were pooled per genotype and treatment. Only three of these tissues (hippocampus, choroid plexus, and lung) are included in this thesis. The biological averaging hypothesis suggests reduced biological variability when pooling samples and increased power to detect DEGs, yet at a lower cost than to sequence individual samples. However, a pooling bias, which refers to disparities between the mean value of the pool and the corresponding individual values, can occur (Rajkumar et al. 2015). To validate the RNA-seq results, we investigated a subset of target genes by qPCR that comprised both DEGs and non-DEGs in all three tissues

and PBMCs. Generally, we observed a strong correlation between expression levels obtained by RNA-seq and qPCR, both in individual sequencing (Paper II) and pooled samples (Papers III and IV). This finding is in line with similar studies (Liu et al. 2013; Wang et al. 2014b). Nevertheless, we also observed some discrepancies during validation. For instance, hippocampal *SAA3* was not detected by RNA-seq in saline groups, and the levels were only about 1-2 FPKM after LPS challenge. In contrast, a significant increase in *SAA3* transcripts was detected by qPCR, which implies that alterations of genes with very low expression may not be detected by RNA-seq.

Histology and immunohistochemistry

Histological samples were prepared from paraffin-embedded tissue by standard methods. Sections from all animals were stained with hematoxylin and eosin and used to assess morphology and inflammatory changes in the hippocampus, choroid plexus, and lung (Papers III and IV). Martius-Scarlet-Blue (MSB) staining was used to detect fibrin effusion in the lungs as red fibrillary material (Paper IV). A positive control of acute fibrinous pneumonia was included. The MSB stain can occasionally be difficult to interpret since fresh fibrin can appear yellow while older fibrin can appear blue.

The basic principle of immunohistochemistry (IHC) is to selectively visualize antigens by the interaction of target epitopes with specific antibodies (Ramos-Vara 2005). The antigen-antibody binding can be visualized in multiple ways. In the most common approach, the primary (direct) or secondary (indirect) antibody is conjugated to an enzyme that can catalyze a color-producing reaction. Only unconjugated primary antibodies were used in this study in which the secondary antibody targets the isotype of the primary antibody. This process allows for signal amplification because several secondary antibodies bind to each primary antibody and therefore has higher sensitivity than direct detection. Because formalin fixation might form protein cross-links that mask the antigens, trypsin treatment was applied to expose epitopes for the Iba1 IHC. Trypsinization did not improve the GFAP IHC in our pilot tests. In addition, our protocols included inhibition of endogenous peroxidase and blocking of unspecific immunoglobulins present in the tissues. The final steps after unmasking, inhibition, and blocking steps were performed with the EnVision method provided by Dako (K4009).

In this thesis, IHC was used for several purposes. The cell-specific markers GFAP and Iba1 (polyclonal antibodies) were used to investigate the distribution of astrocytes and macrophages or microglia, respectively (Paper III). Initial titration runs were performed to optimize the antibody concentration and avoid nonspecific or background staining. The synthesis of these proteins increases upon inflammation, and increased labelling indicates activation of astrocytes (Brahmachari et al. 2006) and microglia (Chen et al. 2012). Both of these antibodies have previously been evaluated in sheep tissues (Johnston et al. 2013; Dean et al. 2009). Pulmonary S100A8 was predominantly present in neutrophils and was therefore a suitable indicator of neutrophil infiltration in the lungs. The pulmonary distribution of PrP^{C} was investigated using the monoclonal antibodies 6H4 and SAF32 (Paper IV). Anti-PrP antibodies are used to detect both PrP^{C} and PrP^{Sc} with different protocols, and both 6H4 and SAF32 have commonly been used in ruminant tissues (Peralta et al. 2009; Jeffrey et al. 2006). In paper IV, cryosections were used to avoid masking of epitopes. Negative controls included incubation with only buffer to omit the primary antibody, as well as sections without PrP^{C} (*PRNP*$^{Ter/Ter}$) to verify the specificity of the anti-PrP antibodies.

Scoring of histopathology and IHC was performed in a semi-quantitative manner. This method proved to be powerful in detecting pathological effects of the LPS treatment. Any subtle genotype-dependent differences were likely masked by the massive LPS effect and may partly explain why we did not observe morphological differences between genotypes. All evaluations of histology and IHC were scored blindly with respect to genotype and treatment to avoid bias.

SH-SY5Y cell culture

In paper II, human neuroblastoma cells (SH-SY5Y) were transfected with human *PRNP* to test the effect of PrP^{C} on interferon signaling *in vitro*. Originally, SH-SY5Y cells were derived from a metastatic bone tumor biopsy (Biedler et al. 1978) and frequently used to model biological responses in neuronal-like cells. The transfected SH-SY5Y clones were checked with regard to glycosylation and proteolytic cleavage to ensure normal post-translational modification and trafficking of PrP^{C}. Several clones were made to account for inter-assay variation. One important consideration for the use of SH-SY5Y cells is that untransfected SH-SY5Y cells are not completely free of PrP^{C}, although the expression of *PRNP* is very low.

Therefore, we cannot exclude that very low levels of PrP^C can affect the results in the untransfected control. Cell cultures from goats devoid of PrP^C are currently being developed (M. A. Tranulis; personal communication).

Discussion

The introduction of the term 'prion', which implicates a protein as causative agent of scrapie, caused great astonishment when it was discovered in the 1980s (Prusiner 1982). A single protein as a standalone infectious agent without nucleic acids was an entirely new principle and paradigm. From then on, studies have been designed to elucidate the physiological function of the normal form of the prion protein (PrP^C), yet still without a definite answer. The generation of transgene animals with genetic KO of the *Prnp* gene has proven valuable in gaining such information, but it has also been criticized due to pitfalls including the genetic background of transgenic mice. For instance, it was suggested that PrP^C negatively regulates phagocytosis (de Almeida et al. 2005), but polymorphisms in a closely linked locus encoding *Sirpa* were later reported to have confounded these results (Nuvolone et al. 2013). Additionally, early reports proposed a role for PrP^C in synaptic transmission (Collinge et al. 1994) and memory formation (Coitinho et al. 2003), but contradictory results have been reported (Lledo et al. 1996; Lipp et al. 1998). Although PrP^C is expressed in diverse tissues, it is most abundant in the CNS. This distribution reflects many of the major proposed functions of PrP^C, such as neuroprotection, neuronal excitability, glutamate receptor function, neurite outgrowth, and regulation of sleep and circadian rhythm (Reviewed in Wulf et al. 2017). More recently, a role of PrP^C in peripheral myelin maintenance was reported in the strictly co-isogenic ZrchIII mice (Nuvolone et al. 2016) as well as in lines with mixed genetic backgrounds (Bremer et al. 2010).

The identification of a non-sense stop mutation in the *PRNP* gene of Norwegian dairy goats that terminates the synthesis of PrP^C has provided a new approach to study PrP^C physiology (Benestad et al. 2012). In this doctoral work, we have not only utilized this model to study the biological role of PrP^C, but also aim to increase knowledge of how goats respond to systemic endotoxins. The latter aspect, with molecular and histopathological emphasis, is discussed at the end of this section.

Loss of PrP^C induces a primed state of type I interferon-stimulated genes

The expression of PrP^C in peripheral blood mononuclear cells (PBMCs) is moderate and dynamically altered by both activation and developmental status in these cells (Dürig et al. 2000; Reiten et al. 2015). Reports from transgenic mice have proposed several functions for PrP^C in blood immune cells (Isaacs et al. 2006). Based on this, we examined whether loss of PrP^C would elicit a transcriptional response in PBMCs when compared to the normal counterpart (Paper II). About 70 % of the differentially expressed genes between genotypes were characterized as type I interferon-stimulated genes (ISGs). Similarly, a subtle increase in several ISGs was observed in blood leukocytes and tissues before and after LPS challenge (Papers II, III, and IV), and we concluded that PrP^C-deficient goats are in a primed state with respect to ISGs. To the best of our knowledge, this is the first report of PrP^C participating in modulating the expression of genes downstream of type I interferons.

The major type I interferons, IFN-α and IFN-β, can be produced by many cell types in response to sensing microbial products by pattern-recognition receptors. In brief, interferons bind the IFN-α receptor (IFNAR) to initiate the JAK-STAT pathway, which results in the assembly of the ISGF3 complex and transcription of ISGs. More recently, it has been become clear that the regulation of the type I interferon pathway is extremely complex, as it comprises posttranslational modifications, interactions with other transcription factors, epigenetic modification, and interaction with regulatory elements (Reviewed in Ivashkiv et al. 2014). For this reason, we analyzed the expression of a range of genes involved in the regulation and induction of ISGs, but found no significant differences between *PRNP* genotypes (Paper II). These results indicate that the primed state of ISGs is not due to altered transcription of regulatory genes or the IFNAR itself. Nonetheless, protein levels or phosphorylation status of transcription factors and regulatory elements were not investigated, so we cannot exclude such interactions. Importantly, the type I interferon signaling pathway has several amplification steps, and genotype-dependent differences upstream of ISGs may be subtle and difficult to detect.

To cross-validate the results *in vitro*, human *PRNP* was transfected into human neuroblastoma SH-SY5Y cells, which normally express very low levels of PrP^C. When stimulated with IFN-α, the introduction of *PRNP* significantly inhibited the expression of ISGs (*MX2)*, which implies that PrP^C dampens the type I interferon response (Paper II).

Recently, it was shown that PrP^C promotes TACE-mediated cleavage of the TNF-α receptor (TNFAR), thus reducing the sensitivity of recipient cells to TNF-α (Ezpeleta et al. 2017). Since TACE may also cleave the IFNAR (Pioli et al. 2012), a similar regulation of the IFNAR may occur. In that case, loss of PrP^C would provoke internalization of TACE and cause elevated levels of IFNAR at the plasma membrane, which could explain the primed state of ISGs in PrP^C-deficient goats. Interestingly, several studies report increased transcription of ISGs in the early course of prion diseases (Baker et al. 2004; Carroll et al. 2015; Riemer et al. 2000). Consequently, we could speculate whether alterations at the early stages of prion diseases could reflect loss-of-PrP^C function similar to what we report in this thesis. Still, activated glial cells probably contribute to the transcription of ISGs, and this hypothesis needs further investigation.

Modulation of interferon responses is not in direct contrast to effects previously attributed to PrP^C. For instance, several reports proposed that PrP^C protects against apoptosis, possibly by reducing p53-mediated caspase 3 activity and profilin 1 (*PFN1*) expression (Zafar et al. 2017), which are activators of apoptosis (Yao et al. 2013). Notably, expression of both *PFN1* and caspase 3 may be stimulated directly by type I interferons (Yan et al. 2016; Gamero et al. 2006). Furthermore, several of the downstream ISGs can induce and regulate apoptosis directly, such as *IFIT2*, *IFI6,* and *IFI27* (Clemens 2003). Considered together, there are many crossroads between interferons or ISGs and proposed PrP^C functions. Nonetheless, these topics have been extensively studied, which makes such crossroads likely to occur; further experiments are required to revisit these observations.

An immunomodulatory role for PrP^C during LPS-induced acute inflammation

During the last decades, accumulating evidence has pointed towards possible roles of PrP^C in the immune system (Bakkebø et al. 2015; Isaacs et al. 2006; Onodera et al. 2014). Loss of PrP^C seems to exacerbate the development of inflammatory diseases, both in the CNS (Gourdain et al. 2012; Tsutsui et al. 2008; Nasu-Nishimura et al. 2008) and peripheral tissues (Martin et al. 2011). Based on the assumption that goats devoid of PrP^C are more susceptible to systemic inflammation than normal goats, we designed and performed the LPS experiment to study this hypothesis in detail.

As reported in papers I, III, and IV, systemic LPS caused sepsis-like clinical signs including depression, anorexia, fever, tachycardia, tachypnea, and reduced social and locomotor activity. Goats devoid of PrP^C suffered a significantly prolonged period of sickness behavior and had a slightly higher fever and respiratory rate than normal goats (Papers III and IV). This is a new behavioral phenotype attributed the lack of PrP^C, and although we were only partly able to explain this difference, it is one of the major discoveries in this doctoral work. Despite the initial reports that *Prnp* KO mice showed no behavioral abnormalities (Büeler et al. 1992), a variety of behavioral phenotypes were later suggested. Such phenotypes include deficits in locomotor activity and memory (Coitinho et al. 2003), increased aggression (Büdefeld et al. 2014), altered nociception (Meotti et al. 2007), and impaired nest-building behavior (Schmitz et al. 2014), among others. While reports of LPS-induced sickness behavior in *Prnp*-ablated mice are lacking, a depressive-like behavior during standardized stress tests has been described (Gadotti et al. 2012). Another interesting observation is that peripheral LPS/TNF-α challenge exaggerated sickness behavior in mice with pre-clinical prion disease (ME7 prion strain) (Combrinck et al. 2002; Hennessy et al. 2017). The authors concluded that microglia in these mice were in a primed state, thus increasing the brain's susceptibility to systemic inflammation. In light of our results, it is tempting to speculate whether loss of PrP^C in the preclinical stage of prion disease could contribute to the prolonged sickness behavior observed in this experiment.

Based on the clinical finding of prolonged sickness behavior in PrP^C-deficient goats, we performed full transcriptome and histopathological analyses of the choroid plexus and the PrP^C-rich hippocampus. As it is located at the blood-brain interface, the highly vascularized choroid plexus acts as a sensor for systemic inflammation and plays a key role in

transmitting information to the brain by releasing mediators into the cerebrospinal fluid (Marques et al. 2016; Balusu et al. 2016). Although there was a high overlap in the transcriptional response in the two genotypes, several innate immune genes were differentially expressed. Similar to what we observed in unstimulated PBMCs (Paper II), elevated levels of ISGs were observed in the brain of the PrP^C-deficient goats (Paper III) after LPS exposure. To date, the exact relationship between the interferon response and LPS-induced sickness behavior is not clear. Mice without IFNAR exhibited an impaired sickness behavior during systemic challenge with Poly I:C, a synthetic double-stranded RNA mimicking viral infection (Murray et al. 2015). Virus-induced sickness behavior has later been linked to activation of the IFNAR in endothelial and epithelial cells at the blood-brain barrier following *CXCL10*-activation of hippocampal neurons (Blank et al. 2016). Notably, *CXCL10* was prominently upregulated in the hippocampus of LPS-treated goats, but with no significant differences between genotypes.

The primary inducers of sickness behavior, *IL1B* and *TNFA*, were not significantly altered in the hippocampus or choroid plexus at the time of euthanasia (Paper III). However, previous reports show that *IL1B* expression peaks already 1 hour after systemic LPS challenge in the choroid plexus (Marques et al. 2009), and a transient increase may not be detected at later stages. Nevertheless, the IL-1 receptor has a high expression in the dentate gyrus and pyramidal cell layer of the hippocampus (Friedman 2001) as well as in the choroid plexus (Ericsson et al. 1995), which suggests high responsiveness in these tissues to inflammatory signals. Interestingly, higher expression of hippocampal *IL1B* and *TNFA* was observed in *Prnp* KO mice than wild types 24 hours after systemic LPS challenge, but clinical and behavioral evaluation of these animals was not reported (Liu et al. 2014). Similarly, KO of *Prnp* dramatically increased expression of pro-inflammatory cytokines such as *IL1B*, *TNFA,* and *IL6* during *in vitro E. coli* infection of bone marrow-derived macrophages (Wang et al. 2014a). Since the LPS-stimulated goats were clinically normal at the time of euthanasia, we cannot exclude that higher levels of these cytokines were present in PrP^C-deficient goats during the endotoxic phase. To summarize, PrP^C seems to participate in the regulation of crucial inflammatory cytokines that are involved in both sickness behavior and pyrogenic responses. Our findings support a protective role of PrP^C in the brain during acute

inflammation, which possibly occurs by mediating central pathways of innate immunity at the blood-brain interface (Paper III).

To investigate whether PrP^C has a similar function in peripheral tissues, we analyzed the histopathological and transcriptional response in the lungs after LPS challenge (Paper IV). Interestingly, a higher activation score of LPS-responsive genes, particularly those stimulated by pro-inflammatory cytokines such as TNF-α, was observed in PrP^C-deficient goats. This result could be due to increased availability of TNA-α receptors at the plasma membrane, as discussed in an earlier section (Ezpeleta et al. 2017). Additionally, several pathways and gene ontology terms related to the turnover of extracellular matrix were significantly enriched, which indicates increased damage to the lung parenchyma in the absence of PrP^C. We further observed that PrP^C was distributed in several cell types throughout the lungs, and *PRNP* expression increased slightly upon LPS challenge similar to what we observed in the brain and choroid plexus (Paper III). Likewise, *Prnp* was upregulated in two different cell systems upon either *E. coli* or LPS stimulation (Wang et al. 2014a; Wang et al. 2005). In neutrophils, LPS-induced upregulation of PrP^C was dependent on the serum content of TGF-β and glucocorticoids, which implies a neuro-immuno-endocrine regulation of the *Prnp* expression (Mariante et al. 2012). The fact that inflammatory stimuli upregulate *PRNP,* supports that PrP^C has a role in modulating immune responses. Taken together, PrP^C seems to have a protective role both in the CNS and lungs (Papers III and IV) that is demonstrated by prolonged sickness behavior, increased activation of inflammatory pathways, and increased transcription of genes that reflect damage of the lungs parenchyma in PrP^C-deficient goats. The cellular localization of PrP^C and some hypothetical interactions with the inflammatory response and the type I interferon response are visualized in Figure 8.

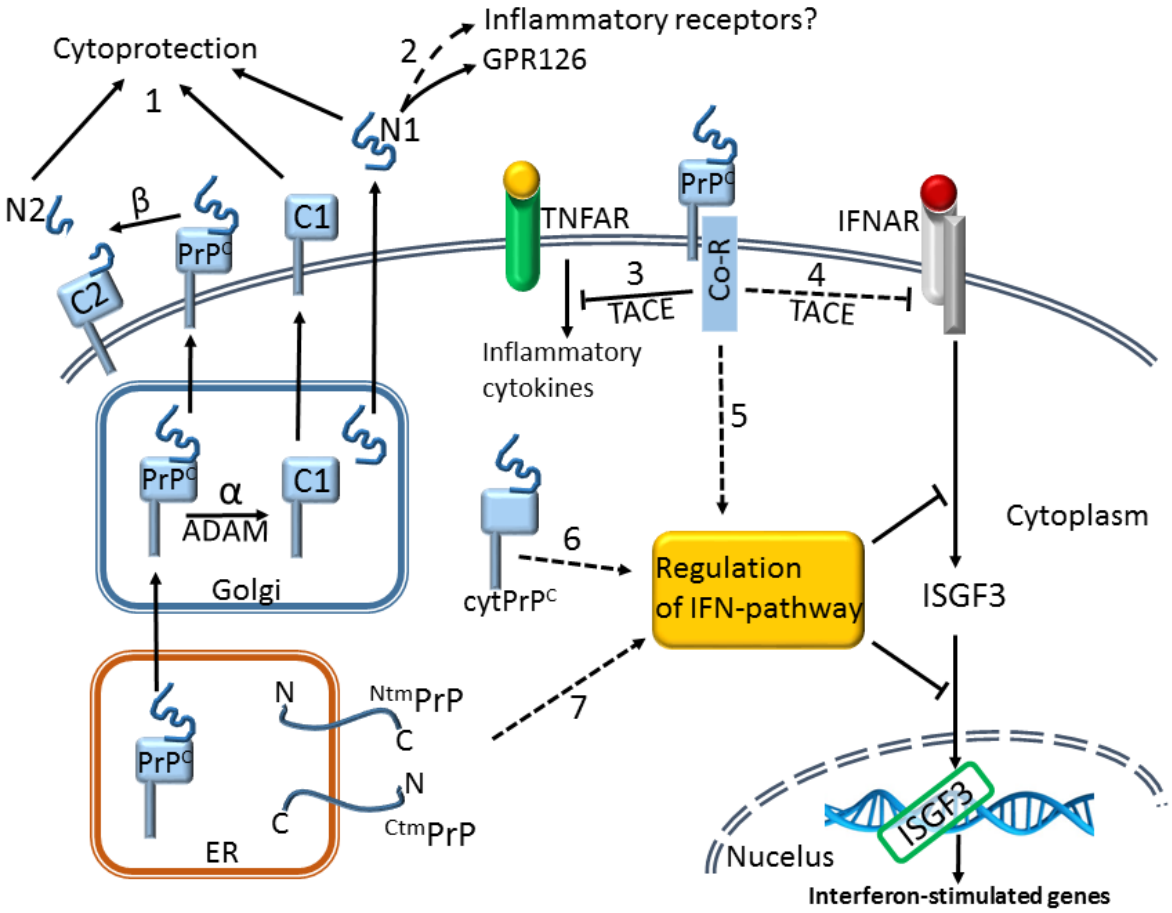

Figure 8. Cellular localization of the prion protein and hypothetical interactions with inflammatory/IFN pathways. As described in the introduction, PrP^C can be proteolytically processed by α- and β-cleavage, and C1, N1, and N2 have cytoprotective properties (1). The N1 fragment can activate receptors, such as the GPR126, and possibly other G-coupled receptors involved in inflammation (2). Cell surface PrP^C probably needs a co-receptor (e.g., β1 integrin) to initiate signaling. PrP^C negatively regulates the availability of the TNF-α-receptor (TNFAR) present at the plasma membrane through TACE, thus reducing inflammatory signaling (3). Because TACE can cleave the interferon receptor (IFNAR) as well, a similar regulation of the IFN-pathway could be possible (4). Proteins involved in the negative regulation of the IFN-pathway may be modulated by signaling through cell surface PrP^C (5), through cytosolic PrP^C (6), or by transmembrane forms of PrP^C in the endoplasmic reticulum (ER) membrane (7). Physiological functions of $cytPrP^C$ (6) and $^{N/Ctm}PrP$ (7), however, are controversial and probably less likely. Arrows indicate promotion or activation, T-shapes indicate inhibition, and dashed lines represent hypothetical interactions.

Could intestinal barrier dysfunction contribute to our results?

The epithelial intestinal barrier is the largest and most important barrier against the external environment. It is maintained by transmembrane proteins that form adhesive complexes called desmosomes, adherent junctions, and tight junctions (Groschwitz et al. 2009). Dysfunction of this barrier can lead to translocation of Gram-negative bacteria,

followed by release of LPS into the bloodstream (Maes et al. 2008). Notably, PrP^C is localized to intestinal cell-cell junctions (Morel et al. 2004), interacts with desmosomal proteins (Morel et al. 2008), and is required for proper organization of tight junctions (Petit et al. 2012). Accordingly, we could speculate that PrP^C-deficient goats have higher levels of circulating LPS due to intestinal barrier dysfunction, which results in a primed state of ISGs in PBMCs and leukocytes (Paper II). Similarly, low levels of LPS might prime glia cells in the brain and immune cells in the lungs (Smith et al. 1994), thus explaining the prolonged sickness behavior and increased inflammatory response in tissues upon experimental LPS challenge (Papers III and IV). Nevertheless, PrP^C also modulated ISG-expression (*MX1*) in cultured cells stimulated with IFN-α (Paper II), which suggests that intestinal dysfunction cannot alone explain our results.

No evidence of PrP^C regulating leukocyte migration

It has been shown that PrP^C is moderately expressed in different compartments of the hematopoietic system (Dürig et al. 2000). Several previous studies propose that PrP^C is involved in extravasation of leukocytes into tissues, although with conflicting results. In a study of zymozan-induced peritonitis, *Prnp* KO mice showed decreased numbers of neutrophils and larger numbers of monocytes in peritoneal infiltrates (de Almeida et al. 2005). When exposed to systemic LPS, the total blood leukocyte counts were higher in *Prnp* KO mice than in wild types, which indicates a slower recruitment of leukocytes into tissues (Liu et al. 2014). A possible explanation is that PrP^C inhibits migration of monocytes by modulating β1 integrin adhesion (Richardson et al. 2015). Based on these findings, blood collected during the LPS study was differentially counted by flow cytometry (Paper III). The levels of neutrophils, lymphocytes, monocytes, and basophils decreased rapidly and similarly in both genotypes, which indicates extravasation into tissues and sequestering in the microcirculation. This result was confirmed by histopathological evaluation and S100A8 IHC of the lungs, in which neutrophils were detected in septal capillaries and alveoli with no differences between genotypes (Paper IV). For this reason, our results do not support a major role of PrP^C in regulating leukocyte migration *in vivo*.

Molecular and histopathological aspects of LPS-induced acute inflammation

In addition to exploring the role of PrP^C in inflammation, the current thesis adds in-depth information of the molecular and histopathological response to endotoxins in small ruminants (Papers I, III, and IV). Previous studies have primarily focused on the clinical and pathophysiological changes evoked by LPS in goats (Takeuchi et al. 1997; Takeuchi et al. 1995), and detailed studies on how systemic inflammation affects the hippocampus, choroid plexus, and lung transcriptome have not been performed. From a clinical perspective, Gram-negative infections, which are important in pneumonia, peritonitis, mastitis, and metritis, can result in endotoxemia (sepsis). Unless treated, unbalanced levels of inflammatory mediators may be lethal. Given the increasing problem of antimicrobial resistance against antibiotics, understanding the molecular events of the innate immunity, as well as identifying biomarkers of sepsis, are key events in developing new therapeutic strategies (Reinhart et al. 2012).

In simple terms, the magnitude of differentially expressed genes reflects the tissue's susceptibility to inflammation. As visualized in Figure 9, the hippocampus transcriptome was only subtly altered, which suggests that this brain area is relatively protected from the effects of circulating endotoxins. Still, the clinical manifestation of sickness behavior and fever, along with activation of GFAP-positive astrocytes, shows the sensitivity of the CNS towards systemic inflammation (Paper III). This sensitivity is probably due to the tight connection between astrocytes and systemic circulation at the blood-brain barrier (Hasegawa-Ishii et al. 2016). Indeed, astrocytes have a central role in regulating neuroinflammation, particularly by driving the system back to homeostasis after injury (Colombo et al. 2016). Conversely, activation of Iba1-positive microglia was not detected in the hippocampus by IHC at the time of euthanasia, yet a later activation seems likely according to a murine study (Chen et al. 2012). Because only minimal amounts of LPS cross the blood-brain barrier (Banks et al. 2010), the observed effects in the hippocampus were probably mediated through neuronal and humoral communication routes, such as the choroid plexus. A particularly interesting observation was that systemic LPS challenge increased the number and labeling intensity of Iba1-positive cells in the choroid plexus (Paper III), thus suggesting recruitment of cells (monocytes) from the circulation (Shechter et al. 2013). Most of the round-bodied Iba1-positive cells were located at the basal side of

the epithelium, with processes extending between the epithelium. These cells probably represent dendritic cell-like macrophages (Ransohoff et al. 2010). Additionally, some cells seemed to transit through the epithelium towards the apical surface. Correspondingly, a considerable activation of the choroid plexus transcriptome was observed after LPS challenge (Figure 9). Notably, 50 of the upregulated genes overlapped between the choroid plexus and lung. When assigned to gene ontology terms, the most enriched biological process was type I interferon signaling comprising ISGs primarily classified as anti-viral (Figure 9). The notion that bacterial LPS stimulates these genes across different tissues (Papers III and IV) and in blood leukocytes (Papers I and II) corroborates a widespread role of these genes in the defense against bacterial infections.

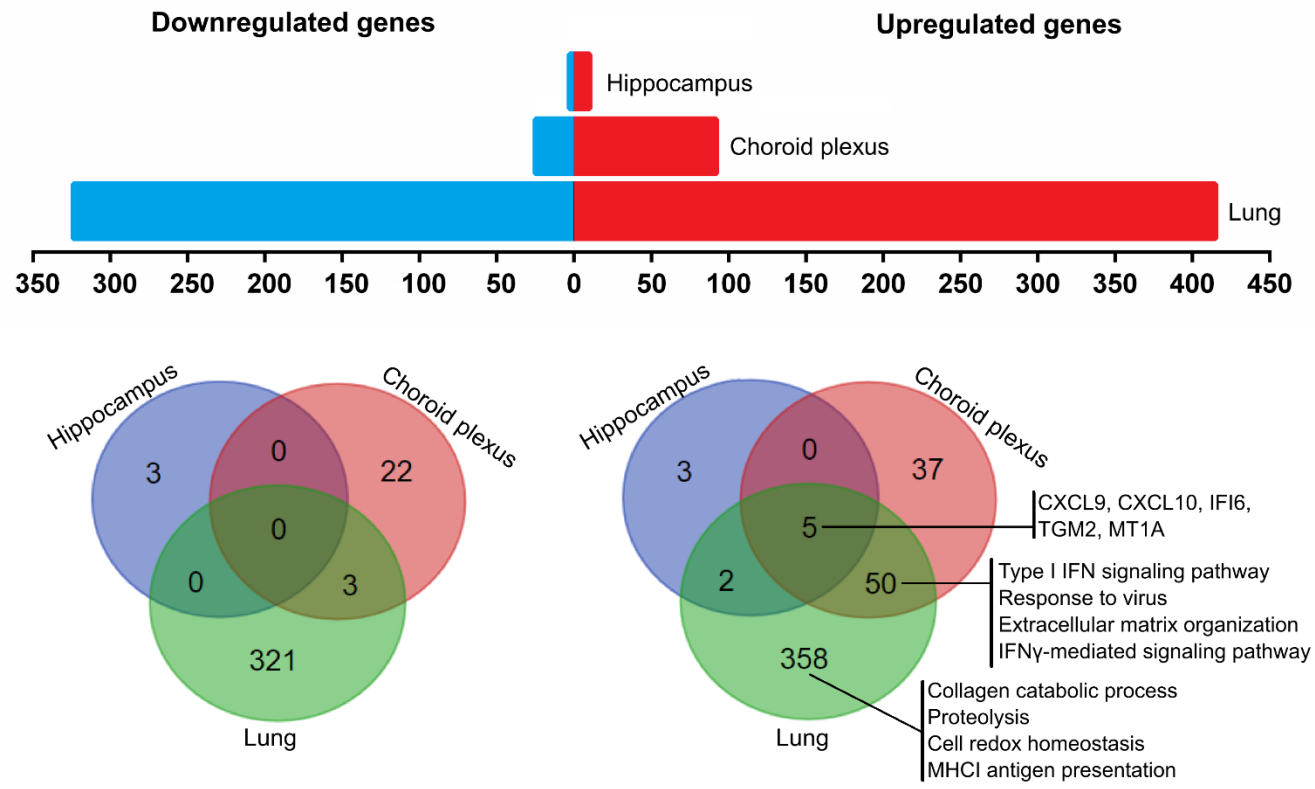

Figure 9. Comparison of up- and downregulated genes in different tissues after LPS challenge. Left Venn diagram shows overlapping downregulated genes across tissues. Right Venn diagram displays overlapping upregulated genes and selected gene ontology terms (biological processes, DAVID) of some subgroups of genes. Included genes were differentially expressed in at least one *PRNP* genotype (Fold change 1.5 and $q < 0.05$).

The lung transcriptome was by far the most affected, which corresponded with gross and histopathological changes. A large amount of the upregulated genes (358 of 455) were lung-specific (Figure 9). These genes were annotated to biological processes such as collagen catabolism, proteolysis, cell redox homeostasis, and MHC I antigen presentation. This reflects a high degree of tissue damage, protein degradation, and turnover, as well as subsequent synthesis of collagen. Importantly, the high susceptibility of caprine lungs to endotoxins suggest that this tissue could be considered the shock organ of small ruminants. Therefore, limiting acute lung injury seems to be an essential step in treating septic patients.

Systemic inflammation upregulates extrahepatic acute phase protein genes in goats

The acute phase response is a complex early-defense system activated by external or internal stress, such as trauma, inflammation, or neoplasia. A key event in this response is the increased hepatic synthesis of serum proteins, collectively known as acute phase proteins (APPs). In goats, serum levels of haptoglobin (HP), serum amyloid A (SAA), acid soluble glycoprotein, and fibrinogen increased upon systemic inflammation induced by turpentine oil (González et al. 2008). Accordingly, we observed a significant increase in serum levels of SAA after LPS challenge and a decrease in albumin, a negative acute phase protein (Paper I). The expression of extrahepatic APPs, however, has only scarcely been previously evaluated in goats.

Extrahepatic APPs serve a variety of functions including opsonization of microbes, promotion of chemotaxis, coagulation, and some have a bactericidal effect by inhibiting microbe iron uptake (Tothova et al. 2014). In paper I, we showed that the leukocyte gene expression of four APPs – *SAA3*, *HP*, lactoferrin, and lipocalin 2 – increased after LPS challenge. This result suggests that leukocytes may contribute to circulating serum levels of APPs in the early stage of systemic inflammation. It is also possible that leukocytes release APPs as they infiltrate inflamed tissues, similar to what has been reported for HP in the mammary gland (Lai et al. 2009). A variety of APPs were also upregulated in the hippocampus, choroid plexus, and lung (Papers III and IV), albeit to a lesser extent than in leukocytes. Infiltration of neutrophils in the lungs was observed histologically, which likely contributes to the increased expression of APPs in this tissue (Paper IV). Considered together, the widespread expression of extrahepatic APPs corroborates findings from

other species (Skovgaard et al. 2009; Marques et al. 2017; Wilson et al. 2005) and suggests that most tissues are capable of mounting a local acute phase response. Generally, *SAA3* was among the most upregulated genes in tissues and increased by more than 400-fold in blood leukocytes 5 hours after LPS challenge (Papers I, II, and IV). As seen in Figure 10, *SAA3* levels varied according to tissue, treatment, and time after LPS challenge. Of importance, there was very little inter-individual variation in gene expression, which suggests that *SAA3* is a robust biomarker of inflammation in goat tissues and leukocytes.

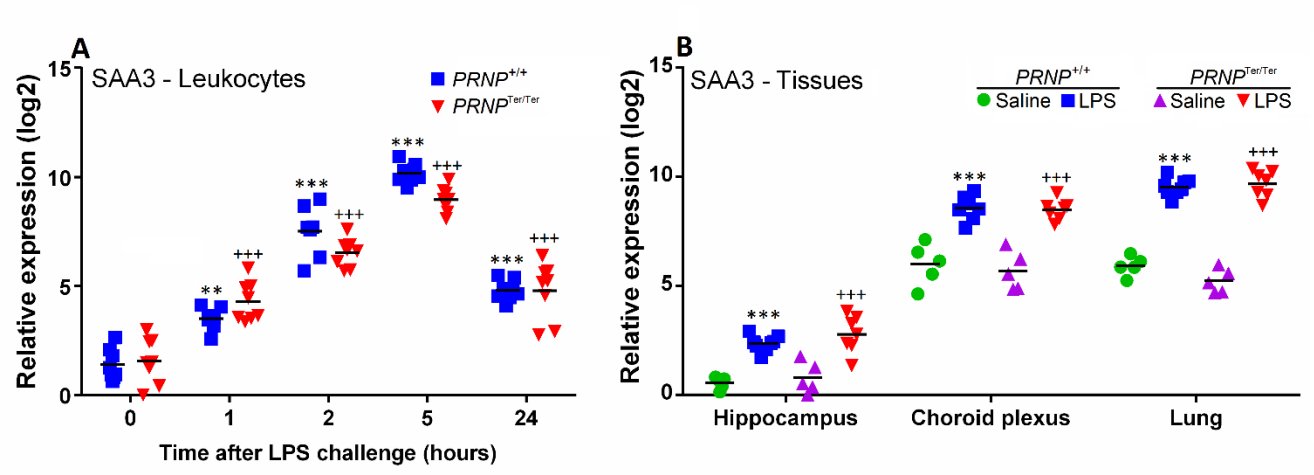

Figure 10. Relative expression of SAA3 in circulating leukocytes (A) and tissues (B) after LPS challenge. Mean expression levels and individual plots are indicated. Symbols * and + represent significantly increased expression compared with baseline (0 hour) or saline control of the matching genotype.

Conclusions

- We propose that PrP^C modulates type I interferon signaling in several cell types and tissues and primarily dampens the expression of interferon-stimulated genes (ISGs). Such ISGs play key roles in the defense against viruses and bacteria, along with cell differentiation and apoptosis, many of which overlap with effects that previously have been attributed PrP^C. These results might also explain molecular signatures identified in the pre-clinical stage of prion disorders.
- When exposed to systemic LPS, loss of PrP^C elicits prolonged sickness behavior, increased activation of pro-inflammatory regulators, and molecular evidence of parenchymal damage in the lungs; all of which indicate that PrP^C protects against systemic inflammation. These findings corroborate the theory of PrP^C as a scaffolding protein, which can regulate various forms of multiprotein complexes at the cell surface to modulate downstream signaling. Elucidating PrP^C functions is important both to understand the pathogenesis of prion disorders and to identify potential side effects of future treatments that involve blocking of PrP^C or removal of the *PRNP* gene.
- The choroid plexus plays a key role in the interplay between the central nervous system and systemic circulation in goats, which is reflected by alterations in the transcriptome. Systemic LPS challenge activates residing Iba1-positive cells and apparently recruits monocytes from the circulation into different parts of the choroid plexus.
- The ISGs are dynamically altered in caprine leukocytes upon LPS challenge and are among the most enriched genes in tissues, such as the choroid plexus and lungs. These findings suggest that ISGs play a global role in the defense against bacterial infections of small ruminants.
- Acute phase proteins (APPs) are substantially upregulated in leukocytes during endotoxemia in goats and could contribute to serum levels of APPs. Extrahepatic APPs were also upregulated in tissues, such as the hippocampus, choroid plexus, and lungs, which indicates that these are capable of mounting a local acute phase response. Serum amyloid A3 seems to be a particularly useful biomarker of inflammation in leukocytes and tissues.

Future perspectives

The current thesis provides the first transcriptome studies of goats naturally devoid of PrP^C, both at rest and after LPS challenge. Since a primed state of ISGs is present even without LPS stimulation, the site of PrP^C modulation is likely at the level of IFNAR or downstream of this receptor. Although transcription of regulatory elements was not altered, future studies should aim to investigate the phosphorylation or activation status of these proteins. Moreover, IFN-α/β stimulation of cultured cells derived from goats should be carried out to validate the results in the absence of possible confounding factors in circulating blood (e.g., viruses, bacteria).

We extracted RNA from tissues as a whole, which means that a variety of cell types were included. Future studies could take advantage of microdissection to study loss of PrP^C in single cell types that normally express high levels of PrP^C. In addition, RNA sequencing of samples without pooling would increase the probability to detect truly differentially expressed genes. Future characterization of polymorphisms in *PRNP*-flanking genes would provide central information of possible confounding genetic factors in the goat model.

We observed prolonged sickness behavior and increased activation of genes stimulated by pro-inflammatory cytokines after LPS challenge. Because transcription of inflammatory cytokines might be transient, further studies should quantify protein levels as well as the availability of receptors that are present at the plasma membrane. Cross-validation of LPS-induced sickness behavior by standardized tests in *Prnp* KO mice would be favorable. Further studies could explore whether PrP^C is proteolytically cleaved by LPS stimulation.

Finally, future research should aim to address some of the major proposed phenotypes in *Prnp* KO mice. Investigations of peripheral nerves, with emphasis on polyneuropathy in aged goats, are of special interest. The PrP^C-deficient line of goats could also be valuable for producing pharmacological products without the risk of prion contamination. In theory, export of semen or embryos could be performed to reduce scrapie in endemic areas, but breeding for a single homozygous trait is probably not desirable considering important production parameters. In addition, one of the conclusions in this doctoral work is that PrP^C has a protective role against inflammatory stress, and this notion should be further investigated in conjunction with important production-related diseases, such as mastitis.

References

Acutis P. L., Martucci F., D'Angelo A., Peletto S., Colussi S., Maurella C., Porcario C., et al. 2012. Resistance to classical scrapie in experimentally challenged goats carrying mutation K_{222} of the prion protein gene. *Vet Res*. 43: 8.

Adle-Biassette H., Verney C., Peoc'h K., Dauge M. C., Razavi F., Choudat L., Gressens P., Budka H., and Henin D. 2006. Immunohistochemical expression of prion protein (PrP^C) in the human forebrain during development. *J Neuropathol Exp Neurol*. 65: 698-706.

Aguilar-Calvo P., Espinosa J. C., Pintado B., Gutiérrez-Adan A., Alamillo E., Miranda A., Prieto I., Bossers A., Andréoletti O., and Torres J. M. 2014. Role of the goat K_{222}-PrP^C-polymorphic variant in prion infection resistance. *J Virol*. 88: 2670-6.

Aguzzi A. 2006. Prion diseases of humans and farm animals: epidemiology, genetics, and pathogenesis. *J Neurochem*. 97: 1726-39.

Alexander C., and Rietschel E. T. 2001. Bacterial lipopolysaccharides and innate immunity. *J Endotoxin Res*. 7: 167-202.

Altmeppen H. C., Prox J., Puig B., Kluth M. A., Bernreuther C., Thurm D., Jorissen E., et al. 2011. Lack of a-disintegrin-and-metalloproteinase ADAM10 leads to intracellular accumulation and loss of shedding of the cellular prion protein *in vivo*. *Mol Neurodegener*. 6: 36.

Annane D., Bellissant E., and Cavaillon J. M. 2005. Septic shock. *Lancet*. 365: 63-78.

Ashley N. T., Weil Z. M., and Nelson R. J. 2012. Inflammation: mechanisms, costs, and natural variation. *Annu Rev Ecol Evol Syst*. 43: 385-406.

Bainbridge J., and Walker K. B. 2005. The normal cellular form of prion protein modulates T cell responses. *Immunol Lett*. 96: 147-50.

Baker C. A., Lu Z. Y., and Manuelidis L. 2004. Early induction of interferon-responsive mRNAs in Creutzfeldt-Jakob disease. *J Neurovirol*. 10: 29-40.

Bakkebø M. K., Mouillet-Richard S., Espenes A., Goldmann W., Tatzelt J., and Tranulis M. A. 2015. The cellular prion protein: a player in immunological quiescence. *Front Immunol.* 6: 450.

Balusu S., Van Wonterghem E., De Rycke R., Raemdonck K., Stremersch S., Gevaert K., Brkic M., et al. 2016. Identification of a novel mechanism of blood-brain communication during peripheral inflammation via choroid plexus-derived extracellular vesicles. *EMBO Mol Med*. 8: 1162-83.

Banks W. A., and Robinson S. M. 2010. Minimal penetration of lipopolysaccharide across the murine blood-brain barrier. *Brain Behav Immun*. 24: 102-9.

Barclay G. R., Houston E. F., Halliday S. I., Farquhar C. F., and Turner M. L. 2002. Comparative analysis of normal prion protein expression on human, rodent, and ruminant blood cells by using a panel of prion antibodies. *Transfusion (Paris)*. 42: 517-26.

Barillet F., Mariat D., Amigues Y., Faugeras R., Caillat H., Moazami-Goudarzi K., Rupp R., et al. 2009. Identification of seven haplotypes of the caprine PrP gene at codons 127, 142, 154, 211, 222 and 240 in French Alpine and Saanen breeds and their association with classical scrapie. *J Gen Virol*. 90: 769-76.

Béland M., and Roucou X. 2013. Homodimerization as a molecular switch between low and high efficiency PrP^C cell surface delivery and neuroprotective activity. *Prion*. 7: 170-4.

Bellingham S. A., Coleman L. A., Masters C. L., Camakaris J., and Hill A. F. 2009. Regulation of prion gene expression by transcription factors SP1 and metal transcription factor-1. *J Biol Chem*. 284: 1291-301.

Benestad S. L., Austbø L., Tranulis M. A., Espenes A., and Olsaker I. 2012. Healthy goats naturally devoid of prion protein. *Vet Res*. 43: 87.

Beraldo F. H., Arantes C. P., Santos T. G., Machado C. F., Roffe M., Hajj G. N., Lee K. S., et al. 2011. Metabotropic glutamate receptors transduce signals for neurite outgrowth after binding of the prion protein to laminin γ1 chain. *FASEB J*. 25: 265-79.

Beraldo F. H., Soares I. N., Goncalves D. F., Fan J., Thomas A. A., Santos T. G., Mohammad A. H., et al. 2013. Stress-inducible phosphoprotein 1 has unique cochaperone activity during development and regulates cellular response to ischemia via the prion protein. *FASEB J*. 27: 3594-607.

Berr C., Richard F., Dufouil C., Amant C., Alperovitch A., and Amouyel P. 1998. Polymorphism of the prion protein is associated with cognitive impairment in the elderly: the EVA study. *Neurology*. 51: 734-7.

Bertuchi F. R., Bourgeon D. M., Landemberger M. C., Martins V. R., and Cerchiaro G. 2012. PrP^C displays an essential protective role from oxidative stress in an astrocyte cell line derived from PrP^C knockout mice. *Biochem Biophys Res Commun*. 418: 27-32.

Besnier L. S., Cardot P., Da Rocha B., Simon A., Loew D., Klein C., Riveau B., et al. 2015. The cellular prion protein PrP^C is a partner of the Wnt pathway in intestinal epithelial cells. *Mol Biol Cell*. 26: 3313-28.

Biedler J. L., Roffler-Tarlov S., Schachner M., and Freedman L. S. 1978. Multiple neurotransmitter synthesis by human neuroblastoma cell lines and clones. *Cancer Res*. 38: 3751-7.

Billinis C., Panagiotidis C. H., Psychas V., Argyroudis S., Nicolaou A., Leontides S., Papadopoulos O., and Sklaviadis T. 2002. Prion protein gene polymorphisms in natural goat scrapie. *J Gen Virol*. 83: 713-21.

Black S. A., Stys P. K., Zamponi G. W., and Tsutsui S. 2014. Cellular prion protein and NMDA receptor modulation: protecting against excitotoxicity. *Front Cell Dev Biol*. 2: 45.

Blank T., Detje C. N., Spieß A., Hagemeyer N., Brendecke S. M., Wolfart J., Staszewski O., et al. 2016. Brain endothelial- and epithelial-specific interferon receptor chain 1 drives virus-induced sickness behavior and cognitive impairment. *Immunity*. 44: 901-12.

Bouzalas I. G., Dovas C. I., Banos G., Papanastasopoulou M., Kritas S., Oevermann A., Papakostaki D., et al. 2010. Caprine *PRNP* polymorphisms at codons 171, 211, 222 and 240 in a Greek herd and their association with classical scrapie. *J Gen Virol*. 91: 1629-34.

Brahmachari S., Fung Y. K., and Pahan K. 2006. Induction of glial fibrillary acidic protein expression in astrocytes by nitric oxide. *J Neurosci*. 26: 4930-9.

Brandner S., Isenmann S., Raeber A., Fischer M., Sailer A., Kobayashi Y., Marino S., Weissmann C., and Aguzzi A. 1996. Normal host prion protein necessary for scrapie-induced neurotoxicity. *Nature*. 379: 339-43.

Bremer J., Baumann F., Tiberi C., Wessig C., Fischer H., Schwarz P., Steele A. D., et al. 2010. Axonal prion protein is required for peripheral myelin maintenance. *Nat Neurosci*. 13: 310-8.

Brown D. R., and Besinger A. 1998. Prion protein expression and superoxide dismutase activity. *Biochem J*. 334: 423-9.

Brown D. R., and Mohn C. M. 1999a. Astrocytic glutamate uptake and prion protein expression. *Glia*. 25: 282-92.

Brown D. R., Nicholas R. S., and Canevari L. 2002. Lack of prion protein expression results in a neuronal phenotype sensitive to stress. *J Neurosci Res*. 67: 211-24.

Brown D. R., Qin K., Herms J. W., Madlung A., Manson J., Strome R., Fraser P. E., et al. 1997a. The cellular prion protein binds copper *in vivo*. *Nature*. 390: 684-7.

Brown D. R., Schulz-Schaeffer W. J., Schmidt B., and Kretzschmar H. A. 1997b. Prion protein-deficient cells show altered response to oxidative stress due to decreased SOD-1 activity. *Exp Neurol*. 146: 104-12.

Brown D. R., Wong B. S., Hafiz F., Clive C., Haswell S. J., and Jones I. M. 1999b. Normal prion protein has an activity like that of superoxide dismutase. *Biochem J*. 344: 1-5.

Brown P., and Gajdusek D. C. 1991. Survival of scrapie virus after 3 years' interment. *Lancet*. 337: 269-70.

Buchanan C. R., Preece M. A., and Milner R. D. 1991. Mortality, neoplasia, and Creutzfeldt-Jakob disease in patients treated with human pituitary growth hormone in the United Kingdom. *BMJ*. 302: 824-8.

Burgess S. T., Shen C., Ferguson L. A., O'Neill G. T., Docherty K., Hunter N., and Goldmann W. 2009. Identification of adjacent binding sites for the YY1 and E4BP4 transcription factors in the ovine PrP (Prion) gene promoter. *J Biol Chem*. 284: 6716-24.

Burton G. J., and Jauniaux E. 2011. Oxidative stress. *Best Pract Res Clin Obstet Gynaecol*. 25: 287-99.

Büdefeld T., Majer A., Jerin A., and Majdic G. 2014. Deletion of the prion gene *Prnp* affects offensive aggression in mice. *Behav Brain Res*. 266: 216-21.

Büeler H., Aguzzi A., Sailer A., Greiner R. A., Autenried P., Aguet M., and Weissmann C. 1993. Mice devoid of PrP are resistant to scrapie. *Cell*. 73: 1339-47.

Büeler H., Fischer M., Lang Y., Bluethmann H., Lipp H. P., DeArmond S. J., Prusiner S. B., Aguet M., and Weissmann C. 1992. Normal development and behaviour of mice lacking the neuronal cell-surface PrP protein. *Nature*. 356: 577-82.

Calzolai L., Lysek D. A., Pérez D. R., Güntert P., and Wüthrich K. 2005. Prion protein NMR structures of chickens, turtles, and frogs. *Proc Natl Acad Sci USA*. 102: 651-5.

Campbell L., Gill A. C., McGovern G., Jalland C. M., Hopkins J., Tranulis M. A., Hunter N., and Goldmann W. 2013. The PrP^{C} C1 fragment derived from the ovine $A_{136}R_{154}R_{171}$ *PRNP* allele is highly abundant in sheep brain and inhibits fibrillisation of full-length PrP^{C} protein *in vitro*. *Biochim Biophys Acta*. 1832: 826-36.

Carroll J. A., Striebel J. F., Race B., Phillips K., and Chesebro B. 2015. Prion infection of mouse brain reveals multiple new upregulated genes involved in neuroinflammation or signal transduction. *J Virol*. 89: 2388-404.

Chang L., and Karin M. 2001. Mammalian MAP kinase signalling cascades. *Nature*. 410: 37-40.

Chen Z., Jalabi W., Shpargel K. B., Farabaugh K. T., Dutta R., Yin X., Kidd G. J., Bergmann C. C., Stohlman S. A., and Trapp B. D. 2012. Lipopolysaccharide-induced microglial activation and neuroprotection against experimental brain injury is independent of hematogenous TLR4. *J Neurosci*. 32: 11706-15.

Chiarini L. B., Freitas A. R., Zanata S. M., Brentani R. R., Martins V. R., and Linden R. 2002. Cellular prion protein transduces neuroprotective signals. *EMBO J*. 21: 3317-26.

Choi S. H., Kim I. C., Kim D. S., Kim D. W., Chae S. H., Choi H. H., Choi I., Yeo J. S., Song M. N., and Park H. S. 2006. Comparative genomic organization of the human and bovine *PRNP* locus. *Genomics*. 87: 598-607.

Clemens M. J. 2003. Interferons and apoptosis. *J Interferon Cytokine Res*. 23: 277-92.

Coitinho A. S., Freitas A. R., Lopes M. H., Hajj G. N., Roesler R., Walz R., Rossato J. I., et al. 2006. The interaction between prion protein and laminin modulates memory consolidation. *Eur J Neurosci*. 24: 3255-64.

Coitinho A. S., Roesler R., Martins V. R., Brentani R. R., and Izquierdo I. 2003. Cellular prion protein ablation impairs behavior as a function of age. *Neuroreport*. 14: 1375-9.

Collinge J. 2016. Mammalian prions and their wider relevance in neurodegenerative diseases. *Nature*. 539: 217-26.

Collinge J., Whittington M. A., Sidle K. C., Smith C. J., Palmer M. S., Clarke A. R., and Jefferys J. G. 1994. Prion protein is necessary for normal synaptic function. *Nature*. 370: 295-7.

Colombo E., and Farina C. 2016. Astrocytes: Key regulators of neuroinflammation. *Trends Immunol*. 37: 608-20.

Combrinck M. I., Perry V. H., and Cunningham C. 2002. Peripheral infection evokes exaggerated sickness behaviour in pre-clinical murine prion disease. *Neuroscience*. 112: 7-11.

Creative Commons License. https://creativecommons.org/licenses/by/4.0/. Accessed 01.09.2017.

Criado J. R., Sánchez-Alavez M., Conti B., Giacchino J. L., Wills D. N., Henriksen S. J., Race R., Manson J. C., Chesebro B., and Oldstone M. B. 2005. Mice devoid of prion protein have cognitive deficits that are rescued by reconstitution of PrP in neurons. *Neurobiol Dis*. 19: 255-65.

Croes E. A., Dermaut B., Houwing-Duistermaat J. J., Van den Broeck M., Cruts M., Breteler M. M., Hofman A., van Broeckhoven C., and van Duijn C. M. 2003. Early cognitive decline is associated with prion protein codon 129 polymorphism. *Ann Neurol*. 54: 275-6.

Crusio W. E. 2004. Flanking gene and genetic background problems in genetically manipulated mice. *Biol Psychiatry*. 56: 381-5.

Dantzer R. 2009. Cytokine, sickness behavior, and depression. *Immunol Allergy Clin North Am*. 29: 247-64.

Dassanayake R. P., Schneider D. A., Herrmann-Hoesing L. M., Truscott T. C., Davis W. C., and O'Rourke K. I. 2012. Cell-surface expression of PrP^C and the presence of scrapie prions in the blood of goats. *J Gen Virol*. 93: 1127-31.

de Almeida C. J., Chiarini L. B., da Silva J. P., PM E. Silva, Martins M. A., and Linden R. 2005. The cellular prion protein modulates phagocytosis and inflammatory response. *J Leukoc Biol*. 77: 238-46.

Dean J. M., Farrag D., Zahkouk S. A., El Zawahry E. Y., Hagberg H., Kjellmer I., and Mallard C. 2009. Cerebellar white matter injury following systemic endotoxemia in preterm fetal sheep. *Neuroscience*. 160: 606-15.

Dehring D. J., and Wismar B. L. 1989. Intravascular macrophages in pulmonary capillaries of humans. *Am Rev Respir Dis*. 139: 1027-9.

Dodelet V. C., and Cashman N. R. 1998. Prion protein expression in human leukocyte differentiation. *Blood*. 91: 1556-61.

Dogan M. D., Ataoglu H., and Akarsu E. S. 2000. Effects of different serotypes of *Escherichia coli* lipopolysaccharides on body temperature in rats. *Life Sci*. 67: 2319-29.

Dürig J., Giese A., Schulz-Schaeffer W., Rosenthal C., Schmücker U., Bieschke J., Dührsen U., and Kretzschmar H. A. 2000. Differential constitutive and activation-dependent expression of prion protein in human peripheral blood leucocytes. *Br J Haematol*. 108: 488-95.

Ericsson A., Liu C., Hart R. P., and Sawchenko P. E. 1995. Type 1 interleukin-1 receptor in the rat brain: distribution, regulation, and relationship to sites of IL-1-induced cellular activation. *J Comp Neurol*. 361: 681-98.

Ermonval M., Mouillet-Richard S., Codogno P., Kellermann O., and Botti J. 2003. Evolving views in prion glycosylation: functional and pathological implications. *Biochimie*. 85: 33-45.

Espenes A., Harbitz I., Skogtvedt S., Fuglestveit R., Berg K. A., Dick G., Krogenæs A., and Tranulis M. A. 2006. Dynamic expression of the prion-like protein Doppel in ovine testicular tissue. *Int J Androl*. 29: 400-8.

Ezpeleta J., Boudet-Devaud F., Pietri M., Baudry A., Baudouin V., Alleaume-Butaux A., Dagoneau N., Kellermann O., Launay J. M., and Schneider B. 2017. Protective role of cellular prion protein against TNFα-mediated inflammation through TACE alpha-secretase. *Sci Rep*. 7: 7671.

Fevrier B., Vilette D., Archer F., Loew D., Faigle W., Vidal M., Laude H., and Raposo G. 2004. Cells release prions in association with exosomes. *Proc Natl Acad Sci USA*. 101: 9683-8.

Forloni G., Angeretti N., Chiesa R., Monzani E., Salmona M., Bugiani O., and Tagliavini F. 1993. Neurotoxicity of a prion protein fragment. *Nature*. 362: 543-6.

Fragkiadaki E. G., Vaccari G., Ekateriniadou L. V., Agrimi U., Giadinis N. D., Chiappini B., Esposito E., Conte M., and Nonno R. 2011. *PRNP* genetic variability and molecular typing of natural goat scrapie isolates in a high number of infected flocks. *Vet Res*. 42: 104.

Friedman W. J. 2001. Cytokines regulate expression of the type 1 interleukin-1 receptor in rat hippocampal neurons and glia. *Exp Neurol*. 168: 23-31.

Gadotti V. M., Bonfield S. P., and Zamponi G. W. 2012. Depressive-like behaviour of mice lacking cellular prion protein. *Behav Brain Res*. 227: 319-23.

Gallego Romero I., Pai A. A., Tung J., and Gilad Y. 2014. RNA-seq: impact of RNA degradation on transcript quantification. *BMC Biol*. 12: 42.

Gamero A. M., Potla R., Sakamoto S., Baker D. P., Abraham R., and Larner A. C. 2006. Type I interferons activate apoptosis in a Jurkat cell variant by caspase-dependent and independent mechanisms. *Cell Signal*. 18: 1299-308.

Gasperini L., Meneghetti E., Pastore B., Benetti F., and Legname G. 2015. Prion protein and copper cooperatively protect neurons by modulating NMDA receptor through S-nitrosylation. *Antioxid Redox Signal*. 22: 772-84.

Gauczynski S., Peyrin J. M., Haik S., Leucht C., Hundt C., Rieger R., Krasemann S., et al. 2001. The 37-kDa/67-kDa laminin receptor acts as the cell-surface receptor for the cellular prion protein. *EMBO J*. 20: 5863-75.

Georgsson G., Sigurdarson S., and Brown P. 2006. Infectious agent of sheep scrapie may persist in the environment for at least 16 years. *J Gen Virol*. 87: 3737-40.

Giachin G., Mai P. T., Tran T. H., Salzano G., Benetti F., Migliorati V., Arcovito A., et al. 2015. The non-octarepeat copper binding site of the prion protein is a key regulator of prion conversion. *Sci Rep*. 5: 15253.

Goldmann W., Chong A., Foster J., Hope J., and Hunter N. 1998. The shortest known prion protein gene allele occurs in goats, has only three octapeptide repeats and is non-pathogenic. *J Gen Virol*. 79: 3173-6.

González F. H., Tecles F., Martínez-Subiela S., Tvarijonaviciute A., Soler L., and Cerón J. J. 2008. Acute phase protein response in goats. *J Vet Diagn Invest*. 20: 580-4.

Gough K. C., and Maddison B. C. 2010. Prion transmission: prion excretion and occurrence in the environment. *Prion*. 4: 275-82.

Gourdain P., Ballerini C., Nicot A. B., and Carnaud C. 2012. Exacerbation of experimental autoimmune encephalomyelitis in prion protein (PrP^C)-null mice: evidence for a critical role of the central nervous system. *J Neuroinflammation*. 9: 25.

Graner E., Mercadante A. F., Zanata S. M., Forlenza O. V., Cabral A. L., Veiga S. S., Juliano M. A., et al. 2000. Cellular prion protein binds laminin and mediates neuritogenesis. *Brain Res Mol Brain Res*. 76: 85-92.

Groschwitz K. R., and Hogan S. P. 2009. Intestinal barrier function: molecular regulation and disease pathogenesis. *J Allergy Clin Immunol*. 124: 3-20.

Guillot-Sestier M. V., Sunyach C., Druon C., Scarzello S., and Checler F. 2009. The alpha-secretase-derived N-terminal product of cellular prion, N1, displays neuroprotective function *in vitro* and *in vivo*. *J Biol Chem*. 284: 35973-86.

Haddon D. J., Hughes M. R., Antignano F., Westaway D., Cashman N. R., and McNagny K. M. 2009. Prion protein expression and release by mast cells after activation. *J Infect Dis*. 200: 827-31.

Hailman E., Lichenstein H. S., Wurfel M. M., Miller D. S., Johnson D. A., Kelley M., Busse L. A., Zukowski M. M., and Wright S. D. 1994. Lipopolysaccharide (LPS)-binding protein accelerates the binding of LPS to CD14. *J Exp Med*. 179: 269-77.

Hajj G. N., Lopes M. H., Mercadante A. F., Veiga S. S., da Silveira R. B., Santos T. G., Ribeiro K. C., et al. 2007. Cellular prion protein interaction with vitronectin supports axonal growth and is compensated by integrins. *J Cell Sci*. 120: 1915-26.

Haldar S., Tripathi A., Qian J., Beserra A., Suda S., McElwee M., Turner J., Hopfer U., and Singh N. 2015. Prion protein promotes kidney iron uptake via its ferrireductase activity. *J Biol Chem*. 290: 5512-22.

Halliday S., Houston F., and Hunter N. 2005. Expression of PrP^C on cellular components of sheep blood. *J Gen Virol*. 86: 1571-9.

Harris D. A., and True H. L. 2006. New insights into prion structure and toxicity. *Neuron*. 50: 353-7.

Harrison P. M., Khachane A., and Kumar M. 2010. Genomic assessment of the evolution of the prion protein gene family in vertebrates. *Genomics*. 95: 268-77.

Hasegawa-Ishii S., Inaba M., Umegaki H., Unno K., Wakabayashi K., and Shimada A. 2016. Endotoxemia-induced cytokine-mediated responses of hippocampal astrocytes transmitted by cells of the brain-immune interface. *Sci Rep*. 6: 25457.

Hegde R. S., Mastrianni J. A., Scott M. R., DeFea K. A., Tremblay P., Torchia M., DeArmond S. J., Prusiner S. B., and Lingappa V. R. 1998. A transmembrane form of the prion protein in neurodegenerative disease. *Science*. 279: 827-34.

Hennessy E., Gormley S., Lopez-Rodriguez A. B., Murray C., Murray C., and Cunningham C. 2017. Systemic TNF-alpha produces acute cognitive dysfunction and exaggerated sickness behavior when superimposed upon progressive neurodegeneration. *Brain Behav Immun*. 59: 233-44.

Herrmann L. M., and Caughey B. 1998. The importance of the disulfide bond in prion protein conversion. *Neuroreport*. 9: 2457-61.

Hetz C., Maundrell K., and Soto C. 2003. Is loss of function of the prion protein the cause of prion disorders? *Trends Mol Med*. 9: 237-43.

Hickie I., and Lloyd A. 1995. Are cytokines associated with neuropsychiatric syndromes in humans? *Int J Immunopharmacol*. 17: 677-83.

Higuchi R., Fockler C., Dollinger G., and Watson R. 1993. Kinetic PCR analysis: real-time monitoring of DNA amplification reactions. *Biotechnology (N Y)*. 11: 1026-30.

Holada K., and Vostal J. G. 2000. Different levels of prion protein (PrP^C) expression on hamster, mouse and human blood cells. *Br J Haematol*. 110: 472-80.

Hornshaw M. P., McDermott J. R., and Candy J. M. 1995. Copper binding to the N-terminal tandem repeat regions of mammalian and avian prion protein. *Biochem Biophys Res Commun*. 207: 621-9.

Houston F., Foster J. D., Chong A., Hunter N., and Bostock C. J. 2000. Transmission of BSE by blood transfusion in sheep. *Lancet*. 356: 999-1000.

Hu W., Nessler S., Hemmer B., Eagar T. N., Kane L. P., Leliveld S. R., Müller-Schiffmann A., et al. 2010. Pharmacological prion protein silencing accelerates central nervous system autoimmune disease via T cell receptor signalling. *Brain*. 133: 375-88.

Huber R., Deboer T., and Tobler I. 1999. Prion protein: a role in sleep regulation? *J Sleep Res*. 8: 30-6.

Huber R., Deboer T., and Tobler I. 2002. Sleep deprivation in prion protein deficient mice and control mice: genotype dependent regional rebound. *Neuroreport*. 13: 1-4.

Hunter N., Foster J., Chong A., McCutcheon S., Parnham D., Eaton S., MacKenzie C., and Houston F. 2002. Transmission of prion diseases by blood transfusion. *J Gen Virol*. 83: 2897-905.

Hutter G., Heppner F. L., and Aguzzi A. 2003. No superoxide dismutase activity of cellular prion protein *in vivo*. *Biol Chem*. 384: 1279-85.

Isaacs J. D., Jackson G. S., and Altmann D. M. 2006. The role of the cellular prion protein in the immune system. *Clin Exp Immunol*. 146: 1-8.

Ivashkiv L. B., and Donlin L. T. 2014. Regulation of type I interferon responses. *Nat Rev Immunol*. 14: 36-49.

Jackson G. S., Murray I., Hosszu L. L., Gibbs N., Waltho J. P., Clarke A. R., and Collinge J. 2001. Location and properties of metal-binding sites on the human prion protein. *Proc Natl Acad Sci USA*. 98: 8531-5.

Jalland C. M. 2017. Influence of base-excision-repair pathway enzymes on prion pathogenesis. PhD Thesis. ISBN: 978-82-575-1996-4. Norwegian University of Life Sciences.

Jeffrey M., González L., Chong A., Foster J., Goldmann W., Hunter N., and Martin S. 2006. Ovine infection with the agents of scrapie (CH1641 isolate) and bovine spongiform encephalopathy: immunochemical similarities can be resolved by immunohistochemistry. *J Comp Pathol*. 134: 17-29.

Jeffrey M., Goodsir C. M., Race R. E., and Chesebro B. 2004. Scrapie-specific neuronal lesions are independent of neuronal PrP expression. *Ann Neurol*. 55: 781-92.

Johnston M. G., Del Bigio M. R., Drake J. M., Armstrong D., Di Curzio D. L., and Bertrand J. 2013. Pre- and post-shunting observations in adult sheep with kaolin-induced hydrocephalus. *Fluids Barriers CNS*. 10: 24.

Kagan J. C., and Medzhitov R. 2006. Phosphoinositide-mediated adaptor recruitment controls Toll-like receptor signaling. *Cell*. 125: 943-55.

Kazlauskaite J., Young A., Gardner C. E., Macpherson J. V., Vénien-Bryan C., and Pinheiro T. J. 2005. An unusual soluble beta-turn-rich conformation of prion is involved in fibril formation and toxic to neuronal cells. *Biochem Biophys Res Commun*. 328: 292-305.

Kim S. J., and Hegde R. S. 2002. Cotranslational partitioning of nascent prion protein into multiple populations at the translocation channel. *Mol Biol Cell*. 13: 3775-86.

Kim T. W., Staschke K., Bulek K., Yao J., Peters K., Oh K. H., Vandenburg Y., et al. 2007. A critical role for IRAK4 kinase activity in Toll-like receptor-mediated innate immunity. *J Exp Med*. 204: 1025-36.

Kim Y., Lee J., and Lee C. 2008. *In silico* comparative analysis of DNA and amino acid sequences for prion protein gene. *Transbound Emerg Dis*. 55: 105-14.

Komuro T., Yomota C., Kimura T., and Galanos C. 1989. Comparison of R- and S-form lipopolysaccharides fractionated from *Escherichia coli* UKT-B lipopolysaccharide in pyrogen and Limulus tests. *FEMS Microbiol Lett*. 51: 79-83.

Koussounadis A., Langdon S. P., Um I. H., Harrison D. J., and Smith V. A. 2015. Relationship between differentially expressed mRNA and mRNA-protein correlations in a xenograft model system. *Sci Rep*. 5: 10775.

Kubista M., Andrade J. M., Bengtsson M., Forootan A., Jonák J., Lind K., Sindelka R., et al. 2006. The real-time polymerase chain reaction. *Mol Aspects Med*. 27: 95-125.

Küffer A., Lakkaraju A. K., Mogha A., Petersen S. C., Airich K., Doucerain C., Marpakwar R., et al. 2016. The prion protein is an agonistic ligand of the G protein-coupled receptor Adgrg6. *Nature*. 536: 464-8.

Lacroux C., Corbière F., Tabouret G., Lugan S., Costes P., Mathey J., Delmas J. M., et al. 2007. Dynamics and genetics of PrP^{Sc} placental accumulation in sheep. *J Gen Virol*. 88: 1056-61.

Lacroux C., Simon S., Benestad S. L., Maillet S., Mathey J., Lugan S., Corbière F., et al. 2008. Prions in milk from ewes incubating natural scrapie. *PLoS Pathog*. 4: e1000238.

Lai I. H., Tsao J. H., Lu Y. P., Lee J. W., Zhao X., Chien F. L., and Mao S. J. 2009. Neutrophils as one of the major haptoglobin sources in mastitis affected milk. *Vet Res*. 40: 17.

Landolt H. P., Glatzel M., Blättler T., Achermann P., Roth C., Mathis J., Weis J., Tobler I., Aguzzi A., and Bassetti C. L. 2006. Sleep-wake disturbances in sporadic Creutzfeldt-Jakob disease. *Neurology*. 66: 1418-24.

Lee I. Y., Westaway D., Smit A. F., Wang K., Seto J., Chen L., Acharya C., et al. 1998. Complete genomic sequence and analysis of the prion protein gene region from three mammalian species. *Genome Res*. 8: 1022-37.

Lee S. D., Lai T. W., Lin S. Z., Lin C. H., Hsu Y. H., Li C. Y., Wang H. J., et al. 2013. Role of stress-inducible protein-1 in recruitment of bone marrow derived cells into the ischemic brains. *EMBO Mol Med*. 5: 1227-46.

Lewis V., Johanssen V. A., Crouch P. J., Klug G. M., Hooper N. M., and Collins S. J. 2016. Prion protein "gamma-cleavage": characterizing a novel endoproteolytic processing event. *Cell Mol Life Sci*. 73: 667-83.

Linden R. 2017. The biological function of the prion protein: A cell surface scaffold of signaling modules. *Front Mol Neurosci*. 10: 77.

Linden R., Martins V. R., Prado M. A., Cammarota M., Izquierdo I., and Brentani R. R. 2008. Physiology of the prion protein. *Physiol Rev*. 88: 673-728.

Lipp H. P., Stagliar-Bozicevic M., Fischer M., and Wolfer D. P. 1998. A 2-year longitudinal study of swimming navigation in mice devoid of the prion protein: no evidence for neurological anomalies or spatial learning impairments. *Behav Brain Res*. 95: 47-54.

Liu J., Zhao D., Liu C., Ding T., Yang L., Yin X., and Zhou X. 2014. Prion protein participates in the protection of mice from lipopolysaccharide infection by regulating the inflammatory process. *J Mol Neurosci*. 55: 279-87.

Liu S., Wang X., Sun F., Zhang J., Feng J., Liu H., Rajendran K. V., et al. 2013. RNA-Seq reveals expression signatures of genes involved in oxygen transport, protein synthesis, folding, and degradation in response to heat stress in catfish. *Physiol Genomics*. 45: 462-76.

Lledo P. M., Tremblay P., DeArmond S. J., Prusiner S. B., and Nicoll R. A. 1996. Mice deficient for prion protein exhibit normal neuronal excitability and synaptic transmission in the hippocampus. *Proc Natl Acad Sci USA*. 93: 2403-7.

Lobão-Soares B., Walz R., Carlotti C. G., Jr., Sakamoto A. C., Calvo F., Terzian A. L., da Silva J. A., Wichert-Ana L., Coimbra N. C., and Bianchin M. M. 2007. Cellular prion protein regulates the motor behaviour performance and anxiety-induced responses in genetically modified mice. *Behav Brain Res*. 183: 87-94.

Longa E. Z., Weinstein P. R., Carlson S., and Cummins R. 1989. Reversible middle cerebral artery occlusion without craniectomy in rats. *Stroke*. 20: 84-91.

Lopes M. H., Hajj G. N., Muras A. G., Mancini G. L., Castro R. M., Ribeiro K. C., Brentani R. R., Linden R., and Martins V. R. 2005. Interaction of cellular prion and stress-inducible protein 1 promotes neuritogenesis and neuroprotection by distinct signaling pathways. *J Neurosci*. 25: 11330-9.

Lye E., Dhanji S., Calzascia T., Elford A. R., and Ohashi P. S. 2008. IRAK-4 kinase activity is required for IRAK-4-dependent innate and adaptive immune responses. *Eur J Immunol*. 38: 870-6.

Lysek D. A., Schorn C., Nivon L. G., Esteve-Moya V., Christen B., Calzolai L., von Schroetter C., et al. 2005. Prion protein NMR structures of cats, dogs, pigs, and sheep. *Proc Natl Acad Sci USA*. 102: 640-5.

Mabbott N. A., Brown K. L., Manson J., and Bruce M. E. 1997. T-lymphocyte activation and the cellular form of the prion protein. *Immunology*. 92: 161-5.

Maes M., Kubera M., and Leunis J. C. 2008. The gut-brain barrier in major depression: intestinal mucosal dysfunction with an increased translocation of LPS from Gram negative enterobacteria (leaky gut) plays a role in the inflammatory pathophysiology of depression. *Neuro Endocrinol Lett*. 29: 117-24.

Magalhães A. C., Silva J. A., Lee K. S., Martins V. R., Prado V. F., Ferguson S. S., Gomez M. V., Brentani R. R., and Prado M. A. 2002. Endocytic intermediates involved with the intracellular trafficking of a fluorescent cellular prion protein. *J Biol Chem*. 277: 33311-8.

Mahal S. P., Asante E. A., Antoniou M., and Collinge J. 2001. Isolation and functional characterisation of the promoter region of the human prion protein gene. *Gene*. 268: 105-14.

Maiti N. R., and Surewicz W. K. 2001. The role of disulfide bridge in the folding and stability of the recombinant human prion protein. *J Biol Chem*. 276: 2427-31.

Mallucci G., Dickinson A., Linehan J., Klöhn P. C., Brandner S., and Collinge J. 2003. Depleting neuronal PrP in prion infection prevents disease and reverses spongiosis. *Science*. 302: 871-4.

Mallucci G. R., Ratté S., Asante E. A., Linehan J., Gowland I., Jefferys J. G., and Collinge J. 2002. Post-natal knockout of prion protein alters hippocampal CA1 properties, but does not result in neurodegeneration. *EMBO J*. 21: 202-10.

Manson J. C., Clarke A. R., Hooper M. L., Aitchison L., McConnell I., and Hope J. 1994. 129/Ola mice carrying a null mutation in PrP that abolishes mRNA production are developmentally normal. *Mol Neurobiol*. 8: 121-7.

Manson J. C., Hope J., Clarke A. R., Johnston A., Black C., and MacLeod N. 1995. PrP gene dosage and long term potentiation. *Neurodegeneration*. 4: 113-4.

Mariante R. M., Nóbrega A., Martins R. A., Areal R. B., Bellio M., and Linden R. 2012. Neuroimmunoendocrine regulation of the prion protein in neutrophils. *J Biol Chem*. 287: 35506-15.

Marioni J. C., Mason C. E., Mane S. M., Stephens M., and Gilad Y. 2008. RNA-seq: an assessment of technical reproducibility and comparison with gene expression arrays. *Genome Res*. 18: 1509-17.

Marques A. T., Nordio L., Lecchi C., Grilli G., Giudice C., and Ceciliani F. 2017. Widespread extrahepatic expression of acute-phase proteins in healthy chicken (*Gallus gallus*) tissues. *Vet Immunol Immunopathol*. 190: 10-17.

Marques F., Sousa J. C., Brito M. A., Pahnke J., Santos C., Correia-Neves M., and Palha J. A. 2016. The choroid plexus in health and in disease: dialogues into and out of the brain. *Neurobiol Dis*. 107: 32-40.

Marques F., Sousa J. C., Coppola G., Falcao A. M., Rodrigues A. J., Geschwind D. H., Sousa N., Correia-Neves M., and Palha J. A. 2009. Kinetic profile of the transcriptome changes induced in the choroid plexus by peripheral inflammation. *J Cereb Blood Flow Metab*. 29: 921-32.

Martin G. R., Keenan C. M., Sharkey K. A., and Jirik F. R. 2011. Endogenous prion protein attenuates experimentally induced colitis. *Am J Pathol*. 179: 2290-301.

Masel J., Genoud N., and Aguzzi A. 2005. Efficient inhibition of prion replication by PrP-Fc_2 suggests that the prion is a PrP^{Sc} oligomer. *J Mol Biol*. 345: 1243-51.

Mays C. E., Kim C., Haldiman T., van der Merwe J., Lau A., Yang J., Grams J., et al. 2014. Prion disease tempo determined by host-dependent substrate reduction. *J Clin Invest*. 124: 847-58.

McDonald A. J., and Millhauser G. L. 2014. PrP overdrive: does inhibition of alpha-cleavage contribute to PrP^{C} toxicity and prion disease? *Prion*. 8: 183-91.

McHugh P. C., Wright J. A., Williams R. J., and Brown D. R. 2012. Prion protein expression alters APP cleavage without interaction with BACE-1. *Neurochem Int*. 61: 672-80.

McMahon H. E., Mangé A., Nishida N., Créminon C., Casanova D., and Lehmann S. 2001. Cleavage of the amino terminus of the prion protein by reactive oxygen species. *J Biol Chem*. 276: 2286-91.

Medori R., Tritschler H. J., LeBlanc A., Villare F., Manetto V., Chen H. Y., Xue R., et al. 1992. Fatal familial insomnia, a prion disease with a mutation at codon 178 of the prion protein gene. *N Engl J Med*. 326: 444-9.

Meotti F. C., Carqueja C. L., Gadotti Vde M., Tasca C. I., Walz R., and Santos A. R. 2007. Involvement of cellular prion protein in the nociceptive response in mice. *Brain Res*. 1151: 84-90.

Mitsios N., Saka M., Krupinski J., Pennucci R., Sanfeliu C., Miguel Turu M., Gaffney J., et al. 2007. Cellular prion protein is increased in the plasma and peri-infarcted brain tissue after acute stroke. *J Neurosci Res*. 85: 602-11.

Mitteregger G., Vosko M., Krebs B., Xiang W., Kohlmannsperger V., Nölting S., Hamann G. F., and Kretzschmar H. A. 2007. The role of the octarepeat region in neuroprotective function of the cellular prion protein. *Brain Pathol*. 17: 174-83.

Moore R. C., Lee I. Y., Silverman G. L., Harrison P. M., Strome R., Heinrich C., Karunaratne A., et al. 1999. Ataxia in prion protein (PrP)-deficient mice is associated with upregulation of the novel PrP-like protein doppel. *J Mol Biol*. 292: 797-817.

Morel E., Fouquet S., Chateau D., Yvernault L., Frobert Y., Pincon-Raymond M., Chambaz J., Pillot T., and Rousset M. 2004. The cellular prion protein PrP^{C} is expressed in human enterocytes in cell-cell junctional domains. *J Biol Chem*. 279: 1499-505.

Morel E., Fouquet S., Strup-Perrot C., Pichol Thievend C., Petit C., Loew D., Faussat A. M., et al. 2008. The cellular prion protein PrP^{C} is involved in the proliferation of epithelial cells and in the distribution of junction-associated proteins. *PLoS One*. 3: e3000.

Moser M., Colello R. J., Pott U., and Oesch B. 1995. Developmental expression of the prion protein gene in glial cells. *Neuron*. 14: 509-17.

Murray C., Griffin É. W., O'Loughlin E., Lyons A., Sherwin E., and Ahmed S. 2015. Interdependent and independent roles of type I interferons and IL-6 in innate immune, neuroinflammatory and sickness behaviour responses to systemic poly I:C. *Brain Behav Immun.* 48: 274-86.

Nagel-Alne G. E., Asheim L. J., Hardaker J. B., Sølverød L., Lindheim D., and Valle P. S. 2014. The Norwegian healthier goats programme - a financial cost-benefit analysis. *Prev Vet Med*. 114: 96-105.

Nasu-Nishimura Y., Taniuchi Y., Nishimura T., Sakudo A., Nakajima K., Ano Y., Sugiura K., Sakaguchi S., Itohara S., and Onodera T. 2008. Cellular prion protein prevents brain damage after encephalomyocarditis virus infection in mice. *Arch Virol*. 153: 1007-12.

Negro A., Ballarin C., Bertoli A., Massimino M. L., and Sorgato M. C. 2001. The metabolism and imaging in live cells of the bovine prion protein in its native form or carrying single amino acid substitutions. *Mol Cell Neurosci*. 17: 521-38.

Nico P. B., de-Paris F., Vinadé E. R., Amaral O. B., Rockenbach I., Soares B. L., Guarnieri R., et al. 2005. Altered behavioural response to acute stress in mice lacking cellular prion protein. *Behav Brain Res*. 162: 173-81.

Nuvolone M., Hermann M., Sorce S., Russo G., Tiberi C., Schwarz P., Minikel E., Sanoudou D., Pelczar P., and Aguzzi A. 2016. Strictly co-isogenic C57BL/6J-*Prnp*$^{-/-}$ mice: A rigorous resource for prion science. *J Exp Med*. 213: 313-27.

Nuvolone M., Kana V., Hutter G., Sakata D., Mortin-Toth S. M., Russo G., Danska J. S., and Aguzzi A. 2013. SIRPα polymorphisms, but not the prion protein, control phagocytosis of apoptotic cells. *J Exp Med*. 210: 2539-52.

Onodera T., Sakudo A., Tsubone H., and Itohara S. 2014. Review of studies that have used knockout mice to assess normal function of prion protein under immunological or pathophysiological stress. *Microbiol Immunol*. 58: 361-74.

Paavola K. J., Sidik H., Zuchero J. B., Eckart M., and Talbot W. S. 2014. Type IV collagen is an activating ligand for the adhesion G protein-coupled receptor GPR126. *Science Signaling*. 7: ra76.

Papassotiropoulos A., Wollmer M. A., Aguzzi A., Hock C., Nitsch R. M., and de Quervain D. J. 2005. The prion gene is associated with human long-term memory. *Hum Mol Genet*. 14: 2241-6.

Park B. S., Song D. H., Kim H. M., Choi B. S., Lee H., and Lee J. O. 2009. The structural basis of lipopolysaccharide recognition by the TLR4-MD2 complex. *Nature*. 458: 1191-5.

Parkin E. T., Watt N. T., Hussain I., Eckman E. A., Eckman C. B., Manson J. C., Baybutt H. N., Turner A. J., and Hooper N. M. 2007. Cellular prion protein regulates β-secretase cleavage of the Alzheimer's amyloid precursor protein. *Proc Natl Acad Sci USA*. 104: 11062-7.

Pauly P. C., and Harris D. A. 1998. Copper stimulates endocytosis of the prion protein. *J Biol Chem*. 273: 33107-10.

Peralta O. A., and Eyestone W. H. 2009. Quantitative and qualitative analysis of cellular prion protein (PrP^C) expression in bovine somatic tissues. *Prion*. 3: 161-70.

Peralta O. A., Huckle W. R., and Eyestone W. H. 2012. Developmental expression of the cellular prion protein (PrP^C) in bovine embryos. *Mol Reprod Dev*. 79: 488-98.

Perera W. S., and Hooper N. M. 2001. Ablation of the metal ion-induced endocytosis of the prion protein by disease-associated mutation of the octarepeat region. *Curr Biol*. 11: 519-23.

Petersen S. C., Luo R., Liebscher I., Giera S., Jeong S. J., Mogha A., Ghidinelli M., et al. 2015. The adhesion GPCR GPR126 has distinct, domain-dependent functions in Schwann cell development mediated by interaction with laminin-211. *Neuron*. 85: 755-69.

Petit C. S. V., Barreau F., Besnier L., Gandille P., Riveau B., Chateau D., Roy M., et al. 2012. Requirement of cellular prion protein for intestinal barrier function and mislocalization in patients with inflammatory bowel disease. *Gastroenterology*. 143: 122-32.

Pfaffl M. W. 2001. A new mathematical model for relative quantification in real-time RT-PCR. *Nucleic Acids Res*. 29: e45.

Pioli P. D., Saleh A. M., El Fiky A., Nastiuk K. L., and Krolewski J. J. 2012. Sequential proteolytic processing of an interferon-α receptor subunit by TNF-α converting enzyme and presenilins. *J Interferon Cytokine Res*. 32: 312-25.

Pritzkow S., Morales R., Moda F., Khan U., Telling G. C., Hoover E., and Soto C. 2015. Grass plants bind, retain, uptake, and transport infectious prions. *Cell Rep*. 11: 1168-75.

Prusiner S. B. 1982. Novel proteinaceous infectious particles cause scrapie. *Science*. 216: 136-44.

Prusiner S. B., Groth D., Serban A., Koehler R., Foster D., Torchia M., Burton D., Yang S. L., and DeArmond S. J. 1993. Ablation of the prion protein (PrP) gene in mice prevents scrapie and facilitates production of anti-PrP antibodies. *Proc Natl Acad Sci USA*. 90: 10608-12.

Puckett C., Concannon P., Casey C., and Hood L. 1991. Genomic structure of the human prion protein gene. *Am J Hum Genet*. 49: 320-9.

Rachidi W., Vilette D., Guiraud P., Arlotto M., Riondel J., Laude H., Lehmann S., and Favier A. 2003. Expression of prion protein increases cellular copper binding and antioxidant enzyme activities but not copper delivery. *J Biol Chem*. 278: 9064-72.

Rajkumar A. P., Qvist P., Lazarus R., Lescai F., Ju J., Nyegaard M., Mors O., Borglum A. D., Li Q., and Christensen J. H. 2015. Experimental validation of methods for differential gene expression analysis and sample pooling in RNA-seq. *BMC Genomics*. 16: 548.

Ramos-Vara J. A. 2005. Technical aspects of immunohistochemistry. *Vet Pathol*. 42: 405-26.

Ransohoff R. M., and Cardona A. E. 2010. The myeloid cells of the central nervous system parenchyma. *Nature*. 468: 253-62.

Reinhart K., Bauer M., Riedemann N. C., and Hartog C. S. 2012. New approaches to sepsis: molecular diagnostics and biomarkers. *Clin Microbiol Rev*. 25: 609-34.

Reiten M. R., Bakkebø M. K., Brun-Hansen H., Lewandowska-Sabat A. M., Olsaker I., Tranulis M. A., Espenes A., and Boysen P. 2015. Hematological shift in goat kids naturally devoid of prion protein. *Front Cell Dev Biol*. 3: 44.

Reynolds K., Novosad B., Hoffhines A., Gipson J., Johnson J., Peters J., Gonzalez F., Gimble J., and Hill M. 2002. Pretreatment with troglitazone decreases lethality during endotoxemia in mice. *J Endotoxin Res*. 8: 307-14.

Rial D., Duarte F. S., Xikota J. C., Schmitz A. E., Dafré A. L., Figueiredo C. P., Walz R., and Prediger R. D. 2009. Cellular prion protein modulates age-related behavioral and neurochemical alterations in mice. *Neuroscience*. 164: 896-907.

Richardson D. D., Tol S., Valle-Encinas E., Pleguezuelos C., Bierings R., Geerts D., and Fernandez-Borja M. 2015. The prion protein inhibits monocytic cell migration by stimulating β1 integrin adhesion and uropod formation. *J Cell Sci*. 128: 3018-29.

Richt J. A., Kasinathan P., Hamir A. N., Castilla J., Sathiyaseelan T., Vargas F., Sathiyaseelan J., et al. 2007. Production of cattle lacking prion protein. *Nat Biotechnol*. 25: 132-8.

Rieger R., Edenhofer F., Lasmézas C. I., and Weiss S. 1997. The human 37-kDa laminin receptor precursor interacts with the prion protein in eukaryotic cells. *Nat Med*. 3: 1383-8.

Riemer C., Queck I., Simon D., Kurth R., and Baier M. 2000. Identification of upregulated genes in scrapie-infected brain tissue. *J Virol*. 74: 10245-8.

Roesler R., Walz R., Quevedo J., de-Paris F., Zanata S. M., Graner E., Izquierdo I., Martins V. R., and Brentani R. R. 1999. Normal inhibitory avoidance learning and anxiety, but increased locomotor activity in mice devoid of PrP^{C}. *Brain Res Mol Brain Res*. 71: 349-53.

Russell W. M. S., and Burch R. L. 1959. The removal of inhumanity: The three R's. *In:* The principles of humane experimental technique. London, Methuen & Co. Ltd.

Sakaguchi S., Katamine S., Nishida N., Moriuchi R., Shigematsu K., Sugimoto T., Nakatani A., et al. 1996. Loss of cerebellar Purkinje cells in aged mice homozygous for a disrupted PrP gene. *Nature*. 380: 528-31.

Sakudo A., Hamaishi M., Hosokawa-Kanai T., Tuchiya K., Nishimura T., Saeki K., Matsumoto Y., Ueda S., and Onodera T. 2003. Absence of superoxide dismutase activity in a soluble cellular isoform of prion protein produced by baculovirus expression system. *Biochem Biophys Res Commun*. 307: 678-83.

Sánchez-Alavez M., Conti B., Moroncini G., and Criado J. R. 2007. Contributions of neuronal prion protein on sleep recovery and stress response following sleep deprivation. *Brain Res*. 1158: 71-80.

Santuccione A., Sytnyk V., Leshchyns'ka I., and Schachner M. 2005. Prion protein recruits its neuronal receptor NCAM to lipid rafts to activate p59fyn and to enhance neurite outgrowth. *J Cell Biol*. 169: 341-54.

Sarnataro D., Campana V., Paladino S., Stornaiuolo M., Nitsch L., and Zurzolo C. 2004. PrP^C association with lipid rafts in the early secretory pathway stabilizes its cellular conformation. *Mol Biol Cell*. 15: 4031-42.

Sato S., Sanjo H., Takeda K., Ninomiya-Tsuji J., Yamamoto M., Kawai T., Matsumoto K., Takeuchi O., and Akira S. 2005. Essential function for the kinase TAK1 in innate and adaptive immune responses. *Nat Immunol*. 6: 1087-95.

Schiepers O. J., Wichers M. C., and Maes M. 2005. Cytokines and major depression. *Prog Neuropsychopharmacol Biol Psychiatry*. 29: 201-17.

Schmitz M., Greis C., Ottis P., Silva C. J., Schulz-Schaeffer W. J., Wrede A., Koppe K., et al. 2014. Loss of prion protein leads to age-dependent behavioral abnormalities and changes in cytoskeletal protein expression. *Mol Neurobiol*. 50: 923-36.

Schumann R. R., Leong S. R., Flaggs G. W., Gray P. W., Wright S. D., Mathison J. C., Tobias P. S., and Ulevitch R. J. 1990. Structure and function of lipopolysaccharide binding protein. *Science*. 249: 1429-31.

Seok J., Warren H. S., Cuenca A. G., Mindrinos M. N., Baker H. V., Xu W., Richards D. R., et al. 2013. Genomic responses in mouse models poorly mimic human inflammatory diseases. *Proc Natl Acad Sci USA*. 110: 3507-12.

Shechter R., London A., and Schwartz M. 2013. Orchestrated leukocyte recruitment to immune-privileged sites: absolute barriers versus educational gates. *Nat Rev Immunol*. 13: 206-18.

Shyng S. L., Heuser J. E., and Harris D. A. 1994. A glycolipid-anchored prion protein is endocytosed via clathrin-coated pits. *J Cell Biol*. 125: 1239-50.

Shyng S. L., Huber M. T., and Harris D. A. 1993. A prion protein cycles between the cell surface and an endocytic compartment in cultured neuroblastoma cells. *J Biol Chem*. 268: 15922-8.

Shyu W. C., Chen C. P., Saeki K., Kubosaki A., Matusmoto Y., Onodera T., Ding D. C., et al. 2005a. Hypoglycemia enhances the expression of prion protein and heat-shock protein 70 in a mouse neuroblastoma cell line. *J Neurosci Res*. 80: 887-94.

Shyu W. C., Kao M. C., Chou W. Y., Hsu Y. D., and Soong B. W. 2000. Heat shock modulates prion protein expression in human NT-2 cells. *Neuroreport*. 11: 771-4.

Shyu W. C., Lin S. Z., Chiang M. F., Ding D. C., Li K. W., Chen S. F., Yang H. I., and Li H. 2005b. Overexpression of PrP^C by adenovirus-mediated gene targeting reduces ischemic injury in a stroke rat model. *J Neurosci*. 25: 8967-77.

Shyu W. C., Lin S. Z., Saeki K., Kubosaki A., Matsumoto Y., Onodera T., Chiang M. F., Thajeb P., and Li H. 2004. Hyperbaric oxygen enhances the expression of prion protein and heat shock protein 70 in a mouse neuroblastoma cell line. *Cell Mol Neurobiol*. 24: 257-68.

Singh A., Haldar S., Horback K., Tom C., Zhou L., Meyerson H., and Singh N. 2013. Prion protein regulates iron transport by functioning as a ferrireductase. *J Alzheimers Dis*. 35: 541-52.

Singh A., Isaac A. O., Luo X., Mohan M. L., Cohen M. L., Chen F., Kong Q., Bartz J., and Singh N. 2009a. Abnormal brain iron homeostasis in human and animal prion disorders. *PLoS Pathog*. 5: e1000336.

Singh A., Kong Q., Luo X., Petersen R. B., Meyerson H., and Singh N. 2009b. Prion protein (PrP) knock-out mice show altered iron metabolism: a functional role for PrP in iron uptake and transport. *PLoS One*. 4: e6115.

Singh A., Mohan M. L., Isaac A. O., Luo X., Petrak J., Vyoral D., and Singh N. 2009c. Prion protein modulates cellular iron uptake: a novel function with implications for prion disease pathogenesis. *PLoS One*. 4: e4468.

Skovgaard K., Mortensen S., Boye M., Poulsen K. T., Campbell F. M., Eckersall P. D., and Heegaard P. M. 2009. Rapid and widely disseminated acute phase protein response after experimental bacterial infection of pigs. *Vet Res*. 40: 23.

Smith P. D., Suffredini A. F., Allen J. B., Wahl L. M., Parrillo J. E., and Wahl S. M. 1994. Endotoxin administration to humans primes alveolar macrophages for increased production of inflammatory mediators. *J Clin Immunol*. 14: 141-8.

Sone Y., Serikov V. B., and Staub N. C., Sr. 1999. Intravascular macrophage depletion attenuates endotoxin lung injury in anesthetized sheep. *J Appl Physiol*. 87: 1354-9.

Spudich A., Frigg R., Kilic E., Kilic U., Oesch B., Raeber A., Bassetti C. L., and Hermann D. M. 2005. Aggravation of ischemic brain injury by prion protein deficiency: role of ERK-1/-2 and STAT-1. *Neurobiol Dis*. 20: 442-9.

Stahl N., Borchelt D. R., Hsiao K., and Prusiner S. B. 1987. Scrapie prion protein contains a phosphatidylinositol glycolipid. *Cell*. 51: 229-40.

Steele A. D., Zhou Z., Jackson W. S., Zhu C., Auluck P., Moskowitz M. A., Chesselet M. F., and Lindquist S. 2009. Context dependent neuroprotective properties of prion protein (PrP). *Prion*. 3: 240-9.

Stewart R. S., and Harris D. A. 2005. A transmembrane form of the prion protein is localized in the Golgi apparatus of neurons. *J Biol Chem*. 280: 15855-64.

Takeuchi Y., Kikusui T., Kizumi O., Ohnishi H., and Mori Y. 1997. Pathophysiological changes evoked by lipopolysaccharide administration in goats. *J Vet Med Sci*. 59: 125-7.

Takeuchi Y., Kikusui T., and Mori Y. 1995. Changes in the behavioral parameters following the lipopolysaccharide administration in goats. *J Vet Med Sci*. 57: 1041-4.

Talwar S., Munson P. J., Barb J., Fiuza C., Cintron A. P., Logun C., Tropea M., et al. 2006. Gene expression profiles of peripheral blood leukocytes after endotoxin challenge in humans. *Physiol Genomics*. 25: 203-15.

Tapping R. I., Akashi S., Miyake K., Godowski P. J., and Tobias P. S. 2000. Toll-like receptor 4, but not toll-like receptor 2, is a signaling receptor for *Escherichia* and *Salmonella* lipopolysaccharides. *J Immunol*. 165: 5780-7.

Thiemermann C., Ruetten H., Wu C. C., and Vane J. R. 1995. The multiple organ dysfunction syndrome caused by endotoxin in the rat: attenuation of liver dysfunction by inhibitors of nitric oxide synthase. *Br J Pharmacol*. 116: 2845-51.

Thomzig A., Schulz-Schaeffer W., Wrede A., Wemheuer W., Brenig B., Kratzel C., Lemmer K., and Beekes M. 2007. Accumulation of pathological prion protein PrP^{Sc} in the skin of animals with experimental and natural scrapie. *PLoS Pathog*. 3: e66.

Tobler I., Gaus S. E., Deboer T., Achermann P., Fischer M., Rülicke T., Moser M., Oesch B., McBride P. A., and Manson J. C. 1996. Altered circadian activity rhythms and sleep in mice devoid of prion protein. *Nature*. 380: 639-42.

Tothova C., Nagy O., and Kovac G. 2014. Acute phase proteins and their use in the diagnosis of diseases in ruminants: a review. *Vet Med (Praha)*. 59: 163-80.

Tranulis M. A. 2002. Influence of the prion protein gene, *Prnp*, on scrapie susceptibility in sheep. *APMIS*. 110: 33-43.

Tranulis M. A., Espenes A., Comincini S., Skretting G., and Harbitz I. 2001. The PrP-like protein Doppel gene in sheep and cattle: cDNA sequence and expression. *Mamm Genome*. 12: 376-9.

Treiber C., Pipkorn R., Weise C., Holland G., and Multhaup G. 2007. Copper is required for prion protein-associated superoxide dismutase-I activity in *Pichia pastoris*. *FEBS J*. 274: 1304-11.

Tremblay P., Bouzamondo-Bernstein E., Heinrich C., Prusiner S. B., and DeArmond S. J. 2007. Developmental expression of PrP in the post-implantation embryo. *Brain Res*. 1139: 60-7.

Tsutsui S., Hahn J. N., Johnson T. A., Ali Z., and Jirik F. R. 2008. Absence of the cellular prion protein exacerbates and prolongs neuroinflammation in experimental autoimmune encephalomyelitis. *Am J Pathol*. 173: 1029-41.

Vaure C., and Liu Y. 2014. A comparative review of toll-like receptor 4 expression and functionality in different animal species. *Front Immunol*. 5: 316.

Walmsley A. R., Watt N. T., Taylor D. R., Perera W. S., and Hooper N. M. 2009. Alpha-cleavage of the prion protein occurs in a late compartment of the secretory pathway and is independent of lipid rafts. *Mol Cell Neurosci*. 40: 242-8.

Walter E. D., Stevens D. J., Visconte M. P., and Millhauser G. L. 2007. The prion protein is a combined zinc and copper binding protein: Zn^{2+} alters the distribution of Cu^{2+} coordination modes. *J Am Chem Soc*. 129: 15440-1.

Wang M., Zhao D., Yang Y., Liu J., Wang J., Yin X., Yang L., and Zhou X. 2014a. The cellular prion protein negatively regulates phagocytosis and cytokine expression in murine bone marrow-derived macrophages. *PLoS One*. 9: e102785.

Wang S., Furmanek T., Kryvi H., Krossoy C., Totland G. K., Grotmol S., and Wargelius A. 2014b. Transcriptome sequencing of Atlantic salmon (*Salmo salar L.*) notochord prior to development of the vertebrae provides clues to regulation of positional fate, chordoblast lineage and mineralisation. *BMC Genomics*. 15: 141.

Wang V., Chuang T. C., Hsu Y. D., Chou W. Y., and Kao M. C. 2005. Nitric oxide induces prion protein via MEK and p38 MAPK signaling. *Biochem Biophys Res Commun*. 333: 95-100.

Wang Z., Gerstein M., and Snyder M. 2009. RNA-Seq: a revolutionary tool for transcriptomics. *Nat Rev Genet*. 10: 57-63.

Watt N. T., Routledge M. N., Wild C. P., and Hooper N. M. 2007. Cellular prion protein protects against reactive-oxygen-species-induced DNA damage. *Free Radic Biol Med*. 43: 959-67.

Watt N. T., Taylor D. R., Gillott A., Thomas D. A., Perera W. S., and Hooper N. M. 2005. Reactive oxygen species-mediated beta-cleavage of the prion protein in the cellular response to oxidative stress. *J Biol Chem*. 280: 35914-21.

Watt N. T., Taylor D. R., Kerrigan T. L., Griffiths H. H., Rushworth J. V., Whitehouse I. J., and Hooper N. M. 2012. Prion protein facilitates uptake of zinc into neuronal cells. *Nat Commun*. 3: 1134.

Watts J. C., Drisaldi B., Ng V., Yang J., Strome B., Horne P., Sy M. S., et al. 2007. The CNS glycoprotein Shadoo has PrP^{C}-like protective properties and displays reduced levels in prion infections. *EMBO J*. 26: 4038-50.

Weise J., Crome O., Sandau R., Schulz-Schaeffer W., Bähr M., and Zerr I. 2004. Upregulation of cellular prion protein (PrP^{C}) after focal cerebral ischemia and influence of lesion severity. *Neurosci Lett*. 372: 146-50.

Welker E., Wedemeyer W. J., and Scheraga H. A. 2001. A role for intermolecular disulfide bonds in prion diseases? *Proc Natl Acad Sci USA*. 98: 4334-6.

Whitehouse I. J., Brown D., Baybutt H., Diack A. B., Kellett K. A., Piccardo P., Manson J. C., and Hooper N. M. 2016. Ablation of prion protein in wild type human amyloid precursor protein (APP) transgenic mice does not alter the proteolysis of APP, levels of amyloid-beta or pathologic phenotype. *PLoS One*. 11: e0159119.

Whittington M. A., Sidle K. C., Gowland I., Meads J., Hill A. F., Palmer M. S., Jefferys J. G., and Collinge J. 1995. Rescue of neurophysiological phenotype seen in PrP null mice by transgene encoding human prion protein. *Nat Genet*. 9: 197-201.

Wilson T. C., Bachurski C. J., Ikegami M., Jobe A. H., and Kallapur S. G. 2005. Pulmonary and systemic induction of SAA3 after ventilation and endotoxin in preterm lambs. *Pediatr Res*. 58: 1204-9.

Winklhofer K. F., Tatzelt J., and Haass C. 2008. The two faces of protein misfolding: gain- and loss-of-function in neurodegenerative diseases. *EMBO J*. 27: 336-49.

Wong B. S., Brown D. R., Pan T., Whiteman M., Liu T., Bu X., Li R., et al. 2001a. Oxidative impairment in scrapie-infected mice is associated with brain metals perturbations and altered antioxidant activities. *J Neurochem*. 79: 689-98.

Wong B. S., Liu T., Li R., Pan T., Petersen R. B., Smith M. A., Gambetti P., et al. 2001b. Increased levels of oxidative stress markers detected in the brains of mice devoid of prion protein. *J Neurochem*. 76: 565-72.

Wopfner F., Weidenhöfer G., Schneider R., von Brunn A., Gilch S., Schwarz T. F., Werner T., and Schätzl H. M. 1999. Analysis of 27 mammalian and 9 avian PrPs reveals high conservation of flexible regions of the prion protein. *J Mol Biol*. 289: 1163-78.

Wright J. A., McHugh P. C., Stockbridge M., Lane S., Kralovicova S., and Brown D. R. 2009. Activation and repression of prion protein expression by key regions of intron 1. *Cell Mol Life Sci*. 66: 3809-20.

Wulf M. A., Senatore A., and Aguzzi A. 2017. The biological function of the cellular prion protein: an update. *BMC Biol*. 15: 34.

Yamamoto M., Sato S., Hemmi H., Hoshino K., Kaisho T., Sanjo H., Takeuchi O., et al. 2003. Role of adaptor TRIF in the MyD88-independent toll-like receptor signaling pathway. *Science*. 301: 640-3.

Yan X. B., Li C. Y., Wang S., Lv O., and Xuan M. W. 2016. Effect of interferon-beta on the expression of cytoskeleton and cellular elasticity associated protein in astrocytes. *Int J Clin Exp Med*. 9: 23102-10.

Yao W., Cai X., Liu C., Qin Y., Cheng H., Ji S., Xu W., et al. 2013. Profilin 1 potentiates apoptosis induced by staurosporine in cancer cells. *Curr Mol Med*. 13: 417-28.

Yu G., Chen J., Yu H., Liu S., Chen J., Xu X., Sha H., et al. 2006. Functional disruption of the prion protein gene in cloned goats. *J Gen Virol*. 87: 1019-27.

Zafar S., Behrens C., Dihazi H., Schmitz M., Zerr I., Schulz-Schaeffer W. J., Ramljak S., and Asif A. R. 2017. Cellular prion protein mediates early apoptotic proteome alternation and phospho-modification in human neuroblastoma cells. *Cell Death Dis*. 8: e2557.

Zafar S., von Ahsen N., Oellerich M., Zerr I., Schulz-Schaeffer W. J., Armstrong V. W., and Asif A. R. 2011. Proteomics approach to identify the interacting partners of cellular prion protein and characterization of Rab7a interaction in neuronal cells. *J Proteome Res*. 10: 3123-35.

Zahn R., Liu A., Lührs T., Riek R., von Schroetter C., López García F., Billeter M., Calzolai L., Wider G., and Wüthrich K. 2000. NMR solution structure of the human prion protein. *Proc Natl Acad Sci USA*. 97: 145-50.

Zanata S. M., Lopes M. H., Mercadante A. F., Hajj G. N., Chiarini L. B., Nomizo R., Freitas A. R., et al. 2002. Stress-inducible protein 1 is a cell surface ligand for cellular prion that triggers neuroprotection. *EMBO J*. 21: 3307-16.

Zhang C. C., Steele A. D., Lindquist S., and Lodish H. F. 2006. Prion protein is expressed on long-term repopulating hematopoietic stem cells and is important for their self-renewal. *Proc Natl Acad Sci USA*. 103: 2184-9.

Zocche Soprana H., Canes Souza L., Debbas V., and Martins Laurindo F. R. 2011. Cellular prion protein (PrP^{C}) and superoxide dismutase (SOD) in vascular cells under oxidative stress. *Exp Toxicol Pathol*. 63: 229-36.

Enclosed papers I, II, III and IV.

Paper I

Salvesen et al. BMC Veterinary Research (2016) 12:241
DOI 10.1186/s12917-016-0870-x

BMC Veterinary Research

RESEARCH ARTICLE Open Access

Activation of innate immune genes in caprine blood leukocytes after systemic endotoxin challenge

Øyvind Salvesen[1], Malin R. Reiten[1], Peter M. H. Heegaard[2], Michael A. Tranulis[1], Arild Espenes[1], Kerstin Skovgaard[2] and Cecilie Ersdal[1*]

Abstract

Background: Sepsis is a serious health problem associated with a range of infectious diseases in animals and humans. Early events of this syndrome can be mimicked by experimental administration of lipopolysaccharides (LPS). Compared with mice, small ruminants and humans are highly sensitive to LPS, making goats valuable in inflammatory models. We performed a longitudinal study in eight Norwegian dairy goats that received LPS (0.1 μg/kg, *Escherichia coli* O26:B6) intravenously. A control group of five goats received corresponding volumes of sterile saline. Clinical examinations were performed continuously, and blood samples were collected throughout the trial.

Results: Characteristic signs of acute sepsis, such as sickness behavior, fever, and leukopenia were observed within 1 h of LPS administration. A high-throughput longitudinal gene expression analysis of circulating leukocytes was performed, and genes associated with the acute phase response, type I interferon signaling, LPS cascade and apoptosis, in addition to cytokines and chemokines were targeted. Pro-inflammatory genes, such as IL1B, CCL3 and IL8, were significantly up-regulated. Interestingly, increased mRNA levels of seven interferon stimulated genes (ISGs) were observed peaking at 2 h, corroborating the increasing evidence that ISGs respond immediately to bacterial endotoxins. A slower response was manifested by four extrahepatic acute phase proteins (APP) (SAA3, HP, LF and LCN2) reaching maximum levels at 5 h.

Conclusions: We report an immediate induction of ISGs in leukocytes in response to LPS supporting a link between the interferon system and defense against bacterial infections. The extrahepatic expression of APPs suggests that leukocytes contribute to synthesis of these proteins at the beginning of a systemic inflammation. Taken together, these findings provide insights into the dynamic regulation of innate immune genes, as well as raising new questions regarding the importance of ISGs and extrahepatic APPs in leukocytes after systemic endotoxin challenge.

Keywords: Interferon stimulated genes, Extrahepatic acute phase proteins, Systemic inflammation, Lipopolysaccharide (LPS), Endotoxemia, Blood leukocyte gene expression, Innate immunity, Goat

* Correspondence: cecilie.ersdal@nmbu.no
[1]Faculty of Veterinary Medicine and Biosciences, Norwegian University of Life Sciences, Oslo, Norway
Full list of author information is available at the end of the article

Background

Sepsis is a life-threatening condition caused by a dysregulated host response that can occur in a range of bacterial, viral, or toxic diseases in animals and humans [1]. Initial events of this syndrome can be mimicked by experimental administration of LPS, derived from the cell-wall of gram-negative bacteria. The host response to LPS is complex and reveals major species differences [2–4]. Interestingly, some species such as mice and the Rhesus monkey, have developed tolerance by limiting harmful inflammation even when the pathogen loads are high [4]. At the other end of the sensitivity spectrum are humans, rabbits and small ruminants, which are extremely sensitive to endotoxins [2–4]. This marked difference in sensitivity towards LPS has led scientists to question the validity of extrapolation of rodent inflammatory responses to human medicine [5].

LPS is a potent stimulator of the innate immune system that provides the first line of defense against pathogens and initiates the acute phase response (APR) [6]. Among leukocytes, circulating monocytes and neutrophils are the primary target cells involved in protection against LPS. These cells constitutively express membrane-bound CD14 and Toll-like receptor 4 (TLR4), important for endotoxin recognition and activation of the innate immune system [6, 7]. Upon LPS stimulation, the CD14-MD-2-TLR4-complex initiates signaling through MyD88-dependent or TRIF-dependent pathways [8], leading to the expression of pro-inflammatory cytokines, chemokines and enzymes [6, 9, 10]. The ensuing physiological response culminate in a behavioral state referred to as sickness behavior [11].

Activated immune cells release pro-inflammatory mediators, such as IL-1, IL-6, IL-8 and TNF-α, which stimulate the liver to produce positive acute phase proteins (APPs) [12] and simultaneously down-regulate negative APPs [13]. The major APPs in goat, serum amyloid A (SAA) and haptoglobin (HP), serve several functions in the APR [14] and are valuable diagnostic indicators of inflammation [13, 15]. APPs are also released from extrahepatic tissues such as mammary gland [16, 17], lungs [18], adipose tissue [19, 20], colon [20], and lymphoid organs [12], but their patho-physiological significance is incompletely understood. The role of APPs released from leukocytes during infections or endotoxemia has been the subject of only a few previous studies [12].

Increasing evidence show that LPS induces transcription of interferon stimulated genes (ISGs), originally considered exclusively anti-viral, but with accumulating data indicating a range of other immunomodulatory properties [21]. The in vivo regulation of these genes in leukocytes, however, has not been described in detail.

In 2013, the worldwide population of small ruminants comprised about 1006 million goats and 1073 million sheep [22]. Large herds and intensive production increase the number of endotoxin-related diseases such as acute ruminal acidosis, per-acute mastitis, toxic metritis, and septic peritonitis. Additionally, failure of, or insufficient, passive transfer of colostral immunoglobulins is a common cause of neonatal sepsis in lambs and goat kids [23]. Circulating leukocytes play a crucial role in initiating the APR in all sepsis-related diseases. Thus, investigation of changes in blood leukocyte gene expression will provide a better understanding of the biological processes during endotoxemia. In a microarray study of human mononuclear cells, more than 800 genes were differentially expressed 6 h post challenge, highlighting the complexity of the response to systemic endotoxins [24]. Here, we report a longitudinal in vivo LPS study in goat comprising clinical, biochemical, and hematological responses, as well as leukocyte transcriptional profiles of selected immune genes.

Methods

Goats

A total of 13 Norwegian dairy goats, non-pregnant females, were recruited from a research herd at the Norwegian University of Life Sciences (NMBU). The mean age ± SD was 7.1 ± 1.8 months and the mean body weight ± SD was 25.1 ± 4.1 kg. Before the experiment, the goats were housed for at least 21 days to acclimatize. They were kept under a 16 h light/8 h dark cycle and housed in groups of 2–4 goats. Hay and water was provided *ad libitum*, and they were fed a commercial goat pellet concentrate twice a day. During this period, a full clinical examination was performed three times, and all goats were clinically normal. Fecal parasite egg counts were low and hematology was within reference values before the experiment.

LPS challenge

LPS (*Escherichia coli* O26:B6, L2654 Sigma-Aldrich, USA) was diluted in 0.9 % sterile saline to a concentration of 1.5 μg/ml. The goats were divided into two groups as follows: Eight goats receiving 0.1 μg/kg LPS intravenously, and a control group of five goats receiving corresponding volumes of sterile saline. The dosage was based on existing literature [25–27] and a pilot titration study involving three animals (data not included).

Clinical examination

After LPS challenge, clinical examination was performed at 12 time points during the first 7 h and once the next morning (24 h). The general condition was determined evaluating body posture (standing, lying), head- and ear-position, pupil size, appetite, grooming, shivering and social interaction. Respiratory frequency was recorded by observation, and ruminal contraction and heart frequency by auscultation. To ensure accurate rectal temperatures, all measurements were repeated three times

at each time point. Clinical examination was performed at corresponding time points in control animals.

Blood samples

Blood samples (EDTA, whole blood and PAX blood tubes) were drawn from *v. jugularis* using a vacutainer system (BD Company, USA). Baseline samples (0 h) were taken within half an hour of the LPS challenge. The other sampling times were 1 h, 2 h, 5 h and 24 h after LPS administration. To investigate if handling stress itself affects the quantified parameters, two blood samples were taken from the controls, a baseline sample (0 h) before saline administration and another sample 1 h later.

Hematological and biochemical analysis

A complete blood cell count including differential count was performed immediately after sampling using the ADVIA 120 Hematology system (caprine analyzing program) (Siemens, Germany). Whole blood was centrifuged and serum stored at −20 °C until biochemical analysis. Serum total protein, albumin and glucose were analyzed by ABX Pentra 400 (Horiba, France). Circulating levels of serum amyloid A (SAA) were analyzed by an ELISA method (Tridelta multispecies assay kit, Ireland) at three of the sampling time points (0 h, 5 h and 24 h).

RNA isolation

After blood sampling, PAX-gene blood RNA tubes (PreAnalytiX, Switzerland) were gently inverted 8–10 times. The tubes were incubated overnight at room temperature followed by storage at −80 °C. The isolation of total RNA was performed according to the manufacturer's instructions using PAXgene Blood miRNA kit (Qiagen, Germany). Isolated RNA was quantified at optical density (OD) 260, and purity evaluated by OD260/280 and OD260/230 ratios using DeNovix DS-11 spectrophotometer. RNA integrity was analyzed by RNA 600 Nano chips in compliance with the Bioanalyzer 2100 system (Agilent, USA) and each sample was assigned a RNA integrity number (RIN) from 1 to 10, with 10 being non-degraded RNA. The mean RIN value of included samples ± SD was 9.1 ± 0.30. All samples were treated with DNase while bound to columns to remove any contaminating genomic DNA, and stored at −80 °C.

cDNA synthesis

Two separate cDNA replicates were made for each sample. 250 ng of total RNA was converted into first strand cDNA using QuantiTect Reverse Transcription Kit (Qiagen, Germany) according to the manufacturer's instructions. A non-reverse transcriptase control (NoRT) and no template control (NTC) were included, and all cDNA samples were stored at −20 °C.

Primer design

A total of 44 genes associated with the LPS signaling cascade, early pro-inflammatory response, cytokines, chemokines, ISGs, APPs and apoptosis were chosen for investigation. Primer sequences and gene abbreviations can be found in Additional file 1.

Nucleic acid sequences were obtained from online genome databases and primers were designed by the Primer 3 software [28]. For previously untested primer assays, two primer pairs were designed for each transcript to validate that the correct transcript was being amplified. Additionally, the primer specificity was verified *in silico* using nucleic BLAST search against the *Capra hircus* genome. Primers were synthesized by Sigma-Aldrich (Germany). When possible, primers were designed to span exon/exon boundaries and to cover all known splice variants.

Fluidigm biomark HD qPCR

Preamplification and endonuclease treatment

A preamplification of target genes was performed to ensure adequate amounts of templates for high-throughput quantitative real time PCR (qPCR). Equal amounts of all primers used in the study were pooled in a 200 nM primer mix in low Tris-EDTA (TE) buffer, pH 8.0. A total of 10 μl comprising 2.5 μl primer mix, 2.5 μl of cDNA and 5 μl of TaqMan PreAmp was prepared per sample. Preamplification was carried out in a thermal cycler using the following program: Initial denaturation for 10 min at 95 °C followed by 20 cycles of 15 s at 95 °C and 4 min at 60 °C for annealing and elongation. To prevent carry-over of unincorporated primers after preamplification, 4 μl of 4U/μl exonuclease was added to the samples and incubated for 30 min at 37 °C and 15 min at 80 °C. Finally, cDNA was diluted 1:5 in TE buffer before qPCR.

Preparation of primer and sample assays

For each primer assay, a primer mix consisting of 3 μl of 2X Assay loading Reagent (Fluidigm, USA) and 3 μl of 20 μM specific forward/reverse primer was prepared. A sample mix consisting of 3 μl 2X TaqMan Gene Expression Mastermix, 0.3 μl 20X DNA binding Dye, 0.3 μl EvaGreen 20X, 0.9 μl TE buffer and 1.5 μl preamplified and exonuclease treated cDNA was made for each sample line.

Dynamic array qPCR analysis

Preparation and loading of Fluidigm 96.96 Dynamic Array IFC (integrated fluidic circuit), which combines 96 samples with 96 primer assays in 9216 simultaneous reactions, was performed according to manufacturer's instructions and as previously described [29]. Using Fluidigm Real-Time Analysis software 3.0.2, expression

data were visualized as a heat map based on Cq values. All amplifications and melting curves were evaluated and only genes with a single melting peak were accepted. Each chip included a NTC, a NoRT and three interplate calibrators. NTCs and melting curves were used to assess non-specific amplification or sample contamination. NoRT controls were used to evaluate potential genomic DNA background signals. No sample contamination or interfering genomic DNA signals were detected.

For each primer assay, a pool of all preamplified and exonuclease-treated cDNA samples were used to make three separate dilution series with the following dilutions: 1:2, 1:10, 1:50, 1:250 and 1:1250. Standard curves were constructed to obtain primer amplification efficiencies, correlations and dynamic range. To cover the dynamic range of genes with low expression, an additional standard dilution was made using four "high responding" samples. In 6 of the 96 primer assays, construction of standard curves was not possible and they were not included in further analyses. Primer efficiencies of included assays varied between 0.95 and 1.11 and had a correlation coefficient above 0.95. Four of the genes (IL6, IL12, CCL20 and MMP8) and one reference gene (ACACA) had very low expression in the samples and not subject to further investigation.

Light cycler 480 qPCR

The expression of IFNB1 gene was investigated by Light cycler 480 qPCR using SYBR Green PCR Master Mix under the following conditions: Initial denaturation for 5 min at 95 °C, followed by 40 amplification cycles (10 s at 95 °C, 10 s at 60 °C and 15 s at 72 °C) and construction of melting curves. IFNB1 primer sequences were adapted from [30] and can be found in Additional file 1.

Preprocessing of data

Heat map data were analyzed using GenEx5 software (MultiD, Sweden). First, interplate calibration was performed and each primer assay was corrected for primer efficiencies. Six potential reference genes (HPRT 1, HMBS, ACTB, HSP90AA1, ALAS 1 and GADPH) were validated using the integrated geNorm and Normfinder software in GenEx5. HPRT1, HMBS, ACTB and HSP90AA1 were used for the final normalization. Three of the samples were excluded due to high variation between cDNA replicates. After averaging cDNA duplicates, genes with more than 15 % missing data (IL10, INFG and CASP3) were removed and the remaining missing data (1.6 %) were replaced with the highest Cq value +1. Expression levels for each gene were then scaled to 1 for the sample with lowest expression, and all other samples for that specific gene calculated relative to this. Finally, expression data were transformed from Cq (log2) to relative quantities (relative fold change, linear scale).

Descriptive and statistical analysis

Data are presented as mean ± standard error of the mean (SEM). Graphical and statistical analyses were performed in GraphPad Prism 6 (GraphPad software Inc., USA) and Microsoft Excel 2013. To account for multiple comparisons, a one-way ANOVA and Dunnett's post hoc test was performed on Log2 transformed expression data. Differential expression was assessed by a limit of ± 2 fold change in expression compared with baseline samples and p values with the following significance levels: $P < 0.05$; $P < 0.01$; $P < 0.001$.

Results

Clinical and hematological responses

The mean rectal temperature increased in a biphasic manner from 38.9 °C (±0.09) to 40.5 °C (±0.28) 3.5 h after LPS injection (Fig. 1). Within the first 45 min, the goats displayed tachypnea, head shaking, anorexia and reduced locomotor activity, accompanied by a period of shivering, lasting 15–25 min. In five of the goats, a second period of shivering was observed between 1 h 45 m and 2 h 30 m after LPS administration. Also, all goats displayed an elevated heart frequency and decreased rumen motility. Overall, clinical signs were most prominent during the first five hours, which correlated with profound leukopenia, acute in neutrophils and more gradual in lymphocytes. The number of basophils and eosinophils declined significantly (data not shown), and a distinct monocytopenia was observed throughout all post-injection time points (Fig. 1). The goats gradually improved and by 7 h post injection all were considered clinically normal, but with an elevated heart frequency. The number of neutrophils had normalized at 5 h post challenge, but was elevated at 24 h compared with baseline levels. None of the control animals displayed alterations in clinical or hematological parameters during the experimental period.

Blood chemistry

Total protein and albumin decreased throughout the experiment, and albumin levels were significantly reduced 24 h after LPS injection. Circulating SAA was below detection limit (470 ng/ml) in all animals before challenge, and reached 215 000 ± 55 600 ng/ml at 24 h (Fig. 2). Serum glucose increased significantly towards 2 h, followed by a decrease at 5 h, but all values were within the reference range.

Gene expression analysis

The regulated genes and fold changes are summarized in Table 1. The magnitude of the fold change reflects the gene expression alterations relative to baseline levels (0 h) scaled to 1. Of the 37 target genes analyzed after preprocessing, 28 were significantly regulated at least at

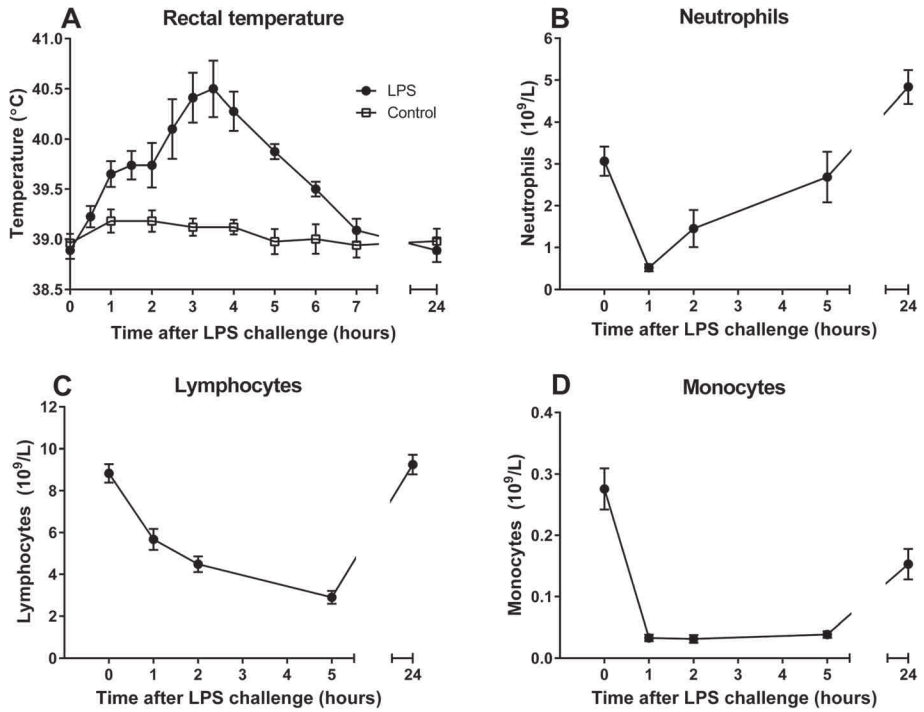

Fig. 1 Rectal temperature and hematology after systemic LPS challenge. Rectal temperature (**a**), and blood leukocyte count including neutrophils (**b**), lymphocytes (**c**) and monocytes (**d**) following 0.1 μg/kg intravenous LPS administration. Values are mean ± SEM, $n = 8$

one time point after LPS injection, with a minimum fold change of ± 2 compared with baseline levels. Expression levels of TNF, BPI, BCL2, BAX, ITGAM, ANAX1, C3 and STIP1 were not significantly altered at any of the time points.

The transcription of CXCL10 and ISG15 increased already 1 h after LPS challenge. All ISGs (CXCL10, ISG15, IFI6, ISG20, OAS1, IFIT1 and MX1) and STAT1, involved in interferon signaling [31], were significantly up-regulated at 2 h and 5 h post injection. IFNB1 increased of about 2-fold at 2 h, but this was not statistically significant. The expression of IFI6 and ISG15 remained elevated at 24 h, but only with a fold change of 3 and 4, compared with baseline levels (Fig. 3).

The mRNA levels of APP genes, HP, LF, LCN2 and SAA3 increased 1 h post injection, and peaked at 5 h before returning to baseline levels at 24 h, except SAA3 which remained up-regulated (Fig. 2). SAA3 was by far

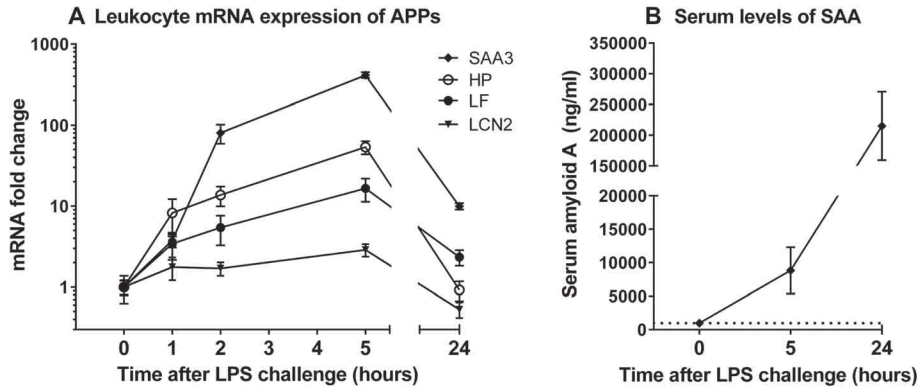

Fig. 2 Acute phase protein (APP) genes and serum levels of SAA after systemic LPS challenge. **a** Relative mRNA expression of serum amyloid A3 (SAA3), haptoglobin (HP), lactoferrin (LF) and lipocalin 2 (LCN2), compared with baseline levels (0 h) scaled to 1. Real time qPCR was performed on RNA extracted from circulating leukocytes at the indicated time points. Results are shown as mean relative fold change ± SEM. **b** Circulating levels of serum amyloid A (SAA) shown as mean serum concentration (ng/ml) ± SEM. The y-axis dotted line indicates the lower detection limit of the ELISA (470 ng/ml). $n = 8$

Table 1 Fold change in gene expression of selected immune genes after LPS challenge

	Gene	mRNA fold change				*P*		Gene	mRNA fold change				*P*
		1 h	2 h	5 h	24 h				1 h	2 h	5 h	24 h	
Interferon stimulated genes	CXCL10	4	**85**	11	2	**<0.001**	LPS-pathway	TLR4	−2	2	**3**	1	**<0.05**
	ISG15	2	**43**	17	4	**<0.001**		CD14	**−4**	1	1	1	**<0.01**
	ISG20	1	**9**	7	3	**<0.001**		MyD88	**−3**	1	1	1	**<0.05**
	IFIT1	1	**9**	3	1	**<0.01**		TRAF6	1	−2	**−2**	−2	**<0.01**
	OAS1	1	**14**	7	2	**<0.001**	IFN-pathway	STAT1	1	**2**	2	1	**<0.001**
	IFI6	1	5	**5**	3	**<0.001**	Cytokines and chemokines	IL1B	2	2	**3**	2	**<0.01**
	MX1	1	**17**	11	2	**<0.001**		IL8	2	**3**	2	1	**<0.01**
Acute phase proteins	SAA3	4	80	**412**	10	**<0.001**		CCL3	3	2	**4**	1	**<0.001**
	LF	3	5	**17**	2	**<0.001**		CCL5	−4	−3	−1	**−5**	**<0.001**
	HP	8	14	**54**	1	**<0.001**		IL18	−3	**−3**	−3	1	**<0.01**
	LCN2	2	2	**3**	−2	**<0.01**		IL1RN	1	**14**	7	1	**<0.05**
Enzymes	HSPA1A	1	3	**13**	1	**<0.001**	Other immune- related genes	TICAM	1	−3	**−3**	−2	**<0.001**
	S100A9	1	8	**18**	3	**<0.001**		ITGB2	−2	−2	**−4**	1	**<0.001**
	SOD2	−3	3	**3**	1	**<0.001**		MHCII	1	−2	**−3**	1	**<0.001**

Relative gene expression following intravenous LPS (0.1 μg/kg) administration in goats. Fluidigm qPCR was performed on RNA extracted from circulating leukocytes at the indicated time points. Results are expressed as mean fold change relative to baseline samples (0 h) scaled to 1. The most regulated time point for each gene is highlighted in bold, and significance level at this time point is given

the most up-regulated gene, reaching a fold change of 412 at 5 h post LPS challenge, and its expression strongly correlated with that of S100A9 ($R = 0.90$), which is involved in leukocyte extravasation [32]. Expression levels of LPS pathway genes (TLR4, CD14, MyD88, TRAF6) were stable throughout the experiment, however TLR4 was slightly (3-fold) up-regulated after 5 h. Three early pro-inflammatory cytokines (IL1B, IL8 and CCL3) were up-regulated during the first few hours.

Overall, genes involved in the LPS pathway, cell migration, and apoptosis displayed fold changes below 5, whereas most ISGs, APPs and genes involved in the later response were regulated by more than 10-fold.

Discussion

Despite the many endotoxin-related diseases in small ruminants and the advantage as a model for human endotoxemia, studies of LPS-induced inflammation are limited in these species. In the present study we describe 28 genes that were significantly (*±2 fold change*, $p < 0.05$) regulated in blood leukocytes during a 24 h experimental period.

Interestingly, all ISGs investigated were significantly up-regulated, peaking already at 2 h after LPS injection. Of these, CXCL10 showed the greatest up-regulation with an 85-fold increase compared with baseline levels. In murine peripheral leukocytes, a 2-fold to 3-fold increase in the expression of CXCL10 and IFIT1 was observed 48 h after a single intraperitoneal LPS administration, but the immediate response was not studied [33].

ISGs, which are induced by type I interferon (IFN) activation, are multifunctional genes traditionally ascribed important roles in anti-viral defense, including chemotaxis, cell differentiation, and apoptosis [21, 34, 35]. The fact that bacterial products such as LPS stimulate the expression of ISGs, has led to experiments addressing the role of type I IFN signaling during bacterial challenge. Two different lines of transgenic mice with genetic knock-out of IFN-β or the IFN-α/β receptor, displayed reduced survival against both streptococci and *Escherichia coli* compared with wild type mice [36]. This suggests an essential role of type I IFN-signaling in host resistance against both gram-positive and gram-negative bacteria. Previous in vitro studies describe a TLR4-mediated IFNβ-dependent induction of ISGs in monocyte-derived macrophages [37–39] and an IFN-independent induction of ISGs (MX1 and ISG15) in neutrophils [38]. However, transcriptional activity in neutrophils is considered low compared with other leukocytes [40], and their contribution to the total ISG pool is presumably limited. Although STAT1 phosphorylation levels were not analyzed in this study, we observed increased expression of STAT1, suggesting that interferon signaling was stimulated. IFNB1 was not significantly altered, but as leukocytes expressing IFNB1 and STAT1 extravasate after LPS challenge, the initial transcription levels of these genes are probably underestimated. Thus, a subtle or transient induction of IFNB1 will be difficult to detect in our model. To our knowledge, the present study is the first report of an immediate induction of ISGs in leukocytes upon LPS challenge, and it further supports a link between

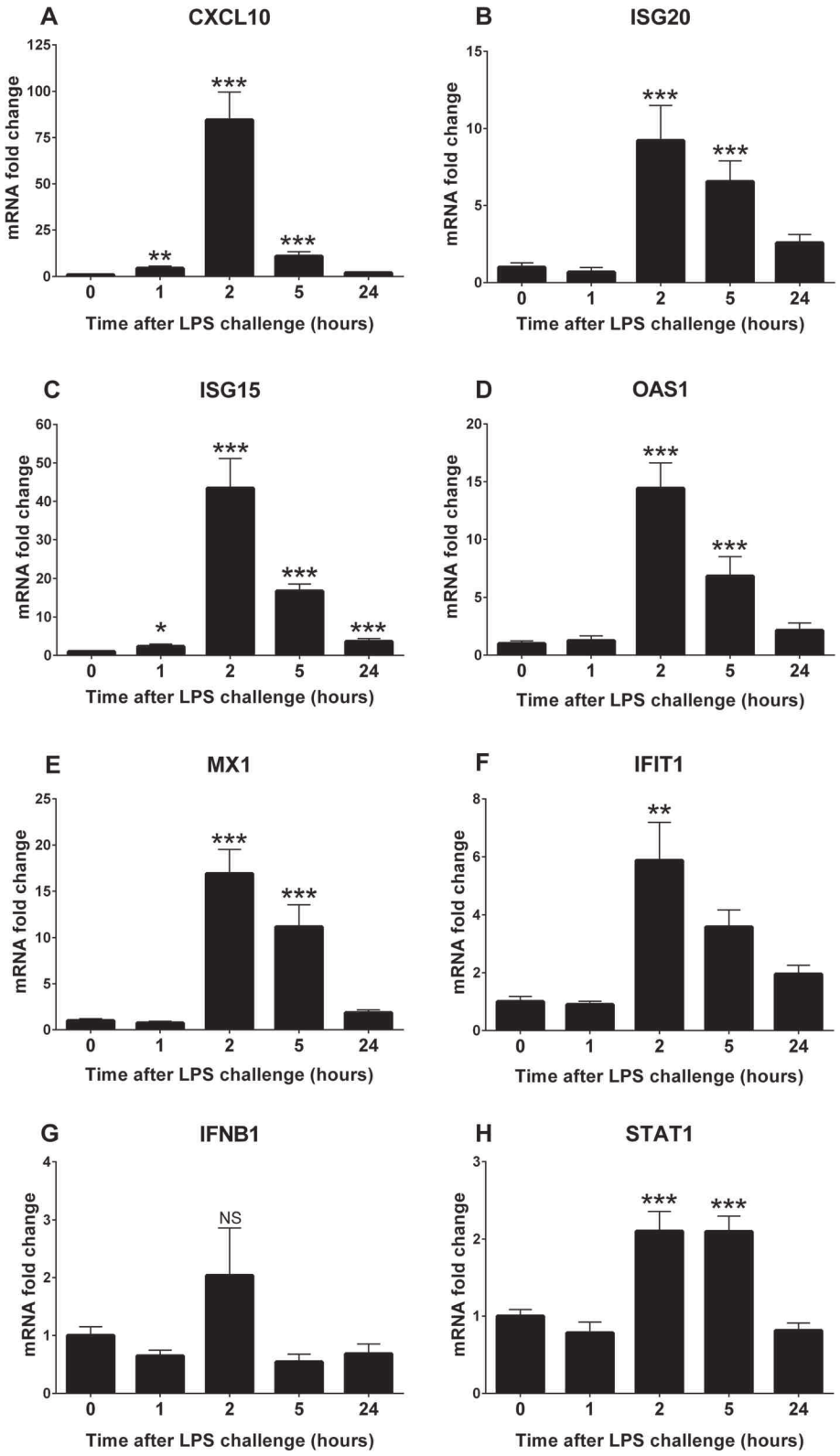

Fig. 3 Gene expression of leukocyte ISGs (**a**-**f**), IFNB1 (**g**) and STAT1 (**h**) after systemic LPS challenge. Relative mRNA fold change compared with baseline levels (0 h) scaled to 1. Real time qPCR was performed on RNA extracted from circulating leukocytes at the indicated time points. Results are expressed as mean relative fold change ± SEM, $n = 8$. NS = not significant. *$P < 0.05$; **$P < 0.01$; ***$P < 0.001$

interferon signaling and defense against bacterial infections [21, 36, 39].

APPs are a group of proteins that undergo substantial quantitative changes following external or internal stress, such as inflammation, neoplasia, or trauma [13]. As part of the innate immune system, these proteins contribute in basic defense mechanisms. Although APPs are mainly generated by the liver, increasing evidence indicate a local production in a number of tissues and cell types [12, 16–20, 41, 42]. Strikingly, mRNA levels of serum amyloid A3 (SAA3), lactoferrin (LF), haptoglobin (HP) and lipocalin (LCN2) were up-regulated in leukocytes upon LPS stimulation in the present study. SAA3 had the highest expression, reaching more than 400 times the baseline level at 5 h post challenge. This molecule is one of several SAA isoforms and is thought to be involved in cholesterol metabolism, modulating the innate immune response, as well as being a monocyte chemoattractant [43]. Recombinant SAA3 is also reported to have antimicrobial activity against *Escherichia coli*, *Streptococccus uberis* and *Pseudomonas aeruginosa* in the bovine mammary gland [44]. In murine colon, SAA3 synthesis has been linked to the TLR4 signaling axis and expression of the SAA3 gene was significantly reduced in mice with genetic knockout of MyD88 [20]. HP, LF and LCN2, also have bacteriostatic properties [45–47], mediated by binding and sequestering of iron. The first two are synthesized during differentiation of neutrophilic granulocytes and stored in specific granules that can be released upon activation [42, 48]. LCN2 has recently been reported to be a major APP in rat and mouse, as mRNA levels dramatically increase in both leukocytes and liver following inflammation [46, 49, 50]. In the current study, LCN2 mRNA was modestly up-regulated (3-fold), suggesting that this gene should be considered a minor APP in caprine leukocytes.

It is not clear if the increased mRNA levels of SAA3, HP, LF and LCN2 in leukocytes contribute to elevated protein levels in serum, or if the proteins are secreted after extravasation of the leukocytes. It has been shown that HP can be released by neutrophils present in milk following intramammary administration of endotoxin [41]. Thus, it is plausible that activated leukocytes release APPs after extravasation in response to local stimulation. Baseline serum concentrations of SAA were below detection limit (470 ng/ml) in all eight goats and increased dramatically towards 24 h after LPS challenge, reaching a mean concentration of 215 000 ng/ml. Although the liver must be considered the main source of SAA, particularly SAA1 and SAA2, it cannot be excluded that leukocyte SAA3 contribute to the circulating pool since the measurements do not differ between the different isoforms of SAA. In a murine obesity model, increased SAA3 mRNA expression in adipocytes did not affect circulating SAA levels [51], but these cells are extravascular and cannot be directly compared to cells in blood. Whether stimulated blood leukocytes release their APP products while in circulation, or just prepare for secretion to occur once migrated into tissues, remains to be investigated.

The decreased expression of CD14 and MyD88 mRNA detected 1 h post injection, was unexpected because these genes are crucial for recognition of LPS and initiating TLR4 signaling [6]. In the present study, mRNA was extracted from total leukocytes, hence the composition of circulating white blood cells affects the mRNA levels. CD14 and MyD88 genes are profoundly expressed in neutrophils and monocytes, two cell types that were dramatically decreased at 1 h due to tissue extravasation (Fig. 1). Thus, the decreased mRNA levels probably reflect the reduced numbers of neutrophils and monocytes in the circulating cell population, rather than down-regulation due to LPS.

Among the early pro-inflammatory cytokines we report an increased expression of IL8, CCL3, and IL1B within the first hours after LPS administration, similar to that described in an equine model [52]. IL-8 and CCL3 primarily stimulate chemotaxis of granulocytes, as well as inducing phagocytosis at the site of infection, whereas IL1β is a key mediator of the inflammatory response, being involved in cell differentiation, proliferation and apoptosis [53]. Intravenous injection of IL1β induces sickness behavior and has been directly linked to fever [54] and anorexia [55]. Consequently, the increased levels of mRNA coding for IL1β is in agreement with the development of sickness behavior and fever manifested in the study. We also investigated the anti-inflammatory IL1 antagonist (IL-1RN) that inhibits IL1 activity by binding the IL1 receptors without generating signal transduction. Indeed, increased mRNA levels of IL-1RN were observed simultaneously with increased IL1B expression, exemplifying the tightly regulated innate immune response.

The clinical picture, with behavioral changes and alteration in parameters like temperature, heart rate, respiration and rumination described in the present study, corresponds with the duration of the reported changes in gene expression, and with previous clinical studies in goats [25–27]. These signs are characteristic of the acute phase of a systemic inflammatory response, and reflect the reorganization of the organism's priorities to cope with infection. Notably, the behavioral changes demonstrate the profound effects systemic inflammation can have on the CNS [11].

Conclusion

Our results demonstrate a brief and tightly regulated transcriptional response to systemic LPS administration in caprine leukocytes. Characteristic clinical signs of sepsis were accompanied by leukopenia and the induction

of a range of immune-related genes. The increased mRNA levels of several ISGs substantiate the growing evidence that these genes possess multifunctional roles in the innate immune response. Extrahepatic expression of four APPs was also observed in caprine leukocytes, and increased dramatically upon stimulation, suggesting that leukocytes contribute to the synthesis of these proteins.

Additional file

Additional file 1: Gene name, gene abbreviations and primer sequences used in the real time qPCR analysis. For previously untested primer assays, two primer pairs were designed for each transcript. (DOCX 22 kb)

Abbreviations

APP: Acute phase protein; APR: Acute phase response; CNS: Central nervous system; ELISA: Enzyme-linked immunosorbent assay; ISG: Interferon stimulated gene; LPS: Lipopolysaccharide; NoRT: No reverse transcriptase; NTC: No template control; qPCR: Quantitative real-time polymerase chain reaction; RIN: RNA integrity number

Acknowledgements

The authors gratefully thank Karin Tarp for invaluable help with the RT-qPCR analysis, Siri Bjerkreim Hamre and Wenche Okstad for performing hematological and biochemical analyses, and Diana Anette Allen for performing the SAA ELISA. The authors acknowledge Lucy Robertson for proofreading the manuscript.

Funding

The research was supported by The Research Council of Norway.

Availability of data and materials

Data and material supporting the conclusions is contained within the manuscript. Any additional data are available upon request. Primer sequences used for qPCR analysis are shown in Additional file 1.

Authors' contributions

CE, MAT, AE and ØS designed the study and ØS, MRR, CE, AE and MAT performed the experiments. KS designed primers and participated in designing laboratory procedures and pre-processing of the expression data. ØS carried out laboratory procedures, performed the statistical analysis and drafted the manuscript. CE participated in the interpretation of analytical data and in drafting the manuscript. PMHH coordinated the expression and serum analysis in Copenhagen. All authors have critically read and approved the final manuscript.

Competing interest

The authors declare that they have no competing interests.

Consent to publication

Not applicable.

Ethics approval

The animal experiment was performed in compliance with ethical guidelines, and approved by the Norwegian Animal Research Authority (ID 7881) with reference to the Norwegian regulation on animal experimentation (FOR-2015-06-18-761).

Author details

[1]Faculty of Veterinary Medicine and Biosciences, Norwegian University of Life Sciences, Oslo, Norway. [2]Innate Immunology Group, Section for Immunology and Vaccinology, National Veterinary Institute, Technical University of Denmark, Frederiksberg, Denmark.

Received: 28 July 2016 Accepted: 20 October 2016
Published online: 28 October 2016

References

1. Annane D, Bellissant E, Cavaillon JM. Septic shock. Lancet. 2005;365(9453):63–78.
2. Schiffer ER, Reber G, De Moerloose P, Morel DR. Evaluation of unfractionated heparin and recombinant hirudin on survival in a sustained ovine endotoxin shock model. Crit Care Med. 2002;30(12):2689–99.
3. Reynolds K, Novosad B, Hoffhines A, Gipson J, Johnson J, Peters J, et al. Pretreatment with troglitazone decreases lethality during endotoxemia in mice. J Endotoxin Res. 2002;8(4):307–14.
4. Warren HS, Fitting C, Hoff E, Adib-Conquy M, Beasley-Topliffe L, Tesini B, et al. Resilience to bacterial infection: difference between species could be due to proteins in serum. J Infect Dis. 2010;201(2):223–32.
5. Seok J, Warren HS, Cuenca AG, Mindrinos MN, Baker HV, Xu W, et al. Genomic responses in mouse models poorly mimic human inflammatory diseases. Proc Natl Acad Sci U S A. 2013;110(9):3507–12.
6. Park BS, Lee JO. Recognition of lipopolysaccharide pattern by TLR4 complexes. Exp Mol Med. 2013;45:e66.
7. Muzio M, Bosisio D, Polentarutti N, D'Amico G, Stoppacciaro A, Mancinelli R, et al. Differential expression and regulation of toll-like receptors (TLR) in human leukocytes: selective expression of TLR3 in dendritic cells. J Immunol. 2000;164(11):5998–6004.
8. Park BS, Song DH, Kim HM, Choi BS, Lee H, Lee JO. The structural basis of lipopolysaccharide recognition by the TLR4-MD-2 complex. Nature. 2009;458(7242):1191–5.
9. Kawai T, Akira S. The role of pattern-recognition receptors in innate immunity: update on Toll-like receptors. Nat Immunol. 2010;11(5):373–84.
10. Akira S. Pathogen recognition by innate immunity and its signaling. Proc Jpn Acad Ser B Phys Biol Sci. 2009;85(4):143–56.
11. Dantzer R, O'Connor JC, Freund GG, Johnson RW, Kelley KW. From inflammation to sickness and depression: when the immune system subjugates the brain. Nat Rev Neurosci. 2008;9(1):46–56.
12. Skovgaard K, Mortensen S, Boye M, Poulsen KT, Campbell FM, Eckersall PD, et al. Rapid and widely disseminated acute phase protein response after experimental bacterial infection of pigs. Vet Res. 2009;40(3):23.
13. Jain S, Gautam V, Naseem S. Acute-phase proteins: As diagnostic tool. J Pharm Bioallied Sci. 2011;3(1):118–27.
14. González FH, Tecles F, Martinez-Subiela S, Tvarijonaviciute A, Soler L, Cerón JJ. Acute phase protein response in goats. J Vet Diagn Invest. 2008;20(5):580–4.
15. Eckersall PD, Bell R. Acute phase proteins: Biomarkers of infection and inflammation in veterinary medicine. Vet J. 2010;185(1):23–7.
16. Hiss S, Mielenz M, Bruckmaier RM, Sauerwein H. Haptoglobin concentrations in blood and milk after endotoxin challenge and quantification of mammary Hp mRNA expression. J Dairy Sci. 2004;87(11):3778–84.
17. McDonald TL, Larson MA, Mack DR, Weber A. Elevated extrahepatic expression and secretion of mammary-associated serum amyloid A3 (M-SAA3) into colostrum. Vet Immunol Immunopathol. 2001;83(3–4):203–11.
18. Yang F, Ghio AJ, Herbert DC, Weaker FJ, Walter CA, Coalson JJ. Pulmonary expression of the human haptoglobin gene. Am J Respir Cell Mol Biol. 2000;23(3):277–82.
19. Friedrichs WE, Navarijo-Ashbaugh AL, Bowman BH, Yang F. Expression and inflammatory regulation of haptoglobin gene in adipocytes. Biochem Biophys Res Commun. 1995;209(1):250–6.
20. Reigstad CS, Lunden GO, Felin J, Backhed F. Regulation of serum amyloid A3 (SAA3) in mouse colonic epithelium and adipose tissue by the intestinal microbiota. PLoS One. 2009;4(6):e5842.
21. Decker T, Muller M, Stockinger S. The yin and yang of type I interferon activity in bacterial infection. Nat Rev Immunol. 2005;5(9):675–87.
22. FAO Statistical Pocketbook 2015. http://www.fao.org/documents/card/en/c/383d384a-28e6-47b3-a1a2-2496a9e017b2/. Accessed 22 Feb 2016
23. Hedegaard CJ, Heegaard PM. Passive immunisation, an old idea revisited: Basic principles and application to modern animal production systems. Vet Immunol Immunopathol. 2016;174:50–63.
24. Talwar S, Munson PJ, Barb J, Fiuza C, Cintron AP, Logun C, et al. Gene expression profiles of peripheral blood leukocytes after endotoxin challenge in humans. Physiol Genomics. 2006;25(2):203–15.
25. Takeuchi Y, Kikusui T, Kizumi O, Ohnishi H, Mori Y. Pathophysiological changes evoked by lipopolysaccharide administration in goats. J Vet Med Sci. 1997;59(2):125–7.
26. Takeuchi Y, Kikusui T, Mori Y. Changes in the behavioral parameters following the lipopolysaccharide administration in goats. J Vet Med Sci. 1995;57(6):1041–4.
27. Ismail M. A pharmacokinetic study of danofloxacin in febrile goats following repeated administration of endotoxin. J Vet Pharmacol Ther. 2006;29(4):313–6.

28. Primer3 software. http://bioinfo.ut.ee/primer3-0.4.0/primer3/. Accessed 25 Oct 2015
29. Brogaard L, Heegaard PM, Larsen LE, Mortensen S, Schlegel M, Durrwald R, et al. Late regulation of immune genes and microRNAs in circulating leukocytes in a pig model of influenza A (H1N2) infection. Sci Rep. 2016;6:21812.
30. Zeng X, Wang S, Chi X, Chen SL, Huang S, Lin Q, et al. Infection of goats with goatpox virus triggers host antiviral defense through activation of innate immune signaling. Res Vet Sci. 2016;104:40–9.
31. Ramana CV, Chatterjee-Kishore M, Nguyen H, Stark GR. Complex roles of Stat1 in regulating gene expression. Oncogene. 2000;19(21):2619–27.
32. Pruenster M, Kurz AR, Chung KJ, Cao-Ehlker X, Bieber S, Nussbaum CF, et al. Extracellular MRP8/14 is a regulator of beta2 integrin-dependent neutrophil slow rolling and adhesion. Nat Commun. 2015;6:6915.
33. Thomson CA, McColl A, Cavanagh J, Graham GJ. Peripheral inflammation is associated with remote global gene expression changes in the brain. J Neuroinflammation. 2014;11:73.
34. Schoggins JW, Rice CM. Interferon-stimulated genes and their antiviral effector functions. Curr Opin Virol. 2011;1(6):519–25.
35. Schneider WM, Chevillotte MD, Rice CM. Interferon-stimulated genes: a complex web of host defenses. Annu Rev Immunol. 2014;32:513–45.
36. Mancuso G, Midiri A, Biondo C, Beninati C, Zummo S, Galbo R, et al. Type I IFN signaling is crucial for host resistance against different species of pathogenic bacteria. J Immunol. 2007;178(5):3126–33.
37. Sheikh F, Dickensheets H, Gamero AM, Vogel SN, Donnelly RP. An essential role for IFN-beta in the induction of IFN-stimulated gene expression by LPS in macrophages. J Leukoc Biol. 2014;96(4):591–600.
38. Malcolm KC, Worthen GS. Lipopolysaccharide stimulates p38-dependent induction of antiviral genes in neutrophils independently of paracrine factors. J Biol Chem. 2003;278(18):15693–701.
39. Toshchakov V, Jones BW, Perera PY, Thomas K, Cody MJ, Zhang S, et al. TLR4, but not TLR2, mediates IFN-beta-induced STAT1alpha/beta-dependent gene expression in macrophages. Nat Immunol. 2002;3(4):392–8.
40. Tecchio C, Micheletti A, Cassatella MA. Neutrophil-derived cytokines: facts beyond expression. Front Immunol. 2014;5:508.
41. Lai IH, Tsao JH, Lu YP, Lee JW, Zhao X, Chien FL, et al. Neutrophils as one of the major haptoglobin sources in mastitis affected milk. Vet Res. 2009;40(3):17.
42. Theilgaard-Mönch K, Jacobsen LC, Nielsen MJ, Rasmussen T, Udby L, Gharib M, et al. Haptoglobin is synthesized during granulocyte differentiation, stored in specific granules, and released by neutrophils in response to activation. Blood. 2006;108(1):353–61.
43. Uhlar CM, Whitehead AS. Serum amyloid A, the major vertebrate acute-phase reactant. Eur J Biochem. 1999;265(2):501–23.
44. Molenaar AJ, Harris DP, Rajan GH, Pearson ML, Callaghan MR, Sommer L, et al. The acute-phase protein serum amyloid A3 is expressed in the bovine mammary gland and plays a role in host defence. Biomarkers. 2009;14(1):26–37.
45. Eaton JW, Brandt P, Mahoney JR, Lee Jr JT. Haptoglobin: a natural bacteriostat. Science. 1982;215(4533):691–3.
46. Flo TH, Smith KD, Sato S, Rodriguez DJ, Holmes MA, Strong RK, et al. Lipocalin 2 mediates an innate immune response to bacterial infection by sequestrating iron. Nature. 2004;432(7019):917–21.
47. Arnold RR, Brewer M, Gauthier JJ. Bactericidal activity of human lactoferrin: sensitivity of a variety of microorganisms. Infect Immun. 1980;28(3):893–8.
48. Lomax KJ, Gallin JI, Rotrosen D, Raphael GD, Kaliner MA, Benz Jr EJ, et al. Selective defect in myeloid cell lactoferrin gene expression in neutrophil specific granule deficiency. J Clin Invest. 1989;83(2):514–9.
49. Sultan S, Pascucci M, Ahmad S, Malik IA, Bianchi A, Ramadori P, et al. Lipocalin-2 is a major acute-phase protein in a rat and mouse model of sterile abscess. Shock. 2012;37(2):191–6.
50. Fannin RD, Auman JT, Bruno ME, Sieber SO, Ward SM, Tucker CJ, et al. Differential gene expression profiling in whole blood during acute systemic inflammation in lipopolysaccharide-treated rats. Physiol Genomics. 2005;21(1):92–104.
51. Chiba T, Han CY, Vaisar T, Shimokado K, Kargi A, Chen MH, et al. Serum amyloid A3 does not contribute to circulating SAA levels. J Lipid Res. 2009;50(7):1353–62.
52. Vinther AM, Skovgaard K, Heegaard PM, Andersen PH. Dynamic expression of leukocyte innate immune genes in whole blood from horses with lipopolysaccharide-induced acute systemic inflammation. BMC Vet Res. 2015;11:134.
53. Turner MD, Nedjai B, Hurst T, Pennington DJ. Cytokines and chemokines: At the crossroads of cell signalling and inflammatory disease. Biochim Biophys Acta. 2014;1843(11):2563–82.
54. Wang J, Ando T, Dunn AJ. Effect of homologous interleukin-1, interleukin-6 and tumor necrosis factor-alpha on the core body temperature of mice. Neuroimmunomodulation. 1997;4(5–6):230–6.
55. Swiergiel AH, Dunn AJ. The roles of IL-1, IL-6, and TNFalpha in the feeding responses to endotoxin and influenza virus infection in mice. Brain Behav Immun. 1999;13(3):252–65.

Paper II

PLOS ONE

RESEARCH ARTICLE

Loss of prion protein induces a primed state of type I interferon-responsive genes

Giulia Malachin[1], Malin R. Reiten[1], Øyvind Salvesen[1], Håvard Aanes[2], Jorke H. Kamstra[1], Kerstin Skovgaard[3], Peter M. H. Heegaard[3], Cecilie Ersdal[1], Arild Espenes[1], Michael A. Tranulis[1☯*], Maren K. Bakkebø[1☯]

1 Faculty of Veterinary Medicine, Norwegian University of Life Sciences, Oslo, Norway, **2** Department of Microbiology, Division of diagnostics and intervention, Institute of Clinical Medicine, Oslo University Hospital, Rikshospitalet, Oslo, Norway, **3** Innate Immunology Group, Section for Immunology and Vaccinology, National Veterinary Institute, Technical University of Denmark, Kgs. Lyngby, Denmark

☯ These authors contributed equally to this work.
* Michael.Tranulis@nmbu.no

Citation: Malachin G, Reiten MR, Salvesen Ø, Aanes H, Kamstra JH, Skovgaard K, et al. (2017) Loss of prion protein induces a primed state of type I interferon-responsive genes. PLoS ONE 12 (6): e0179881. https://doi.org/10.1371/journal.pone.0179881

Editor: Sophie Mouillet-Richard, INSERM, FRANCE

Received: April 18, 2017

Accepted: June 6, 2017

Published: June 26, 2017

Data Availability Statement: All FASTQ files are available from the SRA database (SRA study accession number SRP102642).

Funding: MAT received funding from the Norwegian Research Council, Grant number 227386/E40 (http://www.forskningsradet.no/no/Forsiden/1173185591033). The funders had no role in study design, data collection and analysis, decision to publish, or preparation of the manuscript.

Competing interests: The authors have declared that no competing interests exist.

Abstract

The cellular prion protein (PrP^C) has been extensively studied because of its pivotal role in prion diseases; however, its functions remain incompletely understood. A unique line of goats has been identified that carries a nonsense mutation that abolishes synthesis of PrP^C. In these animals, the PrP-encoding mRNA is rapidly degraded. Goats without PrP^C are valuable in re-addressing loss-of-function phenotypes observed in *Prnp* knockout mice. As PrP^C has been ascribed various roles in immune cells, we analyzed transcriptomic responses to loss of PrP^C in peripheral blood mononuclear cells (PBMCs) from normal goat kids ($n = 8$, $PRNP^{+/+}$) and goat kids without PrP^C ($n = 8$, $PRNP^{Ter/Ter}$) by mRNA sequencing. PBMCs normally express moderate levels of PrP^C. The vast majority of genes were similarly expressed in the two groups. However, a curated list of 86 differentially expressed genes delineated the two genotypes. About 70% of these were classified as interferon-responsive genes. In goats without PrP^C, the majority of type I interferon-responsive genes were in a primed, modestly upregulated state, with fold changes ranging from 1.4 to 3.7. Among these were *ISG15*, *DDX58* (RIG-1), *MX1*, *MX2*, *OAS1*, *OAS2 and DRAM1*, all of which have important roles in pathogen defense, cell proliferation, apoptosis, immunomodulation and DNA damage response. Our data suggest that PrP^C contributes to the fine-tuning of resting state PBMCs expression level of type I interferon-responsive genes. The molecular mechanism by which this is achieved will be an important topic for further research into PrP^C physiology.

Introduction

The cellular prion protein (PrP^C) can misfold into disease-provoking conformers (PrP scrapie; PrP^{Sc}) that give rise to several neurodegenerative prion diseases, such as Creutzfeldt-Jakob disease (CJD) in humans, scrapie in sheep and goats, and bovine spongiform encephalopathy in

cattle [1]. The seeding of PrP^{Sc} in brain tissue acts as a template for further misfolding of PrP^{C}, ultimately leading to severe neurodegeneration and neuronal death [1].

PrP^{C} is abundant throughout the nervous system, and, albeit at lower levels, in most other tissues of the body [2]. The protein is conserved in mammalian species [3, 4] and expressed already during early embryonal stages [5]. It was therefore surprising that *Prnp*$^{0/0}$ mice developed normally and revealed no major phenotypes besides being prion-disease resistant [6–8]. Interestingly, in four *Prnp*$^{0/0}$ mouse models (*Ngsk*, *Rcm0*, *ZrchII*, and *Rikn*), ablation of the *Prnp* gene induced severe degeneration of cerebellar Purkinje neurons [9–12]. This was, however, subsequently shown to be caused by ectopic expression of the prion-like protein Doppel (*Dpl*) in the brain, as a side-effect of the transgenic protocols [10]. Two additional *Prnp*-ablated mouse lines (*ZrchI* and *Npu*) displayed no neurodegeneration [7, 8]. Furthermore, other experiments have shown that a polymorphism in another *Prnp* flanking gene, *Sirp-alpha*, could significantly influence the interpretation of data that concerns the roles for PrP^{C} in phagocytosis [13]. Despite these inherent challenges with *Prnp*-null models [14], collectively known as the flanking-gene problem, the *Prnp*$^{0/0}$ lines have proven extremely valuable in exploring PrP^{C} physiology. They have provided clues regarding maintenance of axonal myelin [15–17], modulation of circadian rhythms [18], and neuronal excitability [19], in addition to protective roles in severe stress such as ischemia [20] and hypoxic brain damage [21].

A more general problem is the gap between mice and human physiologies [22–24]. The two species diverged about 65 million years ago, and differ substantially in both size and life span. Mice have evolved into short-lived animals relying on massive reproductive capacity, whereas humans reside at the other end of the spectrum, with low reproduction rates and life spans of approximately 80 years. This is of particular significance in modeling chronic human diseases that take decades to develop, and often involve subtle immunological imbalances [22]. In addition, translation to human medicine has proven challenging.

Recently, we identified what seems to be a unique line of dairy goats carrying a nonsense mutation that completely abolishes synthesis of PrP^{C} [25]. This spontaneous, non-transgenic model, is referred to as *PRNP*$^{Ter/Ter}$. Approximately 10 percent of the Norwegian dairy goat population carries the mutated allele. These animals appear to have normal fertility and behavior in all aspects of standard husbandry. We have no data to suggest that they are over-represented in disease statistics or otherwise failing in production performance. Careful analysis of hematological and blood biochemical parameters, as well as basic immunological features, did not reveal any abnormalities [26]. It was, however, noted that goats without PrP^{C} had slightly elevated numbers of red blood cells, identical to an observation in transgenic cattle without PrP^{C} [27], suggesting that this is a true biological loss-of-function phenotype, at least in ruminants.

Peripheral blood mononuclear cells (PBMCs) express moderate, but dynamic, levels of PrP^{C} [28]. We observed that goats heterozygous for the mutation (*PRNP*$^{+/Ter}$) express half the amount of cell surface PrP^{C} on PBMCs [26]; however, a 50 percent reduction in levels compared to PBMCs from *PRNP*$^{+/+}$ goats did not stimulate compensatory expression from the normal allele. Intrigued by this, and the fact that many reports have pointed to putative functions for PrP^{C} in immune cells (reviewed in [29], [30, 31]), mRNA sequencing of PBMCs derived from normal goats and goats without PrP^{C} was performed. The main goal of this study was to evaluate whether the loss of PrP^{C} elicits a transcriptional response in PBMCs that could reveal biological processes involving PrP^{C}. Our findings show that in the absence of PrP^{C}, a subtle, but highly significant change in the transcriptional profile of PBMCs is seen, dominated by upregulation in the expression of type I interferon-responsive genes.

Results

RNA-seq data quality control

High quality RNA sequencing data (FASTQ) were derived from Beijing Genome Institute (BGI), with an average total reads of 58,806,319 per sample, average total mapped reads of 42,168,758, and average uniquely mapped reads of 38,253,898 per sample (S1 Fig). To validate the sequencing data, primers (S1 Table) were designed for 12 randomly selected differentially expressed genes (DEGs), using reverse transcription (RT) quantitative real-time PCR (qPCR) on the original RNA. As shown in Fig 1, qPCR analysis of mRNA levels correlated well with the RNA-seq analysis ($r = 0.9616$, $p < 0.0001$, Pearson correlation). Minor discrepancies could be due to sample variations, as RNA from only six goats per group were used for qPCR validation, compared with eight goats per group for RNA-seq analysis.

Lack of PrP^C subtly alters the transcriptome in immune cells

A high correlation was observed between averaged $PRNP^{+/+}$ and $PRNP^{Ter/Ter}$ normalized gene expression data ($r = 0.99$, Pearson correlation). However, we found that not all $PRNP^{+/+}$ and $PRNP^{Ter/Ter}$ goats could be clearly separated from each other, probably reflecting the phenotypic diversity of the goats (S2 Fig). Despite this, using edgeR [32] and a p-value cut-off < 0.05, 735 genes were differentially expressed between the two genotypes (S1 File). Further filtration of the gene list using cut offs for fold change (log2 FC ± 0.5) and mean number of reads (> 100 reads in one of the groups) generated a high-confidence gene list of 127 DEGs, of which 67 were upregulated and 60 were downregulated in the $PRNP^{Ter/Ter}$ genotype (S2 Table). Of note, as we have previously shown that the PBMC cell populations, mainly T cells, B cells and monocytes, are stable between the two genotypes compared in our study [26], the DEGs result from real genotype-associated shifts in gene expression, not shifts in the cell populations. Reassuringly, the *PRNP* gene was among the DEGs, with very few reads mapping to this locus in the mutant. The chromosomal distribution of the DEGs is found in S3 Fig. The *PRNP* gene is located on chromosome 13 in goats. Only 1 (*SIGLEC1*) of the 86 annotated DEGs also maps to

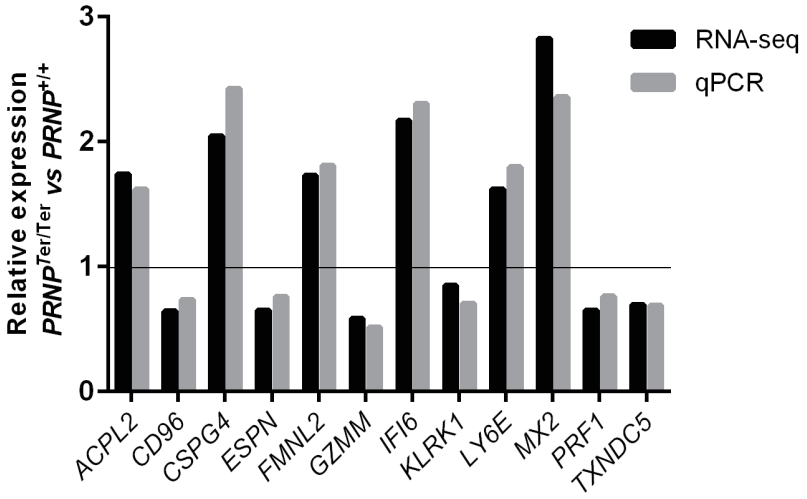

Fig 1. Validation of RNA sequencing data with quantitative PCR. Validation of 12 randomly chosen, differentially expressed genes was performed with qPCR using the original RNA. Expression data from the two methods are presented as relative expression between $PRNP^{Ter/Ter}$ and $PRNP^{+/+}$ animals (RNA-seq data $n = 8$, qPCR $n = 6$; $r = 0.9616$, $p < 0.0001$, Pearson correlation).

https://doi.org/10.1371/journal.pone.0179881.g001

chromosome 13. This gene is expressed at a low level and is irrelevant for the findings in our study.

Of the average total number of genes expressed in PBMCs from both genotypes, only 0.7 percent of the genes were altered upon loss of PrP^C (Fig 2A). Using Ingenuity Pathway Analysis (IPA), of the 127 high-confidence DEGs, 86 genes were functionally annotated. Interestingly, 22 of these genes were categorized as "Viral infection" (p-value = $3.27x10^{-5}$), and additional genes were related to other anti-virus-associated terms. The majority of these genes were upregulated in the $PRNP^{Ter/Ter}$ genotype compared with the $PRNP^{+/+}$ genotype. Of the top canonical pathways, "Interferon signaling" was by far the most affected (p-value = $8.92x10^{-6}$). Due to these findings, we performed further analyses of the annotated DEGs using the Interferome database [33]. Strikingly, 60 of the 86 annotated DEGs were interferon-responsive genes (Fig 2B). Of these, 42 were upregulated (red bar) and 18 downregulated (blue bar) in the $PRNP^{Ter/Ter}$ genotype. Fig 2C shows the inter-individual variation in gene expression of all samples represented in a heatmap, and hierarchical clustering analysis of the 60 interferon-responsive genes revealed a clustering of downregulated and upregulated genes between the $PRNP^{+/+}$ and $PRNP^{Ter/Ter}$ genotypes.

Since the observed data could be due to altered expression levels of interferons or components in type I interferon signaling, we analyzed expression levels of a number of genes that could affect the expression of interferon-responsive genes. However, differences between the genotypes were not detected (Table 1), except for *IFNB2-like*, which was slightly downregulated in the $PRNP^{Ter/Ter}$ genotype (p-value = 0.025).

Introduction of *PRNP* inhibited *MX2* gene expression in SH-SY5Y cells

To test whether PrP^C could influence IFN-α responsiveness in a cell culture system with a different genetic makeup, we used human neuroblastoma SH-SY5Y cells, which normally express extremely low levels of PrP^C. SH-SY5Y clones stably expressing human PrP^C were generated (SH-SY5Y PrP^{high}) and assessed with regard to glycosylation and proteolytic processing to ensure physiological post-translational modification and trafficking of PrP^C (S4 Fig). Eight clones stably expressing PrP^C as well as untransfected SH-SY5Y cells were exposed to 3 U/ml IFN-α for 3h. One of the transfected clones showed aberrantly high *MX2* gene expression levels and was excluded from the analysis. Of the seven clones included in the experiment, six displayed a significantly reduced response to IFN- α, as assessed by the interferon-responsive gene *MX2* expression levels, compared with the untransfected SH-SY5Y cells, using Dunnett's post hoc test for multiple comparisons (Fig 3) ($n = 4$, mean ± SEM). The levels of PrP^C expression did not directly correlate with the degree of *MX2* expression-level inhibition; however, this was not expected due to the complexity of the interferon signaling pathway, and the possible distance between PrP^C interference and *MX2* gene expression. On average, the clones showed a significantly inhibited response to IFN- α (p-value = 0.0001) compared with the untransfected SH-SY5Y cells, using a two-way ANOVA.

Increased interferon-responsive gene expression in blood leukocytes devoid of PrP^C after LPS challenge

In an independent, parallel study [34, 35], goats were challenged intravenously with lipopolysaccharide (LPS), thereby indirectly stimulating interferon pathways. RNA was extracted from circulating blood leukocytes, and gene expression of interferon-responsive genes was assessed by FLUIDIGM qPCR. As shown in Fig 4A, basal level expression (0h) of several interferon-responsive genes was slightly higher in the $PRNP^{Ter/Ter}$ ($n = 13$) genotype than in the $PRNP^{+/+}$ ($n = 12$) genotype, albeit being significantly different for only *IFI6* (p-value = 0.037). Moreover,

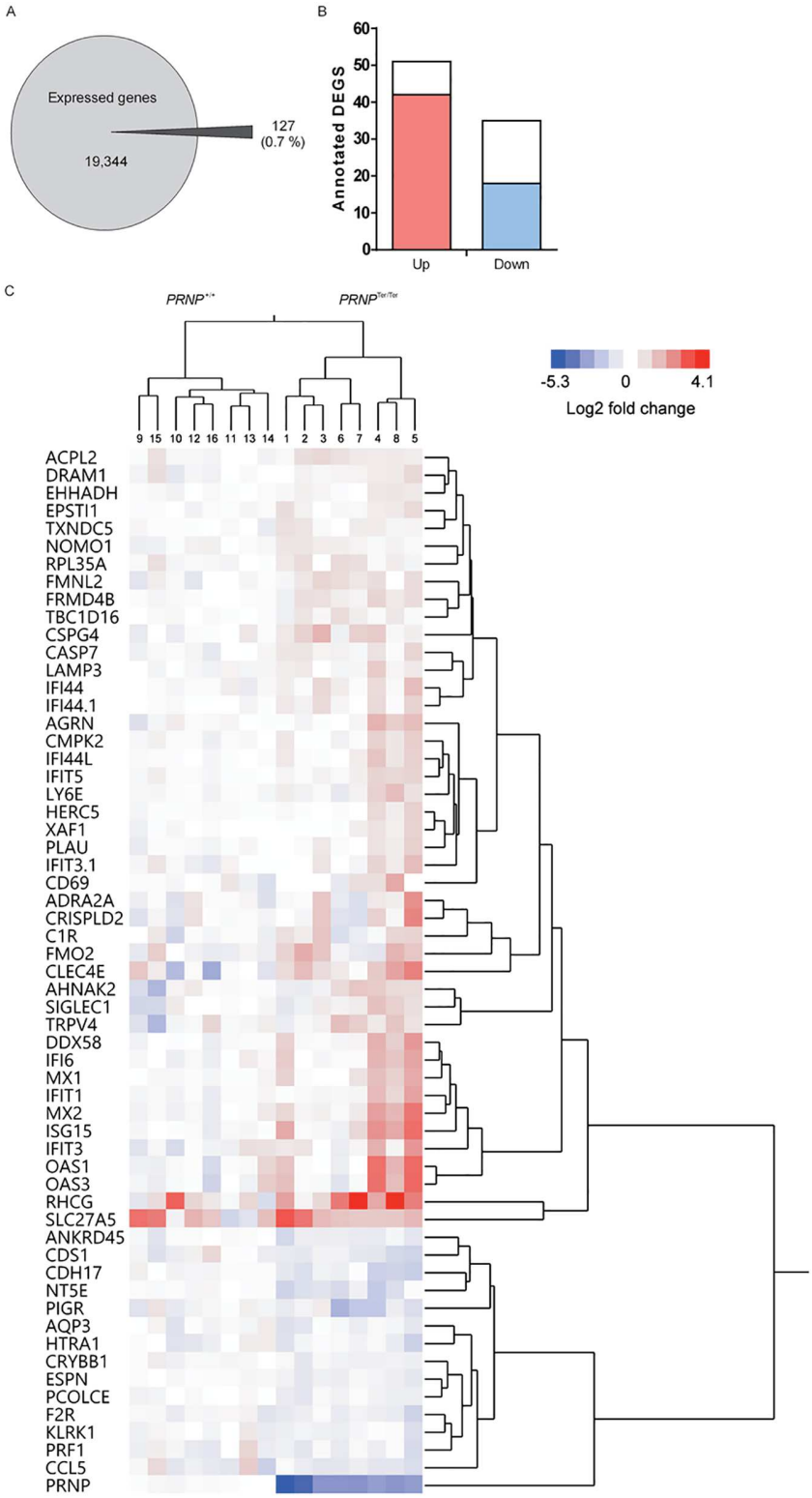

Fig 2. Interferon-responsive genes dominate among the differentially expressed genes in goats lacking PrP^{C}. Graphical presentation of (A) the total number and percentage of differentially expressed genes (DEGs) between the two genotypes, compared to the average total number of genes expressed in peripheral blood mononuclear cells from both genotypes, and (B) the total number of upregulated and

downregulated annotated DEGs. The fraction of upregulated (red) and downregulated (blue) interferon-responsive genes among the DEGs are also shown. (C) Hierarchical clustering of the interferon-responsive genes among the DEGs and expression data from all individual goats of both genotypes. Hierarchical clustering was performed using the ward algorithm on log2-normalized fold changes.

https://doi.org/10.1371/journal.pone.0179881.g002

STAT1 mRNA expression levels did not differ between the genotypes. One hour after LPS challenge, the mRNA expression level of interferon-responsive genes increased slightly and the difference between the two genotypes was more pronounced (Fig 4B), with three genes showing a statistically significant difference in expression level (*ISG15* (p-value = 0.049), *IFIT1* (p-value = 0.02), and *MX1* (p-value = 0.019), assessed by multiple t-tests).

Discussion

Similar to observations in transgenic mice [6], goats [36], and cattle [27] with knockout (KO) of *PRNP*, the $PRNP^{Ter/Ter}$ goats display no obvious loss-of-function phenotype [25, 26]. Consequently, only subtle transcriptomic alterations were expected, corroborating data from KO mouse models [37–41]. Accordingly, this study revealed subtle expression differences affecting less than a percent of the expressed genes. However, analysis of the annotated DEGs using the Interferome database [33], identified a distinct expression profile, with 70 percent of the DEGs being classified as interferon responsive, of which several were among the top upregulated genes. Importantly, animals were age-matched and derived from the same research flock. The health status of this herd is frequently monitored and considered excellent. Prior to sampling, animals were assessed clinically by a veterinarian and found healthy, which was also confirmed by hematological analysis in an accompanying study [26]. Furthermore, we were unable to detect any differences in gene expression levels of neither interferons nor IFN signaling components. A flanking gene problem will also be present in the $PRNP^{Ter/Ter}$ goats; however, preliminary data indicate that this is very limited compared to inbred knockout mouse models. In the absence of alternative explanations, we consider the observed gene expression profile to be a true signature of PrP^{C} loss-of-function. It is likely that this profile, which is evident at rest in the outbred and immunocompetent goats, might be even weaker or absent in inbred transgenic mice, housed in pathogen-depleted environments. It is, however, interesting to note that studies of prion disease in mice have revealed a gene expression profile similar to that observed in PrP^{C}-deficient goats. Analysis of transcripts from mouse whole brain throughout the course of experimental CJD revealed an upregulation of several interferon-responsive genes, e.g. *OAS*, *ISG15*, and *IRF*-family members. Importantly, the upregulation of these genes occurred very early in the course of the disease, approximately 50 days before the onset of neuropathological signs and detection of PrP^{Sc} [42]. Similar findings were recently reported in another study of prion-infected mice [43]. In a hamster model of scrapie, several interferon-responsive genes, including those encoding OAS and Mx protein, were upregulated during development of scrapie [44]. In addition, three interferon-responsive genes, assessed by qPCR studies, were moderately upregulated in a hamster model and different mouse models inoculated with scrapie strains [45]. Recently, transcriptomic data from cerebellar organotypic cultured slices infected with prions showed that a slight upregulation of several interferon-responsive genes was evident at 38 and 45 days post infection [46]. It is tempting to speculate that some of the observed gene expression alterations at very early stages of prion disease could, at least partly, reflect induced loss-of-PrP^{C} function, and, thus, explain the similarity with the expression profile reported here. Further investigations are clearly needed to test this hypothesis.

Studies of human SH-SY5Y neuroblastoma cells transfected with human *PRNP* displayed a significantly dampened response (MX2 expression) to a low-level IFN-α stimulation,

Table 1. Mean unique reads of genes related to Interferon signaling from *PRNP*$^{+/+}$ (*n* = 8, ± SEM) and *PRNP*$^{Ter/Ter}$ (*n* = 8, ± SEM) goats.

Gene symbol	Transcript ID	*PRNP*$^{+/+}$	*PRNP*$^{Ter/Ter}$
Interferons			
IFNA-H-like	XM_005683618.1	0.3 ± 0.3	0.0 ± 0.0
IFNB2-like	XM_005702021.1	63.0 ± 5.3	43.4 ± 4.2 *
IFNK	XM_005683589.1	0.1 ± 0.1	0.0 ± 0.0
IFNO1-like	XM_005683620.1	26.5 ± 6.8	19.1 ± 4.9
IFNT2A	XM_005683606.1	0.9 ± 0.4	0.9 ± 0.5
IFNG	XM_005680208.1	38.4 ± 10.9	27.8 ± 4.5
IFNL3	XM_005692539.1	0.1 ± 0.1	0.0 ± 0.0
IFNL4-like	XM_005692540.1	0.5 ± 0.3	0.3 ± 0.2
Interferon receptors			
IFNAR1	XM_005674742.1	11565.5 ± 613.5	11818.3 ± 683.0
IFNAR2	XM_005674684.1	3484.1 ± 245.4	3664.9 ± 188.7
IFNGR1	XM_005684807.1	3056.4 ± 268.9	3772.4 ± 252.6
IFNGR2	XM_005674741.1	7492.8 ± 179.1	8209.5 ± 408.9
IFNLR1	XM_005677011.1	95.5 ± 10.8	122.4 ± 22.4
Interferon signaling components			
JAK1	XM_005678310.1	31579.9 ± 920.9	31909.0 ± 908.7
JAK2	XM_005683698.1	2399.1 ± 109.3	2587.5 ± 84.7
JAK3	XM_005682189.1	11636.9 ± 600.5	9816.8 ± 603.9
TYK2	XM_005682457.1	4528.3 ± 205.6	4775.3 ± 328.4
STAT1	XM_005676277.1	26477.4 ± 2414.9	28314.6 ± 1119.4
STAT2	XM_005680347.1	5548.9 ± 332.1	6363.6 ± 408.4
STAT3	XM_005693850.1	98.5 ± 10.5	92.5 ± 8.2
STAT4	XM_005676278.1	2101.9 ± 158.6	1949.5 ± 120.6
STAT5A	XM_005693847.1	5250.6 ± 172.7	5365.3 ± 194.9
STAT5B	XM_005693846.1	4604.1 ± 137.3	4511.0 ± 155.2
STAT6	XM_005680308.1	15197.3 ± 704.8	15596.6 ± 692.7
IRF1	XM_005682621.1	12308.6 ± 1155.2	10936.5 ± 1329.5
IRF2	XM_005698710.1	624.5 ± 26.6	663.4 ± 17.1
IRF3	XM_005692726.1	1073.9 ± 74.3	1169.1 ± 60.4
IRF4	XM_005696935.1	1482.5 ± 157.3	1379.5 ± 140.9
IRF5	XM_005679456.1	764.9 ± 61.4	811.8 ± 65.6
IRF6	XM_005691036.1	7.3 ± 2.2	5.4 ± 1.9
IRF8	XM_005691907.1	3565.8 ± 219.0	3824.8 ± 210.8
IRF9	XM_005685224.1	205.8 ± 16.7	234.5 ± 28.2
Inhibitors and enhancers			
IRF2BP-like	XM_005686182.1	2686.3 ± 135.5	2794.5 ± 123.7
IRF2BP1	XM_005692789.1	1265.3 ± 33.0	1232.4 ± 32.3
IRF2BP2	XM_005699013.1	8090.8 ± 600.5	8588.9 ± 793.4
PIAS1	XM_005685148.1	1266.8 ± 66.9	1320.0 ± 86.4
PIAS2	XM_005697179.1	390.6 ± 16.9	405.0 ± 19.2
PIAS3	XM_005677741.1	99.1 ± 7.8	99.5 ± 8.1
PIAS4	XM_005682570.1	39.4 ± 2.7	40.0 ± 4.8
SOCS2	XM_005679820.1	0.8 ± 0.4	1.4 ± 0.6
SOCS3	XM_005694412.1	372.0 ± 48.8	346.4 ± 47.5
SOCS4	XM_005685884.1	845.4 ± 24.5	823.3 ± 28.0
SOCS5	XM_005686570.1	1748.9 ± 82.0	1737.6 ± 75.8

(*Continued*)

Table 1. (*Continued*)

Gene symbol	Transcript ID	*PRNP*$^{+/+}$	*PRNP*$^{Ter/Ter}$
SOCS6	XM_005709580.1	137.5 ± 14.4	144.6 ± 14.0
SOCS7	XM_005709575.1	2286.3 ± 193.8	2144.5 ± 198.7
IL18	XM_005689450.1	21.3 ± 4.5	18.9 ± 3.6
PTK2	XM_005688815.1	82.4 ± 11.4	92.1 ± 7.4
PTK2B	XM_005684041.1	99.3 ± 11.6	114.5 ± 17.5

*: p = 0.025

https://doi.org/10.1371/journal.pone.0179881.t001

compared with untransfected cells that are virtually devoid of PrP^{C}. Furthermore, in an independent, parallel study involving older goat kids than those recruited for the RNA seq study, animals were challenged with LPS, which is a potent pro-inflammatory compound. In contrast to mice, which are relatively tolerant towards LPS, goats have a similar sensitivity as humans [34, 35]. In line with data from the present RNA sequencing study, resting state expression levels of interferon-responsive genes in leukocytes were slightly elevated in the *PRNP*$^{Ter/Ter}$ genotype. Interestingly, the expression differences between the genotypes were increased one hour after LPS injection. Apparently, leukocytes without the expression of PrP^{C} upregulated interferon-responsive genes more rapidly than their PrP^{C}-expressing counterparts. The regulation of interferon-responsive genes expression level is multifaceted and tightly controlled at several levels [47, 48], involving receptor downregulation, upregulation of a plethora of inhibitors as well as epigenetic modifications.

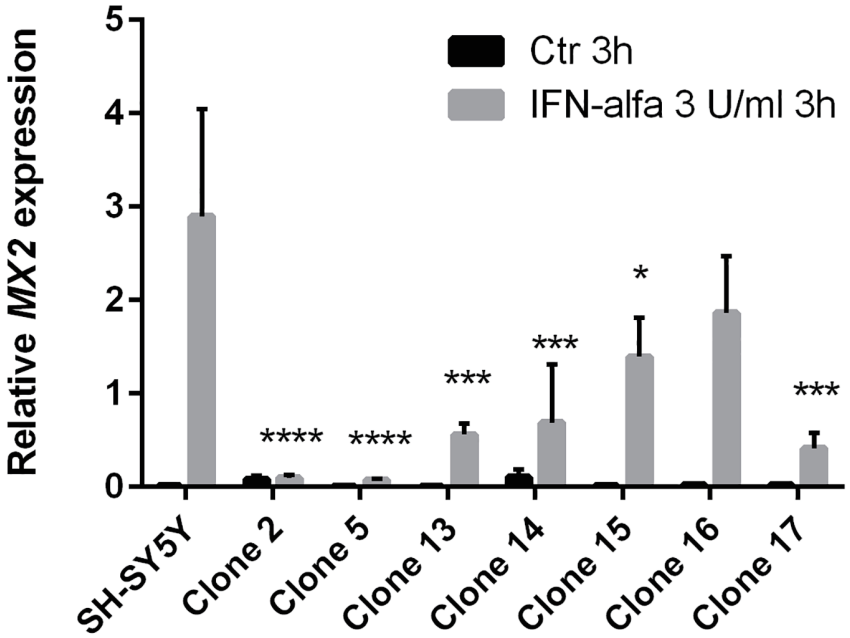

Fig 3. PrP^{C} suppresses upregulation of *MX2* gene expression upon INF-α stimulation in SH-SY5Y cells. Untransfected human neuroblastoma SH-SY5Y cells and seven different clones transfected with a plasmid containing human *PRNP* to produce SH-SY5Y clones expressing human PrP^{C}, were stimulated for 3h with IFN-α (3 U/ml) (mean ± SEM, $n = 4$), and *MX2* gene expression was assessed. Six out of seven clones displayed a significantly lower response to IFN-α compared with the untransfected SH-SY5Y cells, using Dunnett's post hoc test for multiple comparisons.

https://doi.org/10.1371/journal.pone.0179881.g003

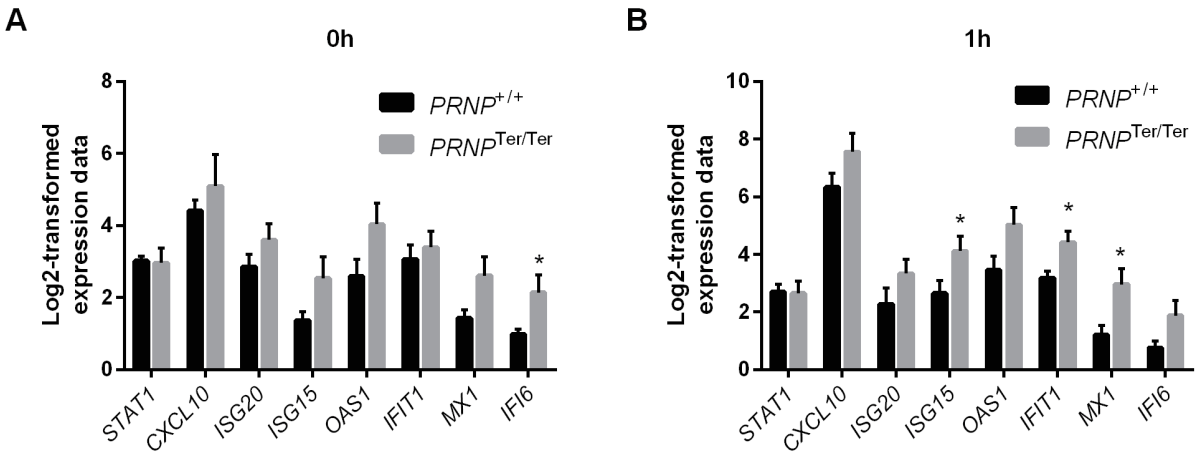

Fig 4. Expression of interferon-responsive genes in blood leukocytes after *in vivo* lipopolysaccharide (LPS) challenge in goats without PrP^C. RNA was extracted from circulating blood leukocytes from both genotypes, and gene expression was analyzed by FLUIDIGM qPCR. (A) Basal expression level (0 h) of selected interferon-responsive genes and *STAT1* in $PRNP^{+/+}$ ($n = 12$) and $PRNP^{Ter/Ter}$ ($n = 13$) animals. (B) Gene expression of interferon-responsive genes and *STAT1* after *in vivo* LPS challenge (1 h) from $PRNP^{+/+}$ ($n = 7$) and $PRNP^{Ter/Ter}$ ($n = 8$) animals. Values are mean ± SEM. Statistical significance is indicated by *, p-value < 0.05, as assessed by multiple t-tests.

https://doi.org/10.1371/journal.pone.0179881.g004

Taken together, our data suggest that PrP^C contributes to dampening of type I interferon signaling at rest and that loss of PrP^C induces a primed state of interferon-responsive genes. Accordingly, direct or indirect stimulation of type I IFN signaling, elicits a somewhat stronger immediate response when PrP^C is absent. These data do not conflict with roles acclaimed to the prion protein. Indeed, they might strengthen previous observations and provide mechanistic hints of PrP^C physiology.

Material and methods

Animals

The animals (FOTS approval number ID 8058) included in the study were of the Norwegian Dairy Goat Breed obtained from a research herd of approximately 100 winter-fed goats at the Norwegian University of Life Sciences. Based on health surveillance through membership in the Goat health monitoring service and The Norwegian Association of Sheep and Goat Farmers and daily monitoring, the general health status of the herd is considered to be good. The entire flock was previously genotyped [25] concerning *PRNP* genotypes, and through selective breeding, goat kids with the two genotypes $PRNP^{+/+}$ ($n = 8$; 4 female and 4 male) and $PRNP^{Ter/Ter}$ ($n = 8$; 4 female and 4 male) were retrieved. Prior to inclusion in the experiment, all goat kids were examined clinically and found to be healthy.

Isolation of peripheral blood mononuclear cells

Blood was sampled from the jugular vein into EDTA tubes at 2–3 months of age. Peripheral blood mononuclear cells (PBMCs) were isolated by gradient centrifugation (Lymphoprep®, Axis-Shield, Dundee, Scotland) at 1760 x *g* without brake, and washed with PBS supplemented with EDTA (2 mM). Red blood cells were lysed by brief exposure to sterile water, and washed with PBS supplemented with EDTA (2 mM) prior to counting and trypan blue viability assessment using a Countess® Automated Cell Counter (Life Technologies, Thermo Fisher Scientific, Waltham, MA).

Cell culture studies

Human neuroblastoma SH-SY5Y cells (Sigma-Aldrich, Merck, Kenilworth, NJ) were cultured in Eagle's Minimum Essential Medium and Ham's F12 (1:1) (Sigma-Aldrich) supplemented with 10% heat-inactivated fetal bovine serum (FBS), glutamine and antibiotics (1% streptomycin and penicillin) (all from Gibco, Thermo Fisher Scientific), and cultivated in T25 flasks at 37˚C with 5% (v/v) CO_2 at saturated humidity. SH-SY5Y cells were stably transfected with a plasmid construct, pCI-neo (Promega, Madison, WI) encoding human *PRNP*, using jetPRIME (Polyplus, Illkirch, France) according to the manufacturer's instructions. Transfected cells were grown under selection pressure of Geneticin (Thermo Fisher Scientific), and nine different single clones with variable levels of PrP^{C} (SH-SY5Y PrP^{high}) were isolated (S4 Fig). Clone no. 8 showed an abnormal phenotype, and was excluded from the studies.

Western blotting

Untransfected SH-SY5Y cells and transfected SH-SY5Y PrP^{high} clones were lysed in homogenizer buffer (Tris HCl 50 uM, NaCl 150 mM, EDTA 1 mM, DOC 0.25%, NP40 1%) supplemented with protease inhibitor cocktail (Roche complete, Roche Holding AG, Basel, Switzerland). Protein concentrations were measured using Protein assay (Bio-Rad, Hercules, CA). To obtain deglycosylated protein, 20 μg of total protein were incubated overnight with PNGase-F (New England Biolabs, Ipswich, MA), according to the manufacturer's instructions.

Fifty μg of protein or the deglycosylated samples were separated on sodium dodecyl sulfate (SDS) polyacrylamide gel electrophoresis (12% Criterion™ XT Bis-Tris, Bio-Rad), and transferred to polyvinylidene fluoride (PVDF) membranes (GE Healthcare, Little Chalfont, United Kingdom). After incubation with blocking buffer (5% non-fat milk in TBS-Tween) for 90 minutes at room temperature, samples were incubated in 1% non-fat milk in TBS-Tween containing mouse anti-PrP^{C} primary antibody diluted 1:4000 (6H4, Prionics, Thermo Fischer Scientific) over-night at 4˚C. Subsequently, the membrane was washed and incubated for 90 minutes in 1% non-fat milk containing Alkaline Phosphatase (AP)-conjugated anti-mouse IgG diluted 1:4000 (Novex, Life Technologies, Thermo Fischer Scientific). Membrane was developed using EFC™ substrate (GE Healthcare) and visualized with Typhoon 9200 (Amersham Bioscience, GE Healthcare).

Isolation and sequencing of RNA

Total RNA was extracted using the Qiagen RNeasy mini plus kit (Qiagen, Germantown, MD) following the manufacturer's instructions. RNA concentration and purity was analyzed using NanoDrop-1000 Spectrophotometer (Thermo Fisher Scientific) or Epoch Microplate Spectrophotometer (BioTek Instruments Inc, Winooski, VT), and quality was assessed before RNA sequencing using RNA Nano Chips on an Agilent 2100 Bioanalyzer (both from Agilent Technologies, Santa Clara, CA). RNA was stored at -80˚C. Individual RNA samples of high quality (RIN $\geq$ 9.8) were sequenced by mRNA poly-A-tail, paired-end sequencing (Illumina HiSeq 2000) with 91 bp read-lengths (Beijing Genomics Institute (BGI), Hong Kong), retrieving a minimum depth of 5G clean data per sample. In detail, after the total RNA extraction and DNase I treatment, magnetic beads with Oligo (dT) were used to isolate mRNA. Mixed with the fragmentation buffer, the mRNA was fragmented into short fragments, and cDNA was synthesized using the mRNA fragments as templates. Short fragments were purified and resolved with EB buffer for end reparation and single nucleotide A (adenine) addition. The short fragments were connected with adapters. After agarose gel electrophoresis, the suitable fragments were selected for the PCR amplification as templates. During the QC steps, Agilent

2100 Bioanalyzer and ABI StepOnePlus Real-Time PCR System were used in quantification and qualification of the sample library.

For the IFN-studies, RNA quality was assessed by TAE/formamide RNA gel electrophoresis. RNA samples were mixed with formamide (50% v/v, Sigma) and orange loading dye (New England Biolabs), denatured by heating for 5 min at 65˚C, put on ice, and loaded on 1% agarose gel containing 1xTAE buffer (0.04 M Tris-acetate, 1 mM EDTA) and visualized with SYBR™ Safe (Invitrogen, Thermo Fisher Scientific).

Analysis of RNA sequencing data

Reads were mapped to the goat genome assembly (CHIR_1.0) using SOAP2 [49]. Reads per gene were obtained using SOAP2 and the goat genome annotation (RefSeq, CHIR_1.0). Read counts were normalized to reads per kilobase per million mapped reads (RPKM) [50]. Testing for differentially expressed genes was performed using the function exactTest in edgeR [32].

Expression analysis by reverse transcription (RT) quantitative real-time PCR (qPCR) analysis

cDNA was synthesized using SuperScript III Reverse Transcriptase, RNase Out, dNTP mix and Random Primers (all from Invitrogen, Thermo Fisher Scientific) at the following conditions: 5 min at 65˚C, >1 min on ice, 5 min at 25˚C, 1 h at 50˚C and 15 min at 70˚C.

For the RNA sequencing validation study, qPCR was conducted with LightCycler 480 Sybr Green I Master mix (Roche). cDNA corresponding to 2.5 ng RNA was used per reaction. The samples were run in duplicates in a total volume of 20 μl on a LightCycler 96 System (Roche). Conditions: 5 min at 95˚C; 40 cycles of 10 sec at 95˚C, 10 sec at 60˚C and 10 sec at 72˚C; and melting curve with 5 sec at 95˚C, 1 min at 65˚C and 97˚C. Relative expression levels were calculated using a standard curve generated from one randomly selected animal, run in triplicate, with GAPDH as a reference gene, and one randomly selected animal as a positive control. The average of six $PRNP^{Ter/Ter}$ animals was divided by the average of six $PRNP^{+/+}$ animals, and compared relative to RNA sequencing data.

For the interferon-treatment studies using SH-SY5Y cells, qPCR was conducted with LightCycler 480 Sybr Green I Master mix (Roche). cDNA corresponding to 10 ng RNA was used per reaction. The samples were run in triplicate in a total volume of 10 μl on a LightCycler 96 System (Roche). Conditions: 5 min at 95˚C; 40 cycles of 10 sec at 95˚C, 10 sec at 60˚C and 10 sec at 72˚C; and melting curve with 5 sec at 95˚C, 1 min at 65˚C and 97˚C. Relative expression levels were calculated using the ΔΔCt method. ActB was used as a reference gene. An inter-run calibrator was included on every plate as a positive control. The qPCR-amplified sample was run on a 1% agarose gel, and visualized using SYBR™ Safe (Thermo Fisher Scientific).

LPS challenge and FLUIDIGM qPCR of whole blood leukocyte interferon-responsive genes

An intravenous LPS challenge was performed (0.1 μg/kg, *Escherichia coli* O26:B6) in 16 Norwegian dairy goats age 6–7 months (*8* $PRNP^{+/+}$ (female) and 8 $PRNP^{Ter/Ter}$ (7 female, 1 castrated male)) (FOTS approval number IDs 5827, 6903, and 7881), and 10 controls were included (5 of each genotype). In brief, blood samples were collected in PAX-gene blood RNA tubes before (0 h) and after LPS challenge (1 h). High quality RNA (RIN 9.0 ± 0.34) was extracted using the PAXgene Blood miRNA kit, and cDNA synthesis was performed in two replicates (QuantiTect Reverse Transcription Kit). The relative expression of ISGs in

circulating leukocytes was assessed after qPCR on the Fluidigm Biomark HD platform and data analysis using GenEx5 software (MultiD, Sweden). The full study protocol, method description, and primer sequences can be found in [34, 35].

Statistical analysis

Multiple *t*-tests or two-way ANOVA followed by Dunnett's post hoc test for multiple comparisons were used for statistical analysis of the data using Graph Pad Prism v. 6.07 (Graphpad, La Jolla, CA). For correlation analysis, the Pearson correlation coefficient was calculated. Mean values are presented ± SEM.

Ethics statement

The animal experiments were performed in compliance with ethical guidelines, and approved by the Norwegian Animal Research Authority (FOTS approval number IDs 8058, 5827, 6903, and 7881) with reference to the Norwegian regulation on animal experimentation (FOR-2015-06-18-761).

Supporting information

S1 Fig. Individual number of reads obtained from RNA sequencing. Total reads, total mapped reads and uniquely mapped reads across all samples, $n = 16$, 8 of each genotype.
(TIF)

S2 Fig. Hierarchical clustering dendrogram. Hierarchical clustering dendrogram of all genes after normalization of expression data (RPKM) using Euclidean distance and complete linkage.
(TIF)

S3 Fig. Chromosomal distribution of differentially expressed genes. (A) Frequency of differentially expressed genes (735 genes) per chromosome. Total number of genes per chromosome were obtained from National Center for Biotechnology Information (NCBI), based on the Capra hircus CHIR_1.0-Primary Assembly. (B) Chromosomal distribution of annotated differentially expressed genes (86 genes).
(TIF)

S4 Fig. Clones of human neuroblastoma SH-SY5Y cells expressing human *PRNP*. Protein expression of PrP^C for untreated and PNGase-F-treated untransfected human neuroblastoma SH-SY5Y cells and SH-SY5Y clones transfected with human *PRNP* ($n = 8$), determined by Western Blot analysis using 6H4 mouse anti-PrP^C as the primary antibody. Protein bands correspond to glycosylated PrP^C, deglycosylated PrP^C and PrP^C C1 fragment as indicated.
(TIF)

S1 Table. Forward and reverse primers used for qPCR.
(DOCX)

S2 Table. Differentially expressed genes between $PRNP^{Ter/Ter}$ ($n = 8$) and $PRNP^{+/+}$ ($n = 8$) goats (127 genes).
(DOCX)

S1 File. Differentially expressed genes (735 genes).
(XLSX)

Acknowledgments

We thank Susan Skogtvedt Røed and Berit Christophersen for skillful laboratory work, Agnes Klouman and the staff at the Animal Production Experimental Centre, and Dag Inge Våge and Torfinn Nome for technical help with the sequencing data. The authors acknowledge Lucy Robertson for proofreading the manuscript, and Ingrid Olsaker for use of the Ingenuity Pathway Analysis software.

Author Contributions

Conceptualization: Cecilie Ersdal, Arild Espenes, Michael A. Tranulis, Maren K. Bakkebø.

Data curation: Giulia Malachin, Malin R. Reiten, Øyvind Salvesen, Håvard Aanes, Jorke H. Kamstra, Kerstin Skovgaard, Peter M. H. Heegaard, Cecilie Ersdal, Michael A. Tranulis, Maren K. Bakkebø.

Formal analysis: Giulia Malachin, Malin R. Reiten, Øyvind Salvesen, Håvard Aanes, Jorke H. Kamstra, Kerstin Skovgaard, Peter M. H. Heegaard, Cecilie Ersdal, Michael A. Tranulis, Maren K. Bakkebø.

Funding acquisition: Michael A. Tranulis.

Investigation: Giulia Malachin, Malin R. Reiten, Øyvind Salvesen, Maren K. Bakkebø.

Methodology: Håvard Aanes, Kerstin Skovgaard, Peter M. H. Heegaard, Cecilie Ersdal, Arild Espenes, Michael A. Tranulis, Maren K. Bakkebø.

Project administration: Cecilie Ersdal, Arild Espenes, Michael A. Tranulis, Maren K. Bakkebø.

Resources: Håvard Aanes, Jorke H. Kamstra, Kerstin Skovgaard, Peter M. H. Heegaard, Arild Espenes, Michael A. Tranulis.

Supervision: Michael A. Tranulis, Maren K. Bakkebø.

Validation: Giulia Malachin, Øyvind Salvesen, Maren K. Bakkebø.

Visualization: Giulia Malachin, Øyvind Salvesen, Håvard Aanes, Jorke H. Kamstra, Maren K. Bakkebø.

Writing – original draft: Michael A. Tranulis, Maren K. Bakkebø.

Writing – review & editing: Giulia Malachin, Malin R. Reiten, Øyvind Salvesen, Håvard Aanes, Jorke H. Kamstra, Kerstin Skovgaard, Peter M. H. Heegaard, Cecilie Ersdal, Arild Espenes, Michael A. Tranulis, Maren K. Bakkebø.

References

1. Prusiner SB. Prions. Proceedings of the National Academy of Sciences. 1998; 95(23):13363–83. https://doi.org/10.1073/pnas.95.23.13363
2. Linden R, Martins VR, Prado MAM, Cammarota M, Izquierdo I, Brentani RR. Physiology of the prion protein. Physiological Reviews. 2008; 88(2):673–728. https://doi.org/10.1152/physrev.00007.2007 PMID: 18391177
3. Wopfner F, Weidenhöfer G, Schneider R, von Brunn A, Gilch S, Schwarz TF, et al. Analysis of 27 mammalian and 9 avian PrPs reveals high conservation of flexible regions of the prion protein. Journal of Molecular Biology. 1999; 289(5):1163–78. https://doi.org/https://doi.org/10.1006/jmbi.1999.2831 PMID: 10373359
4. Rongyan Z, Xianglong L, Lanhui L, Xiangyun L, Fujun F. Evolution and differentiation of the prion protein gene (*PRNP*) among species. Journal of Heredity. 2008; 99(6):647–52. https://doi.org/10.1093/jhered/esn073 PMID: 18799453

5. Peralta OA, Huckle WR, Eyestone WH. Developmental expression of the cellular prion protein (PrP^C) in bovine embryos. Molecular Reproduction and Development. 2012; 79(7):488–98. https://doi.org/10.1002/mrd.22057 PMID: 22674901
6. Bueler H, Fischer M, Lang Y, Bluethmann H, Lipp H-P, DeArmond SJ, et al. Normal development and behaviour of mice lacking the neuronal cell-surface PrP protein. Nature. 1992; 356(6370):577–82. https://doi.org/10.1038/356577a0 PMID: 1373228
7. Manson JC, Clarke AR, Hooper ML, Aitchison L, McConnell I, Hope J. 129/Ola mice carrying a null mutation in PrP that abolishes mRNA production are developmentally normal. Mol Neurobiol. 1994; 8 (2–3):121–7. https://doi.org/10.1007/BF02780662 PMID: 7999308
8. Büeler H, Aguzzi A, Sailer A, Greiner RA, Autenried P, Aguet M, et al. Mice devoid of PrP are resistant to scrapie. Cell. 1993; 73(7):1339–47. https://doi.org/https://doi.org/10.1016/0092-8674(93)90360-3 PMID: 8100741
9. Sakaguchi S, Katamine S, Nishida N, Moriuchi R, Shigematsu K, Sugimoto T, et al. Loss of cerebellar Purkinje cells in aged mice homozygous for a disrupted PrP gene. Nature. 1996; 380(6574):528–31. https://doi.org/10.1038/380528a0 PMID: 8606772
10. Moore RC, Mastrangelo P, Bouzamondo E, Heinrich C, Legname G, Prusiner SB, et al. Doppel-induced cerebellar degeneration in transgenic mice. Proceedings of the National Academy of Sciences of the United States of America. 2001; 98(26):15288–93. https://doi.org/10.1073/pnas.251550798 PMID: 11734625
11. Rossi D, Cozzio A, Flechsig E, Klein MA, Rülicke T, Aguzzi A, et al. Onset of ataxia and Purkinje cell loss in PrP null mice inversely correlated with Dpl level in brain. Journal Article. 2001; 20(4):694–702. https://doi.org/10.1093/emboj/20.4.694 PMID: 11179214
12. Yokoyama T, Kimura KM, Ushiki Y, Yamada S, Morooka A, Nakashiba T, et al. *In vivo* conversion of cellular prion protein to pathogenic isoforms, as monitored by conformation-specific antibodies. Journal of Biological Chemistry. 2001; 276(14):11265–71. https://doi.org/10.1074/jbc.M008734200 PMID: 11152682
13. Nuvolone M, Kana V, Hutter G, Sakata D, Mortin-Toth SM, Russo G, et al. SIRPα polymorphisms, but not the prion protein, control phagocytosis of apoptotic cells. The Journal of Experimental Medicine. 2013; 210(12):2539–52. https://doi.org/10.1084/jem.20131274 PMID: 24145514
14. Steele AD, Lindquist S, Aguzzi A. The prion protein knockout mouse: A phenotype under challenge. Prion. 2007; 1(2):83–93. PMID: 19164918
15. Baumann F, Tolnay M, Brabeck C, Pahnke J, Kloz U, Niemann HH, et al. Lethal recessive myelin toxicity of prion protein lacking its central domain. Journal Article. 2007; 26(2):538–47. https://doi.org/10.1038/sj.emboj.7601510 PMID: 17245436
16. Bremer J, Baumann F, Tiberi C, Wessig C, Fischer H, Schwarz P, et al. Axonal prion protein is required for peripheral myelin maintenance. Nat Neurosci. 2010; 13(3):310–8. http://www.nature.com/neuro/journal/v13/n3/suppinfo/nn.2483_S1.html. https://doi.org/10.1038/nn.2483 PMID: 20098419
17. Nuvolone M, Hermann M, Sorce S, Russo G, Tiberi C, Schwarz P, et al. Strictly co-isogenic C57BL/6J-$Prnp^{-/-}$ mice: A rigorous resource for prion science. The Journal of Experimental Medicine. 2016; 213 (3):313–27. https://doi.org/10.1084/jem.20151610 PMID: 26926995
18. Tobler I, Gaus SE, Deboer T, Achermann P, Fischer M, Rulicke T, et al. Altered circadian activity rhythms and sleep in mice devoid of prion protein. Nature. 1996; 380(6575):639–42. https://doi.org/10.1038/380639a0 PMID: 8602267
19. Walz R, Amaral OB, Rockenbach IC, Roesler R, Izquierdo I, Cavalheiro EA, et al. Increased sensitivity to seizures in mice lacking cellular prion protein. Epilepsia. 1999; 40(12):1679–82. https://doi.org/10.1111/j.1528-1157.1999.tb01583.x PMID: 10612329
20. Spudich A, Frigg R, Kilic E, Kilic Ü, Oesch B, Raeber A, et al. Aggravation of ischemic brain injury by prion protein deficiency: Role of ERK-1/-2 and STAT-1. Neurobiology of Disease. 2005; 20(2):442–9. https://doi.org/https://doi.org/10.1016/j.nbd.2005.04.002 PMID: 15893468
21. McLennan NF, Brennan PM, McNeill A, Davies I, Fotheringham A, Rennison KA, et al. Prion protein accumulation and neuroprotection in hypoxic brain damage. The American Journal of Pathology. 2004; 165(1):227–35. https://doi.org/10.1016/S0002-9440(10)63291-9 PMID: 15215178
22. Mestas J, Hughes CCW. Of mice and not men: Differences between mouse and human immunology. The Journal of Immunology. 2004; 172(5):2731–8. https://doi.org/10.4049/jimmunol.172.5.2731 PMID: 14978070
23. Davis MM. A prescription for human immunology. Immunity. 2008; 29(6):835–8. https://doi.org/10.1016/j.immuni.2008.12.003 PMID: 19100694
24. Bolker J. Model organisms: There's more to life than rats and flies. Nature. 2012; 491(7422):31–3. https://doi.org/10.1038/491031a PMID: 23128209

25. Benestad S, Austbo L, Tranulis M, Espenes A, Olsaker I. Healthy goats naturally devoid of prion protein. Veterinary Research. 2012; 43(1):87. https://doi.org/10.1186/1297-9716-43-87 PMID: 23249298

26. Reiten MR, Bakkebø MK, Brun-Hansen H, Lewandowska-Sabat AM, Olsaker I, Tranulis MA, et al. Hematological shift in goat kids naturally devoid of prion protein. Frontiers in Cell and Developmental Biology. 2015; 3:44. https://doi.org/10.3389/fcell.2015.00044 PMID: 26217662

27. Richt JA, Kasinathan P, Hamir AN, Castilla J, Sathiyaseelan T, Vargas F, et al. Production of cattle lacking prion protein. Nature biotechnology. 2007; 25(1):132. https://doi.org/10.1038/nbt1271 PMID: 17195841

28. Dürig J, Giese A, Schulz-Schaeffer W, Rosenthal C, Schmücker U, Bieschke J, et al. Differential constitutive and activation-dependent expression of prion protein in human peripheral blood leucocytes. British Journal of Haematology. 2000; 108(3):488–95. https://doi.org/10.1046/j.1365-2141.2000.01881.x PMID: 10759704

29. Isaacs JD, Jackson GS, Altmann DM. The role of the cellular prion protein in the immune system. Clinical and Experimental Immunology. 2006; 146(1):1–8. https://doi.org/10.1111/j.1365-2249.2006.03194.x PMID: 16968391

30. Isaacs JD, Garden OA, Kaur G, Collinge J, Jackson GS, Altmann DM. The cellular prion protein is preferentially expressed by $CD4^+$ $CD25^+$ $Foxp3^+$ regulatory T cells. Immunology. 2008; 125(3):313–9. https://doi.org/10.1111/j.1365-2567.2008.02853.x PMID: 18462346

31. Mariante RM, Nóbrega A, Martins RAP, Areal RB, Bellio M, Linden R. Neuroimmunoendocrine regulation of the prion protein in neutrophils. The Journal of Biological Chemistry. 2012; 287(42):35506–15. https://doi.org/10.1074/jbc.M112.394924 PMID: 22910907

32. Robinson MD, McCarthy DJ, Smyth GK. edgeR: a Bioconductor package for differential expression analysis of digital gene expression data. Bioinformatics. 2010; 26(1):139–40. https://doi.org/10.1093/bioinformatics/btp616 PMID: 19910308

33. Rusinova I, Forster S, Yu S, Kannan A, Masse M, Cumming H, et al. INTERFEROME v2.0: an updated database of annotated interferon-regulated genes. Nucleic Acids Research. 2013; 41(Database issue): D1040–D6. https://doi.org/10.1093/nar/gks1215 PMID: 23203888

34. Salvesen Ø, Reiten MR, Heegaard PMH, Tranulis MA, Espenes A, Skovgaard K, et al. Activation of innate immune genes in caprine blood leukocytes after systemic endotoxin challenge. BMC Veterinary Research. 2016; 12:241. https://doi.org/10.1186/s12917-016-0870-x PMID: 27793136

35. Salvesen Ø, Reiten MR, Espenes A, Bakkebø MK, Tranulis MA, Ersdal C. LPS-induced systemic inflammation reveals an immunomodulatory role for the prion protein at the blood-brain interface. Journal of Neuroinflammation. 2017; 14:106. https://doi.org/10.1186/s12974-017-0879-5 PMID: 28532450

36. Yu G, Chen J, Xu Y, Zhu C, Yu H, Liu S, et al. Generation of goats lacking prion protein. Molecular Reproduction and Development. 2009; 76(1):3–. https://doi.org/10.1002/mrd.20960 PMID: 18951376

37. Benvegnù S, Roncaglia P, Agostini F, Casalone C, Corona C, Gustincich S, et al. Developmental influence of the cellular prion protein on the gene expression profile in mouse hippocampus. Physiol Genomics. 2011; 43(12):711–25. https://doi.org/10.1152/physiolgenomics.00205.2010 PMID: 21406608

38. Satoh J-i, Kuroda Y, Katamine S. Gene expression profile in prion protein-deficient fibroblasts in culture. The American Journal of Pathology. 2000; 157(1):59–68. PMID: 10880376

39. Ramljak S, Asif AR, Armstrong VW, Wrede A, Groschup MH, Buschmann A, et al. Physiological role of the cellular prion protein (PrP^C): Protein profiling study in two cell culture systems. Journal of Proteome Research. 2008; 7(7):2681–95. https://doi.org/10.1021/pr7007187 PMID: 18537284

40. Chadi S, Young R, Le Guillou S, Tilly G, Bitton F, Martin-Magniette M-L, et al. Brain transcriptional stability upon prion protein-encoding gene invalidation in zygotic or adult mouse. BMC Genomics. 2010; 11:448–. https://doi.org/10.1186/1471-2164-11-448 PMID: 20649983

41. Crecelius AC, Helmstetter D, Strangmann J, Mitteregger G, Fröhlich T, Arnold GJ, et al. The brain proteome profile is highly conserved between $Prnp^{-/-}$ and $Prnp^{+/+}$ mice. NeuroReport. 2008; 19(10):1027–31. https://doi.org/10.1097/WNR.0b013e3283046157 PMID: 18580573

42. Baker CA, Lu ZY, Manuelidis L. Early induction of interferon-responsive mRNAs in Creutzfeldt-Jakob disease. Journal of NeuroVirology. 2004; 10:29–40. PMID: 14982726

43. Carroll JA, Striebel JF, Race B, Phillips K, Chesebro B. Prion infection of mouse brain reveals multiple new upregulated genes involved in neuroinflammation or signal transduction. Journal of Virology. 2015; 89(4):2388–404. https://doi.org/10.1128/JVI.02952-14 PMID: 25505076

44. Riemer C, Queck I, Simon D, Kurth R, Baier M. Identification of upregulated genes in scrapie-infected brain tissue. Journal of Virology. 2000; 74(21):10245–8. PMID: 11024157

45. Stobart MJ, Parchaliuk D, Simon SLR, LeMaistre J, Lazar J, Rubenstein R, et al. Differential expression of interferon responsive genes in rodent models of transmissible spongiform encephalopathy disease. Molecular Neurodegeneration. 2007; 2:5–. https://doi.org/10.1186/1750-1326-2-5 PMID: 17367538

46. Herrmann US, Sonati T, Falsig J, Reimann RR, Dametto P, O'Connor T, et al. Prion infections and anti-PrP antibodies trigger converging neurotoxic pathways. PLoS Pathogens. 2015; 11(2):e1004662. https://doi.org/10.1371/journal.ppat.1004662 PMID: 25710374

47. Ivashkiv LB, Donlin LT. Regulation of type I interferon responses. Nat Rev Immunol. 2014; 14(1):36–49. https://doi.org/10.1038/nri3581 PMID: 24362405

48. Porritt RA, Hertzog PJ. Dynamic control of type I IFN signalling by an integrated network of negative regulators. Trends in Immunology. 2015; 36(3):150–60. https://doi.org/https://doi.org/10.1016/j.it.2015.02.002 PMID: 25725583

49. Li R, Yu C, Li Y, Lam T-W, Yiu S-M, Kristiansen K, et al. SOAP2: an improved ultrafast tool for short read alignment. Bioinformatics. 2009; 25(15):1966–7. https://doi.org/10.1093/bioinformatics/btp336 PMID: 19497933

50. Mortazavi A, Williams BA, McCue K, Schaeffer L, Wold B. Mapping and quantifying mammalian transcriptomes by RNA-Seq. Nat Meth. 2008; 5(7):621–8. http://www.nature.com/nmeth/journal/v5/n7/suppinfo/nmeth.1226_S1.html.

Paper III

Salvesen et al. Journal of Neuroinflammation (2017) 14:106
DOI 10.1186/s12974-017-0879-5

Journal of Neuroinflammation

RESEARCH Open Access

LPS-induced systemic inflammation reveals an immunomodulatory role for the prion protein at the blood-brain interface

Ø. Salvesen, M. R. Reiten, A. Espenes, M. K. Bakkebø, M. A. Tranulis and C. Ersdal*

Abstract

Background: The cellular prion protein (PrP^C) is an evolutionary conserved protein abundantly expressed not only in the central nervous system but also peripherally including the immune system. A line of Norwegian dairy goats naturally devoid of PrP^C (*PRNP*$^{Ter/Ter}$) provides a novel model for studying PrP^C physiology.

Methods: In order to explore putative roles for PrP^C in acute inflammatory responses, we performed a lipopolysaccharide (LPS, *Escherichia coli* O26:B6) challenge of 16 goats (8 *PRNP*$^{+/+}$ and 8 *PRNP*$^{Ter/Ter}$) and included 10 saline-treated controls (5 of each *PRNP* genotype). Clinical examinations were performed continuously, and blood samples were collected throughout the trial. Genome-wide transcription profiles of the choroid plexus, which is at the blood-brain interface, and the hippocampus were analyzed by RNA sequencing, and the same tissues were histologically evaluated.

Results: All LPS-treated goats displayed clinical signs of sickness behavior, which were of significantly ($p < 0.01$) longer duration in animals without PrP^C. In the choroid plexus, a substantial alteration of the transcriptome and activation of Iba1-positive cells were observed. This response included genotype-dependent differential expression of several genes associated with the immune response, such as *ISG15*, *CXCL12*, *CXCL14*, and acute phase proteins, among others. Activation of cytokine-responsive genes was skewed towards a more profound type I interferon response, and a less obvious type II response, in PrP^C-deficient goats. The magnitude of gene expression in response to LPS was smaller in the hippocampus than in the choroid plexus. Resting state expression profiles revealed a few differences between the *PRNP* genotypes.

Conclusions: Our data suggest that PrP^C acts as a modulator of certain pathways of innate immunity signaling, particularly downstream of interferons, and probably contributes to protection of vulnerable tissues against inflammatory damage.

Keywords: Cellular prion protein, Systemic inflammation, Lipopolysaccharide (LPS), Innate immunity, Choroid plexus, Hippocampus, Transcriptome, Sickness behavior

Background

The cellular prion protein (PrP^C) has been extensively studied for decades, but its normal function is still not fully understood. However, expression of this highly conserved protein across tissues in vertebrates suggests that it may have roles in a variety of physiological functions [1]. Accumulation of the misfolded isoform (PrP^{Sc}) occurs in all prion disorders, and it has been postulated that loss of PrP^C function participates in the progression of these diseases [2]. Thus, identifying the normal function of PrP^C is considered an essential step in understanding the pathogenesis of prion disorders.

PrP^C is abundantly expressed not only in the central nervous system (CNS) but also in non-neural tissues such as gonads, the pregnant uterus, and the immune system [3–5]. Several roles for PrP^C in immunological processes have been suggested (reviewed in [6]). Lack of PrP^C seems to exacerbate inflammation, both in the periphery [7] and in the CNS [8], as well as ischemic

* Correspondence: cecilie.ersdal@nmbu.no
Faculty of Veterinary Medicine, Norwegian University of Life Sciences, Sandnes, Norway

[9–11] and traumatic [12] brain lesions. Likewise, PrP^C has been linked to regulation of pro- and anti-inflammatory cytokines upon systemic lipopolysaccharide (LPS) challenge [13].

Systemic administration of LPS activates the Toll-like receptor 4 signaling cascade in a range of immune cells, resulting in synthesis and release of a variety of pro-inflammatory cytokines [14]. This, in turn, induces characteristic signs of sickness behavior, which includes depression, periods of shivering, and reduced appetite and locomotor activity [15]. We recently demonstrated that LPS is a potent activator of innate immunity in goats, describing a dynamic regulation of leukocyte genes involved in immunological processes [16]. Because only small amounts of LPS and cytokines cross the blood-brain barrier (BBB) [17], information from the periphery is transmitted to the CNS through neuronal and humoral communication routes. Pro-inflammatory cytokines and LPS can stimulate the vagus nerve, directly initiating afferent signaling to the brain [18]. The humoral route is characterized by circulating cytokines that activate endothelial cells of the BBB or act on tissues that lack BBB, such as the circumventricular organs and choroid plexus (ChP) [19]. Consequently, a mirror image of peripheral cytokines is created within the brain. The ChP is localized within the brain ventricular system and is composed of vascularized stroma surrounded by a monolayer of epithelial cells. The epithelial cells are responsible for the production of cerebrospinal fluid and can release cytokines into the ventricular system. Thus, the ChP plays a key role in transmitting signals into the brain during inflammatory conditions [20, 21]. The cellular composition of the stroma can be dynamically altered through recruitment of circulating immune cells, such as lymphocytes, neutrophils, and monocytes [22, 23]. Although the hippocampus is considered more immunoprivileged than the ChP, systemic LPS challenge may also impair hippocampal function [24, 25]. Certainly, cytokine receptors such as IL1R, which is fundamental in the response to inflammatory signals, are expressed in the hippocampus [26].

Recently, a nonsense mutation early in the gene encoding PrP^C (*PRNP*) in Norwegian dairy goats was discovered [27]. The mutation terminates PrP^C synthesis only seven amino acids into the mature protein. Goats homozygous for the mutation ($PRNP^{Ter/Ter}$) are devoid of PrP^C and postulated to be scrapie-resistant [27, 28]. Physiological and immunological studies have not identified major disturbances under normal herd conditions, which is in agreement with studies in transgenic animals without PrP^C [29, 30]. However, closer phenotypic characterization indicates a small increase in red blood cell count of PrP^C-deficient goats compared both with normal animals and with goats heterozygous for the mutation [28]. These outbred, non-transgenic goats provide a new model for studying PrP^C physiology.

We hypothesized that goats without PrP^C are more susceptible to inflammation or stressful stimuli. To investigate this, we performed a longitudinal LPS study in normal ($PRNP^{+/+}$) and PrP^C-deficient goats ($PRNP^{Ter/Ter}$) comprising clinical, biochemical, and hematological responses, as well as end-point tissue transcriptional profiles and characterization of morphological changes. In the current paper, we focus on the PrP^C-rich hippocampus, which is important in behavior and memory, as well as the ChP, an essential tissue in the interplay between the periphery and the brain.

Methods

Animals

A total of 26 Norwegian dairy goat kids, 13 $PRNP^{Ter/Ter}$ and 13 $PRNP^{+/+}$ animals, were included in the study. The goats were kept under a 16-h light/8-h dark cycle, housed in groups of two to four, and acclimatized at least 21 days before the experiment. Hay and water were provided ad libitum, and they were fed a commercial goat pellet concentrate. During the acclimatizing period, clinical examinations were performed three times, and fecal and blood samples were analyzed to ensure that the animals were healthy before the experiment. An overview of the study groups including treatment, animal number, age, weight, and gender can be found in Additional file 1a.

LPS challenge

The goats were split in groups as follows: 16 goats (8 $PRNP^{Ter/Ter}$ and 8 $PRNP^{+/+}$) that received LPS intravenously and a control group of 10 goats (5 $PRNP^{Ter/Ter}$ and 5 $PRNP^{+/+}$) that were given corresponding volumes of sterile saline. Based on existing literature [31, 32] and a pilot titration study (data not included), the LPS group received a dual dose of LPS (*Escherichia coli* O26:B6, L2654 Sigma-Aldrich, USA) with a 24-h time interval between doses; 0.1 μg/kg (day 1) and 0.05 μg/kg (day 2). As goats are very sensitive to LPS, the second dosage was reduced to avoid the risk of sensitization and mortalities. The animals were euthanized by an overdose of pentobarbital 5 h after the second LPS challenge. An overview of the study protocol is given in Additional file 1b.

Clinical examination

Clinical examination, including rectal temperature, heart and respiratory rate, and rumen contraction frequency was performed by veterinary surgeons at 12 time points during the first 7 h of day 1 and at 9 time points after the second LPS injection. Measurements of rectal temperature were repeated three times at each time point. Clinical examination was performed correspondingly, but at fewer time points, in control animals.

The clinical examination and evaluation of sickness behavior were scored blinded with respect to genotype. Signs of sickness behavior were recorded by evaluating body position (standing, lying, head and ear position), locomotor activity, social interaction, appetite, and shivering. Based on this, goats were scored as presenting "sickness behavior" (S) or "no sickness behavior" (N) every 15 min. The animals were evaluated until three consecutive "N" scorings were recorded, and the total duration of sickness behavior was calculated.

Blood sampling, hematology and biochemistry

Blood samples (EDTA and whole blood) were drawn from *v. jugularis* using a vacutainer system (BD Company, USA). Baseline samples (0 h) were taken within 30 min before LPS challenge. The other sampling times were 1, 2, 5, and 24 h after the day 1 LPS administration. Hematology, including a complete blood count, was performed immediately by using the ADVIA 120 Hematology system (caprine analyzing program). Whole blood tubes were centrifuged, and serum stored at −20 °C until biochemical analysis. Serum total protein, albumin, and glucose were analyzed by ABX Pentra 400 (Horiba, France) and ceruloplasmin by Cobas Mira Plus (Roche). Copper was quantified by AAnalyst 300 atomic absorption spectrometer (PerkinElmer, USA).

Histological examination

The left half of the brain was removed immediately from euthanized goats and immersion-fixed in 4% formaldehyde for 1 week. Defined brain slices were then dehydrated in graded ethanol and paraffin embedded. Morphological changes, including neuronal chromatolysis, single-cell necrosis, and inflammatory cell infiltration, were evaluated by analysis of hematoxylin and eosin-stained 4-μm-thick tissue sections. Brain regions, including hippocampus, ChP in the lateral ventricle, and obex, were investigated.

Immunohistochemistry and semi-quantitative scoring

Paraffin sections (4 μm thick) from the abovementioned areas were mounted on Superfrost® Plus slides (Menzel-Gläser, Thermo Scientific). The distribution and morphological appearance of the astrocyte marker, GFAP (Dako, Z0334), and the microglia/macrophage marker, Iba1 (Wako, 019-19741), were investigated by immunohistochemistry. The sections were dried overnight at 58 °C, deparaffinized in xylene, and rehydrated through decreasing concentrations of graded ethanol. For Iba1 analysis, epitope retrieval was performed by trypsinization (10 mg/ml, 1:10 0.1 M Tris/HCl-buffer, 0.1% $CaCl_2$) for 30 min at 37 °C. Endogenous peroxidase activity was blocked by incubation in 3% H_2O_2 in methanol for 10 min at room temperature. The sections were then blocked in normal goat serum (1:50) diluted in 5% bovine serum albumin (BSA) for 20 min and incubated with the primary antibodies anti-Iba1 (1.0 μg/ml) or anti-GFAP (1.9 μg/ml) for 1 h at room temperature. Further steps were performed with EnVison+ kit (Dako, K4009). The sections were counterstained with hematoxylin for 40 s. Washing between steps was in Tris-buffered saline (TBS). All runs included a negative control section where the primary antibody was replaced with 1% BSA/TBS.

The sections were examined by light microscopy and a blinded, semi-quantitative evaluation was performed by an investigator. The labeling intensity of the Iba1 and GFAP signals, the number of and localization of cells, and the appearance of primary and secondary processes were scored as follows: 0 = minimal, 1 = little, 2 = moderate, 3 = strong, including half-step grading.

RNA extraction, quality control, and pooling

Tissue samples were collected from the right half of the brain within 15 min after euthanasia. The samples were dissected into small pieces, immediately immersed in RNAlater and stored at −80 °C. RNA extraction was carried out using RNeasy Lipid Tissue Mini Kit (Qiagen, 74804) according to the manufacturer's instruction. The isolated RNA was quantified at optical density $(OD)_{260}$, and purity was assessed by $OD_{260/280}$ and $OD_{260/230}$ absorbance readings with a DeNovix DS-11 spectrophotometer (Wilmington, USA). RNA integrity was assessed by RNA 600 Nano chips in compliance with the Agilent Bioanalyzer 2100 system in all individual samples before pooling. RNA quality data are summarized in Additional file 1c.

Extracted RNA was diluted to 500 ng/μl and then re-measured three times. Equal amounts (ng) of RNA from individual samples were pooled, reaching a final amount of 15,000 ng. The samples were pooled according to tissue, treatment, and genotype making a total of eight pools. RNA samples were shipped on dry ice to Novogene (Hong Kong) for RNA sequencing. As the transcriptome profile might be sensitive to gender, one buck (LPS, $PRNP^{Ter/Ter}$) was excluded from the material, leaving only female samples.

RNA sequencing

After quality control, messenger RNA (mRNA) was enriched using oligo (dT) beads and then randomly fragmented. First-strand complementary DNA (cDNA) was synthesized using random hexamers and reverse transcriptase. Second-strand synthesis was done by nick-translation using a buffer containing dNTPs, RNase H, and *E. coli* polymerase I (Illumina). The cDNA fragments were processed using an end-repair reaction after the addition of a single "A" base, followed by adapter ligation. These products were then purified and amplified using

PCR to generate the final cDNA library. The quality of each library was evaluated by 2100 Bioanalyzer (Agilent), followed by paired-end 150-bp sequencing on an Illumina HiSeq2000. The quality control summary can be found in Additional file 1d.

Differential expression analysis

Raw reads (FASTQ) were clipped and trimmed of adapter contamination, and those of low quality were removed. Quality-controlled FASTQ files were mapped to the *Capra hircus* (domestic goat) reference genome using the TopHat2 (v2.0.12) software with two mismatches. Mapping status is summarized in Additional file 1e. Differential gene expression analysis (DEA) was performed using DEGSeq2 (1.12.0) with the following criteria: Log2 ratio ±0.59 (fold change ±1.5) and a false discovery rate (FDR) adjusted q-value ($q < 0.05$). For each tissue, four DEAs were performed. Differences in basal transcriptome levels were assessed by comparing $PRNP^{Ter/Ter}$ (saline) to $PRNP^{+/+}$ (saline). The genomic response to LPS in each genotype was assessed by comparing the LPS groups with the saline-treated control of the matching genotype. Finally, DEAs between $PRNP^{Ter/Ter}$ (LPS) and $PRNP^{+/+}$ (LPS) were performed to identify differences between the genotypes during acute inflammation. FPKM (fragments per kilobase of exon per million fragments mapped) values, which take into account the effects of both sequencing depth and gene length, were used to estimate gene expression levels. Genes encoding ribosomal subunit proteins are not included in the tables.

Gene ontology enrichment analysis

To characterize the overall LPS effect, gene ontology (GO) analysis was performed on genes that were differentially expressed (DEGs) in at least one of the *PRNP* genotypes. We used the online PANTHER classification system to identify over-represented biological processes among the DEGs [33, 34]. Because the *C. hircus* genome was not available, and the *Bos taurus* genome resulted in fewer mapped genes, the well-annotated *Homo sapiens* genome was used as reference. The fold enrichment displays the over-representation of genes in a given biological process, compared with the expected number in the reference genome. p values <0.05 represents a statistical significant over-representation and are calculated by the binomial test as described in [33]. In total, eight genes (*SAA3*, *OAS1L*, *MHCI*, *IFI203*, *VCAM*, *ADGRG6*, *C4*, and *C21H14orf132*) were not mapped to the GO reference genome.

Validation of RNA sequencing by qPCR

First, 600 ng total RNA from each individual sample was converted into first-strand cDNA using QuantiTect Reverse Transcription Kit (Qiagen, Germany) according to the manufacturer's instructions. A non-reverse transcriptase control (NoRT) and no template control (NTC) were included.

The expression of *PRNP*, *IFI6*, *CXCL10*, and *SAA3* genes was investigated by Light cycler 480 qPCR using SYBR Green PCR Master Mix under the following conditions: initial denaturation for 5 min at 95 °C, followed by 40 amplification cycles (10 s at 95 °C, 10 s at 60 °C, and 15 s at 72 °C) and construction of melting curves. For each primer assay, a pool of cDNA samples was used to make three separate series with the following dilutions: 1:2, 1:10, 1:50, 1:250, and 1:1250. Standard curves were constructed to obtain primer amplification efficiencies, correlations, and dynamic range. Internal normalization was performed against the *ACTB* reference gene, and relative expression was calculated using the $2^{-\Delta\Delta Cq}$ method [35]. Primer sequences are given in Additional file 1f.

Descriptive and statistical analyses

Clinical, biochemical, hematological, and qPCR expression data are presented as mean ± standard error of the mean (SEM). Graphical and statistical analyses were performed in GraphPad Prism 6 (GraphPad software Inc., USA) and Microsoft Excel 2013. Comparisons between two groups were performed using Student's t test, assuming equal variance.

Results

Prolonged sickness behavior in goats devoid of PrP^C

Within the first 2 hours after LPS administration, all 16 goats displayed characteristic signs of sickness behavior, such as lowered head, hanging ears, and periods of shivering, as well as reduced social interaction, appetite, and locomotor activity. The mean duration of sickness behavior was significantly ($p < 0.01$) longer in the $PRNP^{Ter/Ter}$ group (6.03 ± 0.59 h), than in the $PRNP^{+/+}$ goats (4.16 ± 0.33 h) after day 1 LPS challenge (0.1 μg/kg). The second LPS injection (0.05 μg/kg) induced a significantly shorter period of sickness behavior compared with day 1, but the difference between the genotypes was non-significant (Fig. 1a, b). $PRNP^{Ter/Ter}$ goats displayed a slightly higher mean body temperature at all time points throughout the experiment. The fever response was biphasic, with the lower peak at 1.5 h and the highest temperature at 3.5 h on day 1. A quick onset monophasic fever, peaking at 1.5 h was measured on day 2 (Fig. 1c). Tachycardia was observed in both genotypes, reaching a maximum at 5 h post challenge (data not shown).

The number of white blood cells declined after LPS challenge (Fig. 1d), abruptly in neutrophils and monocytes and more gradually in lymphocytes, with no differences between the genotypes (Additional file 2a). This contrasts with what has been reported in *Prnp*-knock out (KO) mice following systemic LPS injection [13], and

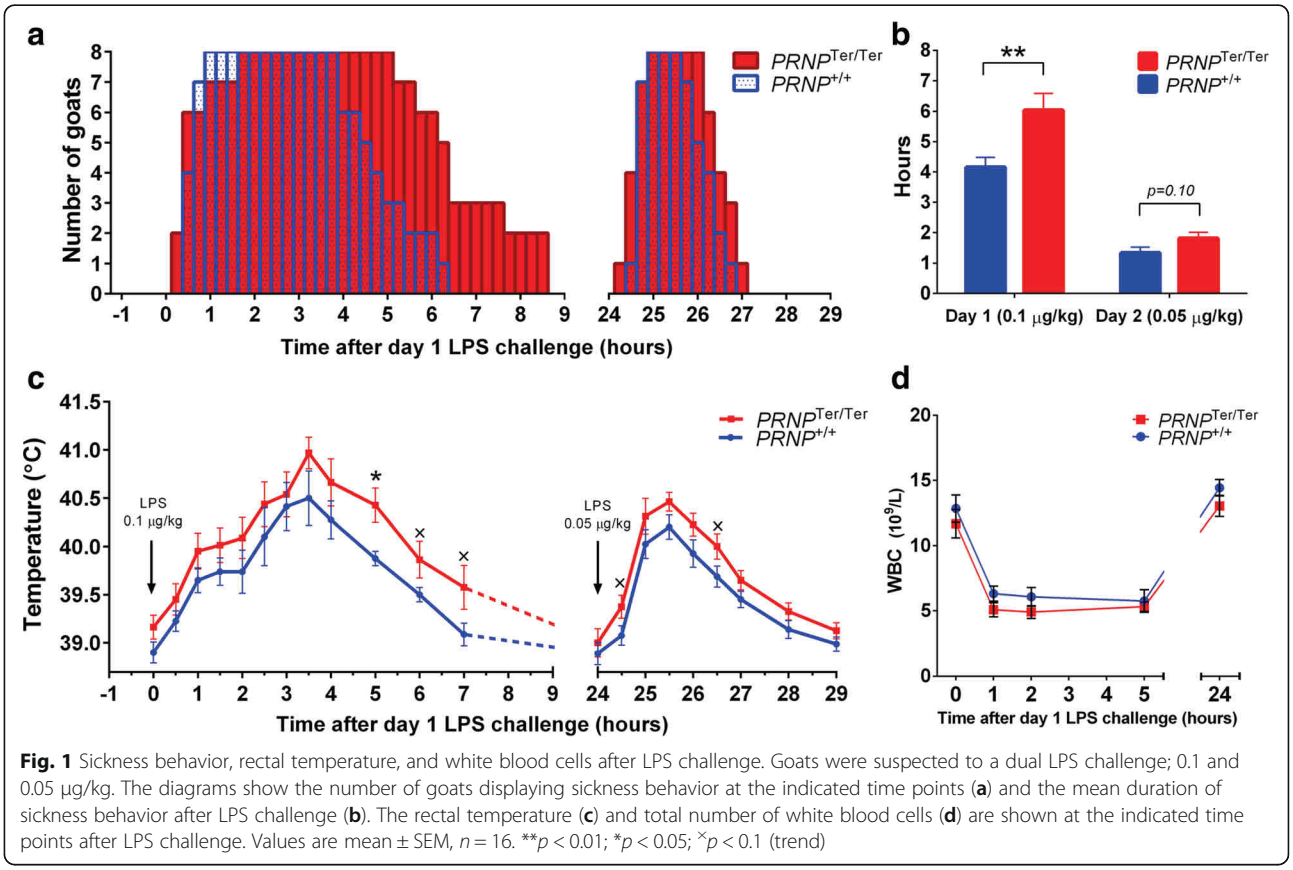

Fig. 1 Sickness behavior, rectal temperature, and white blood cells after LPS challenge. Goats were suspected to a dual LPS challenge; 0.1 and 0.05 μg/kg. The diagrams show the number of goats displaying sickness behavior at the indicated time points (**a**) and the mean duration of sickness behavior after LPS challenge (**b**). The rectal temperature (**c**) and total number of white blood cells (**d**) are shown at the indicated time points after LPS challenge. Values are mean ± SEM, $n = 16$. $^{**}p < 0.01$; $^{*}p < 0.05$; $^{\times}p < 0.1$ (trend)

our data do not support a role for PrP^{C} in leukocyte extravasation and recovery. Total serum protein decreased in both groups, and the level of albumin was significantly lower in $PRNP^{Ter/Ter}$ animals at 5 and 24 h. No differences were observed in serum ceruloplasmin or copper. Although impaired glucose homeostasis has been observed in *Prnp*-KO mice [36], blood glucose was regulated similarly between the two genotypes after LPS challenge (Additional file 2b). None of the control animals displayed alterations in clinical, hematological, or biochemical parameters in response to saline injection and handling stress.

Systemic LPS challenge induces substantial alterations in the choroid plexus transcriptome and reveals differences between *PRNP* genotypes

In the ChP, 92 genes were upregulated and 25 genes downregulated in at least one *PRNP* genotype upon LPS challenge (Fig. 2). Eighty-seven percent of the DEGs were regulated in the same direction in both *PRNP* genotypes, but some had a log2 ratio or *q*-value outside our filtration criteria (Additional file 3). GO enrichment analysis of upregulated genes displayed an over-representation of genes involved in type I interferon (IFN) signaling, collagen catabolism, and leukocyte migration. Additionally, 19 genes were characterized as being involved in the innate immune response and 23 genes were cytokine-responsive (Additional file 4a).

Finally, we identified 25 differentially expressed genes between the two genotypes after LPS treatment, which included several immune genes, as well as genes involved in extracellular matrix stability and oxidative phosphorylation (Table 1). Given the previous report on cytokines being influenced by PrP^{C} [13], we analyzed the 23 genes characterized as cytokine-responsive (GO:0034097) with less stringent criteria (fold change ±1.2 and $p < 0.05$). Comparing the log2 ratio of the these genes after LPS administration, a relatively higher type I IFN response, and less prominent type II IFN response, was noted in the PrP^{C}-deficient goats (Fig. 3).

Systemic LPS challenge induces minor alterations in hippocampus transcriptome in both *PRNP* genotypes

According to the filtration criteria, only 10 genes were upregulated and 3 genes downregulated, in one or both *PRNP* genotypes after LPS challenge (Fig. 2 and Table 2). Five of the upregulated genes (*MT2*, *CXCL9*, *CXCL10*, *TGM2*, and *IFI6*) were classified as being involved in cytokine signaling (Additional file 4b). *CXCL10*, *CXCL9*, and *TGM2* were significantly upregulated in both genotypes, whereas IFI6 was only upregulated in normal goats. The expression of IFI6, however, was already high

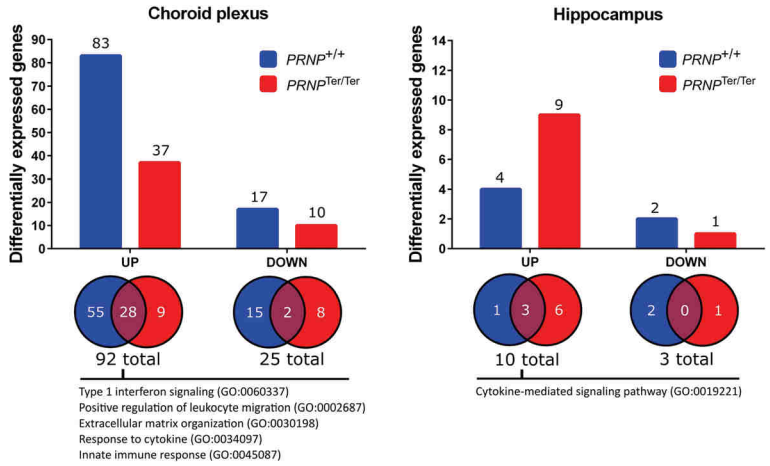

Fig. 2 Upregulated and downregulated genes in the choroid plexus and hippocampus after LPS challenge. Differential expression analyses were performed by comparing the LPS groups to the saline-treated control group of the matching genotype (log2 ratio ±0.59 and $q < 0.05$). Venn diagrams show genes that overlap in the two genotypes. The top over-represented biological functions (GO terms) are included for upregulated genes. LPS, $n = 15$. Saline, $n = 10$

at rest in $PRNP^{Ter/Ter}$ goats (saline group). Six genes (*ATP5I*, *GFAP*, *HOPX*, *MT2*, *MT1A*, and *SLC14A1*) were significantly upregulated in the PrP^{C}-deficient goats and slightly, but non-significantly, upregulated in the normal goats. In the LPS-treated normal goats, a slight increase in *PRNP* expression was observed by RNA sequencing and qPCR, but this was not statistically significant.

Transcriptome analyses of choroid plexus and hippocampus at rest (saline) reveal minor differences between the *PRNP* genotypes

The basal expression was investigated by a differential expression analysis of the saline-treated groups, and only minor differences were observed. $PRNP^{Ter/Ter}$ goats displayed higher expression of IFI6 in both hippocampus and in the ChP. *DKK3*, *CHGA*, and *MYOM2* were slightly upregulated in the PrP^{C}-deficient goats, whereas the transcript levels of *PRNP* were decreased with a log2 ratio of −4.4 in the hippocampus and −2.3 in the ChP. However, as RNA was extracted from tissues as a whole, the dilution effect might mask more subtle phenotypes related to loss of PrP^{C} in certain cell populations.

Systemic LPS activates Iba1-positive cells in the choroid plexus and astrocytes in the hippocampus in both *PRNP* genotypes

In the ChP, expression of the Iba1-encoding allograft inflammatory factor 1 (*AIF1*) and of the microglia/macrophage phenotype activation markers was increased (Fig. 4a, b). This corresponded with increased signal and number of Iba1-positive cells (Fig. 4c, d). These cells were primarily located at the basal side of the epithelial cells and within the stroma, with processes extending between the epithelium and around blood vessels. Some Iba1-positive cells were presumably migrating towards the apical surface and found between the epithelial cells and at the apical surface. No GFAP-labeling was observed in the ChP, confirming that this tissue does not contain astrocytes. Evaluation of the HE-stained sections did not reveal infiltration of inflammatory cells within the stroma (Fig. 4e), but an increased number of leukocytes was observed in the blood vessels (leukostasis).

In the hippocampus, LPS treatment upregulated *GFAP* expression, and increased GFAP signal was detected by immunohistochemistry in the molecular layer, subgranular layer, and hilus (Fig. 5). Activated astrocytes had more distinct primary and secondary processes, than seen in saline controls. Morphological evaluation of Iba1-stained microglia did not identify any effect of treatment or genotype in the hippocampus or obex. Some individuals had a few single-cell necrosis in the granular and subgranular layer, but this was not related to genotype or treatment. No evidence of disruption of the BBB was observed by light microscopy.

Validation of RNA sequencing by qPCR on individual RNA samples

Four target genes (*PRNP*, *IFI6*, *CXCL10*, and *SAA3*) were investigated by qPCR on individual RNA samples from both tissues. A strong correlation ($r = 0.989$, $p < 0.0001$, Pearson correlation) was observed between expression values of RNAseq and qPCR, and differential expression was confirmed in 26 out of 28 comparisons. The increased IFI6 expression in $PRNP^{Ter/Ter}$ goats at rest was primarily due to large biological variability. In the hippocampus, *SAA3* was not detected by RNAseq in saline groups, and comparison

Table 1 Choroid plexus DEGs between *PRNP* genotypes after LPS treatment

Gene ID	Symbol	Gene name	Log2 ratio	Top functions
100860813	MHC II	HA25	1.80	Antigen presentation (extracellular pathway)
102178155	FTSJ1	FtsJ RNA methyltransferase homolog 1	1.53	Methyltransferase
102169982	ISG15	ISG15 ubiquitin-like modifier	0.99	ISGylation, innate immunity
102189650	ANK3	Ankyrin 3	0.75	Cell motility, activation, proliferation,
102187800	UBB	Ubiquitin B	0.73	Targeting of proteins for degradation
102184593	SPOCK2	SPARC/osteonectin, cwcv and kazal-like domains proteoglycan 2	0.68	Extracellular matrix structure
102183219	BGN	Biglycan	−0.60	Extracellular matrix structure, innate immunity
102188061	ATP5E	ATP synthase, H+ transporting, mitochondrial F1 complex, epsilon subunit	−0.63	Catalyzes ATP synthesis, oxidative phosphorylation
102185420	COL24A1	Collagen type XXIV alpha 1 chain	−0.66	Extracellular matrix structure
102172487	CP	Ceruloplasmin	−0.66	Acute phase protein, ferroxidase enzyme
102169556	CXCL12	C-X-C motif chemokine ligand 12	−0.67	Chemoattractant, innate immunity
102172637	LECT1	Leukocyte cell derived chemotaxin 1	−0.69	Promotes chondrocyte growth, inhibit angiogenesis
102170107	ATP5J2	ATP synthase, H+ transporting, mitochondrial Fo complex subunit F2	−0.70	Catalyzes ATP synthesis, oxidative phosphorylation
102181355	PCOLCE	Procollagen C-endopeptidase enhancer	−0.75	Collagen precursor peptidase activator
100860756	OGN	Osteoglycin	−0.76	Growth factor activity
102179198	TNC	Tenascin C	−0.81	Extracellular matrix structure
102182694	CXCL14	C-X-C motif chemokine ligand 14	−0.81	Chemoattractant, immunomodulatory
102177419	NDUFA1	NADH:ubiquinone oxidoreductase subunit A1	−0.85	Component of the respiratory chain, mitochondria
102191086	COCH	Cochlin	−1.03	Extracellular matrix, pro-inflammatory, cytokine regulatory
102187830	COL17A1	Collagen type XVII alpha 1 chain	−1.04	Hemidesmosome component
102189939	ATP5I	ATP synthase, H+ transporting, mitochondrial Fo complex subunit E	−1.58	Catalyze ATP synthesis, oxidative phosphorylation
100860915	ASIP	Agouti signaling protein	−2.14	Paracrine signaling, pigmentation
102180584	MHC I	BOLA class I histocompatibility antigen, alpha chain BL3-7	−2.32	Antigen presentation (cytosolic pathway)
102169975	PRNP	Prion protein	−2.80	Unknown, cytoprotective
102176354	HP	Haptoglobin	−3.25	Acute phase protein, bind hemoglobin

Differential expression analysis was performed by comparing LPS-treated $PRNP^{Ter/Ter}$ vs. $PRNP^{+/+}$ (log2 ratio ± 0.59 and $q < 0.05$). $n = 15$

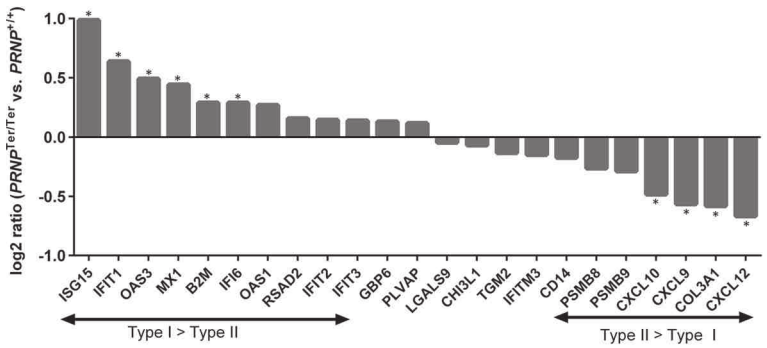

Fig. 3 Comparison of ChP cytokine-responsive genes (GO:0034097) after LPS challenge between genotypes. Expression levels were investigated by transcriptome analysis (Illumina HiSeq 2000) on RNA extracted from the choroid plexus. Transcripts of genes stimulated primarily by type I interferons increased in PrP^{C}-deficient goats compared with $PRNP^{+/+}$ goats, whereas genes stimulated primarily by type II interferons were reduced. *Fold change ±1.2 and $p < 0.05$. $n = 15$

Table 2 Upregulated and downregulated genes in the hippocampus after LPS challenge

			Log2 ratio, LPS vs. saline		
Gene ID	Symbol	Gene name	$PRNP^{+/+}$	$PRNP^{Ter/Ter}$	Top functions
102185230	IFI6	Interferon alpha inducible protein 6	*1.19**	−0.05	Regulation of apoptosis
100860873	CXCL10	C-X-C motif chemokine ligand 10	*3.37**	*3.07**	Chemoattractant
102187851	CXCL9	C-X-C motif chemokine ligand 9	*2.93**	*2.65**	Chemoattractant
102185477	TGM2	Transglutaminase 2	*1.25**	*1.36**	Unclear, involved in phagocytosis
102189939	ATP5I	ATP synthase, H+ transporting, mitochondrial Fo complex subunit E	0.53	*0.76**	Catalyze ATP synthesis
102190069	GFAP	Glial fibrillary acidic protein	0.34	*0.62**	Cell communication, mitosis, BBB function
102178715	HOPX	HOP homeobox	0.35	*0.65**	Unknown
102188072	MT2	Metallothionein-2	0.29	*0.91**	Metal-binding, neuroprotection
102188618	MT1A	Metallothionein-1A	0.58	*1.40**	Metal-binding, neuroprotection
100860878	SLC14A1	Solute carrier family 14 member 1	0.54	*1.59**	Membrane transport (urea)
102186073	AQP4	Aquaporin 4	*−0.61**	−0.31	Membrane transport (water)
102175716	MYO10	Myosin X	*−0.66**	−0.53	Motor molecule, bind actin
102186825	COL9A2	Collagen type IX alpha 2 chain	−0.43	*−0.64**	Extracellular matrix structure

Differential expression analyses were performed by comparing the LPS groups to the saline control group of the matching genotype. Italic values indicate a true differential expression. LPS, $n = 15$. Saline, $n = 10$
*log2 ratio ±0.59, $q < 0.05$

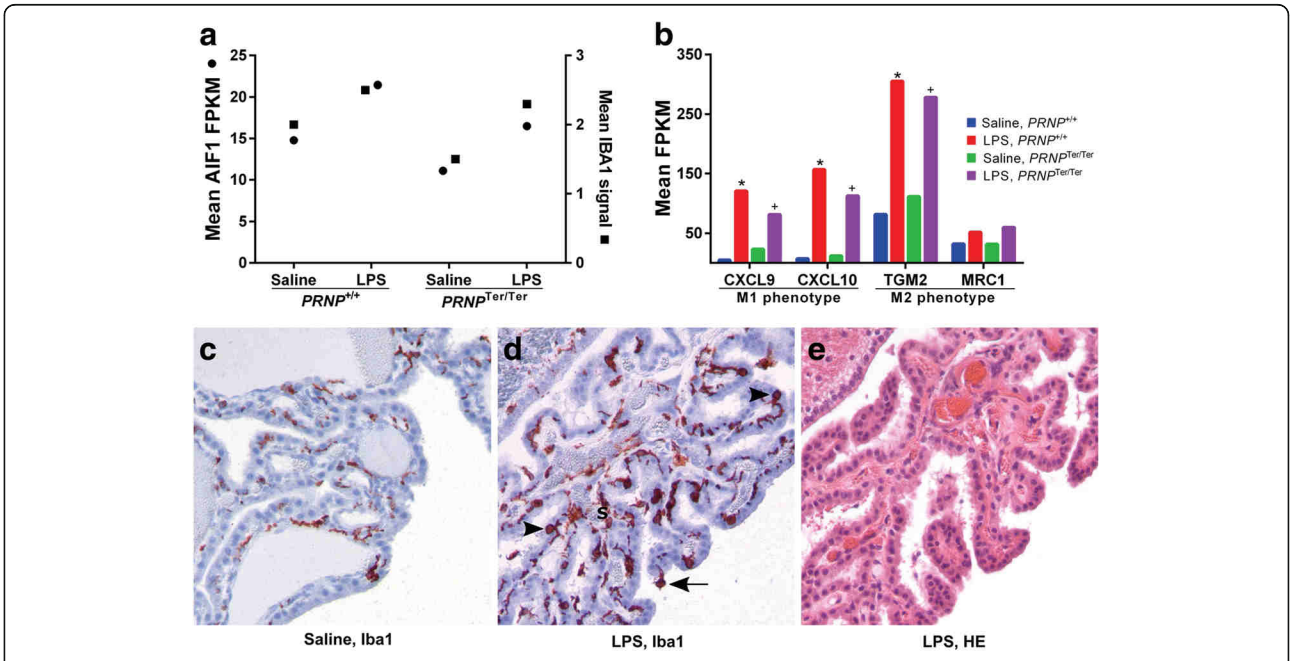

Fig. 4 LPS upregulates AIF1/IBA1 and macrophage/microglia phenotype markers in the choroid plexus. Expression levels were investigated by transcriptome analysis (Illumina HiSeq 2000) on RNA extracted from the choroid plexus. Allograft inflammatory factor 1 (*AIF1*) expression corresponded with increased IBA1 signal detected by immunohistochemistry (**a**). Genes indicating activation of macrophage/microglia phenotype M1 and M2 increased in both *PRNP* genotypes. A significant upregulation (log2 ratio >0.59, $q < 0.05$) in $PRNP^{+/+}$ and $PRNP^{Ter/Ter}$ goats is indicated by an *asterisk* and *plus sign*, respectively (**b**). Some Iba1-positive cells are present in the choroid plexus of saline-treated animals (**c**). The number of Iba1-positive cells is increased, and the cells have a different location and longer processes in LPS-treated animals. Cells are localized within the stroma (*S*), between the epithelial cells (*arrowhead*) and protruding from the apical surface (*arrow*) (**d**). No infiltration of inflammatory cells is observed within the stroma (**e**). ×200 magnification. LPS, $n = 16$. Saline, $n = 10$

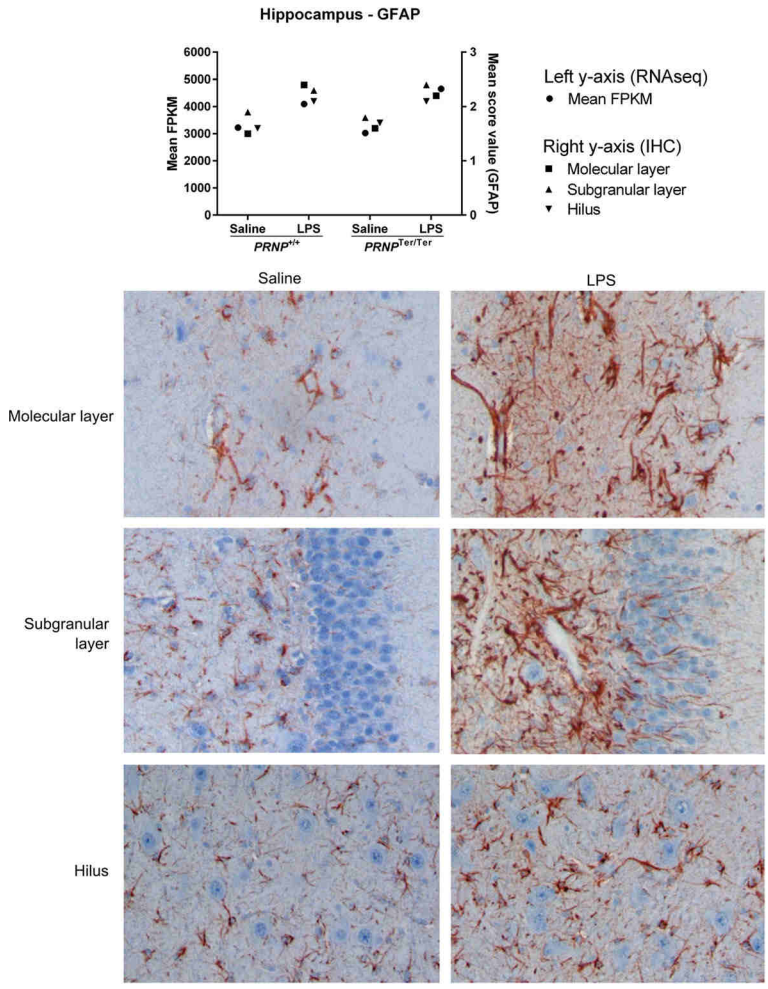

Fig. 5 LPS upregulates *GFAP* expression and GFAP signal in hippocampus in both *PRNP* genotypes. Mean *GFAP* expression was investigated by transcriptome analysis (Illumina HiSeq 2000) on RNA extracted from the hippocampus. GFAP immunohistochemistry (IHC) shows increased GFAP signal in the molecular layer, subgranular layer, and hilus after LPS administration. Activated astrocytes have more distinct primary and secondary processes. ×200 magnification. LPS, $n = 16$. Saline, $n = 10$

with relative qPCR expression was not possible (Additional file 5).

Discussion

The high degree of conservation of the *PRNP* gene across species [37] suggests that the protein possesses important biological functions. These have, however, proven difficult to pin-point even after the creation of *Prnp*-KO mice [38]. It has been proposed that compensatory mechanisms could mask loss-of-function phenotypes under normal conditions and become evident during stress such as inflammation. For instance, *Prnp*-KO mice displayed an exacerbated disease progression of experimental autoimmune encephalomyelitis [8] and colitis [7]. Here, we report the first study of the inflammatory response in a unique, non-rodent model naturally devoid of PrP^C. Considering the high *PRNP* expression in the hippocampus and the role of the choroid plexus (ChP) in responding to inflammatory signals at the blood-brain boundary, we investigated both these tissues by full-scale transcriptome analysis. Our data suggest a role for PrP^C in modulating the innate immune response.

Systemic LPS challenge induced characteristic signs of sickness behavior that was prolonged by about 2 h in $PRNP^{Ter/Ter}$ goats after the initial high dose of LPS (0.1 μg/kg). This is a novel clinical loss-of-function phenotype, pointing to a more potent inflammatory response in the absence of PrP^C. When the dosage was halved on day 2, the mean duration of sickness behavior was only about 1–2 h in both groups. The difference between genotypes was similar as day 1, but not statistically significant ($p = 0.1$). This suggests that the lower dose of LPS did not induce a sufficient amount of inflammatory stress to clearly separate the two genotypes.

In the ChP, a clear acute phase response as well as activation of a range of interferon-stimulated genes was observed, which underlines the widespread role of these genes in the host defense to bacterial endotoxin [16]. Interestingly, several genes associated with the immune response were differentially expressed between the *PRNP* genotypes after LPS challenge. This included acute phase proteins genes and multiple chemokines, as well as *COCH* that has an anti-bacterial role by regulating local cytokine production [39]. Based on previous reports of PrP^C regulating cytokines [13], we compared the 23 genes characterized as cytokine-responsive (GO:0034097) between the two genotypes. Most of these genes are primarily induced by type I and/or type II IFNs [40, 41]. Notably, there was a relatively more pronounced type I IFN response and a weaker type II response in PrP^C-deficient goats, compared with the normal group. A potential role of PrP^C in regulating type II IFN response has been previously suggested, as IFN-γ levels were decreased in ConA-treated PrP 0/0 splenocytes [42], but type I interferon signaling has received less attention. Type I interferons are key modulators of innate immunity and may affect the manifestation of sickness behavior by facilitating the immune activation of other cytokines [43]. Indeed, interferon signaling is involved in many of the effects previously attributed PrP^C, such as apoptosis [44], protection against oxidative stress [45], DNA repair [46], and depressive-like behavior immediately after stress [47, 48]. Taken together, our data indicate that PrP^C contributes as a modulator of innate immunity signaling, particularly downstream of type I interferons, which might affect the duration of sickness behavior.

The substantial activation of the ChP transcriptome, including upregulation of *AIF1* expressed by activated macrophages/microglia, corresponded with a parallel increase in Iba1 signal. Markers of classical activation M1 (*CXCL9*, *CXCL10*) and alternative activation M2 (*TGM2*, *MRC1*) increased [49, 50], suggesting a combination of M1 and M2 phenotype of activated macrophages/Iba1-positive cells. Moreover, cytokines involved in leukocyte migration were upregulated, as well as genes involved in collagen catabolism and extracellular matrix organization, indicating that the integrity of the blood-cerebrospinal fluid barrier was altered. These findings agree with the observation of increased numbers of Iba1-positive cells in the ChP stroma, some of which were presumably migrating through the epithelium. The stromal cells could represent antigen-presenting cells as dendritic cells [51], recently blood-derived monocytes, or residing macrophages [52].

Not surprisingly, alterations in the hippocampus transcriptome were modest compared with those observed in the ChP, yet a somewhat similar cytokine response was present. However, it is possible that the filtration of single genes strictly by fold change and *q*-value might exclude biologically relevant pathways characterized by a subtle increase in a subset of genes. The two most upregulated genes in the hippocampus were *CXCL9* and *CXCL10*, which are primarily induced by IFN-γ signaling [41]. Recently, *CXCL10* expression in hippocampus was traced to activated astrocytes and cells lining the blood vessels [53]. This suggests that endothelial cells within the BBB, as well as nearby glial cells, react to circulating LPS and cytokines by releasing IFN-γ, which, in turn, stimulates expression of *CXCL9* and *CXCL10*. Despite the important role of these chemokines in recruiting immune cells into the brain [54], no inflammatory cell infiltration was observed in our study. Although the overall LPS response in the hippocampus was similar in the two *PRNP* genotypes, two metallothioneins (MT) were significantly upregulated in PrP^C-deficient goats. Metallothioneins bind metals and scavenge free radicals and participate in reducing the inflammatory and oxidative stress [55]. In the brain, MT-I and MT-II are primarily expressed by activated astrocytes [55]. We further found that *GFAP* transcription increased significantly in $PRNP^{Ter/Ter}$ goats, indicating an early activation of astrocytes as previously described [53, 56]. This was confirmed by an increased GFAP labeling after LPS treatment. Given the role of MTs [55] and PrP^C [57] in neuroprotection, it is tempting to speculate that upregulation of metallothioneins in astrocytes could be part of a compensatory mechanism in goats devoid of PrP^C.

Systemic administration of LPS has been shown to activate microglia in the hypothalamus, thalamus, and brainstem as early as 8–24 h after LPS challenge [58], but murine hippocampal microglia were not activated until 48 h post challenge [59]. The latter study is consistent with our results as we did not observe increased AIF1 expression or altered Iba1 immunohistochemical labeling in hippocampus 29 h after the first LPS injection. Altogether, the transcriptional and morphological findings indicate that only a modest inflammation, with a predominance of astrocytes, was present in the hippocampus. This might not be sufficient to manifest clearly potential phenotypes related to the loss of PrP^C and further suggests that this brain region is relatively protected from circulating endotoxins. Still, the clinical signs of sickness behavior, and difference between the *PRNP* genotypes in this respect, demonstrate the sensitivity of the CNS towards inflammatory insult and that this sensitivity is increased in the absence of PrP^C.

Although not statistically significant, LPS upregulated *PRNP* transcripts in both the hippocampus and ChP of $PRNP^{+/+}$ goats, indicating a role for PrP^C in acute inflammation. Similarly, systemic LPS upregulated PrP^C in circulating neutrophils [60], whereas LPS incubation

increased *PRNP* expression in neuronal cell cultures [61]. As expected, *PRNP* expression was low in PrP^C-deficient goats, regardless of treatment, which probably reflects nonsense-mediated mRNA decay [62].

Conclusions

This is the first report of an endotoxin challenge in a non-transgenic goat model naturally devoid of PrP^C. Animals without PrP^C suffered a significantly prolonged period of sickness behavior after LPS challenge. Transcriptome data revealed that in the absence of PrP^C, LPS induced an increased expression of a number of genes downstream of type I interferons. These results, together with the finding that *PRNP* was slightly upregulated upon LPS stimulation in normal goats, point to an immunomodulatory role for PrP^C during inflammation. Importantly, a huge number of proteins contribute to modulating inflammatory responses, balancing pro- and anti-inflammatory signaling. This balancing act is vitally important for the organism and not dependent upon a few proteins or signaling pathways. Considering the many crossroads between innate immunity signaling and various aspects of cellular homeostasis, such as apoptosis and DNA repair, our data contribute to a new understanding of cellular functions previously ascribed to PrP^C and provide directions for future mechanistic studies.

Additional files

Additional file 1: Material and methods. Study groups, experimental protocol, RNA quality control, RNA sequencing quality control and mapping status, and primer sequences. (PDF 395 kb)

Additional file 2: Hematology and biochemistry after LPS challenge. (PDF 590 kb)

Additional file 3: List of upregulated and downregulated genes in choroid plexus after LPS challenge. (PDF 458 kb)

Additional file 4: Gene ontology analyses of DEGs after LPS challenge. (PDF 312 kb)

Additional file 5: Validation of RNAseq data by qPCR. (PDF 484 kb)

Abbreviations

ChP: Choroid plexus; CNS: Central nervous system; DEA: Differential expressed analysis; DEGs: Differentially expressed genes; GO: Gene ontology; IL1R: Interleukin 1 receptor; INF: Interferon; LPS: Lipopolysaccharide; NoRT: No reverse transcriptase; NTC: No template control; qPCR: Quantitative real-time polymerase chain reaction; RIN: RNA integrity number

Acknowledgements

The authors are grateful to Siri Bjerkreim Hamre and Wenche Okstad for skillful laboratory work. The authors acknowledge Lucy Robertson for proofreading the manuscript.

Funding

The research was supported by The Research Council of Norway.

Availability of data and materials

Data and material supporting the conclusions are contained within the manuscript.

Authors' contributions

CE, MAT, AE, MKB, and ØS designed the study. ØS, MRR, CE, AE, and MAT performed the experiments. ØS carried out the laboratory procedures, performed the statistical analysis, and drafted the manuscript. All authors have critically read and approved the final manuscript.

Competing interests

The authors declare that the research was conducted in the absence of any commercial or financial relationships that could be construed as a potential conflict of interest.

Ethics approval

The animal experiment was performed in compliance with the ethical guidelines and approved by the Norwegian Animal Research Authority (ID 5827, 6903, and 7881) with reference to the Norwegian regulation on animal experimentation (FOR-2015-06-18-761).

Publisher's Note

Received: 24 February 2017 Accepted: 9 May 2017
Published online: 22 May 2017

References

1. Linden R, Martins VR, Prado MA, Cammarota M, Izquierdo I, Brentani RR. Physiology of the prion protein. Physiol Rev. 2008;88(2):673–728.
2. Hetz C, Maundrell K, Soto C. Is loss of function of the prion protein the cause of prion disorders? Trends Mol Med. 2003;9(6):237–43.
3. McLennan NF, Rennison KA, Bell JE, Ironside JW. *In situ* hybridization analysis of PrP mRNA in human CNS tissues. Neuropathol Appl Neurobiol. 2001; 27(5):373–83.
4. Tanji K, Saeki K, Matsumoto Y, Takeda M, Hirasawa K, Doi K, et al. Analysis of PrPc mRNA by *in situ* hybridization in brain, placenta, uterus and testis of rats. Intervirology. 1995;38(6):309–15.
5. Bakkebø MK, Mouillet-Richard S, Espenes A, Goldmann W, Tatzelt J, Tranulis MA. The cellular prion protein: a player in immunological quiescence. Front Immunol. 2015;6:450.
6. Isaacs JD, Jackson GS, Altmann DM. The role of the cellular prion protein in the immune system. Clin Exp Immunol. 2006;146(1):1–8.
7. Martin GR, Keenan CM, Sharkey KA, Jirik FR. Endogenous prion protein attenuates experimentally induced colitis. Am J Pathol. 2011;179(5):2290–301.
8. Gourdain P, Ballerini C, Nicot AB, Carnaud C. Exacerbation of experimental autoimmune encephalomyelitis in prion protein (PrPc)-null mice: evidence for a critical role of the central nervous system. J Neuroinflammation. 2012;9:25.
9. Steele AD, Zhou Z, Jackson WS, Zhu C, Auluck P, Moskowitz MA, et al. Context dependent neuroprotective properties of prion protein (PrP). Prion. 2009;3(4):240–9.
10. McLennan NF, Brennan PM, McNeill A, Davies I, Fotheringham A, Rennison KA, et al. Prion protein accumulation and neuroprotection in hypoxic brain damage. Am J Pathol. 2004;165(1):227–35.
11. Spudich A, Frigg R, Kilic E, Kilic U, Oesch B, Raeber A, et al. Aggravation of ischemic brain injury by prion protein deficiency: role of ERK-1/-2 and STAT-1. Neurobiol Dis. 2005;20(2):442–9.
12. Hoshino S, Inoue K, Yokoyama T, Kobayashi S, Asakura T, Teramoto A, et al. Prions prevent brain damage after experimental brain injury: a preliminary report. Acta Neurochir Suppl. 2003;86:297–9.
13. Liu J, Zhao D, Liu C, Ding T, Yang L, Yin X, et al. Prion Protein participates in the protection of mice from lipopolysaccharide infection by regulating the inflammatory process. J Mol Neurosci. 2014;55:279–87.
14. Park BS, Lee JO. Recognition of lipopolysaccharide pattern by TLR4 complexes. Exp Mol Med. 2013;45:e66.
15. Dantzer R. Cytokine, sickness behavior, and depression. Immunol Allergy Clin North Am. 2009;29(2):247–64.
16. Salvesen Ø, Reiten MR, Heegaard PM, Tranulis MA, Espenes A, Skovgaard K, et al. Activation of innate immune genes in caprine blood leukocytes after systemic endotoxin challenge. BMC Vet Res. 2016;12(1):241.
17. Banks WA, Robinson SM. Minimal penetration of lipopolysaccharide across the murine blood-brain barrier. Brain Behav Immun. 2010;24(1):102–9.

18. Bluthé RM, Walter V, Parnet P, Layé S, Lestage J, Verrier D, et al. Lipopolysaccharide induces sickness behaviour in rats by a vagal mediated mechanism. C R Acad Sci III. 1994;317(6):499–503.
19. Bluthé RM, Michaud B, Kelley KW, Dantzer R. Vagotomy blocks behavioural effects of interleukin-1 injected via the intraperitoneal route but not via other systemic routes. Neuroreport. 1996;7(15-17):2823–7.
20. Marques F, Sousa JC, Coppola G, Falcao AM, Rodrigues AJ, Geschwind DH, et al. Kinetic profile of the transcriptome changes induced in the choroid plexus by peripheral inflammation. J Cereb Blood Flow Metab. 2009;29(5):921–32.
21. Marques F, Sousa JC, Coppola G, Geschwind DH, Sousa N, Palha JA, et al. The choroid plexus response to a repeated peripheral inflammatory stimulus. BMC Neurosci. 2009;10:135.
22. Schmitt C, Strazielle N, Ghersi-Egea JF. Brain leukocyte infiltration initiated by peripheral inflammation or experimental autoimmune encephalomyelitis occurs through pathways connected to the CSF-filled compartments of the forebrain and midbrain. J Neuroinflammation. 2012;9:187.
23. Marques F, Mesquita SD, Sousa JC, Coppola G, Gao F, Geschwind DH, et al. Lipocalin 2 is present in the EAE brain and is modulated by natalizumab. Front Cell Neurosci. 2012;6:33.
24. Czerniawski J, Guzowski JF. Acute neuroinflammation impairs context discrimination memory and disrupts pattern separation processes in hippocampus. J Neurosci. 2014;34(37):12470–80.
25. Shaw KN, Commins S, O'Mara SM. Lipopolysaccharide causes deficits in spatial learning in the watermaze but not in BDNF expression in the rat dentate gyrus. Behav Brain Res. 2001;124(1):47–54.
26. Friedman WJ. Cytokines regulate expression of the type 1 interleukin-1 receptor in rat hippocampal neurons and glia. Exp Neurol. 2001;168(1):23–31.
27. Benestad SL, Austbø L, Tranulis MA, Espenes A, Olsaker I. Healthy goats naturally devoid of prion protein. Vet Res. 2012;43:87.
28. Reiten MR, Bakkebø MK, Brun-Hansen H, Lewandowska-Sabat AM, Olsaker I, Tranulis MA, et al. Hematological shift in goat kids naturally devoid of prion protein. Frontiers in cell and developmental biology. 2015;3:44.
29. Büeler H, Aguzzi A, Sailer A, Greiner RA, Autenried P, Aguet M, et al. Mice devoid of PrP are resistant to scrapie. Cell. 1993;73(7):1339–47.
30. Richt JA, Kasinathan P, Hamir AN, Castilla J, Sathiyaseelan T, Vargas F, et al. Production of cattle lacking prion protein. Nat Biotechnol. 2007;25(1):132–8.
31. Takeuchi Y, Kikusui T, Kizumi O, Ohnishi H, Mori Y. Pathophysiological changes evoked by lipopolysaccharide administration in goats. J Vet Med Sci. 1997;59(2):125–7.
32. Ismail M. A pharmacokinetic study of danofloxacin in febrile goats following repeated administration of endotoxin. J Vet Pharmacol Ther. 2006;29(4):313–6.
33. Mi H, Muruganujan A, Casagrande JT, Thomas PD. Large-scale gene function analysis with the PANTHER classification system. Nat Protoc. 2013; 8(8):1551–66.
34. Gene Ontology Consortium enrichment analysis. http://geneontology.org/. Accessed 11 Dec 2016
35. Livak KJ, Schmittgen TD. Analysis of relative gene expression data using real-time quantitative PCR and the 2(-Delta Delta C(T)) Method. Methods. 2001;25(4):402–8.
36. Strom A, Wang GS, Scott FW. Impaired glucose tolerance in mice lacking cellular prion protein. Pancreas. 2011;40(2):229–32.
37. Wopfner F, Weidenhöfer G, Schneider R, von Brunn A, Gilch S, Schwarz TF, et al. Analysis of 27 mammalian and 9 avian PrPs reveals high conservation of flexible regions of the prion protein. J Mol Biol. 1999;289(5):1163–78.
38. Steele AD, Lindquist S, Aguzzi A. The prion protein knockout mouse: a phenotype under challenge. Prion. 2007;1(2):83–93.
39. Py BF, Gonzalez SF, Long K, Kim MS, Kim YA, Zhu H, et al. Cochlin produced by follicular dendritic cells promotes antibacterial innate immunity. Immunity. 2013;38(5):1063–72.
40. Sanda C, Weitzel P, Tsukahara T, Schaley J, Edenberg HJ, Stephens MA, et al. Differential gene induction by type I and type II interferons and their combination. J Interferon Cytokine Res. 2006;26(7):462–72.
41. Carter SL, Müller M, Manders PM, Campbell IL. Induction of the genes for Cxcl9 and Cxcl10 is dependent on IFN-gamma but shows differential cellular expression in experimental autoimmune encephalomyelitis and by astrocytes and microglia in vitro. Glia. 2007;55(16):1728–39.
42. Bainbridge J, Walker KB. The normal cellular form of prion protein modulates T cell responses. Immunol Lett. 2005;96(1):147–50.
43. Murray C, Griffin ÉW, O'Loughlin E, Lyons A, Sherwin E, Ahmed S, et al. Interdependent and independent roles of type I interferons and IL-6 in innate immune, neuroinflammatory and sickness behaviour responses to systemic poly I:C. Brain Behav Immun. 2015;48:274–86.
44. Kuwahara C, Takeuchi AM, Nishimura T, Haraguchi K, Kubosaki A, Matsumoto Y, et al. Prions prevent neuronal cell-line death. Nature. 1999; 400(6741):225–6.
45. Bertuchi FR, Bourgeon DM, Landemberger MC, Martins VR, Cerchiaro G. PrPC displays an essential protective role from oxidative stress in an astrocyte cell line derived from PrPC knockout mice. Biochem Biophys Res Commun. 2012;418(1):27–32.
46. Bravard A, Auvré F, Fantini D, Bernardino-Sgherri J, Sissoëff L, Daynac M, et al. The prion protein is critical for DNA repair and cell survival after genotoxic stress. Nucleic Acids Res. 2015;43(2):904–16.
47. Gadotti VM, Bonfield SP, Zamponi GW. Depressive-like behaviour of mice lacking cellular prion protein. Behav Brain Res. 2012;227(2):319–23.
48. Beckman D, Santos LE, Americo TA, Ledo JH, de Mello FG, Linden R. Prion protein modulates monoaminergic systems and depressive-like behavior in mice. J Biol Chem. 2015;290(33):20488–98.
49. Martinez FO, Gordon S. The M1 and M2 paradigm of macrophage activation: time for reassessment. F1000Prime Rep. 2014;6:13.
50. Martinez FO, Helming L, Milde R, Varin A, Melgert BN, Draijer C, et al. Genetic programs expressed in resting and IL-4 alternatively activated mouse and human macrophages: similarities and differences. Blood. 2013; 121(9):e57–69.
51. Köhler C. Allograft inflammatory factor-1/Ionized calcium-binding adapter molecule 1 is specifically expressed by most subpopulations of macrophages and spermatids in testis. Cell Tissue Res. 2007;330(2):291–302.
52. Colton CA. Immune heterogeneity in neuroinflammation: dendritic cells in the brain. J Neuroimmune Pharmacol. 2013;8(1):145–62.
53. Hasegawa-Ishii S, Inaba M, Umegaki H, Unno K, Wakabayashi K, Shimada A. Endotoxemia-induced cytokine-mediated responses of hippocampal astrocytes transmitted by cells of the brain-immune interface. Sci Rep. 2016;6:25457.
54. Müller M, Carter S, Hofer MJ, Campbell IL. Review: the chemokine receptor CXCR3 and its ligands CXCL9, CXCL10 and CXCL11 in neuroimmunity—a tale of conflict and conundrum. Neuropathol Appl Neurobiol. 2010;36(5):368–87.
55. Pedersen MØ, Jensen R, Pedersen DS, Skjolding AD, Hempel C, Maretty L, et al. Metallothionein-I + II in neuroprotection. Biofactors. 2009;35(4):315–25.
56. Brahmachari S, Fung YK, Pahan K. Induction of glial fibrillary acidic protein expression in astrocytes by nitric oxide. J Neurosci. 2006;26(18):4930–9.
57. Hirsch TZ, Hernandez-Rapp J, Martin-Lannerée S, Launay JM, Mouillet-Richard S. PrP(C) signalling in neurons: from basics to clinical challenges. Biochimie. 2014;104:2–11.
58. Buttini M, Limonta S, Boddeke HW. Peripheral administration of lipopolysaccharide induces activation of microglial cells in rat brain. Neurochem Int. 1996;29(1):25–35.
59. Chen Z, Jalabi W, Shpargel KB, Farabaugh KT, Dutta R, Yin X, et al. Lipopolysaccharide-induced microglial activation and neuroprotection against experimental brain injury is independent of hematogenous TLR4. J Neurosci. 2012;32(34):11706–15.
60. Mariante RM, Nóbrega A, Martins RA, Areal RB, Bellio M, Linden R. Neuroimmunoendocrine regulation of the prion protein in neutrophils. J Biol Chem. 2012;287(42):35506–15.
61. Wang V, Chuang TC, Hsu YD, Chou WY, Kao MC. Nitric oxide induces prion protein via MEK and p38 MAPK signaling. Biochem Biophys Res Commun. 2005;333(1):95–100.
62. Brogna S, Wen J. Nonsense-mediated mRNA decay (NMD) mechanisms. Nat Struct Mol Biol. 2009;16(2):107–13.

Paper IV

PrP^C modulates pathways of inflammation during LPS-induced acute lung injury

Salvesen Ø[1], Reiten MR[2], Kamstra JH[2], Bakkebø MK[2], Espenes A[2], Tranulis MA[2], Ersdal C[1]

[1] Norwegian University of Life Sciences, Faculty of Veterinary Medicine, Department of Production Animal Clinical Sciences, Sandnes, Norway

[2] Norwegian University of Life Sciences, Faculty of Veterinary Medicine, Department of Basic Sciences and Aquatic Medicine, Oslo, Norway

Corresponding author:
Øyvind Salvesen
oyvind.salvesen@nmbu.no

Keywords: acute lung injury, cellular prion protein, systemic inflammation, lipopolysaccharide (LPS), innate immunity, RNA sequencing, ECM remodeling, histopathology

1 Abstract

Background: A naturally occurring mutation in the *PRNP* gene of Norwegian dairy goats terminates synthesis of the cellular prion protein (PrP^C), rendering homozygous goats ($PRNP^{Ter/Ter}$) devoid of the protein. Although extensively studied, the function of PrP^C during acute pulmonary inflammation has not been investigated earlier. We examined transcriptional and morphological alternations in the lungs after lipopolysaccharide (LPS) challenge of goats with and without PrP^C.

Methods: Acute pulmonary inflammation was induced by intravenous injection of LPS (*Escherichia coli* O26:B6) in 16 goats (8 $PRNP^{Ter/Ter}$ and 8 $PRNP^{+/+}$). A control group of 10 goats (5 $PRNP^{Ter/Ter}$ and 5 $PRNP^{+/+}$) received sterile saline. Clinical examinations included recordings of respiratory frequency and signs of respiratory distress. A full necropsy was performed, and lung tissue was collected for RNA sequencing and histopathological analysis.

Results: Systemic LPS challenge induced sepsis-like clinical signs including tachypnea and respiratory distress. A total of 432 ($PRNP^{+/+}$) and 596 ($PRNP^{Ter/Ter}$) genes were differentially expressed compared with the saline control of the matching genotype. When assigned to gene ontology categories, biological processes involved in remodeling of the extracellular matrix (ECM), were exclusively enriched in PrP^C-deficient goats. These genes included a range of collagen-encoding genes, and proteases such as metalloproteinases (*MMP1*, *MMP2*, *MMP14, ADAM15*) and cathepsins. Several pro-inflammatory upstream regulators (TNF-α, IL1-β, IFN-γ, TGF-β) showed increased activation scores in goats devoid of PrP^C. Histological examination of lungs revealed multifocal areas with alveolar bleedings, edema, neutrophil infiltration, and higher numbers of alveolar macrophages, with no significant differences between *PRNP* genotypes.

Conclusion: LPS challenge induced marked alterations in the lung tissue transcriptome that corresponded with histopathological and clinical findings in both genotypes. In goats devoid of PrP^C, increased activation of upstream inflammatory regulators was present, and enrichment of ECM components indicated an augmented damage to the lung parenchyma. This suggests that PrP^C has a protective role during acute pulmonary inflammation, possibly by modulating inflammatory pathways.

2 Introduction

The cellular prion protein (PrP^C) is an evolutionarily conserved protein abundantly expressed in the central nervous system (CNS), and also at moderate levels peripherally, such as in the immune system and lungs [1-4]. Misfolding of PrP^C is the essential step for development of prion disorders in humans and animals [5]. Although intensively studied for several decades, the normal functions of PrP^C have proven difficult to identify. Not surprisingly, the main focus has been on the nervous system, and PrP^C has been linked to neuroprotection, signal transduction, and myelin maintenance, among others [6, 7]. More recently, the association of PrP^C with inflammatory responses and the immune system has been investigated. Lack of PrP^C enhance the inflammatory reaction in several models and organ systems [8-11], and it has been proposed that PrP^C plays important roles in neuroimmune cross-talk [12, 13].

In a line of Norwegian dairy goats, a mutation in the PrP^C-encoding gene (*PRNP*) terminates PrP^C synthesis. Animals homozygous for this mutation ($PRNP^{Ter/Ter}$) are the only known non-transgenic mammals devoid of PrP^C [14]. The goats are postulated to be scrapie-resistant, and constitute a unique animal model for studying PrP^C physiology. No major loss-of-function phenotypes have been observed under normal herd conditions, but a hematological shift in red blood cells [15] and a primed state of type I interferon-stimulated genes are present at rest in these animals [16]. When exposed to systemic lipopolysaccharide (LPS), PrP^C-deficient goats display a prolonged sickness behavior and a slightly different immunological profile that is skewed toward a type I interferon response [17].

Acute lung injury (ALI) and its most severe manifestation, acute respiratory distress syndrome (ARDS), contribute to increased morbidity and mortality in critically ill patients [18, 19]. The most common cause of ALI is sepsis caused by a systemic bacterial infection [20]. Early events in this syndrome can be mimicked by administration of LPS, a component of the outer membrane of Gram-negative bacteria. LPS is recognized by the toll-like receptor 4 (TLR4) complex expressed by innate immune cells, and also by other cells such as endothelial cells within the lung [21]. Systemic administration of LPS initially induces apoptosis of the alveolar endothelium [22] and epithelium [23], and neutrophils are rapidly

recruited. The migration of neutrophils into the alveoli is dependent upon crossing the basement membrane, possibly through gaps in the basal laminae [24], and is facilitated by proteolytic degradation of the highly organized extracellular matrix (ECM) [25]. Once at the site of injury, activated macrophages and infiltrating neutrophils release a variety of pro-inflammatory cytokines, enzymes, and reactive oxygen and nitrogen species. These molecules participate in maintaining the inflammatory state and defeating invading pathogens, but also inflict damage of the lung parenchyma and microvascular structure. This results in proteinaceous edema and hemorrhage, as seen in the exudative phase of ALI [26]. To the best of our knowledge, no studies have used RNA sequencing to investigate the pulmonary inflammatory response in mammals upon systemic LPS challenge.

We hypothesized that PrP^{C}-deficient goats are more susceptible to inflammatory stimuli, and therefore examined the responsiveness to LPS of *PRNP*$^{Ter/Ter}$ goats, compared with normal goats (*PRNP*$^{+/+}$). This study shows a full-scale transcriptional profile coupled to morphological alterations in caprine lungs after systemic LPS-induced inflammation, and investigates whether loss of PrP^{C} affects the initial stage of acute lung injury.

3 Material and methods

3.1 Animals

A total of 26 Norwegian dairy goat kids, 13 *PRNP*$^{Ter/Ter}$ and 13 *PRNP*$^{+/+}$ animals, were included in the study. Details about housing conditions can be found in reference [17] and an overview of the study groups including treatment, animal number, age, weight, and gender can be found in Table S1 in Supplementary Material. The animal experiment was performed in compliance with ethical guidelines, and approved by the Norwegian Animal Research Authority (ID 5827, 6903, and 7881) with reference to the Norwegian regulation on animal experimentation (FOR-2015-06-18-761).

3.2 Experimental protocol

Sixteen goats (8 *PRNP*$^{Ter/Ter}$ and 8 *PRNP*$^{+/+}$) received a dual dose of LPS (*Escherichia coli* O26:B6, L2654 Sigma-Aldrich, USA) intravenously with a 24-hour time interval between doses; 0.1 µg/kg (day 1) and 0.05 µg/kg (day 2). The control group consisted of 10 goats (5 *PRNP*$^{Ter/Ter}$ and 5 *PRNP*$^{+/+}$) and were given corresponding volumes of sterile saline. Clinical examinations, including respiratory rate, were performed at 12 time points during the first 7 h of day 1, and at 9 time points after the second LPS injection. Additionally, episodes of coughing and panting were recorded. The animals were euthanized by an overdose of pentobarbital 5 h after the second LPS challenge.

3.3 Gross pathology and histopathology score

Gross pathology: After euthanasia, goats were fully necropsied. The amount of fluid in the thoracic cavity and airways, and the distribution and amount of bleedings, atelectasis, edema, and emphysema in the lungs were recorded. Additionally, macroscopic changes compatible with lungworm (*Muellerius capillaris*) were noted.

Histopathology: Tissues were collected at standardized areas dorsally and ventrally from the left caudal lung lobe, as well as from areas with gross pathology, mainly bleedings. Tissues were immersion fixed in 4 % formaldehyde for one week, and then dehydrated in graded ethanol and paraffin embedded. Paraffin sections (4 µm) were mounted on slides and

stained with hematoxylin and eosin (HE). Martius-scarlet-blue (MSB) staining was performed on selected sections to evaluate fibrin deposition. The HE sections were examined by light microscopy and a blinded, semi-quantitative evaluation was performed to assess lung pathology. Both the airways and the lung interstitium were evaluated, focusing on the alveolar lumen and septa. Evaluation parameters included bleedings, hyperemia, fibrin deposition, necrosis, and neutrophil and macrophage infiltration. Pathological changes were scored as follows: 0 = minimal; 1 = little/a few, 2 = moderate; 3 = severe, including half-step grading. A total lung histopathology score was calculated for each section by summarizing the values from the above mentioned criteria.

3.4 Immunohistochemistry

6H4 and SAF32: Frozen lung tissue from a control *PRNP*$^{+/+}$ goat were used to evaluate the pulmonary distribution of PrP^{C}. After dissection, lung tissues were frozen in isopentane, transferred to liquid nitrogen, and stored at -70 °C. Sections (8 µm) were cut on a cryostat and mounted on Superfrost® Plus slides (Menzel-Gläser, Thermo Scientific). The sections were fixed in formol-calcium, followed by 5 min inhibition of endogenous peroxidase activity (DAKO Peroxidase Block, Agilent). After blocking in normal goat serum (1:50) for 10 min, the sections were incubated with the primary anti-PrP antibodies 6H4 (1:500, Prionics AG) or SAF32 (1:1000, Cayman) for 1 h at room temperature. Further steps were performed with the Envision+ System-HRP DAB (Dako, K4007), according to the manufacturer's instruction. Antibody specificity was checked by performing the same procedure on lung sections from a *PRNP*$^{Ter/Ter}$ goat.

S100A8: Formalin-fixed, paraffin-embedded sections (4 µm) were mounted on Superfrost® Plus slides (Menzel-Gläser, Thermo Scientific) and dried for 30 min at 58 °C . The sections were deparaffinized in xylene, and rehydrated through decreasing concentrations of graded ethanol. The PT link system (100 °C for 15 min in Tris/EDTA-buffer, pH 9.1) was used for epitope retrieval. Endogenous peroxidase activity was blocked by incubation in 3 % H_2O_2 in methanol for 20 min at room temperature. Sections were then blocked in normal goat serum (1:50), diluted in phosphate buffered saline (PBS), and incubated with the primary

antibody S100A8 (1:3200, Abcam) for 1.5 h at room temperature. Further steps were performed with EnVison+ System-HRP AEC (Dako, K4009).

Washing between steps was performed with PBS for both procedures. Sections were counterstained in hematoxylin, and mounted using Aquatex medium (Merck). All runs included a negative control section in which the primary antibody was replaced with 1 % PBS. The number of cells that were positive for the S100 calcium binding protein A8 (S100A8) was quantified within the field of view of three representative areas in each animal/section (400 X magnification, ⌀ = 450 µm).

3.5 RNA extraction, quality control and pooling

Tissue samples were collected at a standardized area dorsally from the left caudal lung lobe within 15 min after euthanasia, and immediately immersed in RNA later (Invitrogen) and stored at -70 °C. RNA was extracted from approximately 30 mg of lung tissue using the RNeasy Lipid Tissue Mini Kit (Qiagen, 74804) according to the manufacturer's instruction. High quality RNA (RIN > 8) from individuals was pooled in equal amounts per treatment and genotype, reaching a final amount of 15 ug, as described in Salvesen et al [17]. RNA quality data are summarized in Table S2 in Supplementary Material.

3.6 RNA sequencing and differential expression analyses

RNA samples were shipped on dry ice to Novogene (Hong Kong) for RNA sequencing. Paired-end 150 bp sequencing was performed on an Illumina HiSeq2000. Quality control summary and mapping status are given in Table S3-4 in Supplementary Material. Normalization was performed by the trimmed mean of M values (TMM) method, p-value estimation assuming Poisson distribution, and false discovery rate (FDR) estimation by Benjamini-Hochberg correction of multiple testing [27, 28]. Differential gene expression analysis was performed using DEGSeq [28] with the following criteria: Log2 ratio ± 0.59 (fold change ± 1.5) and a FDR-adjusted q-value ($q < 0.05$). The genomic response to LPS in each *PRNP* genotype was assessed by comparing LPS-groups with the saline-treated control of the matching genotype. FPKM (fragments per kilobase of exon per million fragments mapped) values,

which take into account the effects of both sequencing depth and gene length, were used to estimate gene expression levels.

3.7 Ingenuity pathway analysis and gene ontology enrichment

Gene lists from *Capra hircus* were first converted to gene symbols using the NCBI batch converter tool[1]. Pathway analysis was performed with both ingenuity pathway analysis (IPA, v. 36601845) and gene ontology (GO) analysis with the online DAVID 6.8 software [29, 30]. Because the *Capra hircus* genome is not available in both analyses, *Homo sapiens* orthologues were used instead. The lists of differentially expressed genes (DEGs), containing gene identifiers and corresponding expression values, were uploaded into the IPA software (Qiagen). The top enriched canonical pathways, upstream regulators and gene networks were identified by the "core analysis" function, using a cut-off in absolute fold change of 1.5 and a FDR < 0.05. The IPA software uses the Fishers exact test for pathway enrichment and Z scores for pathway activation. A Benjamini-Hochberg adjusted p-value < 0.05 was considered significant for GO analyses. DEGs of the two genotypes were analyzed separately.

3.8 Validation of RNA-seq by real-time qPCR

Complementary DNA was generated using RNA from each individual sample by the QuantiTect Reverse Transcription Kit (Qiagen) according to manufacturer's instructions. A non-reverse transcriptase control and no template control were included. The expression of nine representative target genes (*SAA3.2*, *CXCL10*, *ITGAM*, *CD14*, *IFI6*, *GADPH*, *S100A9*, *PRNP* and *IL1B*) was investigated by the Light cycler 480 qPCR system. Real-time reactions were prepared using SYBR Green PCR Master Mix including 10 µl cDNA (1:10) in each reaction, and qPCR was performed with standard cycling conditions: initial denaturation for 5 min at 95 °C, followed by 40 amplification cycles (10 s at 95 °C, 10 s at 60 °C and 15 s at 72 °C) and construction of melting curves. A standard curve was generated for each target gene to obtain primer amplification efficiencies, correlations, and dynamic range.

[1] https://www.ncbi.nlm.nih.gov/sites/batchentrez

Normalization was performed against the *ACTB* reference gene, which showed no significant change by LPS-treatment in the RNA-seq data, confirming stability as internal control. Relative expression was calculated using the $2^{-\Delta\Delta Cq}$ method as described in [31]. Primer sequences are given in Table S5 in Supplementary Material.

3.9 Descriptive and statistical analyses

Data are presented as mean ± standard error of the mean (SEM). Graphical and statistical analyses were performed in GraphPad Prism 6 (GraphPad software Inc., USA) and Microsoft Excel 2013. A one-way ANOVA, followed by Dunnetts's post hoc test, was performed when comparing three or more groups. Differences in lung histopathology score between two groups were assessed by the Mann-Whitney U test. Significance levels $p < 0.05$; $p < 0.01$; $p < 0.001$ are indicated.

4 Results

4.1 Systemic LPS challenge induces tachypnea and respiratory distress

After LPS challenge, all 8 goats from both genotype groups displayed sepsis-like clinical signs, such as sickness behavior, fever, and tachycardia. PrP^{C}-deficient goats displayed prolonged sickness behavior, and hematological analysis showed a rapid and profound leukopenia in both genotypes as we have previously described [17]. Respiratory rate increased significantly in both genotypes after the initial high dose of LPS (0.1 µg/kg), peaking 1 h post LPS challenge, and remained elevated at all subsequent time points on day 1 (Figure 1A). The mean respiratory rate was higher in the *PRNP*$^{Ter/Ter}$ group at all time points during the first day, albeit not statistically significant. Periods of heavy abdominal breathing, coughing, and panting were observed in 7 out of 8 animals of both genotypes receiving LPS, whereas none of the control animals displayed alterations in clinical parameters. Clinical signs of respiratory distress were less profound on day 2, when the dosage of LPS was halved.

4.2 Systemic LPS challenge induces circulatory disturbances and inflammation

Gross pathology: Multifocal ecchymosis and petechial bleedings were observed in 4 of 8 *PRNP*$^{+/+}$ goats and 5 of 8 *PRNP*$^{Ter/Ter}$ goats receiving LPS. The majority of bleedings were sub-pleural and dorsally located in the caudal lung lobes (Figure 1B). Two *PRNP*$^{Ter/Ter}$ animals had hydrothorax with 90 mL and 400 mL of serous fluid within the thoracic cavity. Both these goats had mild to moderate ventral atelectasis. Four animals (*PRNP*$^{Ter/Ter}$) had sparse to moderate amounts of froth and fluid within the trachea and main bronchi, and one animal had a macroscopically visible lung edema. Sparse lungworm-changes (*Muellerius capillaris*) were equally distributed between the genotypes in both the LPS- and control group.

Histopathological changes: The lung histopathology scores were significantly higher in the LPS-groups than in the saline controls (Figure 2A). Multifocal microscopic bleedings were recorded in 7 out of 8 animals receiving LPS in both genotypes, located both sub-pleurally and deeper within the lung parenchyma. These areas were characterized by alveolar hemorrhage and edema, increased amount of alveolar macrophages, and infiltration of

neutrophils (Figure 2C). Some hyaline membranes were observed lining the alveolar wall (Figure 2D). Focally, an increased number of neutrophils were present in the alveolar septa, accompanied by single cell necrosis and hyperemia (Figure 2E). In these same foci, MSB staining showed fibrin deposition along alveolar septa of a few LPS-treated animals (Figure 2F). Immunohistochemical labeling of S100 calcium binding protein A8 (S100A8) increased upon LPS challenge, and was predominantly expressed by neutrophils, and at lower levels, in alveolar macrophages (Figure 2G-I). The histopathological changes were more profound dorsally than ventrally. There were no significant differences between *PRNP* genotypes.

4.3 *PRNP* expression and cellular distribution of PrP^C

The level of *PRNP* expression in the lungs was similar to that of the choroid plexus, and five times lower than in the hippocampus [17]. After LPS challenge, *PRNP* expression increased by 1.6 fold in the lungs of $PRNP^{+/+}$ goats, albeit not significantly. In $PRNP^{Ter/Ter}$ goats, reads mapping to the *PRNP* locus are reduced to about 25 % (Figure 3A). The localization of PrP^C in the lungs of non-treated animals was investigated by use of the 6H4 antibody. A granular distribution of PrP^C was observed within bronchial and bronchiolar epithelial cells of $PRNP^{+/+}$ goats (Figure 3B). In the alveoli, PrP^C was primarily localized at the luminal side of the alveolar septa, probably associated with alveolar pneumocytes (Figure 3C). No PrP^C was detected in $PRNP^{Ter/Ter}$ goats, confirming the absence of synthesized protein as well as the specificity of the antibodies (Figure 3D). Staining with SAF32 showed similar results (data not shown).

4.4 The lung transcriptome is profoundly altered by systemic LPS challenge

After LPS challenge, a total of 432 (upregulated (UR): 269, downregulated (DR): 163) and 596 (UR: 339, DR: 257) genes were differentially expressed compared to the saline control group in normal and PrP^C-deficient goats, respectively (Data sheet 1 in Supplementary Material). The Venn diagrams show that 146 upregulated and 161 downregulated genes exclusively belonged to the PrP^C-deficient goats when the filtration criteria (log2 ratio 0.59, $q < 0.05$) were applied (Figure 4A). However, closer investigation of the transcriptional data revealed that 95 % of the differentially expressed genes (DEGs) were regulated in the same direction in both genotypes, albeit some excluded by fold change or q-value. Genes

upregulated by a log2 ratio ≥ 3 (Fold change ≥ 8) after LPS challenge are listed in Table 1. The most upregulated gene in both *PRNP* genotypes was the acute phase protein *SAA3* (51 fold, $PRNP^{Ter/Ter}$; 25 fold, $PRNP^{+/+}$). Other highly upregulated genes were cytokines, chemokines, and metal-binding proteins such as metallothioneins and several S100 proteins. The most downregulated gene was *CYP1A1* (24 fold, $PRNP^{Ter/Ter}$; 22 fold, $PRNP^{+/+}$), a member of the cytochrome P450 superfamily (Data sheet 1 in Supplementary Material).

Table 1: Genes upregulated by log2 ratio ≥ 3 (Fold change ≥ 8) after LPS challenge.

Genes upregulated by a log 2 ratio ≥ 3 in both genotypes			**Log2 ratio (LPS vs. saline)**	
Gene ID	**Symbol**	**Gene name**	***PRNP*$^{+/+}$**	***PRNP*$^{Ter/Ter}$**
100860781	SAA3	Serum amyloid A3	4.66	5.69
102188618	MT1A	Metallothionein-1A	4.64	4.80
102174322	FOLR1	Folate receptor alpha	4.27	4.56
102188072	MT2	Metallothionein-2	4.14	3.75
102168428	SAA3.2	Serum amyloid A3.2 protein	3.90	4.63
102177100	ISG20	Interferon-stimulated exonuclease gene 20	3.73	3.09
102182273	S100A9	S100 calcium-binding protein A9	3.22	4.19
Genes upregulated (log 2 ratio ≥ 3) in *PRNP*$^{Ter/Ter}$ goats				
102168876	S100A8	S100 calcium-binding protein A8	2.76	3.67
102173634	GPNMB	Glycoprotein nmb	ND	3.55
102175845	S100G	S100 calcium-binding protein G	ND	3.44
102169149	S100A12	S100 calcium-binding protein A12	2.27	3.17
Genes upregulated (log 2 ratio ≥ 3) in *PRNP*$^{+/+}$ goats				
102169982	ISG15	ISG15 ubiquitin-like modifier	3.53	2.39
102189279	ASIC1	Acid sensing ion channel subunit 1	3.23	2.25
102190797	RSAD2	Radical S-adenosyl methionine domain containing 2	3.19	2.68
102187309	CXCL11	C-X-C motif chemokine ligand 11	3.16	2.34
102183403	CLEC4E	C-type lectin domain family 4 member E	3.06	2.97

ND = not differentially expressed
Differential expression analyses were performed by comparing LPS-treated groups to the saline control group of the matching genotype.

4.5 Affected pathways are linked to LPS challenge and indicate enhanced inflammation and turnover of extracellular matrix in PrP^C-deficient goats

To assess the function of the DEGs, enriched pathways, networks and upstream regulators were identified by ingenuity pathway analysis (IPA). DEGs were also assigned to gene ontology (GO) classifications, including biological process, cellular compartment and molecular function. In general, there was a high degree of overlap in the transcriptional response to LPS in normal and PrP^C-deficient goats. As expected, a considerable amount of the DEGs belonged to the innate immune response and inflammatory response (Data sheet 2 in Supplementary Material), and LPS was identified as the most significant upstream regulator of both genotypes (Figure 4B). The associated p-values indicate more enrichment of genes involved in the LPS-response in *PRNP*$^{Ter/Ter}$ goats, particularly those stimulated by the pro-inflammatory cytokines IL1-β, IFN-γ, TGF-β and TNF-α (Figure 4B). Other notably affected pathways in both genotypes involved acute-phase response signaling, antigen presentation, and granulocyte adhesion and diapedesis (Figure 4D). Although some upstream regulators of interferons were more significantly enriched in PrP^C-deficient goats, predicted activation of interferon signaling were lower than in the normal goats. The full IPA output can be found in Data sheet 3 in Supplementary Material.

Several of the GO-terms, such as collagen catabolic process (GO:0030574), extracellular matrix (ECM) disassembly (GO0022617), and ECM structural constituents (GO:0005201) were exclusively enriched in PrP^C-deficient goats (Data sheet 2 in Supplementary Material). The genes were primarily in an upregulated state, and included collagen-encoding genes, secreted metalloproteinases, such as matrix metalloproteinases (*MMPs*) and *ADAM* genes, as well as cathepsins primarily located within lysosomes (Figure 4C). In line with this, the top canonical pathway in *PRNP*$^{Ter/Ter}$ goats was related to turnover of ECM (Figure 4D). Also, IPA analysis revealed a significantly enriched network involved in connective tissue disorders (-logP 39, Figure 5).

4.6 Validation of RNA-seq data by qPCR

The expression of nine target genes (*SAA3.2*, *CXCL10*, *ITGAM*, *CD14*, *IFI6*, *GADPH*, *S100A9*, *PRNP* and *IL1B*) was investigated by qPCR on individual RNA samples from lung tissue (Figure 6). A strong correlation ($r = 0.975$, $p < 0.0001$, Pearson correlation) was observed between log2-transformed expression values of RNA-seq and qPCR, in line with our previous reports from other tissues [16, 17]. Differential expression was confirmed by qPCR in 34 out of 36 comparisons.

5 Discussion

We observed an increased activation score of genes related to the pro-inflammatory LPS-response along with a significant enrichment of extracellular matrix (ECM) turnover in the *PRNP*$^{Ter/Ter}$ group. Homeostasis of the ECM is of major importance for the physiological function of most organs, and is maintained by secretion of proteases and degradation of ECM components, as well as synthesis of collagens [32]. In addition, both ECM constituents and matrix metalloproteinases (MMPs) may act as modulators of inflammation by regulating barrier function along with cytokine and chemokine activity [25, 33, 34]. Interestingly, more than 70 % of the differentially express genes (DEGs) classified as being involved in collagen catabolic processes belonged exclusively to *PRNP*$^{Ter/Ter}$ goats, and the connective tissue disorder network was significantly enriched. The collagen-encoding genes were primarily upregulated, probably as a result of resident fibroblast activation mediated by TGF-β [35, 36]. Indeed, PrP^{C} modulates B1 integrin signaling [37, 38], which is a key regulator of TGF-β-dependent activation of fibroblasts [39]. Although collagen deposition is an essential step in limiting alveolar damage and initiating repair [40], elevated levels of procollagen (COL3) and proteases (MMP1/3) have also been reported as biomarkers of poor prognosis in human acute lung injury (ALI) patients [41, 42]. Altogether, this indicates that inflammation, ECM degradation and subsequent collagen synthesis occurred to a greater extent in the absence of PrP^{C} following LPS challenge.

Because most PrP^{C} is localized to the cell surface, it has been hypothesized that PrP^{C} binds extracellular proteins and facilitates transmembrane signaling processes [43]. We have

recently proposed that PrP^C protects tissues by modulating certain signaling pathways of innate immunity [17]. When challenged with LPS, the PrP^C-deficient goats displayed a prolonged sickness behavior and innate immune genes were differentially expressed [17]. Similarly, genes associated with pro-inflammatory upstream regulators, such as TNF-α, were more activated in PrP^C-deficient goats in the current study. Accordingly, PrP^C desensitized cells to TNF-α by restricting the level of available TNF-receptor (TNFR) present at the plasma membrane of neuroectodermal cells [37]. We also observed a relatively lower activation score of the interferon response pathway in the *PRNP*$^{Ter/Ter}$ group, but this probably reflects a primed state of interferon-responsive genes at rest [16], rather than a reduced activation. Indeed, type I interferons and some of the downstream effector genes are considered as important regulators of lung inflammation [44]. Taken together, we propose that PrP^C is a modulator of innate immunity across different tissues. This is in agreement with murine studies reporting that lack of PrP^C exacerbates inflammation in different organ systems [8, 9, 11]. Thus, increased expression of MMPs and ECM constituents might demonstrate an aggravated inflammatory damage of the lung parenchyma in goats devoid of PrP^C.

We observed moderate levels of *PRNP* mRNA in the lungs, in accordance with reports from sheep and cattle [3, 4, 45, 46]. After LPS challenge, *PRNP* expression increased slightly (1.6 fold) in *PRNP*$^{+/+}$ goats, indicating a response to inflammatory stimuli. We have earlier published the same tendency in the hippocampus and choroid plexus [17]. Immunohistochemistry showed that PrP^C was distributed in several cell types throughout the lungs, similar to what has been reported in a bovine study [45]. As expected, the absence of PrP^C protein was confirmed in *PRNP*$^{Ter/Ter}$ goats.

Systemic LPS challenge was associated with a dramatic change in the lung transcriptome, in which 432 and 596 genes were differentially expressed in normal and PrP^C-deficient goats, respectively. Besides the genotype-dependent profile in ECM homeostasis, there was a considerable overlap in the molecular response to LPS. Not surprisingly, the majority of the genes were annotated as being involved in the inflammatory and innate immune response, and showed a comparable profile to those reported in other species [47]. The most upregulated gene in both genotypes was the acute phase protein serum amyloid A3 (*SAA3)*, an isoform of the SAA apolipoproteins. Indeed, *SAA3* seems to be a hallmark of acute

inflammation in a range of tissues, at least in ruminants [17, 48, 49]. Interestingly, *SAA3* may act as a ligand for the TLR4-MD2-complex, and play multiple roles in modulating the innate immune response [50]. Four S100 proteins (*S100G*, *S100A8*, *S100A9* and *S100A12)* were also among the most prominently upregulated genes in both genotypes. These low-molecular weight proteins have a Ca^{2+}-binding capacity, and as well as being involved in regulation of proliferation, differentiation and apoptosis [51], also have anti-microbial activity against a variety of micro-organisms [52]. Because *S100A8*/*A9*/*A12* genes are constitutively expressed in neutrophils, as demonstrated by S100A8 IHC in the present study, infiltrating neutrophils probably contribute to the upregulation of these genes in our model [53]. Although the exact functions of S100 proteins in lung inflammation remain currently unresolved, at least S100A8/A9 seem to reduce the development of ALI [54]. The most downregulated gene, *CYP1A1*, plays a key role in the metabolism of xenobiotics and some endogenous substrates [55]. Similarly, systemic LPS suppressed *CYP1A1* expression in the murine liver [56] and lungs [57]. The downregulation could result from the formation of reactive oxygen species (ROS) generated by LPS challenge, as ROS have been shown to suppress *CYP1A1* expression *in vitro* [58]. Conversely, LPS treatment induced *CYP1A1* expression in cultured human dendritic cells and in the thymus [59], suggesting that tissue-specific differences may occur.

Acute inflammation is a balancing act; although it is an essential component of an appropriate response and recovery from an insult, it may also damage the tissue in which it occurs. The multifocal areas with alveolar hemorrhage, edema and infiltration of inflammatory cells shown histologically, indicate disruption of the alveolar/capillary basement membrane. This is probably due to the massive release of proteases and inflammatory mediators [60, 61]. The observed hydrothorax in two PrP^{C}-deficient goats most likely represent transudative pleural effusion resulting from compromised integrity of the lung capillaries. Neutrophils were found sequestered within the pulmonary capillaries and some migrated into the alveoli upon LPS challenge. Correspondingly, several genes mapped to neutrophil chemotaxis, such as *S100A8*/*A9*/*A12* proteins and chemokines (*CCL2*, *CCL5* and *CCL15*), and ingenuity pathway analysis confirmed the involvement of granulocyte diapedesis. In some areas, the normal septal structure was replaced by fibrinous exudate and debris from necrotic cells, compatible with hyaline septa [26]. Although the mean lung

histopathology score was slightly higher in *PRNP*$^{Ter/Ter}$ goats than in normal goats, the difference was not statistically significant. Thus, the genotype-dependent differences in transcriptome probably represent early events that were only detectable at a molecular level, at least at the time of euthanasia.

The substantial activation of the lung transcriptome and histopathological evidence of lung injury corresponded with the clinical signs observed. The presence of pulmonary intravascular macrophages, specialized in removing circulating bacteria and endotoxins, probably means that small ruminants are particularly sensitive to systemic LPS exposure [62]. A significant increase in respiratory rate was observed, peaking at 1 h, and remained elevated the first 7 h post exposure. Moreover, periods of evident respiratory distress were observed in nearly 90 % of the animals receiving LPS, indicating temporarily reduced lung function. This is in agreement with a significant enrichment of genes characterized as hypoxia-responsive. Given that only subtle effects have been attributed to PrP^C, it was not surprising that loss of PrP^C did not affect the overall clinical recovery and outcome.

In conclusion, we demonstrated a potent activation of the lung transcriptome that corresponded with morphological and clinical alterations. Although there was a substantial overlap in the response to LPS in both genotypes, increased turnover of ECM and activation of upstream inflammatory regulators were present in PrP^C-deficient goats. This indicates a protective role for PrP^C during acute pulmonary inflammation.

6 Availability of data and material

Original BAM-files containing sequencing data are available from the SRA database (SRA accession number SRP116648). Data and material supporting the conclusions are contained within the manuscript and supplementing material.

7 Conflict of interest statement

The authors declare that the research was conducted in the absence of any commercial or financial relationships that could be construed as a potential conflict of interest.

8 Authors' contributions

CE, MT, AE, MB, and ØS designed the study and ØS, MR, CE, AE, and MT performed the experiments. ØS carried out laboratory procedures, performed the statistical analysis and drafted the manuscript. MR performed the PrP^C immunohistochemistry. JK performed the ingenuity pathway analysis. All authors have critically read and approved the final manuscript.

9 Funding information

The research was supported by The Research Council of Norway (Grant ID 227386/E40).

10 Acknowledgments

The authors gratefully thank Siri Bjerkreim Hamre and Mari Katharina Aas Ådland for skillful laboratory work. The authors acknowledge Lucy Robertson for proofreading the manuscript.

11 List of abbreviations

LPS, lipopolysaccharide; RIN, RNA integrity number; qPCR, quantitative real-time polymerase chain reaction; DEGs, differentially expressed genes; GO, gene ontology; IPA, ingenuity pathway analysis; IHC, immunohistochemistry; IL, interleukin; IFN, interferon; TNF, tumor necrosis factor; TGF, transforming growth factor

12 References

1. McLennan NF, Rennison KA, Bell JE, Ironside JW. *In situ* hybridization analysis of PrP mRNA in human CNS tissues. Neuropathol Appl Neurobiol. 2001;27(5):373-83.

2. Tanji K, Saeki K, Matsumoto Y, Takeda M, Hirasawa K, Doi K, et al. Analysis of PrP^C mRNA by *in situ* hybridization in brain, placenta, uterus and testis of rats. Intervirology. 1995;38(6):309-15.

3. Tichopad A, Pfaffl MW, Didier A. Tissue-specific expression pattern of bovine prion gene: quantification using real-time RT-PCR. Mol Cell Probes. 2003;17(1):5-10.

4. Moudjou M, Frobert Y, Grassi J, La Bonnardiére C. Cellular prion protein status in sheep: tissue-specific biochemical signatures. J Gen Virol. 2001;82(Pt 8):2017-24.

5. Prusiner SB. Novel proteinaceous infectious particles cause scrapie. Science. 1982;216(4542):136-44.

6. Hirsch TZ, Hernandez-Rapp J, Martin-Lannerée S, Launay JM, Mouillet-Richard S. PrP^C signalling in neurons: from basics to clinical challenges. Biochimie. 2014;104:2-11.

7. Wulf MA, Senatore A, Aguzzi A. The biological function of the cellular prion protein: an update. BMC Biol. 2017;15(1):34.

8. Martin GR, Keenan CM, Sharkey KA, Jirik FR. Endogenous prion protein attenuates experimentally induced colitis. Am J Pathol. 2011;179(5):2290-301.

9. Gourdain P, Ballerini C, Nicot AB, Carnaud C. Exacerbation of experimental autoimmune encephalomyelitis in prion protein (PrP^C)-null mice: evidence for a critical role of the central nervous system. J Neuroinflammation. 2012;9:25.

10. Ding T, Zhou X, Kouadir M, Shi F, Yang Y, Liu J, et al. Cellular prion protein participates in the regulation of inflammatory response and apoptosis in BV2 microglia during infection with *Mycobacterium bovis*. J Mol Neurosci. 2013;51(1):118-26.

11. Liu J, Zhao D, Liu C, Ding T, Yang L, Yin X, et al. Prion protein participates in the protection of mice from lipopolysaccharide infection by regulating the inflammatory process. J Mol Neurosci. 2014;55(1):279-87.

12. Bakkebø MK, Mouillet-Richard S, Espenes A, Goldmann W, Tatzelt J, Tranulis MA. The cellular prion protein: a player in immunological quiescence. Front Immunol. 2015;6:450.

13. Mariante RM, Nóbrega A, Martins RA, Areal RB, Bellio M, Linden R. Neuroimmunoendocrine regulation of the prion protein in neutrophils. J Biol Chem. 2012;287(42):35506-15.

14. Benestad SL, Austbø L, Tranulis MA, Espenes A, Olsaker I. Healthy goats naturally devoid of prion protein. Vet Res. 2012;43(1):87.

15. Reiten MR, Bakkebø MK, Brun-Hansen H, Lewandowska-Sabat AM, Olsaker I, Tranulis MA, et al. Hematological shift in goat kids naturally devoid of prion protein. Front Cell Dev Biol. 2015;3:44.

16. Malachin G, Reiten MR, Salvesen Ø, Aanes H, Kamstra JH, Skovgaard K, et al. Loss of prion protein induces a primed state of type I interferon-responsive genes. PLoS One. 2017;12(6):e0179881.

17. Salvesen Ø, Reiten MR, Espenes A, Bakkebø MK, Tranulis MA, Ersdal C. LPS-induced systemic inflammation reveals an immunomodulatory role for the prion protein at the blood-brain interface. J Neuroinflammation. 2017;14(1):106.

18. Erickson SE, Martin GS, Davis JL, Matthay MA, Eisner MD, Network NNA. Recent trends in acute lung injury mortality: 1996-2005. Crit Care Med. 2009;37(5):1574-9.

19. Gonzales JN, Lucas R, Verin AD. The acute respiratory distress syndrome: Mechanisms and perspective therapeutic approaches. Austin J Vasc Med. 2015;2(1):1009.

20. Rubenfeld GD, Caldwell E, Peabody E, Weaver J, Martin DP, Neff M, et al. Incidence and outcomes of acute lung injury. N Engl J Med. 2005;353(16):1685-93.

21. Andonegui G, Bonder CS, Green F, Mullaly SC, Zbytnuik L, Raharjo E, et al. Endothelium-derived Toll-like receptor-4 is the key molecule in LPS-induced neutrophil sequestration into lungs. J Clin Invest. 2003;111(7):1011-20.

22. Fujita M, Kuwano K, Kunitake R, Hagimoto N, Miyazaki H, Kaneko Y, et al. Endothelial cell apoptosis in lipopolysaccharide-induced lung injury in mice. Int Arch Allergy Immunol. 1998;117(3):202-8.

23. Martin TR, Hagimoto N, Nakamura M, Matute-Bello G. Apoptosis and epithelial injury in the lungs. Proc Am Thorac Soc. 2005;2(3):214-20.

24. Walker DC, Behzad AR, Chu F. Neutrophil migration through preexisting holes in the basal laminae of alveolar capillaries and epithelium during streptococcal pneumonia. Microvasc Res. 1995;50(3):397-416.

25. Korpos E, Wu C, Sorokin L. Multiple roles of the extracellular matrix in inflammation. Curr Pharm Des. 2009;15(12):1349-57.

26. Matthay MA, Ware LB, Zimmerman GA. The acute respiratory distress syndrome. J Clin Invest. 2012;122(8):2731-40.

27. Robinson MD, Oshlack A. A scaling normalization method for differential expression analysis of RNA-seq data. Genome Biol. 2010;11(3):R25.

28. Wang L, Feng Z, Wang X, Wang X, Zhang X. DEGseq: an R package for identifying differentially expressed genes from RNA-seq data. Bioinformatics. 2010;26(1):136-8.

29. Huang da W, Sherman BT, Lempicki RA. Systematic and integrative analysis of large gene lists using DAVID bioinformatics resources. Nat Protoc. 2009;4(1):44-57.

30. Huang da W, Sherman BT, Lempicki RA. Bioinformatics enrichment tools: paths toward the comprehensive functional analysis of large gene lists. Nucleic Acids Res. 2009;37(1):1-13.

31. Livak KJ, Schmittgen TD. Analysis of relative gene expression data using real-time quantitative PCR and the 2(-Delta Delta C(T)) Method. Methods. 2001;25(4):402-8.

32. Bonnans C, Chou J, Werb Z. Remodelling the extracellular matrix in development and disease. Nat Rev Mol Cell Biol. 2014;15(12):786-801.

33. Manicone AM, McGuire JK. Matrix metalloproteinases as modulators of inflammation. Semin Cell Dev Biol. 2008;19(1):34-41.

34. Parks WC, Wilson CL, López-Boado YS. Matrix metalloproteinases as modulators of inflammation and innate immunity. Nat Rev Immunol. 2004;4(8):617-29.

35. Deheinzelin D, Jatene FB, Saldiva PH, Brentani RR. Upregulation of collagen messenger RNA expression occurs immediately after lung damage. Chest. 1997;112(5):1184-8.

36. Armstrong L, Thickett DR, Mansell JP, Ionescu M, Hoyle E, Billinghurst RC, et al. Changes in collagen turnover in early acute respiratory distress syndrome. Am J Respir Crit Care Med. 1999;160(6):1910-5.

37. Ezpeleta J, Boudet-Devaud F, Pietri M, Baudry A, Baudouin V, Alleaume-Butaux A, et al. Protective role of cellular prion protein against TNFα-mediated inflammation through TACE alpha-secretase. Sci Rep. 2017;7(1):7671.

38. Loubet D, Dakowski C, Pietri M, Pradines E, Bernard S, Callebert J, et al. Neuritogenesis: the prion protein controls beta1 integrin signaling activity. FASEB J. 2012;26(2):678-90.

39. Hayashida T. Integrins modulate cellular fibrogenesis at multiple levels; Regulation of TGF-beta signaling. Endocr Metab Immune Disord Drug Targets. 2010;10(4):302-19.

40. González-López A, Albaiceta GM. Repair after acute lung injury: molecular mechanisms and therapeutic opportunities. Crit Care. 2012;16(2):209.

41. Chesnutt AN, Matthay MA, Tibayan FA, Clark JG. Early detection of type III procollagen peptide in acute lung injury. Pathogenetic and prognostic significance. Am J Respir Crit Care Med. 1997;156(3):840-5.

42. Fligiel SE, Standiford T, Fligiel HM, Tashkin D, Strieter RM, Warner RL, et al. Matrix metalloproteinases and matrix metalloproteinase inhibitors in acute lung injury. Hum Pathol. 2006;37(4):422-30.

43. Didonna A. Prion protein and its role in signal transduction. Cell Mol Biol Lett. 2013;18(2):209-30.

44. Makris S, Paulsen M, Johansson C. Type I interferons as regulators of lung inflammation. Front Immunol. 2017;8:259.

45. Peralta OA, Eyestone WH. Quantitative and qualitative analysis of cellular prion protein (PrP^C) expression in bovine somatic tissues. Prion. 2009;3(3):161-70.

46. Han CX, Liu HX, Zhao DM. The quantification of prion gene expression in sheep using real-time RT-PCR. Virus Genes. 2006;33(3):359-64.

47. Pennings JL, Kimman TG, Janssen R. Identification of a common gene expression response in different lung inflammatory diseases in rodents and macaques. PLoS One. 2008;3(7):e2596.

48. Salvesen Ø, Reiten MR, Heegaard PM, Tranulis MA, Espenes A, Skovgaard K. Activation of innate immune genes in caprine blood leukocytes after systemic endotoxin challenge. BMC Vet Res. 2016;12(1):241.

49. Wilson TC, Bachurski CJ, Ikegami M, Jobe AH, Kallapur SG. Pulmonary and systemic induction of SAA3 after ventilation and endotoxin in preterm lambs. Pediatr Res. 2005;58(6):1204-9.

50. Deguchi A, Tomita T, Omori T, Komatsu A, Ohto U, Takahashi S, et al. Serum amyloid A3 binds MD-2 to activate p38 and NF-κB pathways in a MyD88-dependent manner. J Immunol. 2013;191(4):1856-64.

51. Donato R, Cannon BR, Sorci G, Riuzzi F, Hsu K, Weber DJ, et al. Functions of S100 proteins. Curr Mol Med. 2013;13(1):24-57.

52. Hsu K, Champaiboon C, Guenther BD, Sorenson BS, Khammanivong A, Ross KF, et al. Anti-infective protective properties of S100 calgranulins. Antiinflamm Antiallergy Agents Med Chem. 2009;8(4):290-305.

53. Foell D, Wittkowski H, Vogl T, Roth J. S100 proteins expressed in phagocytes: a novel group of damage-associated molecular pattern molecules. J Leukoc Biol. 2007;81(1):28-37.

54. Hiroshima Y, Hsu K, Tedla N, Wong SW, Chow S, Kawaguchi N, et al. S100A8/A9 and S100A9 reduce acute lung injury. Immunol Cell Biol. 2017;95(5):461-72.

55. Androutsopoulos VP, Tsatsakis AM, Spandidos DA. Cytochrome P450 CYP1A1: wider roles in cancer progression and prevention. BMC Cancer. 2009;9:187.

56. Ke S, Rabson AB, Germino JF, Gallo MA, Tian Y. Mechanism of suppression of cytochrome P-450 1A1 expression by tumor necrosis factor-alpha and lipopolysaccharide. J Biol Chem. 2001;276(43):39638-44.

57. Wu D, Li W, Lok P, Matsumura F, Vogel CF. AhR deficiency impairs expression of LPS-induced inflammatory genes in mice. Biochem Biophys Res Commun. 2011;410(2):358-63.

58. Morel Y, Barouki R. Down-regulation of cytochrome P450 1A1 gene promoter by oxidative stress - Critical contribution of nuclear factor 1. J Biol Chem. 1998;273(41):26969-76.

59. Vogel CFA, Khan EM, Leung PSC, Gershwin ME, Chang WLW, Wu DL, et al. Cross-talk between aryl hydrocarbon receptor and the inflammatory response: a role for nuclear factor κB. J Biol Chem. 2014;289(3):1866-75.

60. Pugin J, Verghese G, Widmer MC, Matthay MA. The alveolar space is the site of intense inflammatory and profibrotic reactions in the early phase of acute respiratory distress syndrome. Crit Care Med. 1999;27(2):304-12.

61. Yang G, Hamacher J, Gorshkov B, White R, Sridhar S, Verin A, et al. The dual role of TNF in pulmonary edema. J Cardiovasc Dis Res. 2010;1(1):29-36.

62. Sone Y, Serikov VB, Staub NC, Sr. Intravascular macrophage depletion attenuates endotoxin lung injury in anesthetized sheep. J Appl Physiol. 1999;87(4):1354-9.

13 Figures

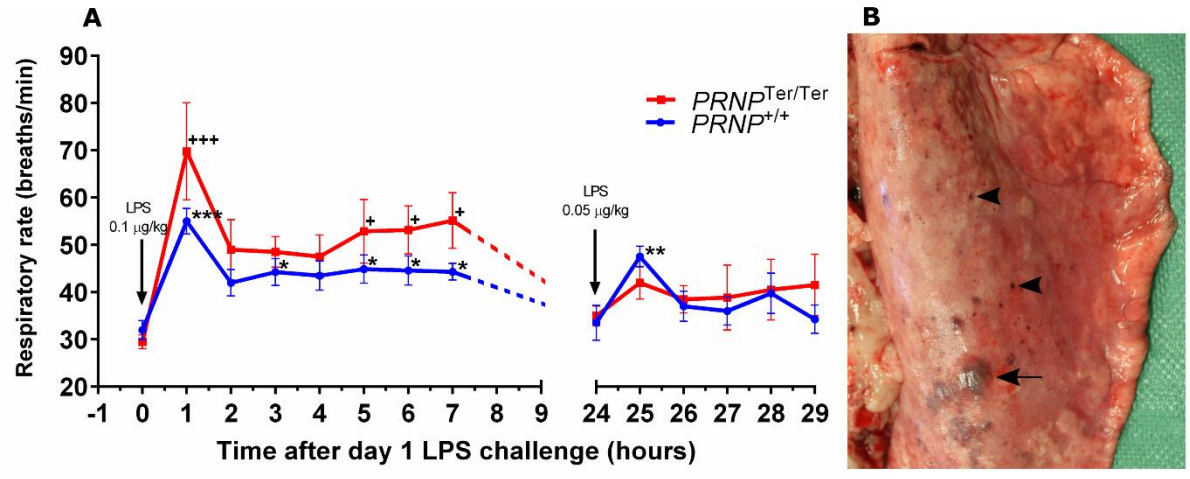

Figure 1: Respiratory rate and lung gross pathology after systemic LPS challenge. Goats were subjected to a dual LPS challenge; 0.1 µg/kg and 0.05 µg/kg with a 24-hour time interval between doses. **(A)** The diagram shows the respiratory rate (breaths/min) after LPS challenge. Values are mean ± SEM. Symbols * and + represent significantly increased respiratory rate compared with baseline samples (0 h) of the matching genotype. **(B)** Dorsal view of the right caudal lung lobe. Sub-plural ecchymosis (arrow) and petechial bleedings (arrowhead) display a multifocal distribution.

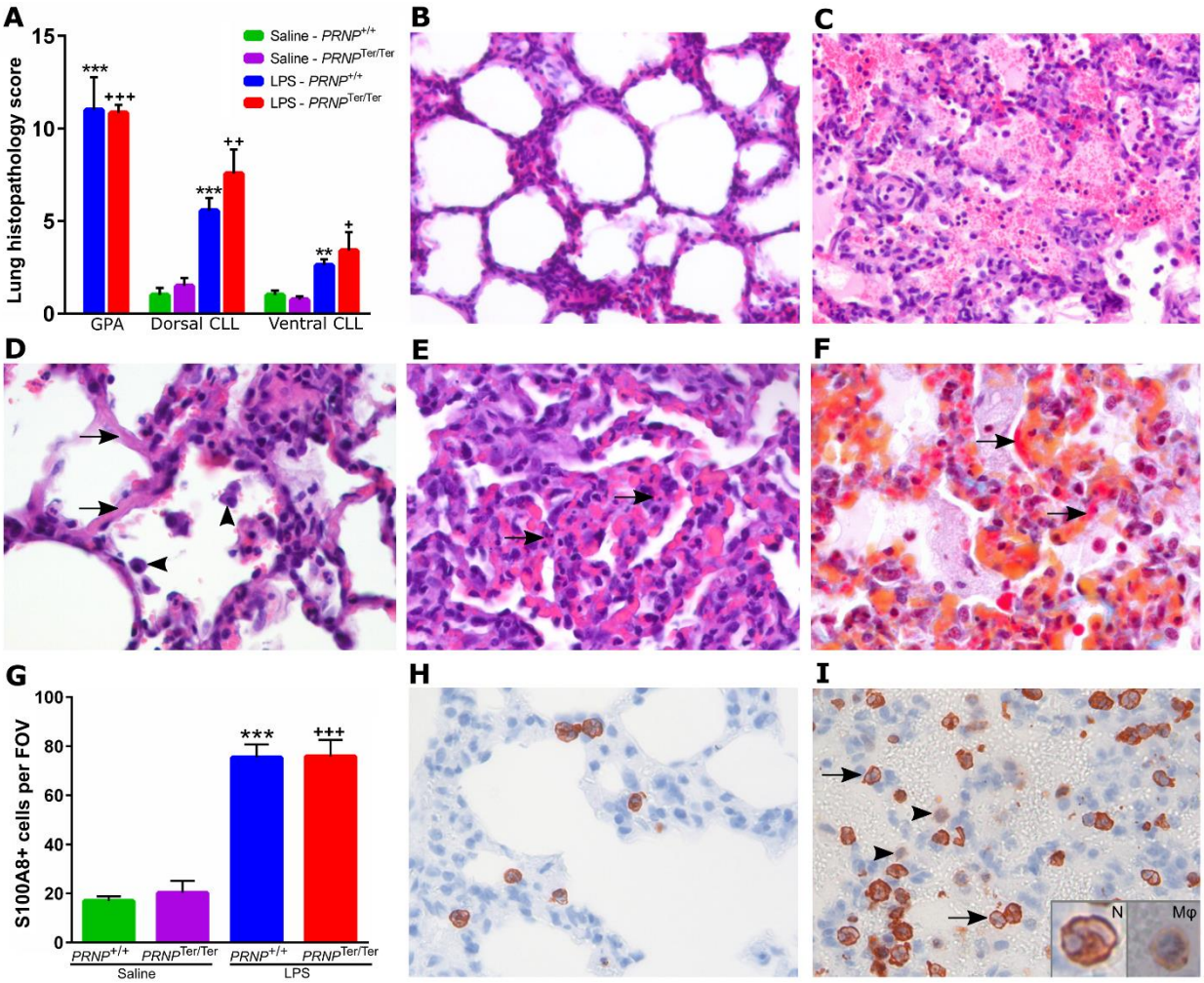

Figure 2: Histopathology after LPS challenge. (A) A blinded scoring of lung histopathology was performed as described in methods. Sections from the dorsal caudal lung lobe (CLL) and ventral CLL were scored in all animals, in addition to sections from areas with gross pathology, mainly bleedings (GPA). Symbols represent significantly increased lung histopathology score compared with saline controls of the matching genotype. GPA are compared with the dorsal CLL of the matching control. **(B)** Normal lung tissue from a saline control goat. **(C)** Alveolar edema and bleedings accompanied by neutrophil infiltration and increased number of alveolar macrophages. **(D)** Hyaline septa (arrows) and increased number of alveolar macrophages (arrowheads). **(E)** Area with moderate atelectasis and hyperemia. Several single cell necroses (arrows) can be seen within the alveolar septa. **(F)** MSB staining shows deposition of fibrin within the septa (arrows) and small amounts in the alveoli. Sections C-F are from areas with pathology in LPS-treated animals. **(G)** Mean number of S100A8-positive cells quantified within a representative 400 X field of view (⌀ = 450 µm). Symbols represent significantly increased levels compared with saline controls of the matching genotype. **(H)** Normal lung tissue from a control animal displaying a few S100A8-positive neutrophils within the alveolar septa. **(I)** After LPS challenge, increased numbers of S100A8-positive neutrophils are sequestered within the septal capillaries and some infiltrate the alveoli (arrows). Alveolar macrophages displayed a weak S100A8-signal (arrowheads). Insertions show a magnified neutrophil (N) with segmented nucleus and an alveolar macrophage (Mϕ). Magnification: B-C, 200 X; D-I, 400 X. Values are mean ± SEM.

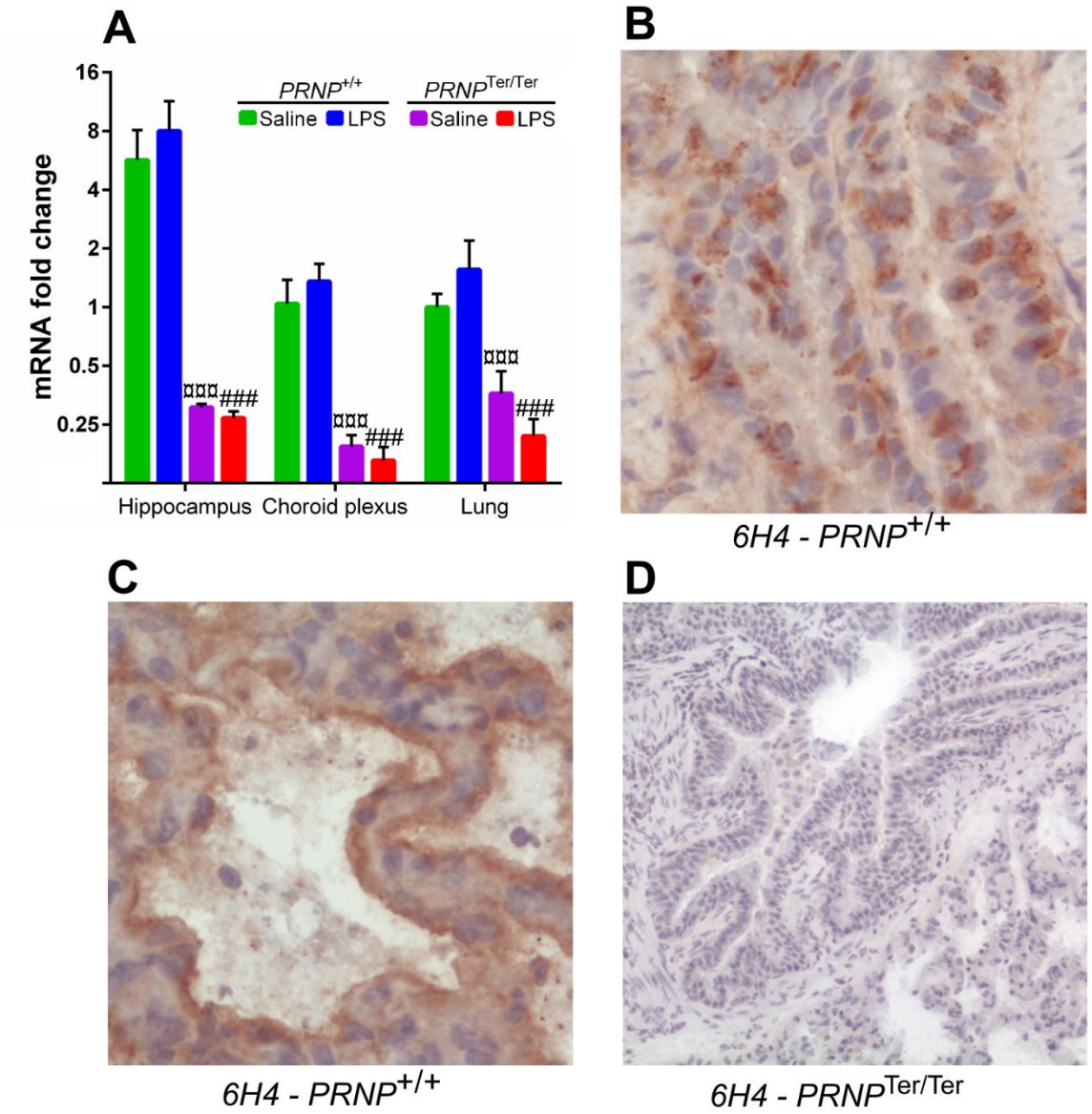

Figure 3. *PRNP* expression and cellular distribution of PrP^C. (A) Comparison of *PRNP* expression in three tissues from Norwegian dairy goats before and after LPS challenge. Symbols represent significantly ($p < 0.001$) reduced expression in $PRNP^{Ter/Ter}$ goats, compared with $PRNP^{+/+}$ goats of the same treatment. **(B)** PrP^C shows a granular distribution within bronchial epithelial cells. **(C)** In the alveoli, PrP^C labeling is associated with the luminal surface of the alveolar septa, probably associated with alveolar pneumocytes. **(D)** No PrP^C was detected in sections from $PRNP^{Ter/Ter}$ goats. All sections are from representative areas stained with the 6H4 antibody. Sections stained with the SAF32 showed a similar distribution of PrP^C (not shown). Magnification B-C, 400 X; D, 100 X.

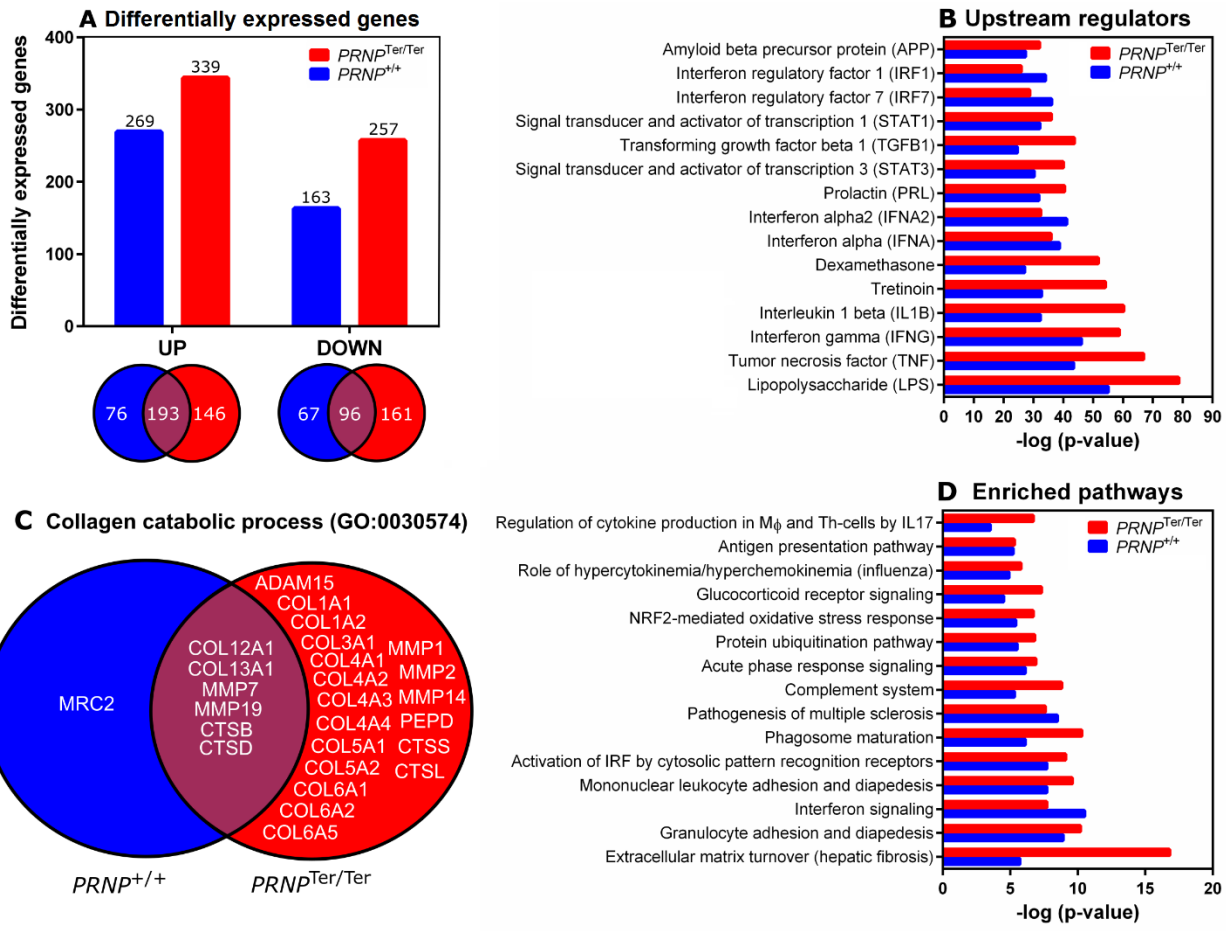

Figure 4. Differentially expressed genes after LPS challenge and biological function analysis. (A) Differential expression analyses were performed by comparing the LPS-groups to the saline control group of the matching genotype (log2 ratio 0.59 and q-value < 0.05). Venn diagrams show genes that overlap between the two genotypes. **(B)** Shown are the top 15 overrepresented upstream regulators identified by ingenuity pathway analysis (IPA). **(C)** Venn diagram showing the distribution of genes characterized as collagen catabolic process (GO:0030574) in the two *PRNP* genotypes. **(D)** The top 15 affected pathways identified by IPA are shown.

.

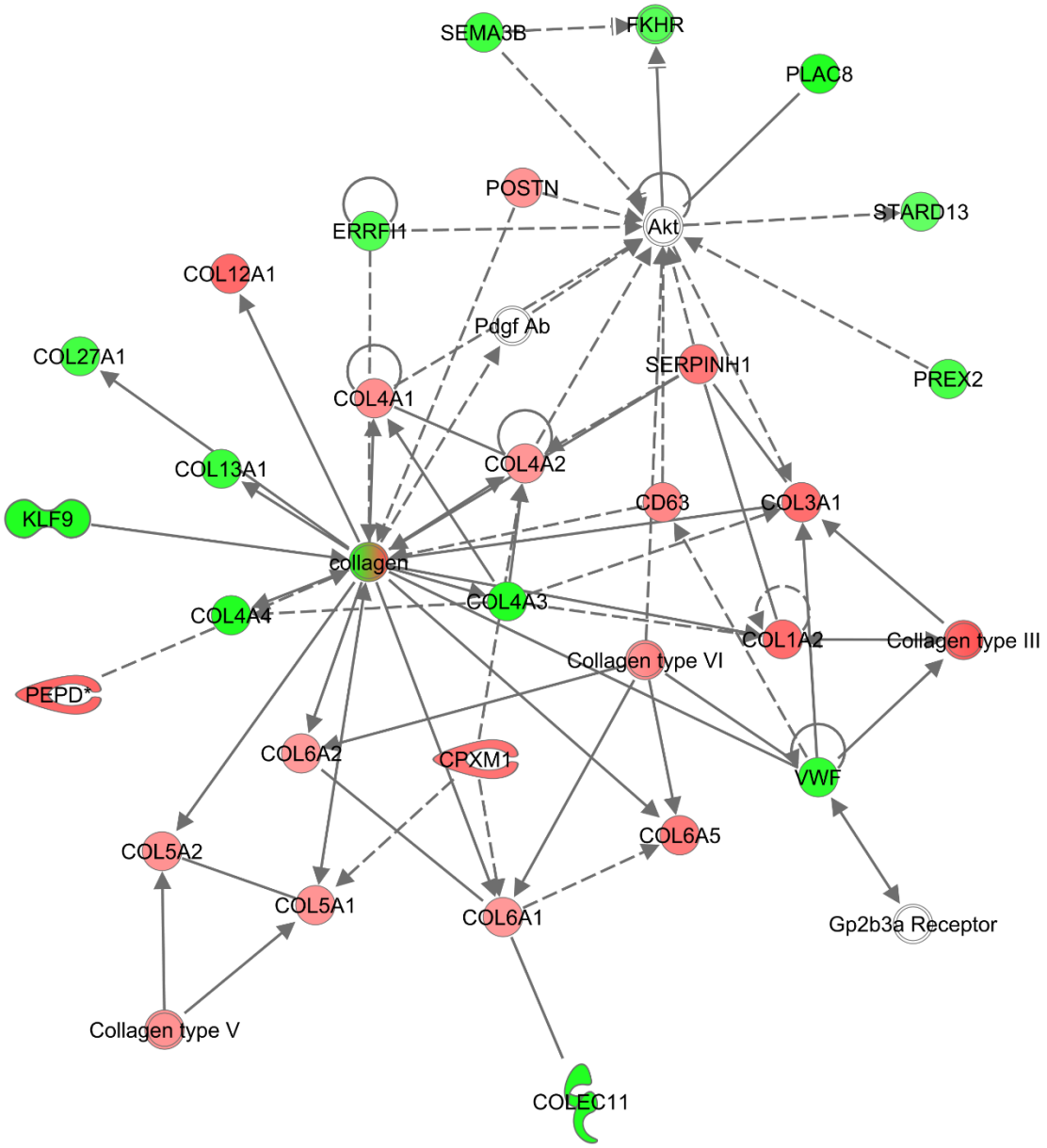

Figure 5. Network of genes related to connective tissue disorders in *PRNP*$^{Ter/Ter}$ goats. An overrepresented network is shown exclusively for *PRNP*$^{Ter/Ter}$ goats of differentially expressed genes and interacting partners related to connective tissue disorders. Red means upregulated, green means downregulated

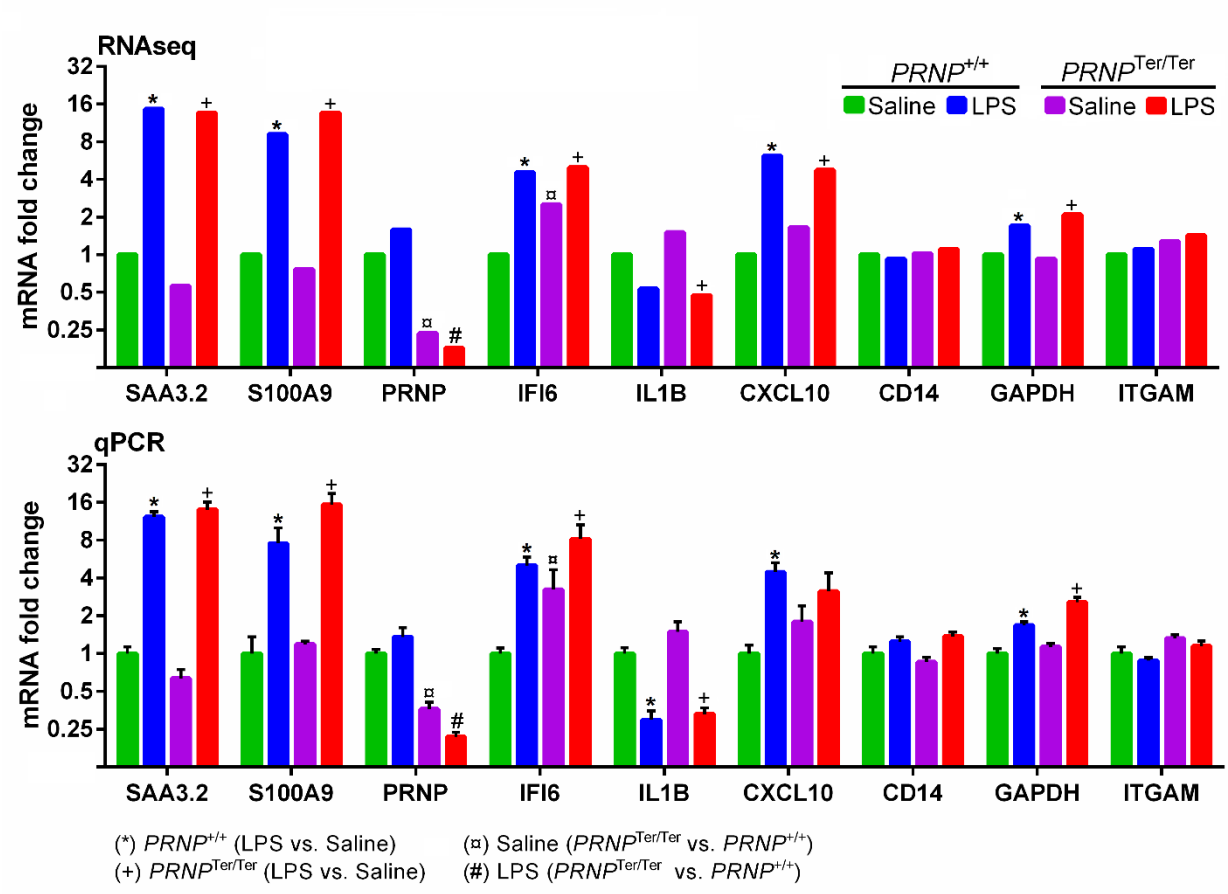

Figure 6. Validation of RNA-seq data by qPCR. Nine target genes representing both differentially expressed and non-differentially expressed genes were measured by qPCR. For each gene, the expression levels are normalized relative to the saline-treated *PRNP*$^{+/+}$ group. RNA-seq symbols above bars represent a significant differential expression (log2 ratio ± 0.59, $q < 0.05$). Bars (qPCR) display mean expression ± SEM with symbols representing significant differences, as assed by multiple t-tests ($p < 0.05$).

frontiers

Supplementary Material

PrP^{C} modulates pathways of inflammation during LPS-induced acute lung injury

Salvesen Ø*, Reiten MR, Kamstra JH, Bakkebø MK, Espenes A, Tranulis MA, Ersdal C

*** Correspondence:** oyvind.salvesen@nmbu.no

Table S1. Study groups showing treatment, animal number, mean age, mean weight and gender.

Treatment	Genotype	Animal number	Mean age (months)	Mean weight (kg)	Gender
LPS	*PRNP*$^{+/+}$	8	7,3 (±0,3)	27,3 (±2,7)	8♀
	PRNP$^{Ter/Ter}$	8	6,7 (±1,1)	26,1 (±4,6)	7♀, 1♂
Saline	*PRNP*$^{+/+}$	5	6,7 (±0,2)	21,5 (±3,2)	5♀
	PRNP$^{Ter/Ter}$	5	6,6 (±0,03)	24,9 (±2,8)	5♀
		26	**6,9 (± 0,7)**	**25,3 (± 3,9)**	**25♀, 1♂**

Table S2. RNA quality control. Purity was based on $OD_{260/280}$ and $OD_{260/230}$ absorbance reading using DeNovix DS-11 spectrophotometer (Wilmington, USA). RNA integrity was assessed by the Agilent Bioanalyzer system.

Treatment	Group	$OD_{260/280}$	$OD_{260/230}$	Mean RIN	Novogene RIN*
LPS	*PRNP*$^{Ter/Ter}$	2.1 (±0.05)	2.2 (±0.08)	8.5 (±0.29)	9.1
	PRNP$^{+/+}$	2.1 (±0.06)	2.2 (±0.03)	8.6 (±0.27)	8.9
Saline	*PRNP*$^{Ter/Ter}$	2.1 (±0.11)	2.2 (±0.04)	8.5 (±0.17)	9.0
	PRNP$^{+/+}$	2.1 (±0.07)	2.1 (±0.12)	8.4 (±0.39)	8.8

* Novogene quality control on samples before RNA sequencing. All samples were assessed as being of the best quality level (A level).

Table S3. RNA sequencing - quality control summary

Sample	Raw reads	Clean reads	Clean bases	Error rate (%)	Q20 (%)	Q30 (%)	GC content (%)
Lu_L_Ter	58928706	57240044	8.59G	0.01	98.14	95.58	52.01
Lu_L_Nrm	40942406	39851306	5.98G	0.01	98.16	95.62	51.24
Lu_C_Ter	47429726	46063496	6.91G	0.01	98.10	95.51	51.94
Lu_C_Nrm	41592070	40369834	6.06G	0.01	98.14	95.60	52.12

Table S4. RNA sequencing - overview of mapping status

Sample	Lu_LPS_Ter	Lu_LPS_Nrm	Lu_Ctrl_Ter	Lu_Ctrl_Nrm
Total reads	57240044	39851306	46063496	40369834
Total mapped	43924351 (76.74%)	31053064 (77.92%)	35377663 (76.8%)	30723965 (76.11%)
Multiple mapped	655985 (1.15%)	464171 (1.16%)	482173 (1.05%)	458717 (1.14%)
Uniquely mapped	43268366 (75.59%)	30588893 (76.76%)	34895490 (75.76%)	30265248 (74.97%)
Read-1	22137382 (38.67%)	15659895 (39.3%)	17887107 (38.83%)	15487734 (38.36%)
Read-2	21130984 (36.92%)	14928998 (37.46%)	17008383 (36.92%)	14777514 (36.61%)
Reads map to '+'	21626721 (37.78%)	15291053 (38.37%)	17439028 (37.86%)	15125398 (37.47%)
Reads map to '-'	21641645 (37.81%)	15297840 (38.39%)	17456462 (37.90%)	15139850 (37.50%)
Non-splice reads	26470495 (46.24%)	19304450 (48.44%)	22101289 (47.98%)	19223946 (47.62%)
Splice reads	16797871 (29.35%)	11284443 (28.32%)	12794201 (27.78%)	11041302 (27.35%)

Table S5. Primer sequences used for qPCR

Gene ID	Symbol	Gene name	Primer sequences	Ref.
102179831	ACTB	Actin beta	F: 5'TGCCCTGAGGCTCTCTTCCA R: 5'TGCGGATGTCGACGTCACA	[1]
102169975	PRNP	Prion protein	F: 5'GTGGCTACATGCTGGGAAGT R: 5'AGCCTGGGATTCTCTCTGGT	
102185230	IFI6	Interferon alpha inducible protein 6	F: 5'TATCGCTGTTCCTGTGCTACC R: 5'AAGCTCGAGTCGCTGTTTTC	
100860873	CXCL10	C-X-C motif chemokine ligand 10	F: 5'ACGCTGTACCTGCATCGAG R: 5'GCAGGATTGACTTGCAGGA	
102168428	SAA3.2	Serum amyloid A3	F: 5'CTGGGCTGCTAAAGTGATCAGTAAC R: 5'CCCTTGAGCAGAGGGTCTGTGATT	[2]
102182273	S100A9	S100 calcium-binding protein A9	F: GAGATCATGGAGGACCTGGA R: GGCCACCAGCATAATGAACT	
102180100	ITGAM	Integrin Subunit Alpha M	F: CTTGAGGCCTCCACCAAATA R: GCCCAGGTTGTTGAACTGAT	
102177056	CD14	Cluster of differentiation 14	F: CCACCCTCAGTCTCCGTAAC R: GTGTGCTTGGGCAATGTTC	
100860816	IL1B	Interleukin 1 beta	F: GACAACAAGATTCCTGTGGCC R: TCTACTTCCTCCAGATGAAGTGT	
100860872	GAPDH	Glyceraldehyde 3-phosphate dehydrogenase	F: GCAAGTTCCACGGCACAGTC R: CCCACTTGATGTTGGCAGGA	[1]

References

1. Zhang Y, Zhang XD, Liu X, Li YS, Ding JP, Zhang XR, et al. Reference gene screening for analyzing gene expression across goat tissue. Asian-Australasian journal of animal sciences. 2013;26(12):1665-71.
2. Brenaut P, Lefevre L, Rau A, Laloe D, Pisoni G, Moroni P, et al. Contribution of mammary epithelial cells to the immune response during early stages of a bacterial infection to Staphylococcus aureus. Vet Res. 2014;45:16.